Enhanced Analysis of Spiral Separation Performance

J.D. Grobler

Department of Materials Science and Metallurgical Engineering, University of Pretoria, South Africa

2015

ENHANCED ANALYSIS OF SPIRAL SEPARATION PERFORMANCE

by

J.D. Grobler

submitted in partial fulfillment of the requirements for the degree

Master's in Metallurgical Engineering

supervised by

Dr J.H. Zietsman

in the

Faculty of Engineering, Built Environment and Information Technology

of the

University of Pretoria

on

February 22, 2016

;

Abstract

Standard material analysis methods used in the heavy minerals industry to characterise spiral separation behaviour is unable to fully quantify performance differences between the available spiral profiles of today. This study proposes an enhanced method to analyse spiral products to identify key separation performance differences between different spiral profiles for specific feed materials. The enhanced analysis method has two major components. The first involves a material characterisation method that was developed using the analytical capability of Qemscan® to simultaneously quantify particle density and particle size. The second involves a data presentation method that was developed by making improvements to the Holland-Batt equation. The standard material characterisation method was compared to the enhanced method using the separation products of two different spiral profiles with two different feed materials. The benefit of the developed method is clearly demonstrated by the additional separation performance information that it produced. This information enables the user to make more informed decisions when identifying spiral performance deviations in current installations, when selecting the correct spiral profile prior to spiral replacement, and during the spiral plant design process.

Keywords:
spiral concentrator, enhanced analysis, Qemscan®, Holland-Batt, separation performance

Dedication

To Christ who inspires and enables excellence

Acknowledgements

I would like to thank my fellow colleagues at Exxaro Metallurgical Services as well as supportive friends and family.

Special thanks to my wife for her continued support.

Special thanks to Dr Johan Zietsman who made such a significant difference in the approach and outcome of this study as well as the quality of the final product.

Contents

List of Figures

List of Tables

Part I

Introduction

Chapter 1

Background

1.1 Project Background

Performance testing of separation equipment in the mineral processing industry is common practice. One of the motivations for performance testing arises from a performance deviation, usually a negative deviation, from target product recovery and/or product grade. The source of the recovery or grade 'problem' needs to be identified quickly in order to be rectified and to minimize any further product losses. Another common motivation is that most separation equipment will come to the end of its life and replacement equipment needs to be evaluated. The normal method for performance testing is to sample the products from the separator and to conduct a series of analyses on the samples.

The spiral concentrator, also simply known as a spiral, has been studied extensively since its introduction into the mineral processing industry in mid-1940, resulting in a large volume of available literature. The main reason for the large amount of performance test-work conducted on spirals is that most spiral profiles have a low capacity (not more than 10 t/h) and are therefore fairly easy to sample by hand. Another reason is that a typical spiral only lasts 10 to 15 years, which will require replacement at least twice during the life of a reasonably sized mineral beneficiation business.

Over the last three decades of spiral development the sample analysis methods applied on spiral products to evaluate separation performance remained unchanged. The major risk of not developing the analysis methods is that the performance benefit of one spiral over the other, for a specific feed material, might not be identified. The careless application of the standard analysis methods could cause product losses in the long term, resulting in significant loss in business profit.

This project was initiated to develop an enhanced material characterisation method coupled with enhanced presentation of test-work data. The developed method was successfully applied to the products from two spirals to improve the understanding of spiral separation performance. This information enables the user to make more informed decisions regarding spiral selection for a specific separation application (feed material and operating conditions). It also enables the user to identify spiral performance deviations in current installations more effectively.

1.2 Spirals in the Heavy Mineral Industry

Spirals play an important role in the mineral beneficiation industry in the separation of low-density mineral particles, consisting mostly of quartz, from high-density particles containing commercially valuable minerals, usually heavy mineral sand, fine chromite or fine iron ore. In the case of coal, low-density mineral particles containing mostly carbon are separated from

higher density mineral particles containing mostly quartz. In most cases spirals are used in primary separation that involves large run-of-mine volumes. This implies large throughput tonnages through multiple units and processing stages.

Heavy mineral sands deposits generally consist of naturally fine grained, free flowing sand due to the way in which the deposit was formed. The size of the heavy minerals market is roughly 8 Mt/a of zircon and titanium combined (Iluka 2013). If an average combined feed grade of 5 % zircon and titanium and an average combined overall product recovery of 80 % are assumed, the resulting run-of-mine feed tons that would require primary spiral beneficiation is 200 Mt/a. The number of spirals required for the processing of this material, assuming 6500 operating hours per annum and assuming an average of 2 t/start and the same number of rougher spirals to other duty spirals, is over 30 000 spirals alone for the heavy mineral sands business. These numbers clearly illustrate the importance of the spiral in the heavy mineral industry.

This project focused on spiral separation performance measurement within the heavy mineral sands industry. Since more than 90 % of the particles are usually smaller than 500 µm, it is common to assume that the separation on the spiral mostly occurs on particle density differences. The standard product sample analysis approach used over the last 70 years, is to perform a sink-float in a high-density organic medium to separate high-density particles, greater than 3 g/cm^3, from low-density particles that are less than 3 g/cm^3. Although it is known in the mineral sands industry that both particle density and particle size influence spiral separation performance, particle size relative to particle density fractions is rarely measured.

This study measured the influence of particle size and particle density on spiral separation performance. It was clear that there were significant differences with particle size variation. The correct quantification of spiral separation performance and the understanding following from correct quantification are therefore critical for the mineral beneficiation business in which it is applied.

1.3 Company Background

Tronox Mineral Sands produces more than 800 000 t/a of final heavy mineral product to the external market as well as to Tronox's own pigment production business. Products from the different mineral beneficiation processes are zircon, rutile and ilmenite. High purity zircon is sold into the open market and used primarily in the ceramic, refractory and zirconium chemical industries. High purity rutile is used as flux in the welding electrode manufacturing and feedstock for the manufacturing of titanium dioxide pigment. The ilmenite product is processed in furnaces to produce high titania slag and pig iron. The titanium dioxide is purified in a chlorination process to produce final TiO_2 pigment.

The company consists of three open-pit mining and beneficiation operations. Namakwa Sands is situated on the west coast of South Africa. Material is mined by various types of 'yellow machines' and conveyed to two separate wet beneficiation plants utilising spiral concentration to produce a heavy mineral concentrate consisting mostly of ilmenite, zircon and rutile. KZN Sands is situated on the east coast of South Africa. Material is mined by high pressure monitoring and pumped to a wet beneficiation plant, also utilising spiral concentration to produce a heavy mineral concentrate containing similar minerals in slightly different ratios. Cooljarloo on the west coast of Australia makes use of dredge mining. Material is mined by a dredge and pumped to a floating concentrator utilising spiral concentration to produce a heavy mineral concentrate with similar mineral ratios. The heavy mineral concentrate from each of the operations is further separated at close-by mineral separation plants to produce high purity zircon, rutile and ilmenite products.

More than 40 000 000 t/ a of run-of-mine material is processed by spirals across the above-mentioned mining and beneficiation operations. These tonnages require more than 3000 first stage spirals (rougher duty) and another 3500 second stage spirals (cleaner and scavenger duty). The selection of optimal spiral profile for the correct separation duty is critical for the business's long term profitability. Spirals are replaced every 10 to 15 years due to trough surface wear and each replacement step is an opportunity to install an improved spiral. A method to accurately measure all the factors influencing spiral separation performance can greatly assist in good decision making with regards to performance deviation control as well as spiral selection.

1.4 Publications from this Study

Two international presentations have thus far been made from the work conducted in this study. The first presentation was at the 7th International Heavy Mineral Conference in 2009 with the topic Gravity separator performance evaluation using Qemscan® particle mineral analysis (Grobler and Bosman 2009). The second presentation was done at the Physical Beneficiation conference in 2010 with the topic Spiral concentrator modelling using Qemscan® (Grobler and Bosman 2010). The article from the Heavy Mineral Conference was reviewed, updated and accepted as a transaction paper in the Journal of the Southern African Institute of Mining and Metallurgy (Grobler and Bosman 2011).

1.5 Document Overview

Part I of this document introduces the reader to the study. Chapter 1 describes the project, industry and company background and the relevance this study has on each. Chapter 2 gives a clear and concise background to spiral concentrators and how separation performance is measured. Readers familiar with these concepts can proceed to Chapter 3, which contains the problem statement, purpose, significance and scope of this study in the light of the background in the first two chapters.

Part II summarises the relevant literature. Chapter 4 focuses on material characterisation using Qemscan®. Background to Qemscan® is provided followed by some literature references on how the technology has been applied previously in a similar fashion to this study.

Part 4.6 presents the research design and methodology. Chapter 3 (research design) provides the structure in which the total study was planned and executed. It also introduces how the enhanced analysis method was developed. Chapter 6 describes the standard analysis methods that were used as building blocks before the enhanced characterisation could commence. Chapter 7 discusses the methods that were developed and validated. This chapter contains validation results and discussions that followed from it. This investigation aimed at developing an enhanced method for spiral performance measurement. The method description and its validation therefore form an integral part of this document. Chapter 8 describes the second component of the enhanced analysis, the data presentation method, and how it was improved in this study.

Part III contains the test-work results from feed and product characterisation. This part of the document is presented as four main components. Chapter 9 contains the first component that presents the feed material data that was generated from standard material characterisation methods as well as the enhanced method. Chapter 10 demonstrates the standard spiral performance analysis based on standard characterisation methods. Chapter 11 introduces the enhanced product characterisation and compares it with the output from the standard product characterisation. Chapter 12, containing the fourth component, focuses on the application of the new enhanced analysis method (enhanced characterisation and enhanced data presentation)

to demonstrate the value this method has in the evaluation and comparison of the separation performance of different spiral profiles.

Part IV is the closure. Chapter 13 summarises the four result and discussion chapters. The final conclusions and the recommendations for future test-work and potential further investigations from this study are listed.

Chapter 2

Spiral Concentrators

This chapter is dedicated to the description of the process and theoretical background of the spiral. It presents a general view on spiral separation performance, while the chapters that follow present the specific scope and contribution of this study. Large parts of this chapter are based on author's own experience. The purpose of the chapter is to give a clear background on the spiral if the reader is not familiar with a spiral concentrator or its performance measurement. Readers familiar with these concepts can proceed to Chapter 3.

The chapter is divided into five separate sections. The first section discusses basic design and the second section the separation mechanism. These two sections provide the theoretical background. The third section addresses the application aspects, the fourth section the measurement of separation performance and the last section factors that influence separation performance, which gives the necessary process background.

2.1 Spiral Design

In this section basic trough geometry, typical auxiliaries on the trough and materials used to manufacture the trough are discussed.

2.1.1 Basic Geometry

A spiral is an open, downward curved trough. The number of turns around a centre column can vary between 3 and 10 and need not be full turns. A typical example is a seven-and-a-half turn spiral. Figure 2.1 shows an example of a five and a quarter turn spiral. Figure 2.2 is an example of a spiral trough cut in two places to demonstrate a half turn of a spiral. The vertical length of spirals can vary between 1 m and 10 m, and the diameter between 0.3 m and 1.5 m. The pitch, also referred to as the spiral slope angle, is simply the number of full rotations divided by the total height of the full rotations. For spiral concentrators the pitch remains constant over the entire length of the spiral. The trough slope angle is the angle of the trough at the cross section from the centre column in the transverse direction. This angle changes from a small angle on the inside of the trough and increases towards the outside of the trough. Figure 2.3 demonstrates the difference between these two angles. These two angle types play a significant role in the separation efficiency for a specific application. Although the spiral seems like an operationally simple unit, the fluid and solid flow phenomena on the trough are complex. The direct relationship between spiral design and separation efficiency is ill-defined in literature, and spiral manufacturers keep whatever information is available close to their chests. There are many patents registered for different slope angles and slope angle combinations. In quite a few cases a certain spiral manufacturer's product outperforms similar spiral products for only a specific feed material.

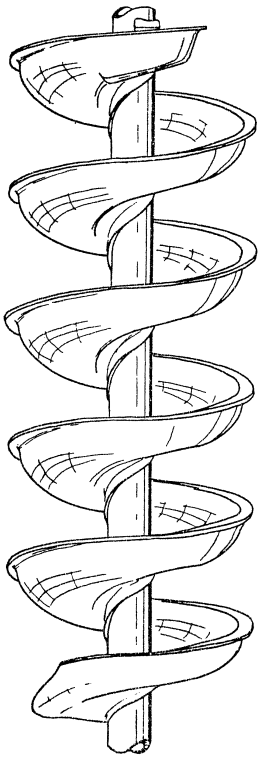

Figure 2.1: Example of a spiral concentrator. (Wright 1982)

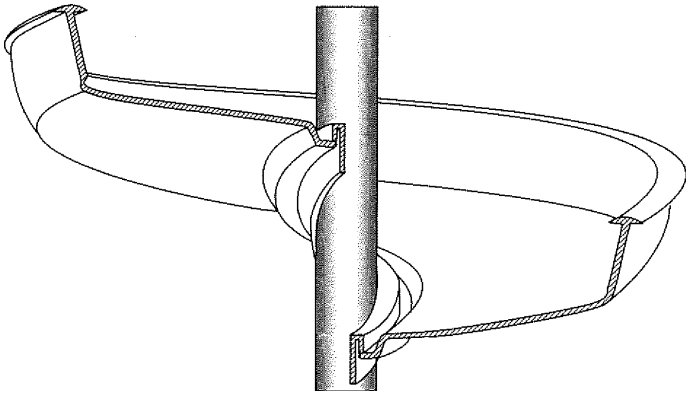

Figure 2.2: Example of spiral intersected at two positions, presenting a half rotation. (Cooke 2011)

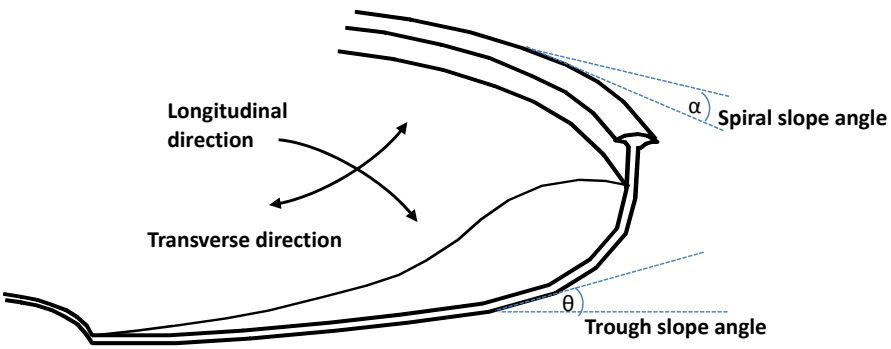

Figure 2.3: Spiral cross sectional profile indicating trough slope angle and spiral slope angle.

2.1.2 Auxiliary Components

Figure 2.4 shows the components discussed here.

The feedbox is the entry point onto the spiral trough. Its purpose is to spread the material evenly across the trough at the correct entry velocity to ensure that separation can commence as soon as possible as the mineral particles progress down the spiral. Figure 2.5 illustrates a feedbox design.

Repulpers are used to recombine a portion of the material on the spiral trough to 'reset' the particle positions and give 'trapped' particles another opportunity to move to their respective transverse equilibrium positions. The transverse direction is indicated in Figure 2.3. An example of repulper design is provided in Figure 2.6.

The auxiliary side splitter can be utilised to extract concentrate into the centre column usually two thirds down the spiral column. The purpose of the auxiliary side splitter is to move high-density particles that have been successfully separated out of the concentrate section to limit particle crowding in the middling section, therefore creating opportunity for other high-density particles to move out of the middling section into the concentrate section. These different separation sections are illustrated in Figure 2.7. The middling section is also known as the separation zone. An example of an auxiliary side splitter design is shown in Figure 2.8.

The product splitter box contains the splitters that separate the material at the trough exit into concentrate, middling and tailing streams. It is important that the product splitter box is well designed to accommodate the flow rates and solids concentration of the different streams. Incorrect design could cause mixing in the product box which will negatively impact spiral separation performance. Figure 2.9 illustrates a product splitter box design.

A wash water system adding water at different trough positions is another example of an auxiliary type component. In this case high quality water is added in the separation zone on the spiral trough. Figure 2.10 illustrates a wash water addition point design.

Different spiral manufacturers make use of different auxiliary component designs, with varying degrees of success. Its success is highly dependent on the specific feed material and operating conditions.

2.1.3 Materials of Construction

The first spirals were constructed from tyres sown or glued together. Later spiral models were produced with a concrete cast (Thompson 1969). The materials of construction improved significantly from the 1950s, and are critical from a frictional force point of view. Poly urethane, poly ethylene, and other plastics are used in manufacturing. The particles on the trough surface experience frictional drag from the material of manufacture as it moves radially (transverse direction, see Figure 2.3) to its equilibrium position and downwards along the spiral trough (longitudinal direction, see Figure 2.3). Different materials of manufacture cause different spiral separation performance. The most suitable materials of manufacture are determined through test-work on different spiral types to decide the best match for a specific feed material. There are no rules regarding matching specific trough materials with a specific feed material.

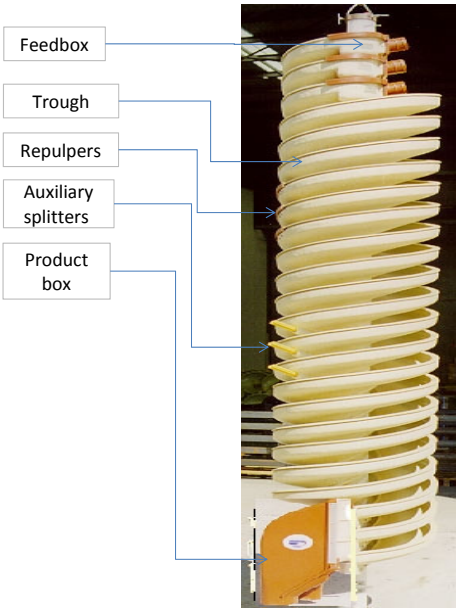

Figure 2.4: Auxiliary components of a typical spiral. (Mineral Technologies 2014)

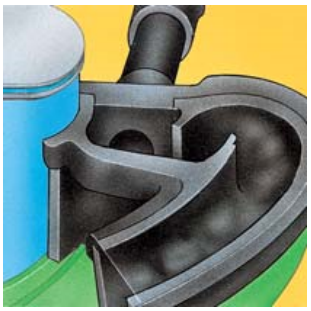

Figure 2.5: Feedbox design on a single spiral start. (Multotec 2014a)

Figure 2.6: Repulper design on a single spiral start. (Multotec 2014b)

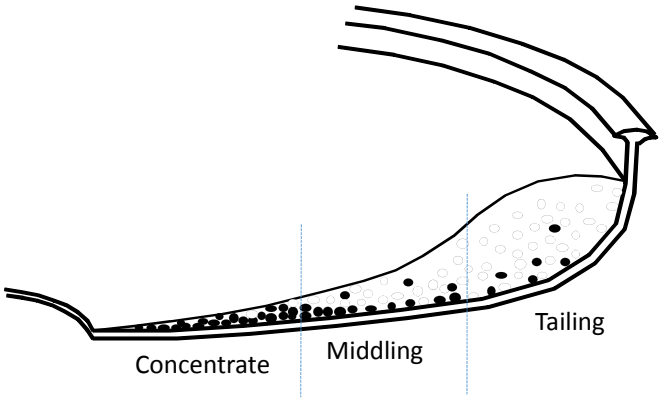

Figure 2.7: Spiral cross sectional profile depicting the different separation sections. (● = high-density particle, ○ = low-density particle)

Figure 2.8: Auxiliary side splitter. (Multotec 2014a)

Figure 2.9: Product splitter box design on a single spiral start. (Multotec 2014b)

Figure 2.10: Wash water addition point. (Multotec 2014b)

2.2 Spiral Separation

In this section the basic separation mechanism is discussed, which includes a simple two-phase example and a description of fluid flow and forces exerted on a particle in the separation environment.

2.2.1 Separation Basics

The spiral is used in the mineral beneficiation industry as a gravity or density separator to separate high-density particles from low-density particles. Figure 2.11 and Figure 2.12 illustrate a basic spiral separation process in which the numbers of particles and not particle masses were considered as an example. A combination of particle properties such as density, size and shape determines the final radial position of a specific particle. Generally particle density is the most considered property in literature since it links directly with minerals that have economic value in the mineral beneficiation industry. Usually the feed to the spiral has a density spectrum, and it is very rarely as simple as depicted in the Figure 2.11.

In Figure 2.11 a particle population with equal numbers of high- and low-density particles enters the spiral. A combination of flows and forces causes separation into two products, namely a concentrate, which is rich in high-density particles, and a tailing, which is rich in low-density particles. The simplified separation on the spiral can be seen in Figure 2.12. Some misplacement occurs with low-density particles reporting to concentrate and vice versa. The result of the separation can be expressed using product grade, recovery and separation efficiency. These terms are discussed in Section 2.4 on page 21.

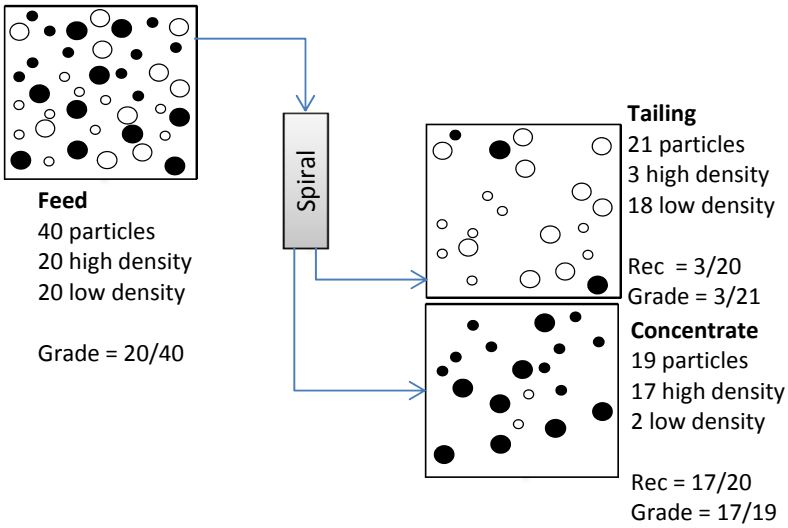

Figure 2.11: Basic functioning of a spiral in mineral beneficiation. (● = high-density particle, ○ = low-density particle, Rec = black particle recovery, Grade = black particle grade)

2.2.2 Water Requirement

The spiral contains no moving parts. The force due to gravity provides the energy required to effect separation. Water and mineral particles are usually mixed in a 30 % particle mass and 70 % water mass ratio and introduced at the top of the spiral column as depicted in Figure 2.13. The different forces that the particles experience while moving down with the fast moving water cause segregation of high- and low-density particles as well as large and small

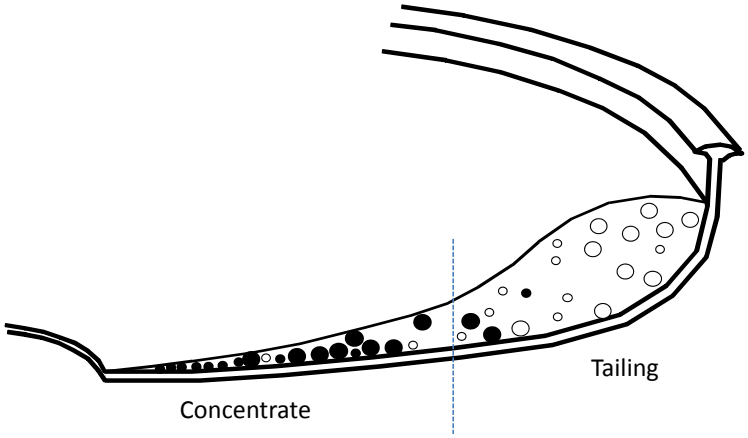

Figure 2.12: Cross sectional profile of a spiral depicting the products from Figure 2.11. (● = high-density particle, ○ = low-density particle, ■ = water concentration)

particles. The ratio of water to solids (particles) is an important parameter since the water acts as the suspension 'space' in which the separation of the particles occurs. Figure 2.14 depicts different water to solid ratios on the spiral, also referred to as solids concentration. High solids concentration limits the suspension 'space' in which separation can occur and hinders effective separation. High solids concentration could cause turbulence that hinders separation, but reduced throughput capacity is the greater concern when solids concentration is reduced. If the amount of water increased and solids loading remained the same, it might exceed the volume capacity of the trough and spill over the side. The general trend is that spiral separation efficiency is more sensitive to increased solids concentration compared with reduced solids concentration.

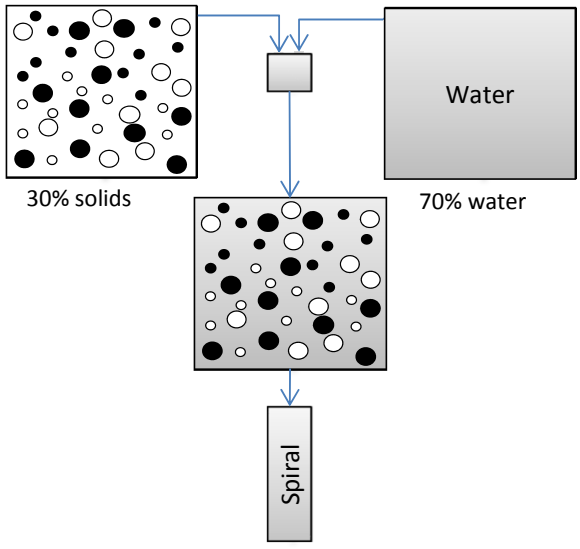

Figure 2.13: Wet separation with water. (● = high-density particle, ○ = low-density particle. ■ = water concentration)

2.2.3 Basic Separation Mechanism

The combination of the different forces that acts on particles in the spiral causes high-density particles to move to the inside of the trough and the lower density particles to the outside. High-density particles settle rapidly and come into contact with the spiral surface. Due to surface

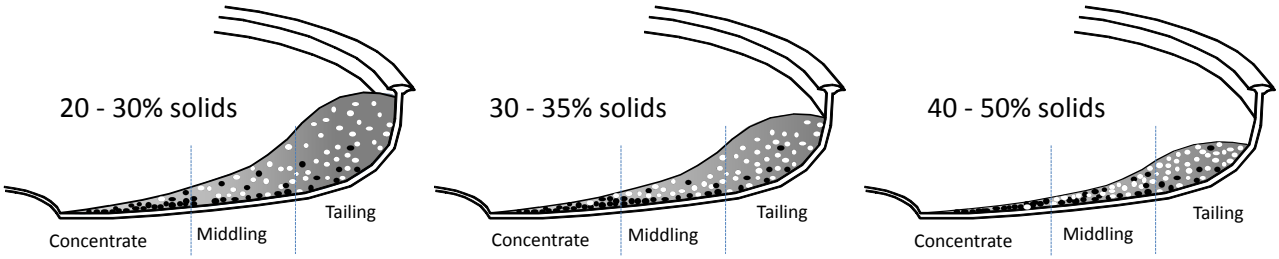

Figure 2.14: Influence of solids concentration on flow profile. (Constant solids throughput (t/h), varying water flow rate.)

friction the particles slow down and move to the inside of the trough. Low-density particles take longer to settle out and remain in suspension due to rapid fluid flow. These particles are pulled towards the outside of the trough by centrifugal force. Figure 2.15 shows the different flow patterns and particle segregation resulting in the three product streams. The adjustable splitter at the end of the spiral trough is positioned to achieve different mass flow rates to the different product streams with the required mineral recovery and product grade. The product splitter box (Figure 2.16) at the trough exit typically divides the mass on the profile into three streams. The high-density-rich stream is typically called concentrate if the high-density particles contain the mineral of economic value. The outside of the trough where the bulk of the water is transported together with the low-density particles is typically called the tailing. The stream that is between the concentrate and the tailing is called the middling. This stream is usually a mixture of the low and high density particles which will require reprocessing. Figure 2.17 shows particle segregation in the production environment with the heavy mineral particles reporting as a black band on the inside of the trough. Ultra-fine particles, also called 'slimes' (less than 10 µm in diameter) are mixed fairly homogeneously in the water due to turbulence and do not separate out.

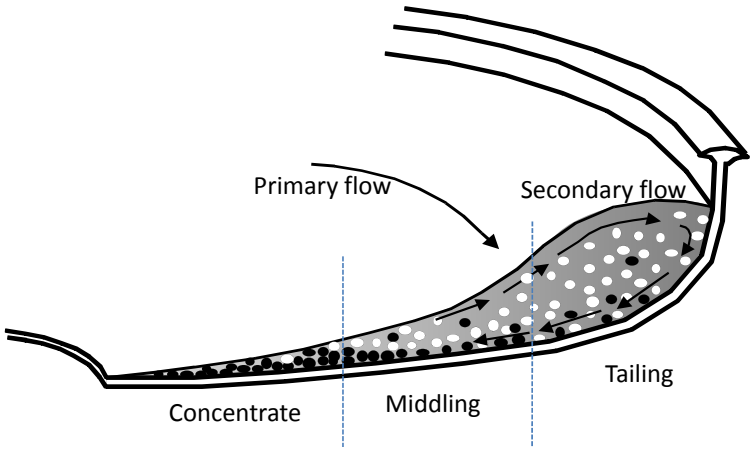

Figure 2.15: Cross sectional profile demonstrating separation mechanism and water profile. (● = high-density particle, ○ = low-density particle, ■= water concentration)

2.2.4 Forces

There are multiple flow regimes present at the different trough positions on the spiral, which implies varying forces that particles experience as they proceed down the spiral. The work done by (Kapur and Meloy 1998) suggests rough estimates for the five principal forces involved,

Figure 2.16: Example of a product splitter box - concentrate on inside for high-density valuable product. (Mine Engineer 2014)

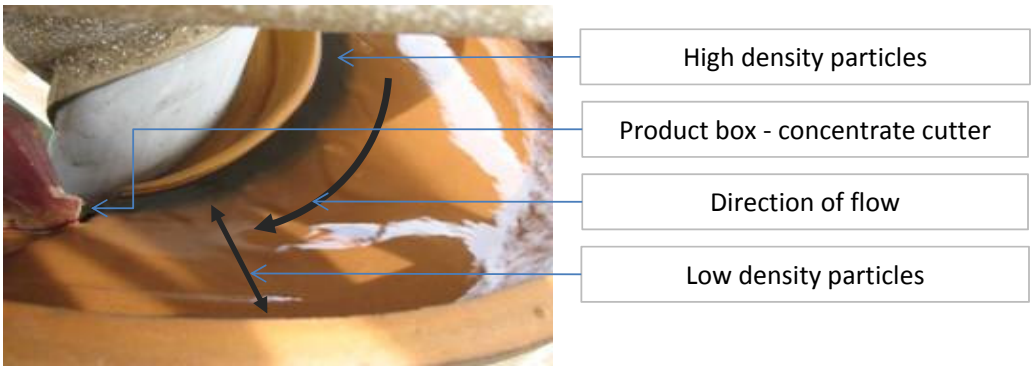

Figure 2.17: Top view of material on spiral trough.

namely gravity, centrifugal, hydrodynamic drag, lift and friction forces. Equations 2.1 to 2.5 show the formulae for these forces.

Gravity is the downward force as a function of the size and density of the particle, considering it is submerged in a liquid, and a buoyancy force is working upwards. Refer to Equation 2.1, Figure 2.18 and Figure 2.19 for a description of the gravity force.

Centrifugal force is significant due to the fast and tightly turning flow on the spiral. The force is dependent on particle mass and velocity as well as distance from the centre column. Refer to Equation 2.2.

Drag force is exerted on the particle due to the fluid flow and pressure differences within the fast moving liquid. It is a function of particle density and volume as well as the depth of flow as given by (Allen 1982). Drag force is a result of the primary and secondary flow as indicated by Figure 2.15. Refer to Equation 2.3.

Lift force is a result of secondary fluid flow in a radial direction to the primary downward spiral flow. Lift forces assist in loosening the particle bed which assists with particle separation. A first order estimation is to relate lift force directly to the drag force of the particle. Refer to Equation 2.4.

Friction force is the resistance to motion of the particle on the spiral trough. This force is proportional to the sum of all the normal components (downward and perpendicular to horizontal plane) of the forces acting on the particle. The constant is a function of the dynamic friction under water, but is similar to the static friction under water (Allen 1982). Refer to Equation 2.5.

The following three important observations were made by Kapur and Meloy (1999) after evaluating the sensitivity of the different force equations.

1. With the exception of gravity force, the other forces are strongly dependant on spiral geometry.
2. The magnitude of the gravity force is comparable to the drag and centrifugal forces for the particle size ranges normally processed on spirals.
3. It is not the magnitude of the individual forces but the rate of change with particle size, particle density and radial position that determines the efficiency of separation on spirals.

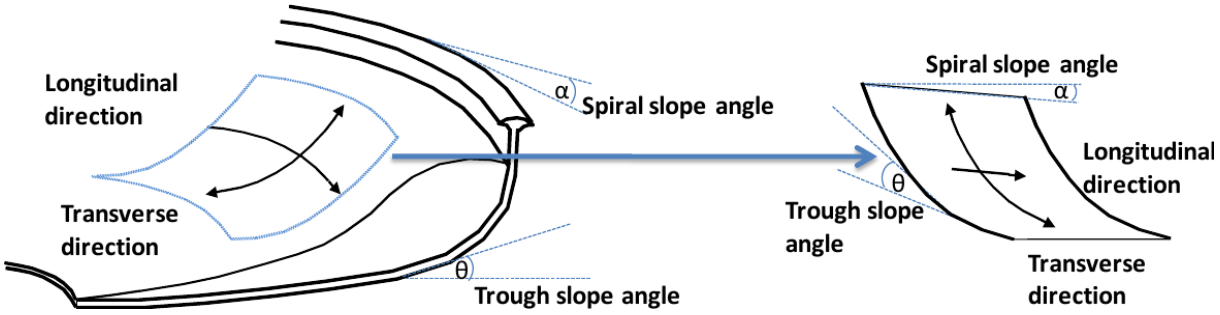

Figure 2.18: Flow directions and different planes for force equations. (Blue block on left is presented on the right to demonstrate different force angles.)

Equations 2.1 to 2.5 present the mathematical formulae for the five main forces involved in spiral separation (Kapur and Meloy 1998).

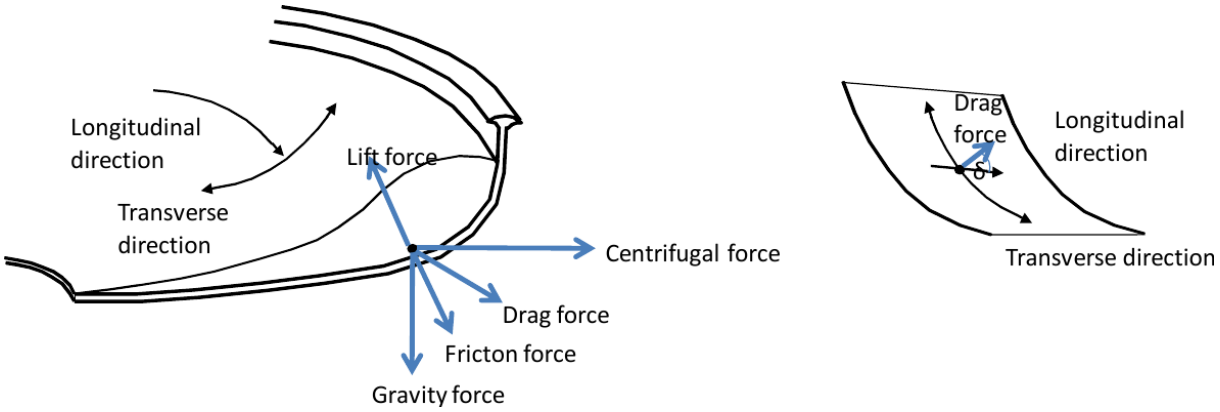

Figure 2.19: Different forces that influence a particle during spiral separation.

$$F_g = \frac{\pi}{6} d^3 g(\sigma - \rho) \qquad (2.1)$$

$$F_c = \frac{\pi}{6} \frac{d^3 v^2 (\sigma - \rho)}{r} \qquad (2.2)$$

$$F_d = \frac{\pi}{4} \rho g h d^2 \sin\alpha \qquad (2.3)$$

$$F_l = k_l F_d \qquad (2.4)$$

$$F_f = k_f F_N \qquad (2.5)$$

d	particle diameter
F_c	centrifugal force
F_d	drag force
F_f	frictional force
F_g	gravitational force
F_l	lift force
F_n	normal component of all relevant forces
g	gravitational acceleration
h	depth of flow
k_l	constant for lift (set as 0.33)
k_f	constant for friction (set as 0.5)
r	radial distance from column centre
v	velocity
α	spiral slope angle
ρ	liquid density
σ	density of particle submerged in a liquid

2.2.5 Fluid Flow

Spirals demonstrate the most complex flow regime of all gravity separators available. There are two important fluid flow phenomena. The first is that the water on the outer concave wall of the trough exceeds that at the inner convex surface by an amount called super-elevation (Kapur and Meloy 1998). This is referred to as the primary flow or flow in the longitudinal direction as indicated in Figure 2.20. The second phenomenon is a transverse secondary circulation in the form of a flattened helical spiral that moves forward in a corkscrew fashion (Kapur and Meloy 1998). This is also referred to as the secondary flow as illustrated in Figure 2.20.

2.3 Spiral Application

This section focuses on where and how spirals are applied in the mineral processing industry.

2.3.1 Importance

The mineral sands industry followed by the iron ore industry is processing the highest tonnages through spiral beneficiation. Some coal and chromite processing are also done with spirals. Coal processing is the only example where the product of economic value is on the outside

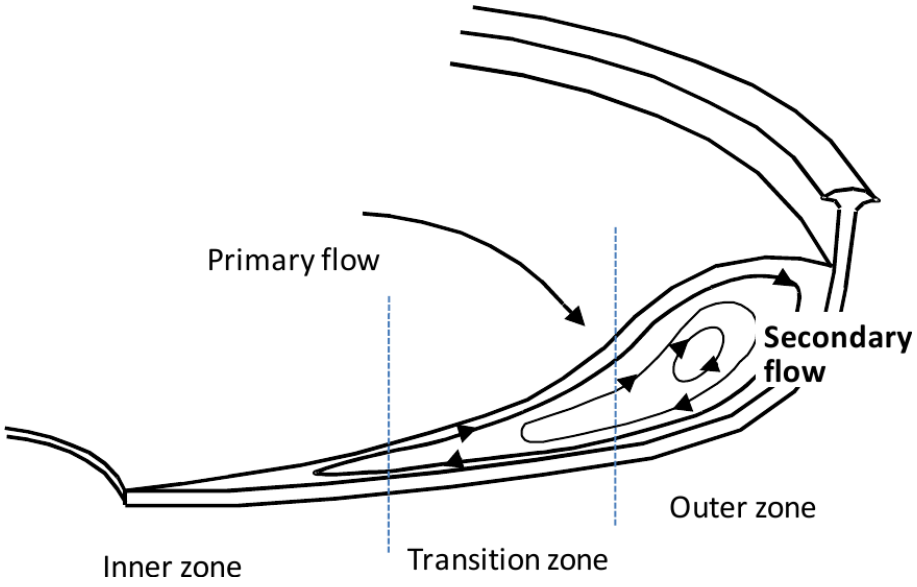

Figure 2.20: Primary and secondary fluid flow on the spiral trough.

of the spiral trough due to the lower density. The spiral troughs differ significantly between coal and other mineral processing industries and cannot be used interchangeably. The iron ore, mineral sands and chromite industries have used similar profiles in the past, but recently spiral developments have seen more specialised spirals tailored for specific commodities.

2.3.2 History

The first commercial spirals were operated in 1943 to concentrate chromite bearing sands (Thompson 1969). Spirals have evolved over the last half century from a generically designed unit to the present status as sophisticated devices with a high level of design optimisation (Holland-Batt 1995). Wright, Richards, and Cross (1986) reported that proof of this sophistication is evident in the fact that in the same period valuable mineral feed grades (titanium sands) diminished from 50 % to 0.5 %, while over the same period the real value of the product has generally dropped. However, over time these sophistication improvements became progressively more subtle following the law of diminishing gains (Richards and Palmer 1997). The focus of the latest developments was on increasing capacity of units and widening the range of application, making units more efficient on both larger and smaller particles (Richards et al. 2000). According to Henderson and MacHunter (2003) the spiral still remains competitive to this day since it is regarded as the most economical option for large fine circuits due to their relatively low operating cost and low capital cost.

2.3.3 Particle Size Range

Different spirals can treat particles as coarse as 2 mm in coal beneficiation circuits, and as fine as 0.05 mm when processing iron ore and mineral sand. Each particle size and particle density range application requires a different spiral geometry. The spiral is generally more efficient in separating near sized particles as opposed to a wide size distribution range. In a free settling environment a large low-density particle will compete with a small high-density particle since they have similar terminal velocities. Although the separation environment on the spiral is more complex than free settling there are also particle size effects that impact separation efficiency. Fine high-density particles are usually recovered best by the spiral.

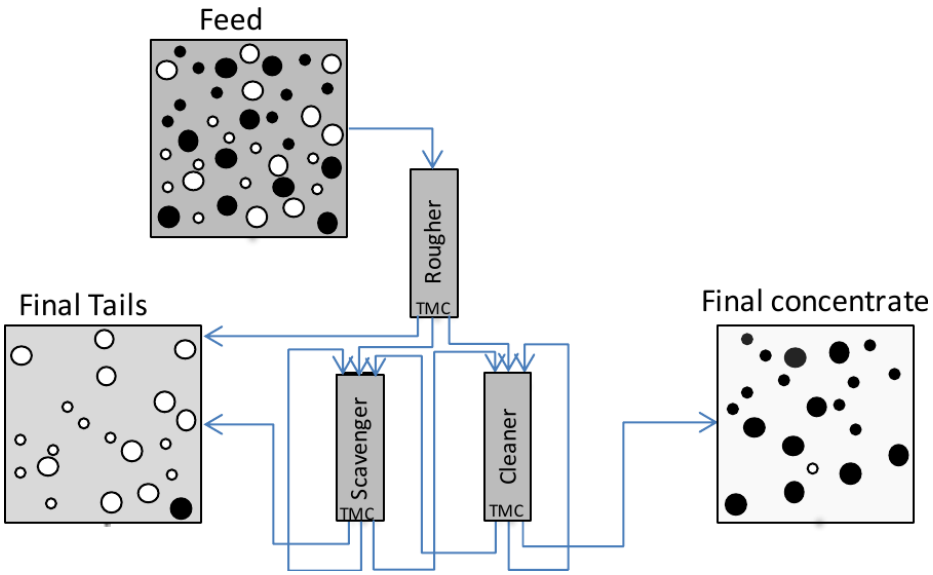

Figure 2.21: A typical three stage spiral circuit configuration. (● = high-density particle, ○ = low-density particle. ■ = water concentration, T=tailing, M=middling, C=concentrate)

2.3.4 Multiple Stages of Separation

The spiral has reasonable separation efficiency, but requires several separation stages to achieve above 90 % recovery of high-density particles and above 90 % concentrate grade of the high-density particles under normal operating conditions and with normal feed material. The primary separation stage is usually referred to as the rougher stage, where most of the valuable mineral is removed from the bulk mass flow. The scavenger stage involves the separation of high-density particles that were trapped in the middling portion of the primary separation stage. The cleaner stage involves the removal of low-density particles from the rougher stage concentrate. There can be up to six different stages of separation and many different flow-sheet configurations. Recirculation of the middling stream on the spiral itself is commonly practised, but has operating risk with material build-up and eventual circuit overload. The most common configuration is a four stage separation in which the concentrate is sent to a re-cleaner circuit. This it is dependent on the concentrate requirements from the next stage processing. Figure 2.21 illustrates an example of a typical three stage circuit.

Different spiral troughs allow for different feed grades. For example, cleaner spiral and scavenger spiral have different trough designs since the flow patterns differ significantly because of large differences in concentration of high-density particles in the feed. The general trend is that the higher the concentration of high-density particles, the lower the throughput must be to achieve acceptable recoveries.

2.3.5 Spirals in Combination with Other Technologies

Spiral circuits are in many cases complemented with other technologies to improve the separation efficiency of the total circuit. To name a few examples fine screening can be used to remove large low-density particles, up-current classification can be used to remove fine low-density particles in the final concentrate and magnetic separation can be used to remove magnetic non-valuable minerals. On the other hand, spirals can be used as complementary technologies in other circuits to remove problematic low-density particles quickly and cost effectively such as in flotation circuits or magnetic separation circuits where the problematic low-density material has similar magnetic or surface characteristics to the valuable product.

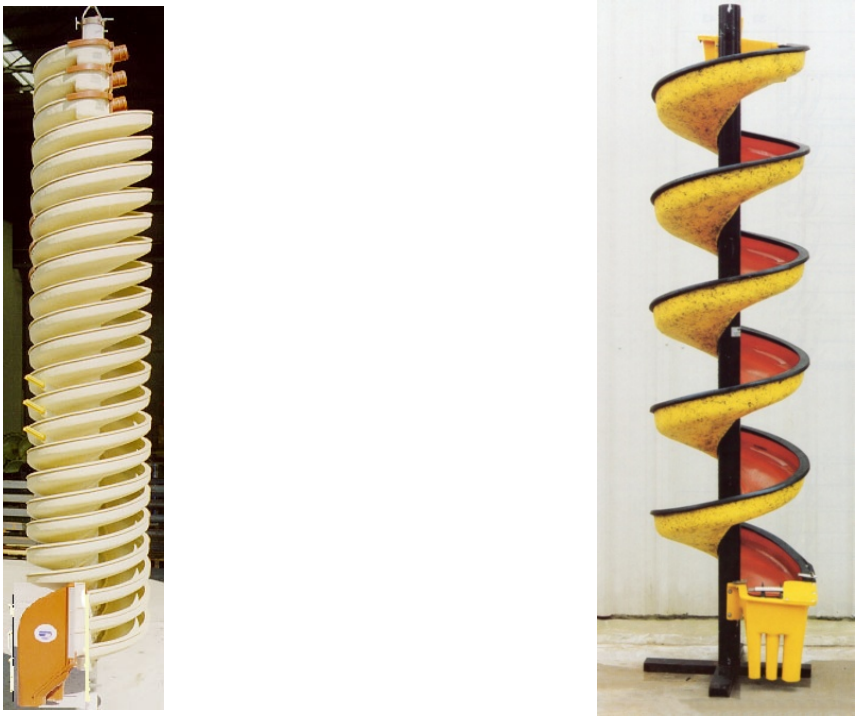

(a) (b)

Figure 2.22: Comparison of a three start (a) and single start spiral (b). (Mineral Technologies 2014; Mine Engineer 2014)

2.3.6 Typical Spiral Throughput

A spiral has a low operating processing capacity and ranges from as low as 500 kg/h up to 5000 kg/h of dry solids per single trough depending on the material being separated as well as the operating conditions. Different spiral troughs allow for different throughput capacities. Recent spiral development has seen higher throughput capacities being achieved of up to 7000 kg/h of dry solids. The general trend is that higher throughput volume will lower the separation efficiency. The most common spiral throughput capacity is around 2000 kg/h of dry solids per start.

2.3.7 Spiral Unit Configuration

A single spiral trough is referred to as a start, which is a single feed entry point. The spiral trough has large spaces in between the different turns, which allows for more than one start on a single centre column. Up to four starts can be accommodated on one column, but will allow little to no space to visually inspect the flow pattern on the different troughs within the column. The standard operating configuration is three starts on a single column. Figure 2.22 illustrates the difference between a single start and triple start spiral. The splitter position at the trough exit point for a triple start spiral column will be the same for all the starts on the column. The purpose of the multiple starts on one column is to maximise the processing capacity per unit footprint area.

The combination of many columns with a feed distribution unit to the different spiral starts is referred to as a spiral bank. A spiral bank is usually designed and sold as a distinct unit fitted with a concentrate, middling and tailing launder at the bottom of the bank that combine the concentrate, middling and tailing streams from each column. Figure 2.23 provides examples of different spiral bank designs.

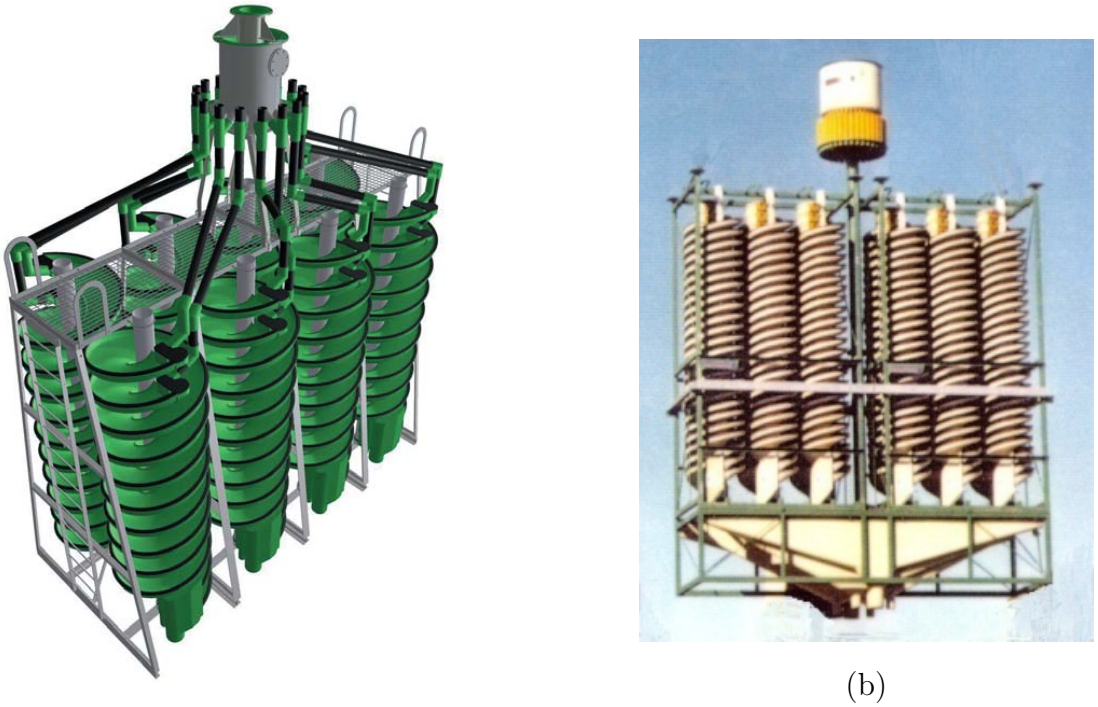

(a) (b)

Figure 2.23: Different spiral bank designs. (a) Eight columns and 16 double starts. (Multotec 2014a) (b) Different product launder at the bottom of the spiral bank - 12 columns and 36 starts. (Mineral Technologies 2014)

2.3.8 Advantages of Spirals

Spirals have no moving parts and the energy required for separation is provided by the water flowing down the trough. This implies that spirals themselves have low operating cost. The pumping of slurry to the feed distributor is the only higher maintenance as well as energy consuming cost component. Spirals don't require any reagents in the slurry to enhance separation. Normal process water can be used for slurry makeup as long as the ultra-fines (slimes, particles below 10 µm) content is below 5 % and it doesn't contain high amounts of residual flocculent or other chemicals that could influence medium viscosity. Some spiral separation applications use sea water. To ensure reasonable water quality and high water recovery, upfront desliming cyclones and thickeners are usually included as part of the spiral circuit.

Spirals don't require operator control other than ensuring that all the splitters on a specific spiral bank are in the same position. Spirals furthermore need to be clean and free from roots and other organic material build-up at the splitter boxes, as well as at intermediate splitters. Since the spiral is very simple in its operation it, does not require a high level of operator skill, which will benefit operating cost further.

Spirals can last up to 15 years and in some cases more than 25 years depending on the abrasiveness of the material being processed. As the surface is abraded away the spiral profile is altered which could influence separation efficiency negatively. The normal life of a spiral is usually 10 years, as conservatively quoted by spiral manufacturers. This low life cycle cost makes it competitive when comparing to capital investments of alternative density separation equipment.

The spiral is fairly forgiving with regards to feed variation. Small variations in solids throughput can be compensated for by the addition or removal of water through simple process control to ensure steady solids concentration on the spiral. Large variations in solids throughput can justify the pumps and control valves, allowing the shutting down or opening of entire spiral

banks.

The combination of different spiral profiles to ensure high separation efficiencies for the different feed grades in each stage of the process, with re-circulating loads giving particles more opportunity to separate, allows for relatively high separation efficiencies.

In summary, the spiral is simple to operate, operationally robust, relatively compact, fairly efficient through multiple processing stages and cost effective from a capital and operating cost point of view. Spirals are here to stay.

2.3.9 Disadvantages of Spirals

Since the spiral (single trough) is a low capacity unit it requires multiple starts, which requires a large number of feed distribution lines. This could easily result in fluctuating feed conditions. In some cases up to 36 spiral starts originate from a single distributor. Any flow variation in the pipe will result in a distribution variation upon exit, which causes inconsistent feed to the different spiral starts. This necessitates special design and operator vigilance surrounding spiral distributors. The length of the distributing lines and height difference between the spiral start entry and distributor exit point should be similar. Large differences result in different feed pressures, which will negatively impact distribution consistency.

A further disadvantage of multiple low capacity units is that it is difficult to pick up which unit is not performing well, since the inefficiency will be blended in with the performance of the other units. For example, if one spiral column splitter is completely open to allow all material into the concentrate, it will reduce the grade of the combined concentrate significantly. Since standard spirals are not equipped with sensors, such as proximity indicators on splitters, it can be months before the specific problem is picked up by routine spiral evaluation. Operator vigilance is again required and a low level of process control on spirals might address this issue as well. In a nutshell, although the spirals don't require a high degree of operator skill it requires a high degree of operator observation to ensure consistent spiral separation performance.

Large numbers of low capacity units require large footprint area and results in large buildings. Due to the pipe network underneath the spiral banks and minimum flow angles required, the buildings are high, which requires more structural strength resulting in more cost. One of the ways that this shortfall is addressed is to put more starts per column, four starts instead of three. This makes it nearly impossible for the operator to view the trough in order to confirm that the flow is still acceptable. Another way is to increase the capacity per spiral start through different trough designs. Some recent developments make use of a rougher spiral on top of a scavenger and cleaner spiral in an effort to reduce the footprint but this will increase building height. It will further increase the necessity for enhanced feed preparation.

A spiral circuit's performance is dependant on feed preparation. The lower the ultra-fines content that could influence medium viscosity, the better the spiral will perform. The control of the solids concentration is also crucial. Once the slurry is on the spiral, nothing can be done to improve separation. In many cases spiral circuits are inefficient because the focus was placed on optimising splitter position instead of optimising feed preparation control through density and flow control from a correct density tank containing a minimum amount of ultra-fines. Although the spiral is simple in operation, feed preparation control is more advanced and costly from a capital and operating cost point of view.

2.4 Measurement of Spiral Separation Performance

A solid understanding of the methods of measuring spiral performance is required before the factors influencing separation performance can be discussed. This section aims to introduce the different separation attributes commonly used for spiral concentrators in the mineral processing

industry. The separation envelope, or extremes, is used to explain each of the attributes. A theoretical example is used for the sake of simplicity followed by a test-work data example to clearly illustrate the meaning of the data, the methods of data gathering and the methods of data presentation.

2.4.1 Separation Attributes

There are four main separation attributes generally referenced in literature using different terms. For the purpose of this document they are termed yield, recovery, grade and efficiency. Each attribute and the relationship with the others are discussed separately and supported with the necessary figures to illustrate the application and calculations clearly.

Three separation scenarios are discussed, namely, typical separation, ideal separation and zero separation. Figure 2.24 demonstrates the three scenarios with the help of simplified cross sectional spiral profiles. The ideal and zero separation scenarios are purely theoretical, but they are important since they define the operational window for each of the different separation attributes to be discussed.

Consider the theoretical case where a cross section of a spiral trough is cut and intersects 100 particles of similar volume at an instant of time as shown in Figure 2.24. There are only two types of mono-mineral particles present, namely high-density particles and low-density particles. Please note that a real cross section can involve billions of particles with a wide density range. For simplicity of demonstration, the number of particles is used for calculation instead of masses. The spiral trough section was divided into three process streams, namely, concentrate, middling and tailing, which would be the function of a splitter at the end of the trough.

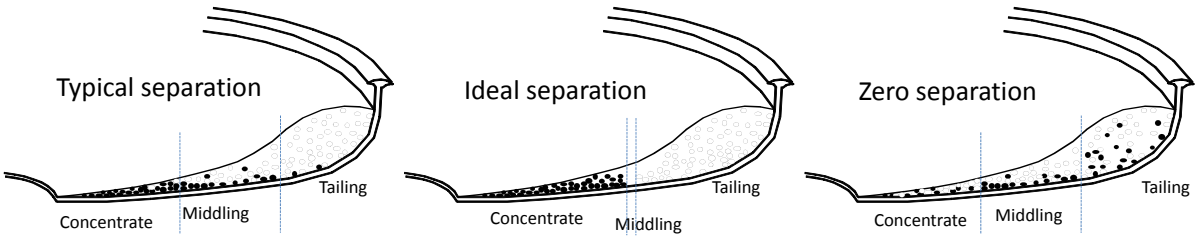

Figure 2.24: Cross sectional profile for the three separation scenarios. (Note: Particles are not according to scale and only for illustration purposes)

The typical separation example in Figure 2.24 is where most of the high-density particles moved to the inside of the trough and most of the low-density particles moved to the outside of the trough due to forces discussed in the earlier sections of this chapter. There are still some particles that are misplaced due to particle crowding and entrapment since the particles were only in this separation environment for a limited time. Because of the inefficiency of the first pass, the middling process stream is re-circulated on the same spiral or sent to another spiral.

In the ideal separation case there is infinite separation time and no operational hindrances. There is therefore no need for a 'mixed' middling stream as this stream contains zero particles. The zero separation case is where no separation takes place and the different particles are distributed representatively across the entire trough profile. At any given point on the trough the composition is similar to that of the feed. For the purposes of explaining the principles of the different separation attributes, a particle analysis is performed on the 100 particles of the typical separation scenario from Figure 2.24. Figure 2.25 is the result of this analysis.
The feed grade is 40 % high-density particles and the spiral is able to upgrade the high-density particles to 92 % grade in the concentrate. A high-density mineral particle recovery of 60 % to

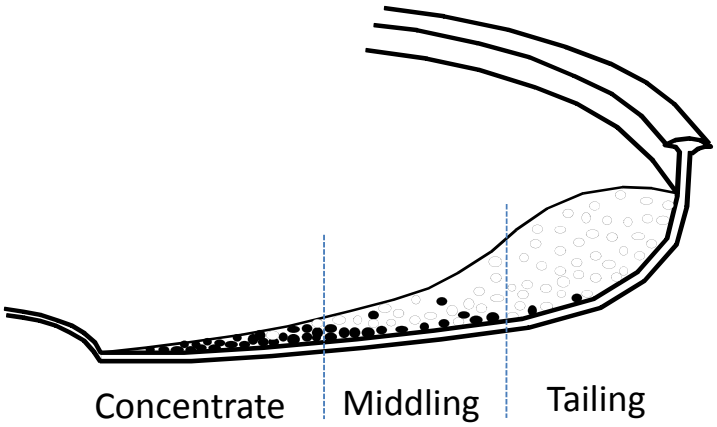

Particle amount	Concentrate	Middling	Tailing	Total
Black Hi	24	14	2	**40**
White Lo	2	17	41	**60**
Fractional Yield%	**26**	**31**	**43**	**100**
Cumulative Yield%	**26**	**57**	**100**	**NA**

Fractional Recovery%	Concentrate	Middling	Tailing	Total
Black Hi	60	35	5	**100**
White Lo	3	28	68	**100**

Cumulative Recovery%	Concentrate	Middling	Tailing
Black Hi	60	95	100
White Lo	3	32	100

Fractional Grade%	Concentrate	Middling	Tailing
Black Hi	92	45	5
White Lo	8	55	95
Total	**100**	**100**	**100**

Cumulative Grade%	Concentrate	Middling	Tailing
Black Hi	92	67	40
White Lo	8	33	60
Total	**100**	**100**	**100**

Figure 2.25: Yield, recovery and grade data for typical separation scenario. (Hi = high density, Lo = low density)

the concentrate is achieved which represents 26 % yield.

2.4.2 Separation Efficiency

The separation attributes of yield, grade and recovery are demonstrated and discussed in the previous section. Separation efficiency is a parameter that considers all three of these attributes.

In any separation process the efficiency of the unit operation drives the economics of the business in which it is utilised. The ideal is to achieve a 100 % recovery of the valuable particle to the concentrate at 100 % grade in the concentrate, referring to the 'ideal separation' in Figure 2.24. No separation process is perfect; referring to 'typical separation' Figure 2.24, the recovery of high-density particles to the concentrate is 24 out of the 40 particles in the feed (60 % recovery). The concentrate grade is 24 out of the 26 particles (92 % grade). The equation for separation efficiency commonly used in literature (Holland-Batt 1990), as well as in this study, is shown in Equation 2.6 and demonstrated in Table 2.1, utilising the same numbers mentioned in Figure 2.25.

$$E = \frac{r - y}{1 - f} \qquad (2.6)$$

E	separation efficiency
r	recovery to concentrate
y	yield to concentrate
f	feed grade

Table 2.1: Separation efficiency for three scenarios.

Typical:	$E = \frac{r-y}{1-f} = \frac{\frac{24}{40} - \frac{26}{100}}{1 - \frac{40}{100}} = 57\,\%$
Ideal:	$E = \frac{r-y}{1-f} = \frac{\frac{40}{40} - \frac{40}{100}}{1 - \frac{40}{100}} = 100\,\%$
Zero:	$E = \frac{r-y}{1-f} = \frac{\frac{13}{40} - \frac{33}{100}}{1 - \frac{40}{100}} = 0\,\%$

2.4.3 Plotting Separation Attributes

Figure 2.26 illustrates the first of three of the most commonly used graphs utilised in literature, the cumulative-recovery vs yield plot. The following important discussion points refer to this figure:

- The grey dotted vertical lines represent the total particle recovery to the different process streams as indicated by the cross sectional profile.
- The recovery line of the high-density particles is presented by the bold black line and the low-density particles by the bold white line. The first point on the black bold line represents 26 % yield that is cut to concentrate. In this fraction 60 % of the high-density particles is recovered. The concentrate grade cannot be read off from this graph, but it can be seen that 3 % of the white low-density particles is also recovered which implies a grade lower than 100 %.
- The ideal separation line is presented by the dotted white and black line, which implies that there are only two cuts and the middling fraction contains zero particles. This separation situation corresponds with the middle picture in Figure 2.24. The solid black line connecting the origin and (100,100) point is the zero separation condition. If no separation occurs the composition of the different process streams is similar to the feed composition and the unit made no distinction on density.

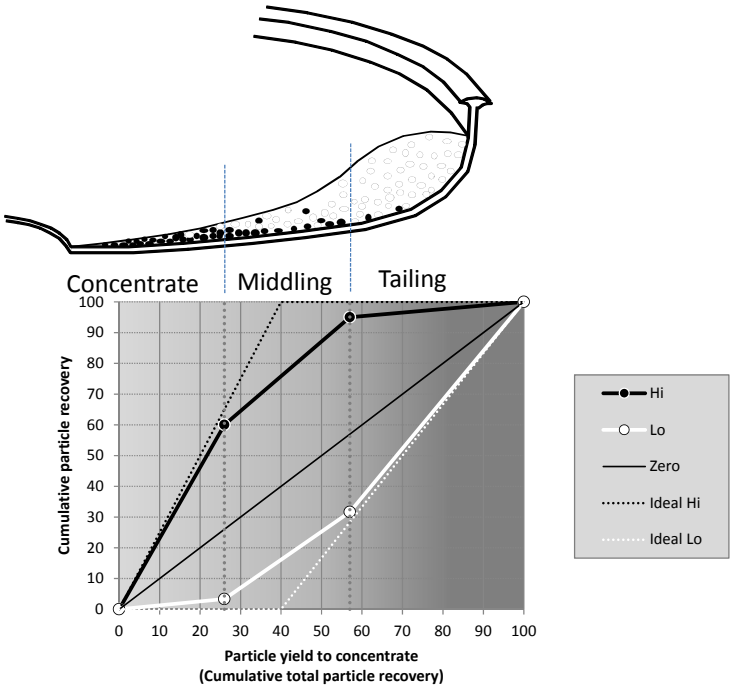

Figure 2.26: The cumulative-recovery vs yield relationship for the typical separation scenario. (Hi = high density, Lo = low density, Zero = zero separation)

Figure 2.27 illustrates the second widely used graph, the cumulative grade vs yield relationship. The same separation conditions as discussed above are considered in plotting the grade curves.

In Figure 2.27 the typical separation condition is depicted by the bold white and black lines. Considering an example where 40 % of particles are cut to concentrate: although there is no test-work point, the line allows for interpolation. At 40 % particle yield (usually mass yield), the resulting product grade in the concentrate is 80 % high-density particles. Since it is only a two density type example, the remaining 20 % is low-density particles. As more particles are cut to concentrate, it equals the original feed composition, which is 40 % high-density and 60 % low-density particles, since the entire stream is 'cut' to the concentrate.

The ideal case is presented by the dotted black and white lines and the zero separation condition is presented by the two horizontal solid lines that correspond with the feed grade. The grade starts at 100 % high-density particles and 0 % low-density particles at 0 % yield and decreases as low-density particles dilute the concentrate. If all the high-density particles are diluted with all the low-density particles it results in the original feed grade. In these theoretical examples all the ideal lines are straight. For a real separation case the ideal lines will most likely be curved following an exponential decay relationship.

If no separation takes place the grade will remain the same as the feed grade. Ideal separation will result in 100 % high-density mineral until it is all isolated at 40 % yield to concentrate after which it will be systematically diluted to the original feed grade condition in the remaining 60 % yield (particle or mass recovery).

Figure 2.28 illustrates the third graph that is often utilised in literature, the efficiency vs yield relationship. The maximum separation efficiency is achieved between 30 and 60 % yield.

The efficiency in Figure 2.28 was calculated using Equation 6. The example used to demonstrate the above-mentioned calculations and principles makes use of only two particle types, single high density and single low density. The most efficient separation of the high-density particles will imply the most efficient separation of the low-density particles, therefore these lines will be exactly the same for both particles and there is no need to plot the low-density line. The ideal separation line reaches the 100 % efficiency point at 40 % mass recovery where

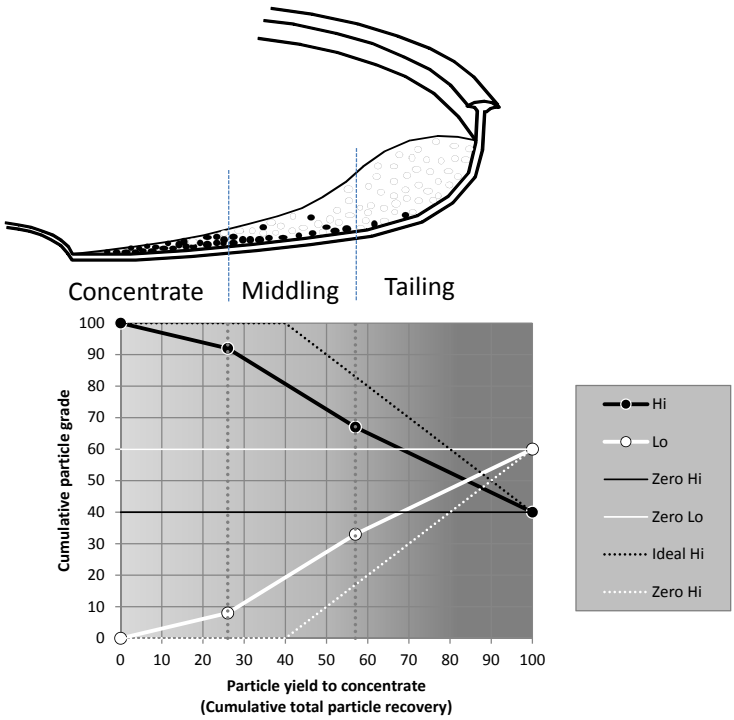

Figure 2.27: Cumulative particle grade vs yield for the typical separation scenario.

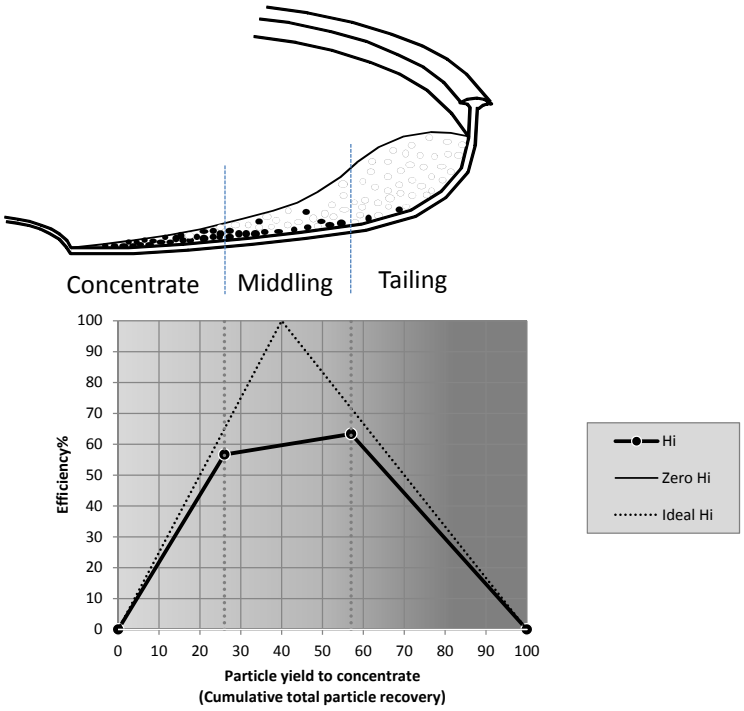

Figure 2.28: Description of the efficiency vs total particle yield.

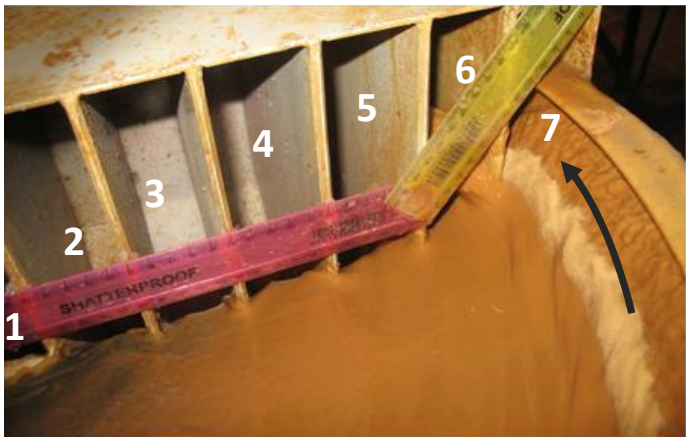

Figure 2.29: A 7 cut mouth-organ. (Inside of trough on the left indicating the darker high-density particles, outside of trough on the right with a foam band on the water, flow direction into box - indicated by arrow.)

optimum separation theoretically takes place for both high and low density particles. Zero separation condition results in the line lying on top of the x-axis.

2.4.4 Mouth-organ Benefit

A mouth-organ is a product splitter box with multiple product cut points fitted at the spiral trough exit. In other words it divides the process stream into more than the three typical process streams. Figure 2.29 provides a real example of a fixed mouth organ that separates the spiral trough into 7 process streams. These mass streams are usually referred to as Cut 1 to Cut 7 and not the usual concentrate, middling and tailing. Cut 1 starts at the concentrate and Cut 7 ends at the tailing.

The benefit of this type of spiral trough sampling is that there are eight points instead of the normal four on the recovery, grade and efficiency curves. Eight points allow for smoother curves and better information on the crucial transition points. It is recommended that spiral profile efficiency comparisons are done with the use of mouth-organ sampling boxes. The smoother curve illustrates the efficiency differences clearly, otherwise the benefit of one spiral over another or effect of certain operating or design parameter could be lost through incorrect splitter position. The other significant benefit in using the mouth-organ during spiral separation performance testing, is that it removes the splitter position as a test variable. The smoother curve allows for more accurate interpolation around the crucial transition points. Figure 2.30 describes the naming and location of the 7 cuts (C1 to C7) and expresses the same data from previous example in a higher resolution format. Figure 2.31 displays the same data as in Figure 2.26, Figure 2.27 and Figure 2.28, but with more trough points resulting in higher resolution and smoother curves.

2.4.5 Standard Analytical and Data Presentation Techniques

This section describes the basic analytical methods followed by the data presentation methods that are typically applied in the mineral sands industry to describe and measure spiral separation performance. The detail of some of the terms is described in previous sections and some details will be discussed in the chapters to follow. Table 2.2 acts as a short description of the acronyms and abbreviations that are used in the section to follow. In the previous sections a theoretical case was used to illustrate the principals, while in the following sections real spiral data is used. The mass attributes, as demonstrated in Figure 2.32 from Table 2.2, are plotted

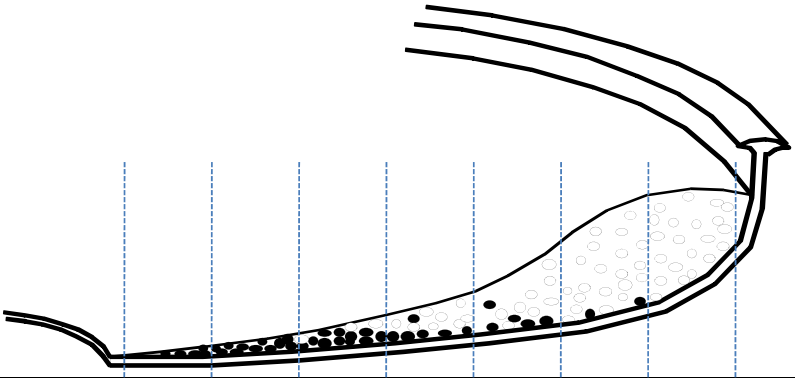

Particle amount	C1	C2	C3	C4	C5	C6	C7	Total
Black Hi	5	11	11	6	5	2	0	**40**
White Lo	0	0	3	8	8	20	21	**60**
Fractional Yield%	**5**	**11**	**14**	**14**	**13**	**22**	**21**	**100**
Cumulative Yield%	**5**	**16**	**30**	**44**	**57**	**79**	**100**	**NA**

Fractional Recovery%	C1	C2	C3	C4	C5	C6	C7	Total
Black Hi	13	28	28	15	13	5	0	**100**
White Lo	0	0	5	13	13	33	35	**100**

Cumulative Recovery%	C1	C2	C3	C4	C5	C6	C7
Black Hi	13	40	68	83	95	100	100
White Lo	0	0	5	18	32	65	100

Fractional Grade%	C1	C2	C3	C4	C5	C6	C7
Black Hi	100	100	79	43	38	9	0
White Lo	0	0	21	57	62	91	100
Total	**100**	**100**	**100**	**100**	**100**	**100**	**100**

Cumulative Grade%	C1	C2	C3	C4	C5	C6	C7
Black Hi	100	100	90	75	67	51	40
White Lo	0	0	10	25	33	49	60
Total	**100**	**100**	**100**	**100**	**100**	**100**	**100**

Figure 2.30: Yield, recovery, grade and efficiency for mouth-organ example.

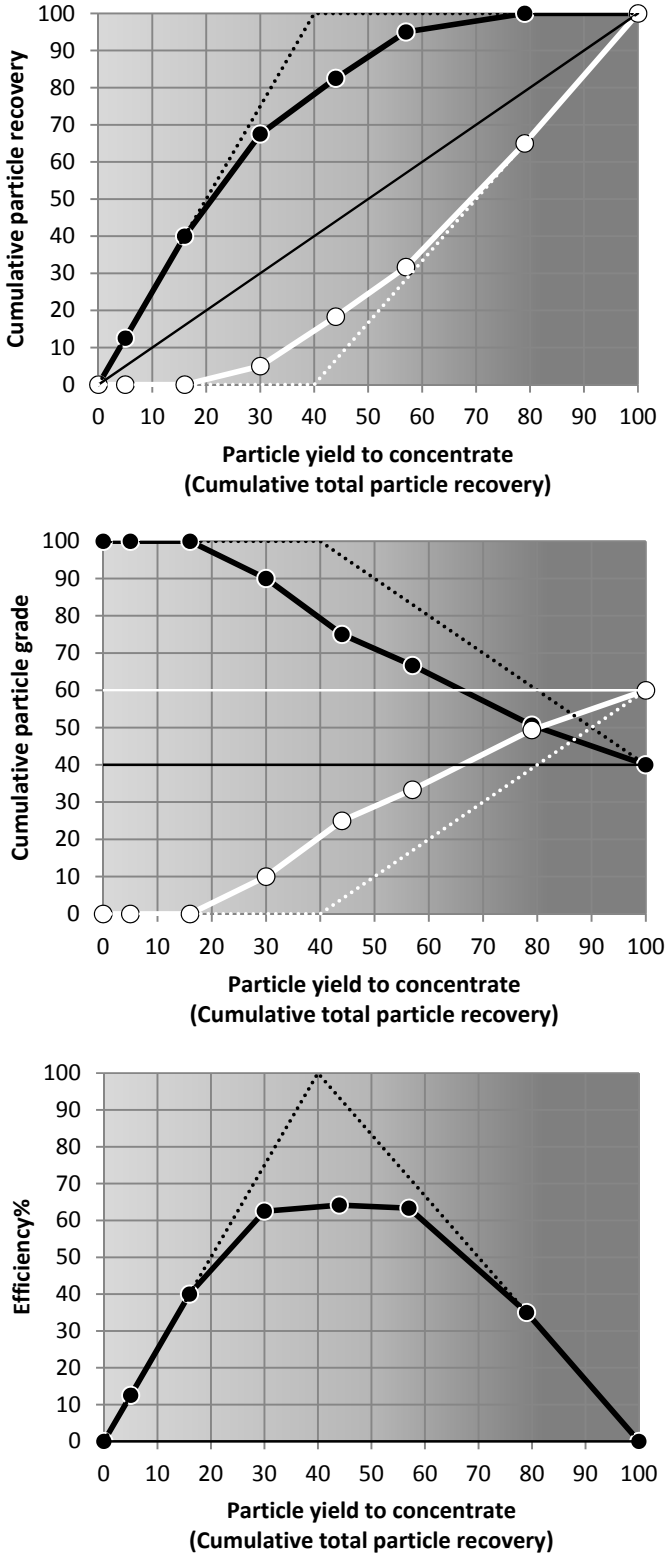

Figure 2.31: Yield, recovery, grade and efficiency data for seven mouth-organ cuts.

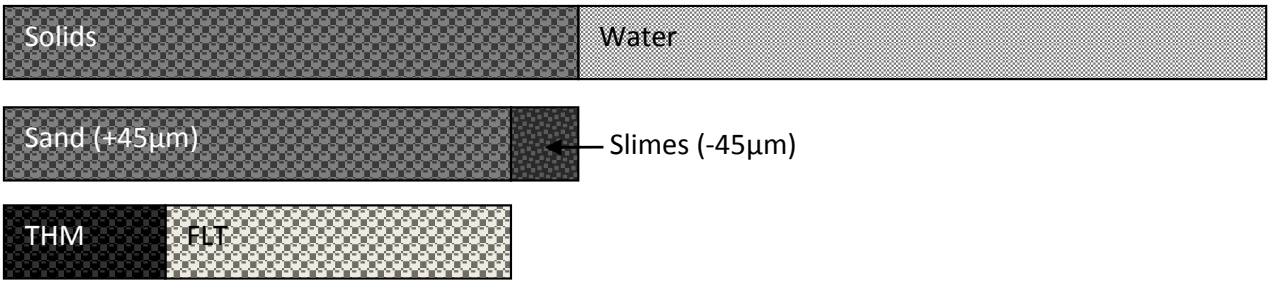

Figure 2.32: Diagram of the mass attributes from Table 2.2. (Note the bars above are not to scale and for explanation purposes only.)

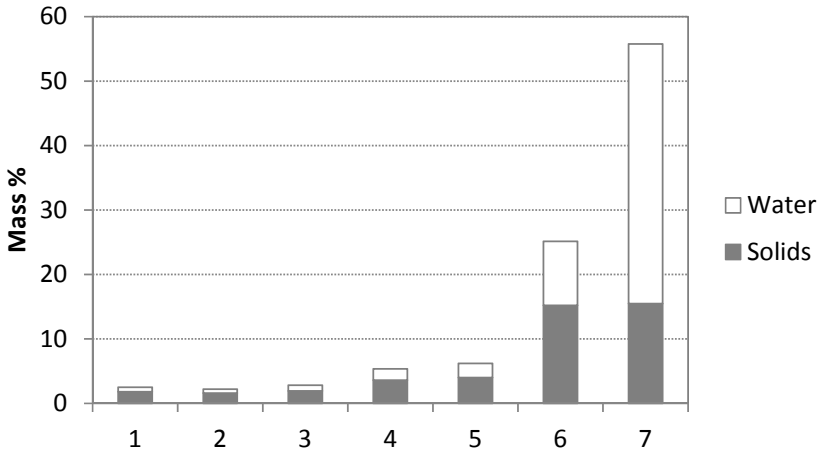

Figure 2.33: Distribution of water and solids across the spiral trough. (Number 1 to 7 on x-axis represent mouth-organ sampler mass cuts. Note the change in the x-axis)

in Figure 2.33, Figure 2.34 and Figure 2.35 show how they vary across the spiral trough as sampled by means of a mouth organ sample cutter.

Table 2.2: Standard terms for mass attributes used in the discussions to follow.

Term	Description
% Solids	Mass percentage of dry solids in mass of liquid (water) and dry solids combined. Includes THM, FLT and slimes and excludes water.
% Sand	Dry mass percentage of particles larger than 45 µm in all solid particles.
% Slimes	Dry mass percentage of particles finer than 45 µm in all solid particles.
% THM	Dry mass percentage of total heavy minerals (density greater than 2.98 g / cm^3) in all sand particles greater than 45 µm.
% FLT	Dry mass percentage of sand particles that floated on heavy liquid (density less than 2.98 g / cm^3) in all sand particles greater than 45 µm.

Figure 2.32 demonstrates how spiral feed is fractionated and demonstrates the three steps of sample analysis. The first step is to remove the water from the solids by decanting clear water after slimes have settled, and drying the mass to remove all moisture. The second step represents wet screening of the dried material on a 45 µm screen. The sand portion is dried again and a sink-float analysis is done on a representative portion of the sand fraction as step three. This mass fractionation or sample analysis divides the spiral into four mass streams, namely water, slimes, THM and FLT. The yield, recovery, grade and separation efficiency of each of these mass streams are shown in Figure 2.36, Figure 2.37 and Figure 2.38.

Figure 2.36 presents the mass data from Figure 2.33, Figure 2.34 and Figure 2.35 in a

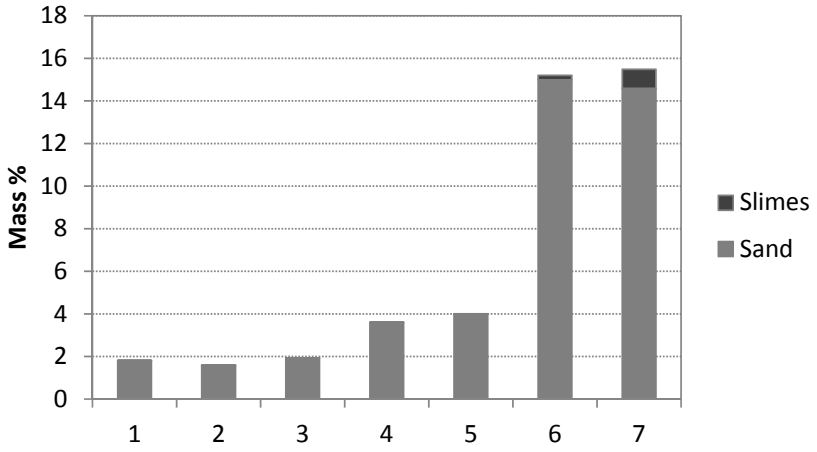

Figure 2.34: Distribution of sand and slimes across the spiral trough. (Number 1 to 7 on x-axis represent mouth-organ sampler mass cuts. Note the change in the x-axis)

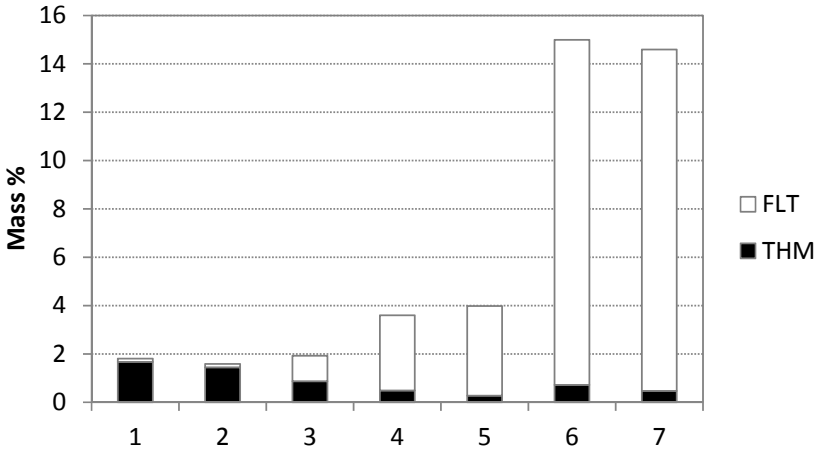

Figure 2.35: Distribution of THM and FLT across the spiral trough. (Number 1 to 7 on x-axis represent mouth-organ sampler mass cuts. Note the change in the x-axis)

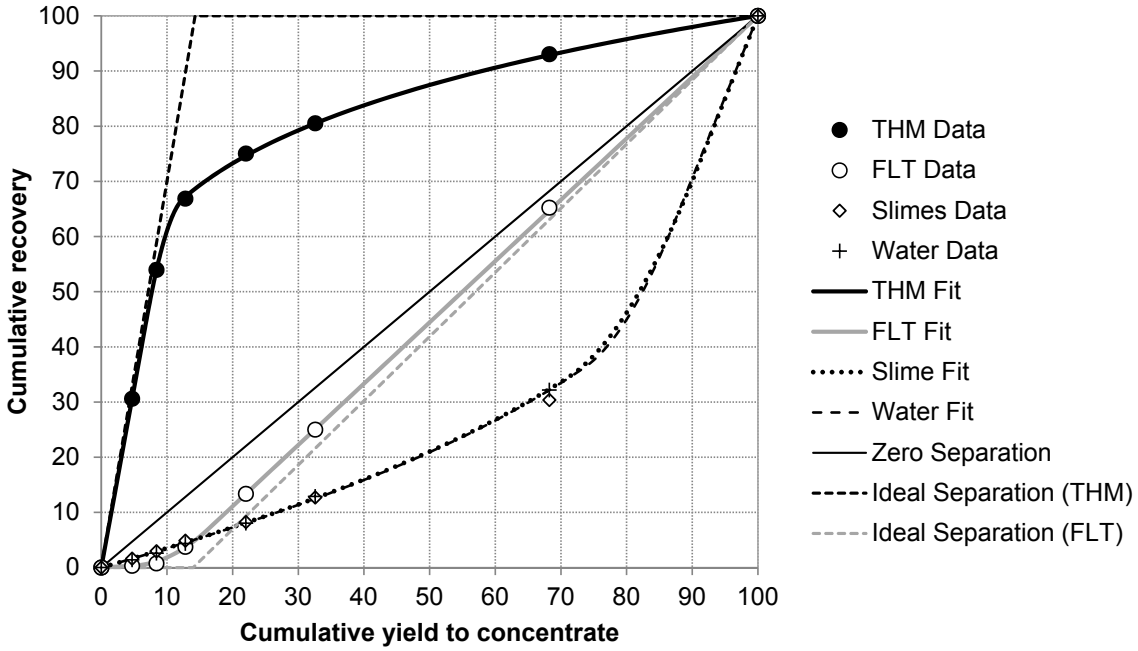

Figure 2.36: Cumulative recovery of the four mass streams across the spiral trough. (THM head grade = 13.5 %, solids concentration 35 %, slimes content 3 %, HC1 spiral)

cumulative recovery form, each mass stream plotted separately. In this case test-work data is utilised with actual mass data instead of the mono-mineral particles and theoretical separation as demonstrated and discussed in previous sections. From the number of data points presented it can be seen that a mouth-organ spiral trough cutter was utilised. The x-axis can be seen according to the spiral trough with the high-density particles accumulating on the left and low-density particles accumulating on the right. The THM curve indicates that most of the high-density particles are recovered on the inside of the spiral trough. The FLT curve shows a mass recovery line close to the zero separation line which is expected since the FLT mass represents 85 % of the solids in the feed. Water recovery and slimes recovery are similar since the slimes (ultra-fine clay particles) are in suspension in the water. The bulk of the water accumulates on the outside of the spiral trough. The cumulative recovery graph, as depicted in Figure 2.36, forms the basis of the other two graphs in Figure 2.37 and Figure 2.38. It uses the same mass data but plots it differently to reveal other aspects of spiral separation performance.

Figure 2.37 demonstrates how the grade of the concentrate varies with mass yield. The 20 % yield point, for example, produces a product with a 49.5 % THM, 49.5 % FLT and 1 % Slimes. 20 % of the water is recovered at the same time into this mixture. The concentrate grade at 100 % mass recovery is the same as the feed grade.

All the data that was on the left hand side of the zero separation line in Figure 2.36 are presented as positive in Figure 2.38. All the lines on the right hand side of the zero separation line in Figure 2.36 are presented as negative in Figure 2.38. In this way Equation 2.6 is applied consistently. For most efficient separation of THM from FLT the mass yield is around 13 % to concentrate. This is the point where the combination of THM grade and THM recovery is most suitable. Mass yield less than this point results in significant recovery losses in THM while mass yield greater than this point results in significant decreases in THM grade.

Note that the lines used in Figure 2.36, Figure 2.37 and Figure 2.38 are not an exact fit between the test-work data points. The lines are the closest fit of the "enhanced Holland-Batt equation" that is discussed in Chapter 8. The data from Figure 2.36 is used to best fit the equation for the four mass streams. Figure 2.37 and Figure 2.38 utilise the curve data from

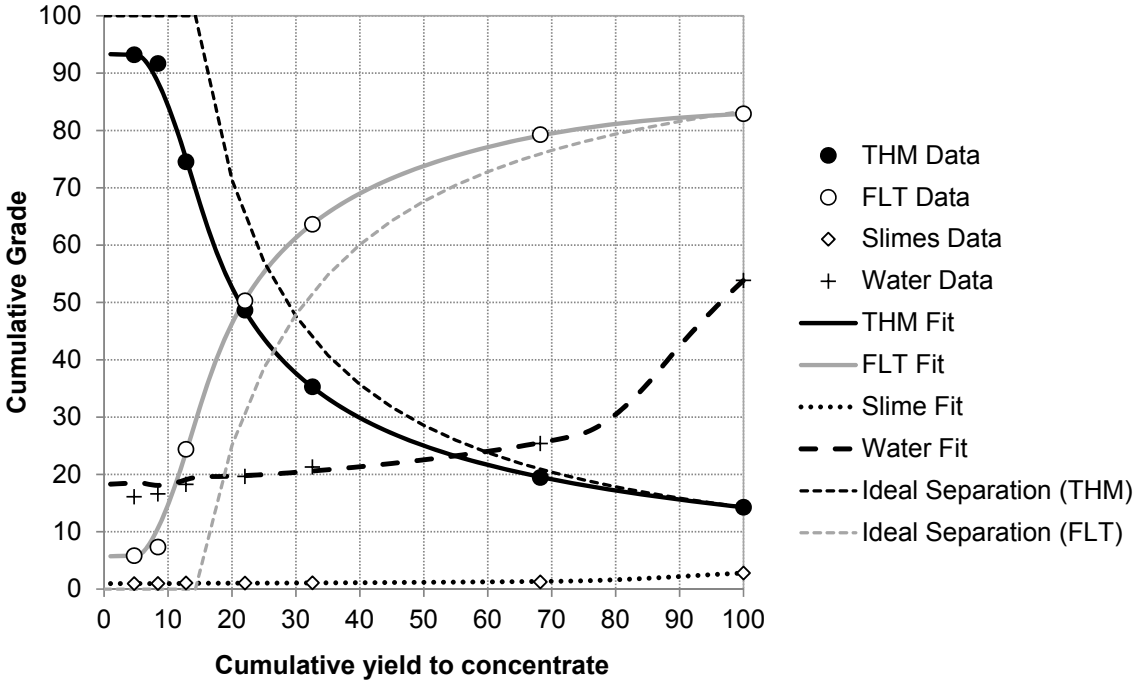

Figure 2.37: Cumulative grade of the four mass streams across the spiral trough. (THM head grade = 13.5 %, solids concentration 35 %, slimes content 3 %, HC1 spiral)

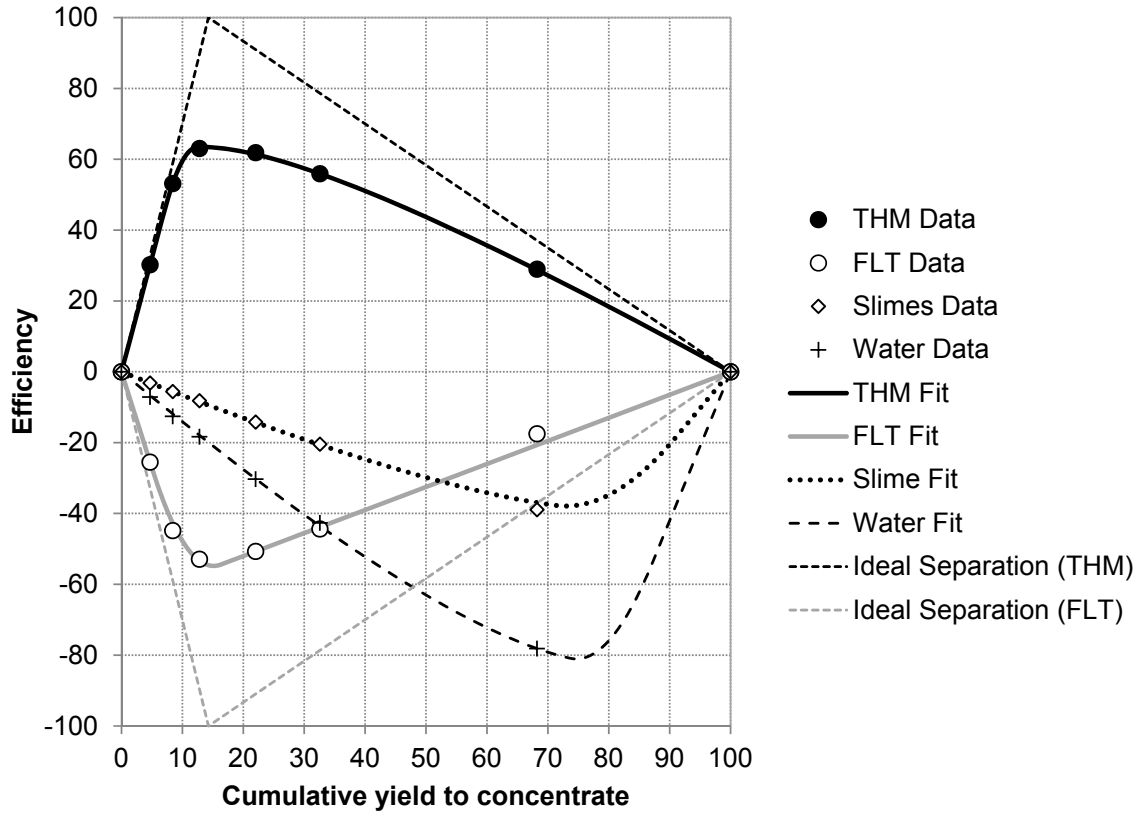

Figure 2.38: Separation efficiency of the four mass streams across the spiral trough. (THM head grade = 13.5 %, solids concentration 35 %, slimes content 3 %, HC1 spiral)

Figure 2.36.

In the next section the above-mentioned analysis methods and data presentation methods are used to demonstrate the influence of different factors.

2.5 Factors Influencing Spiral Separation Performance

The following section uses terms and principles discussed in the previous sections to explain how the different factors influences spiral separation performance and what can be done to control or limit the negative effect. Table 2.3 lists the different factors and divides them into three distinct categories. These factors are discussed in detail in this section.

Table 2.3: Parameters that influence spiral separation performance.

Feed Material Characteristics	**Design Parameters**	**Operating Parameters**
Particle density distribution	Profile (trough design)	Water viscosity (slimes conc.)
Particle size distribution	Trough diameter	Solids concentration
Particle shape distribution	Number of turns	Throughput
Included in above 3 parameters	Trough pitch	Trough cleanliness (housekeeping)
Slimes content (below 45 µm)	Intermediate splitters / cutters	Throughput consistency
Oversize content (above 1 mm)	Flow modifiers / repulpers	Solids concentration consistency
Mineral assemblage	Height above feed point	Final splitter position
Near density mineral content	Feed distribution	Auxiliary splitter position
Milled or natural material	Materials of manufacture	
Liberation of valuable mineral	Wash water addition points	
THM grade		
Abrasiveness		

2.5.1 Feed Material Characteristics

Particle Density

In consideration of the different force equations discussed earlier, particle density played an important role. Gravitational, centrifugal and frictional forces are influenced by particle density. Density difference between particles to be separated is considered as the main driving force for effective separation. In the case where the density difference between high-density and low-density particles are too small, spiral separation efficiency would be uneconomically low. Typically density differences should be greater than $1.0\,\mathrm{g/cm^3}$. In other words, a particle with a density below $3.0\,\mathrm{g/cm^3}$ and a particle with a density above $4.0\,\mathrm{g/cm^3}$ should be able to separate reasonably well using a spiral. The greater the density difference between the low- and high-density populations the greater the separation efficiency would be.

The particle density distribution is a description of the range and quantity of particle densities. This provides information on the entire particle population. In the coal industry it is called a washability curve, and presents the data on a cumulative mass and relative density plot. This information is valuable since other important parameters mentioned in column 1 of Table 2.3 can be derived from it.

The near density mineral content is the amount of material that is close to the separation density of the separator and hinders separation through particle crowding in the separation zone. The force balance on these intermediate density particles places them in the separation zone, which hinders low-density particles moving to the outer zone and high-density particles moving to the inner zone. These particles can consist of intermediate density, or poorly liberated particles that consist of a number of minerals in a single particle.

Another important parameter that can be derived from the particle density distribution is the total heavy mineral content (THM) and valuable mineral content (VHM). The THM is defined by the mass percentage of particles with a density greater than $2.98\,\mathrm{g/cm^3}$.

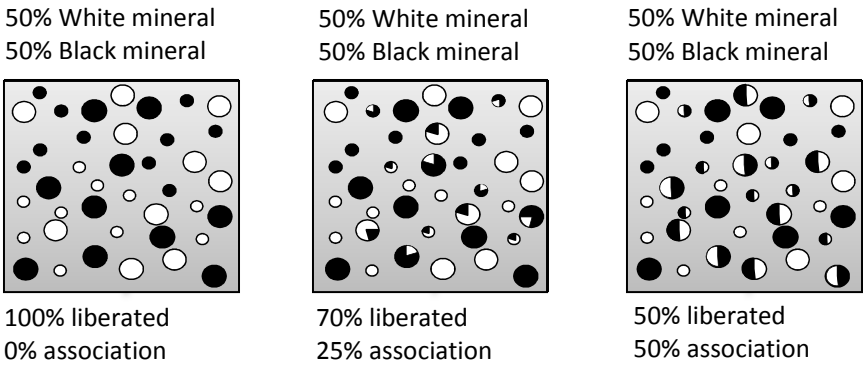

Figure 2.39: Varying degrees of liberation and association for the same bulk mineral composition.

VHM on the other hand is defined by the mass percentage of particles of economic value. In many cases these particles have a density greater than $4.0\,g/cm^3$. The fraction of THM in the feed determines the most suitable spiral trough design, since spirals are designed based on ranges of THM content in the feed material.

The liberation of valuable mineral can also be determined by the particle density distribution curve. If the liberation of the high-density mineral from the low-density mineral is poor, there will be a considerable fraction of intermediate density particles that will limit separation efficiencies noticeably. Figure 2.39 illustrates the impact that mineral association has on particle density. In the case where only 50 % of the particles are liberated with a 50 % association, it implies a particle density that is the average of the two mineral densities. These intermediate density particles cause considerable problems during spiral separation through particle crowding, but will also result in poor mineral recoveries due to poor liberation and not just lower separation efficiencies.

The process to determine a complete particle density distribution for fine particles (less than 300 µm) at higher densities (greater than $2.98\,g/cm^3$) is challenging and is discussed in some of the next sections of this document. The most common method of density separation practised in the heavy mineral industry is a sink-float method using the organic liquid tetrabromo-ethane (TBE), with a homogeneous liquid density of $2.98\,g/cm^3$. The float fraction (FLT), which contains most of the particles with a density less than $2.98\,g/cm^3$, remains on the surface of the organic liquid. The sink fraction (THM), which contains most of the particles with a density greater than $2.98\,g/cm^3$, settles and is tapped off. This sink fraction is also known as total heavy minerals or THM. In most cases the float particles consist out of a single mineral, quartz, while the particles in the THM can contain a range of minerals within a single particle, ranging from a density as low as $3.2\,g/cm^3$ and as high as $5.0\,g/cm^3$.

Figure 2.40 illustrates the steps in a typical sink-float process of separating higher density particles from low-density particles. This process is regarded as the industry standard and almost all literature referenced in this text used this analytical method as the basis for spiral separation data. If the sink-float analysis is done in a controlled and consistent manner, it could be considered to approximate ideal separation. In other words, little to no misplacement occurs in this measurement method.

Particle Size

When considering the different force equations, particle size also plays an important role. All of the force equations are impacted by particle size. Both gravitational force and centrifugal force on the particle is influenced by the particle diameter to the third power.

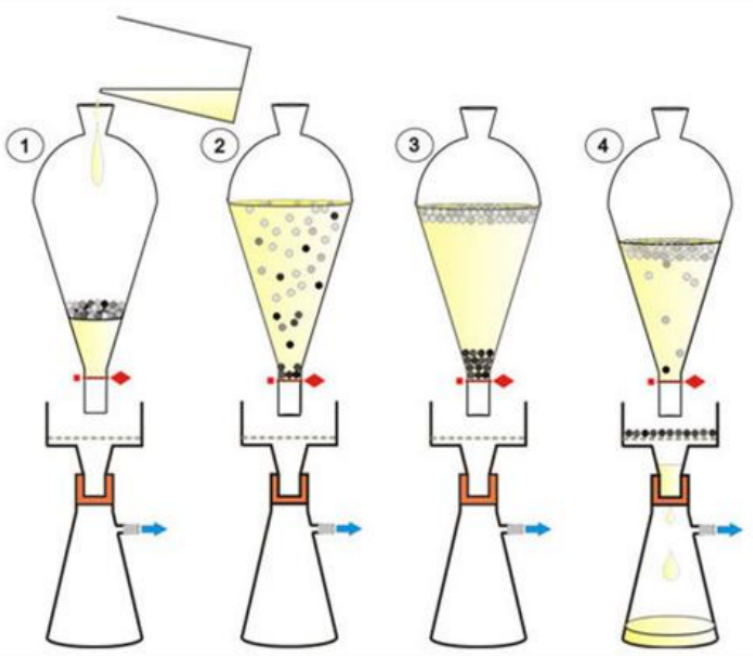

Figure 2.40: The sink-float process to separate high-density particles from low-density particles. (British Geological Society 2014)

Particle size distribution is a description of the range and quantity of different particle sizes. The particle size distribution provides information about the entire particle population. The narrower the particle size distribution, the better spiral separation would be, since there will be less of a particle size effect, and particle density separation will be dominant. This is preferred.

Ultra-fine particles less than 10 µm, also referred to as slimes, cannot be separated on the spiral since they remain captured in the fluid flow. Over-sized particles (greater than 500 µm), irrespective of their density, are rejected towards the outside of the spiral due to secondary flow. The particle size distribution also assists in the selection of the correct spiral trough to maximise separation efficiency based on historical data. The oversize particles and slimes particles form part of the particle size distribution, but are separated during sample analysis. The most common method to determine particle size distributions is screening on multiple screens or laboratory sieves. This method is fairly quick and considered as the industry standard. Figure 2.41 demonstrates a typical laboratory sieve shaker used to determine particle size distributions.

Particle Shape

The drag force, which is similar in magnitude to the gravity and centrifugal forces, is most significantly impacted by particle shape. Elongated or flat particles are pushed to the outer zone through the secondary flow pattern irrespective of their high density. It is therefore important to understand the particle shape distribution of the feed material.

There are many different equations for quantifying shape in literature, but the one most commonly used is the particle perimeter comparison to a circle. If the particle is a perfect sphere it would have a shape factor of 12.4. Elongated particles have shape factors greater than 30. Figure 2.42 illustrates the application of Equation 2.7. It is termed a factor since it is dimensionless.

$$\text{particle shape factor} = \frac{\text{particle perimeter on cross section}^2}{\text{particle cross-sectional area}} \tag{2.7}$$

Figure 2.41: A laboratory sieve shaker to determine particle size distribution. (Fritsh 2014)

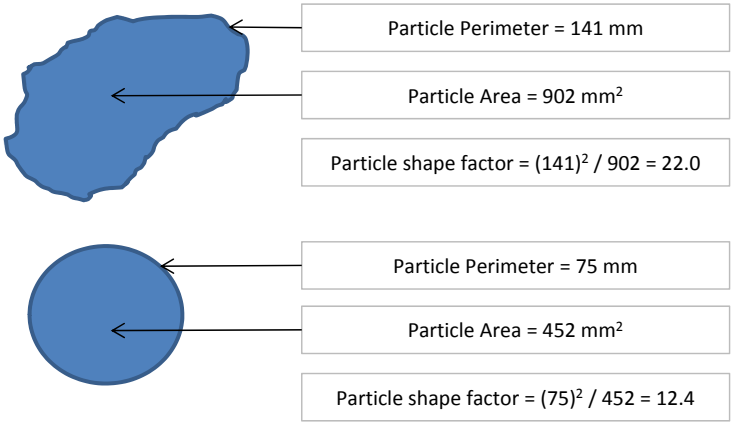

Figure 2.42: Particle perimeter, particle area and particle shape.

Crushed and milled material have a significantly different particle shape distribution compared to naturally occurring beach sands, for example. A good understanding of the feed material with regards to shape can aid the explanation if spiral separation efficiencies are not as expected.

Other Ore Characteristics

Particle abrasiveness is determined by the hardness and sharp edges of the particles. The major impact that high particle abrasiveness can have is not necessarily poorer separation due to potentially higher drag but rather higher wear on the spiral and the equipment (pumps and pipes) that feed the spiral. This can have a significant impact on the operational cost if not identified at the early stages of material characterisation

When considering the impact that ore characteristics has on spiral separation it is important to note there is very little that can be done to manipulate the feed characteristics to more favourable separation conditions. In most cases these parameters are fixed but a thorough upfront characterisation and understanding of the impact it would have on spiral separation can aid in making major investment decisions.

The following could be done to the feed material to create more favourable separation conditions:

Ultra-fines removal: The ultra-fines concentration can be lowered by upfront desliming. The impact that ultra-fines has on water viscosity is significant. It is therefore discussed under operating conditions, since it can be controlled.

Coarse material removal: The removal of coarse material through upfront screening aids spiral separation by minimizing interference in the separation zone

Fine and coarse circuit: If the feed material contains a wide particle size range it can be considered to treat the coarse fraction and fine fraction separately to maximise density separation by minimising particle size effects in the force balance. Different spiral trough designs could also be considered on the coarse and fine fractions.

Recirculation streams: Careful consideration is to be given to recirculation streams in spiral circuits. Intermediate density particles tend to remain in the separation zone or middling stream. If the middling stream is circulated it causes build-up of intermediate density particles that negatively impact the overall circuit efficiency. In this way the feed to the spiral is modified negatively and the number of near density particles is increased.

Further liberation: If particles are not sufficiently liberated, the particles can be milled further. Other spiral profile designs can be considered which are more effective on fine particles.

2.5.2 Design Parameters

The parameters from Table 2.3, column 2, are discussed in the following paragraphs.

Spiral trough design, trough diameter, the number of turns and trough pitch are all considered under spiral geometry. As previously mentioned almost all forces that a particle experienced on the trough, with the exception of gravity force, are significantly influenced by spiral geometry. Over more than 70 years of spiral utilisation in industry there has been well over a 100 different spiral geometries and in most cases the separation efficiency of the specific design can only be determined empirically. In many cases the success of a certain profile is limited to a specific feed material. There is limited information available in literature to correlate a single

spiral geometrical parameter with separation efficiency. Rather it is the combination of all the spiral geometrical parameters that produces a certain separation result.

Intermediate splitters, repulpers, flow modifiers and wash water addition points were previously discussed under spiral auxiliary components. During spiral performance characterisation there are so many operating parameters to be considered that the impact of repulpers and intermediate splitters on spiral separation efficiency is not thoroughly investigated by the beneficiation industry and therefore not well documented in literature. The spiral suppliers would most likely have investigated these effects thoroughly, but would have kept the data in-house as far as possible.

Height above feed point and feedbox design are important to consider since it relates to a hydrostatic pressure and inlet flow velocity. The inlet flow velocity needs to correspond closely to the steady state velocity on the spiral itself to initiate particle separation as soon as possible to limit the number of turns and the resultant column height. The spiral manufacturer usually specifies the height between the distributor discharge and the spiral start inlet. The feedbox design allows for some height variation, since although the distributor discharge points are all at the same height, the entry points on multiple spiral starts differ with up to 300 mm (top and bottom start on a four-start spiral).

The equal feed distribution to multiple spiral starts from a single inlet pipe is crucial to ensure overall circuit efficiency. In some spiral banks there is up to 36 spiral starts that are fed from a single inlet pipe. If the feed distributor is not properly designed and installed some spiral starts will receive more than their design tonnage while other spiral starts will be starved. The solids concentration in the feed to spirals also varies as a result of poor distribution, which in turn leads to poor spiral separation performance.

In the selection of materials of manufacture one needs to consider wear resistance, a suitable friction coefficient for particles to separate, suitable strength, weight of the final product, corrosion resistance and a suitable method of construction.

2.5.3 Operating Parameters

The parameters from Table 2.3, column 3, are discussed in the following paragraphs. The three major operating parameters that are usually considered in the mineral processing industries using spirals are dry tonnage per spiral start or throughput, slurry feed density or solids concentration and water viscosity, which has a strong relationship with slimes content. Throughput is important since it determines the production capacity of the processing plant that directly links to capital cost and profitability of the installation. Solids concentration influences how the feed is presented onto the spiral trough and is typically controlled by the addition of process water to cyclone underflow in a density correction tank. Water viscosity can be controlled upfront, prior to spiral separation, by removing water that contains slimes and adding clean process water to dilute the slimes content to acceptable levels. The following headings discuss these three parameters with regards to their impact on spiral separation performance using the recovery-grade relationship as basis.

Throughput

A specific spiral profile has a well-defined separation volume in which medium flows and particles interact with each other. This separation volume determines how many particles can be processed in a period of time. If this volume is exceeded it would hinder the effective separation of particles due to increased particle-particle interaction. The force equations discussed previously assume that each particle can move to its radial equilibrium position during the time period that it spends on the spiral trough. If the separation volume is too small, most of the particles will not have sufficient time to reach their radial equilibrium positions, which

would result in poor separation performance. Figure 2.43 illustrates this effect with all other operating conditions kept constant. An increase in throughput results in more than 10 % THM recovery decrease at 20 % mass yield to concentrate. The effect of increased throughput can be countered slightly by decreasing the solids concentration in creating more separation volume. However physical limitations will be breached and slurry spilling over the side of the spiral trough can occur, for example.

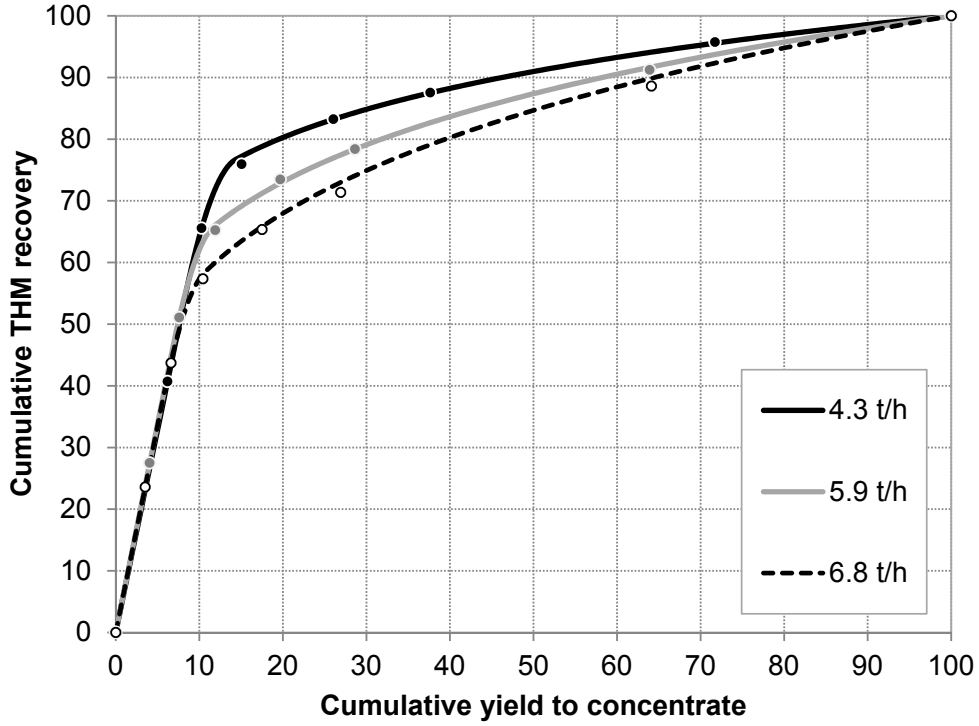

Figure 2.43: Influence of feed rate on spiral separation performance (THM recovery). (THM head grade = 13.5 %, solids concentration 40 %, slimes content 3 %, HC1 spiral)

Solids Concentration

As discussed previously in Section 2.2.2, the water on the spiral trough creates the 'space' in which the particles can move to their respective equilibrium radial positions. High solids concentration increases particle-particle interaction, which will increase the residence time required for effective separation. Low solids concentration will create additional turbulence, but the effect of lower than design solids concentration is significantly less compared with higher than design solids concentration. Figure 2.44 illustrates the effect of solids concentration (% solids by mass, wet basis) for similar operating conditions. A limited measurable difference can be seen for the 3 % variation in solids concentration.

Water Viscosity (slimes content)

Water viscosity is not usually measured during spiral performance analyses, and slimes content (by mass %, dry basis) can easily be determined through conventional wet screening on 45 µm. Slimes content has the effect of increasing the medium viscosity, thereby increasing the drag force on particles while moving through the medium and causing particles to take longer to reach their equilibrium radial positions on the trough. The negative influence of high medium viscosity cannot be overstated, and the THM recovery decreases rapidly after a certain threshold of slimes content is exceeded. Figure 2.45 illustrates the detrimental effect of increased slimes

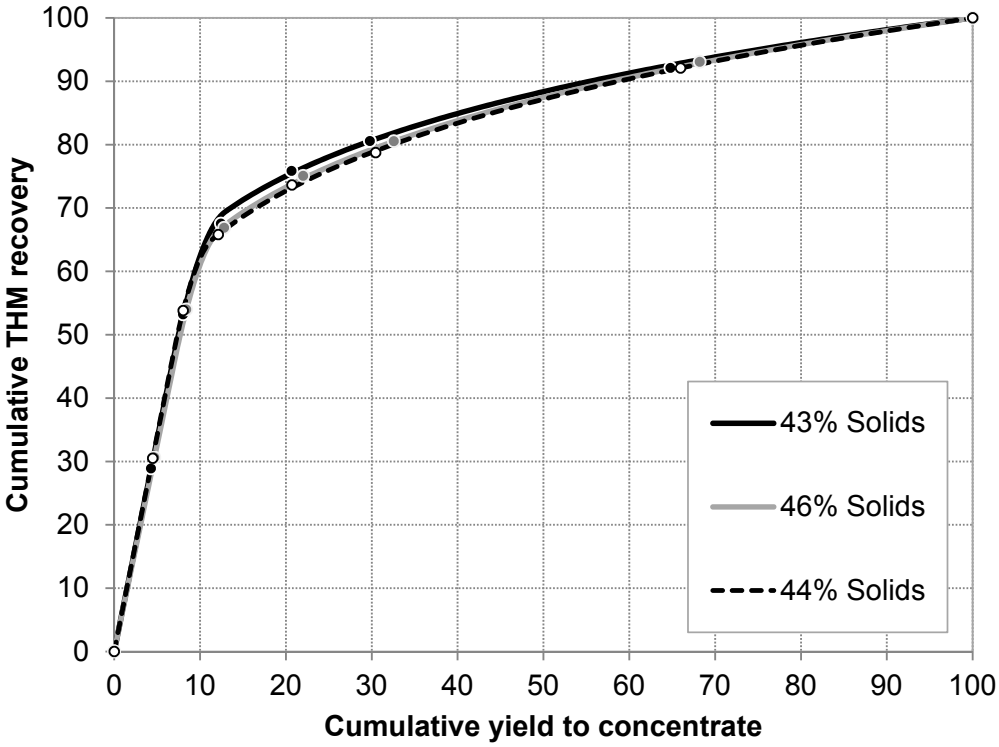

Figure 2.44: Influence of solids concentration on spiral separation performance (THM recovery). (THM head grade = 13.5 %, throughput 5.5 t/h, slimes content 3 %, HC1 spiral)

content while the other operating conditions remained constant. THM recovery variation is more than 65 % at 20 % yield to concentrate for a 26 % variation in slimes content.

2.6 Summary

At the end of this chapter there should be a clear understanding of what a spiral is, of the basic separation mechanism and of the terms that are used in the discussions to follow. The history, scale, benefits and disadvantages of the application of spirals in the mineral industry were discussed to support the relevance of this study and provide a perspective of where it fits into the larger mineral processing environment. The typical measurement and data presentation methods applied on spirals were demonstrated to set a baseline. The measurement methods are further expanded upon in the chapters to follow to demonstrate the contribution of this study. The factors influencing spiral separation performance were briefly discussed, building the platform to present the test-work results from this study.

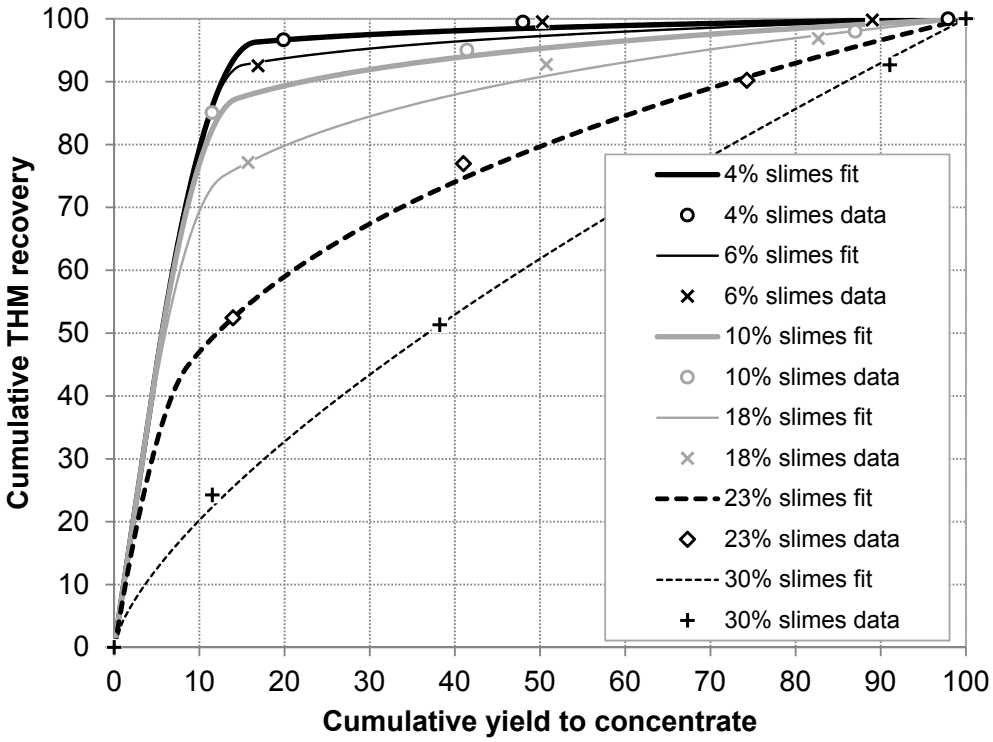

Figure 2.45: Influence of slimes content on spiral separation performance (THM recovery). (THM head grade = 15 %, throughput 1.5 t/h, solids concentration 35 %, MG4B spiral)

Chapter 3

Research Definition

3.1 Problem Statement

The current method of analysing spiral separation performance that is used in industry is insufficient to determine the most suitable spiral trough design for a specific feed material and operational application.

Over the last 20 years there has been significant improvement and specialisation of spiral design from various manufacturers. However, over the same period there has been very little improvement in the analysis methods that are applied to compare spirals with each other. The need to compare spirals usually arises from a spiral replacement requirement or the implementation of a new mineral processing facility, each involving large capital cost.

The standard sink-float (THM) analysis has been applied to analyse spiral products for the last 50 years. The risk of applying this rudimentary method is that unique beneficiation benefits or weaknesses of a specific spiral may not be identified. It is well known that a spiral separates on size and density, yet spiral products are not analysed in this manner. The reason for this is that physical separation of a particle population consisting of billions of particles based on density for analytical purposes remains a challenge.

Traditional sink-float analyses in organic mediums of varying densities are unable and/or unsafe to reach high densities above $3.0\,\mathrm{g/cm^3}$ due to the toxicity of these fluids. Mass fractionation using other density separation devices, such as small shaking tables or elutriators, introduces secondary separation inefficiencies that are unwanted for any analytical method. Due to these limitations almost all literature reports only two particle density categories, namely less than $2.98\,\mathrm{g/cm^3}$ (FLT) and greater than $2.98\,\mathrm{g/cm^3}$ (THM), for the heavy minerals industry.

If a more detailed analysis method can be developed that incorporates particle size and particle density, and that is cost and time effective, it will aid the mineral processing industry in making better decisions regarding spiral selection.

3.2 Research Purpose

This study aimed to develop and validate an enhanced material characterisation method as an improvement on the current industry standard characterisation method and as an alternative to physical separation of spiral product particles.

A secondary aim of the study was to develop an enhanced data presentation method to improve the presentation of spiral test-work data in general. The combination of the two methods, "enhanced material characterisation" and "enhanced data presentation" is termed "enhanced analysis", which is the title of this study.

3.3 Research Objectives

In the development of the enhanced material characterisation method the following objectives had to be met:

- Evaluate the consistency of the individual steps in the standard characterisation method on the spiral products.
- Define the steps of an enhanced material characterisation method and explain how it improves standard characterisation.
- Validate the steps of the enhanced material characterisation method by evaluating the impact on particle population attributes at each step. The definition of the requirements that need to be considered in the enhanced method's application is a natural result from the validation process.
- Demonstrate the value of the enhanced material characterisation method by applying it on the feed material to the spirals as well as on the spiral products.

In the development of the enhanced data presentation method the following objectives had to be met:

- Demonstrate the standard data presentation method and explain the current shortcomings.
- Explain the improvements made to develop an enhanced data presentation method.
- Demonstrate the value of the enhanced data presentation method by application to the test-work data.

3.4 Research Significance

Differences in spiral separation performance under similar operational conditions while processing similar feed material might seem insignificant. However, in the long term these differences cause a cumulative effect that can have a significant impact (negative or positive) on mineral recovery and overall business profitability, depending on the spiral profile design that was selected. A consistent 1% recovery change in zircon for a medium sized operation can easily equate to a revenue change of ZAR4 000 000 per annum, which could easily pay for spiral replacement if the correct spiral was selected in the first place.

The result of this research can equip operating personnel to confidently select the most suitable spiral based on their specific feed material characteristics and operating window. This research can also assist process design teams in the selection of the correct spiral early in the project life cycle, which can save a significant amount of time and money in plant design costs. This spiral selection is achieved by the application of an enhanced analysis method that demonstrates the separation performance differences more clearly.

3.5 Research Scope

This study focused on six main scope areas. Feed material makes reference to the type of material and commodity. Only two spiral profile designs were considered on which the test-work data have direct application. Only typical operating conditions were evaluated and standard

spiral performance quantification methods were used. Qemscan® was selected as the analytical tool for enhanced material characterisation. The Holland-Batt equation was selected as the basis for the structure in which the data was interrogated and presented.

3.5.1 Feed Material

The material under investigation was heavy mineral sand with natural particle size and particle density distribution. No other materials typically processed with spirals, such as fine coal, chromite and iron ore were considered in this study. A heavy mineral sample implies that limited to no particle crushing or liberation was applied to the material. The particle shape is therefore generally well rounded. The slimes content, made up of clay below 10 µm, was of natural origin and was only slightly increased or decreased from its natural content for test-work purposes. Two distinct feed material types with vastly different geological backgrounds were utilised in the investigation. The first sample originated from the south-west coast of Madagascar and the other sample from the west coast of South Africa. Both locations were not close to the shoreline itself, but a few kilometres inland.

3.5.2 Selected Spiral Profiles

Two spirals from a single spiral manufacturer were selected for this investigation. The first spiral (MG4) is an older version that is installed in many operational heavy mineral sands processing plants. The second unit (HC1) is a newer generation spiral with higher processing capacity, which implies more throughput capacity for similar plant footprint. This is typically considered during spiral replacement to increase throughput capacity for the same footprint. Both of these spirals are primary processing units, which are typically installed in a "rougher" application where large volumes of quartz are separated from small volumes of heavy mineral. Heavy mineral content ranged between 5 % and 15 %. No secondary or tertiary processing, "cleaner" or "scavenger" duties, were considered in this investigation. Both of these spirals were fairly new, which implies that limited to no wear had occurred on the spiral trough surface. Spiral wear, especially irregular wear, can have a significant impact on separation performance.

3.5.3 Operating Conditions

The three main operating parameters of throughput, solids concentration and slimes content were considered. Feed grade was varied in only a few instances. The operating window was selected within the typical ranges of processing plant variation for the mentioned parameters. Spiral separation performance at extreme operating conditions was not evaluated. Other parameters such as auxiliary splitter position, and feed stability in terms of rapid changes in throughput and/or solids concentration were also not considered.

3.5.4 Spiral Separation Performance Quantification

Standard separation performance quantification methods as available in literature were utilised in the investigation. The methods as discussed in section 2.4 utilised the four basic separation attributes of yield, recovery, grade and efficiency. The yield-recovery relationship, yield-grade relationship and yield-efficiency relationship were the typical methods of presenting the data to quantify spiral performance. Alternative data presentation was not considered or developed.

3.5.5 Material Characterisation Method

This investigation focused on the development and validation of a characterisation method to quantify particle density and particle size simultaneously. Qemscan®, utilising quantitative electron microscopy, was the analytical tool applied to quantify particle properties and not just bulk mineralogical or chemical attributes. This tool was mainly selected due to its availability within this specific research domain. Other analytical methods having similar particle quantification capabilities were not evaluated due to availability restrictions.

3.5.6 Data Presentation Method

Holland-Batt, well-known spiral separation performance researcher, proposed a mathematical expression (Holland-Batt 1990), which is a combination of a linear and a power law equation, to describe the relationship between mass yield and specific component recovery. This expression was based on large amounts of experimental data from various literature sources, which implies that the expression describes typical or natural spiral separation performance. For the purpose of this investigation the decision was made that this expression would be suitable to be applied to the experimental data to present a continuous mathematical expression rather than interpolation between test-work data points. The test-work result presentation demonstrated the validity of the data fit as well. The advantage of this approach was that a series of discontinuous data points could be presented by a simple continuous mathematical expression. The parameters of the equation could be more effectively compared since it represented the data over the entire mass yield spectrum as opposed to comparison at specific mass-yield-to-concentrate points. This consistent method assisted in identifying test-work "noise" due to slight analytical or test-work errors.

3.6 Research Assumptions

3.6.1 Particle Shape Quantification

Particle shape plays a significant role in the equilibrium position on the spiral trough. Elongated particles or thin plate particles will behave very differently to well-rounded particles of similar density and volume. For this investigation naturally occurring heavy mineral sand samples were utilised. From the particle analyses that were conducted on these samples the majority of the particles were found to be well rounded with limited shape differences. For the purpose of this study the assumption was made that particle shape does not have a significant impact on separation performance and could therefore be ignored. The validity of this assumption was evaluated in the particle analysis method applied and is only applicable on specific feed material. If crushed material, highly irregular material or weathered material was used as feed material to the spiral this assumption would not be valid. The impact of this assumption was a more simplified particle analysis process. Particle shape is a multi-dimensional attribute and there is no general consensus in literature regarding a single metric that can be used for particle shape.

3.7 Definition of Key Terms

The following terms were discussed in Chapter 2, but are repeated here in case the reader skipped Chapter 2 based on familiarity with spiral concentration.

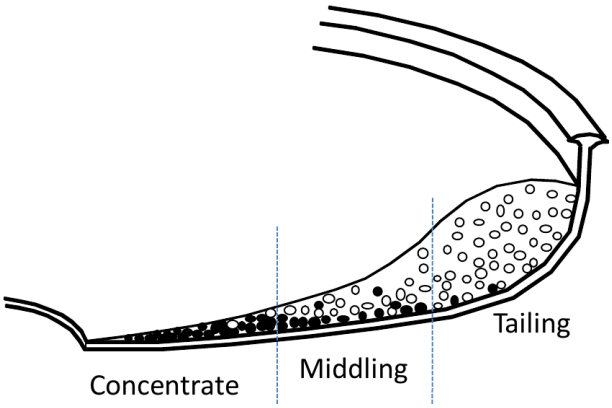

Figure 3.1: Spiral trough with particle separation presentation (not to scale). (● = high-density particle, ○ = low-density particle, ■ = water concentration)

3.7.1 Spiral trough

The surface on which separation occurs is referred to as the trough. The trough slope angle and the spiral slope angle are results of years of spiral development from manufacturing companies. The point at which the material exits the spiral trough is termed the trough exit point. At this point the position of the splitters determines how the particle mass on the trough is divided.

3.7.2 Yield

The dry mass to the concentrate is termed the mass yield (or yield) to concentrate. If the concentrate splitter was to be opened more, the yield to concentrate will change without changing any of the operating parameters of throughput, solids concentration or slimes content. The mass yield or dry mass percentage is typically sub-divided into three process streams called concentrate, middling and tailing that are presented in Figure 3.1.

3.7.3 Total Heavy Mineral Content (THM)

THM (Total heavy mineral content) is an industry term used to indicate the mass of material with a density greater than 2.98 g/cm^3. This density is chosen since it is the density of the organic medium tetra-bromo-ethane (TBE), which is readily available, and the bulk of the particles in mineral sands are quartz with a density of 2.63 g/cm^3. The mass of THM is determined by a sink-float analysis, in which 200 to 300 g of sand sample is mixed with TBE in a glass funnel with a tap at the bottom. The material is allowed to segregate due to density differences and the sink mass fraction is extracted by draining the settled fraction. The quartz particles remain floating and are removed by ladling them from the surface of the medium. This process is not particle size dependant although fine heavy mineral particles would be trapped in large quantities of float fraction (usually quartz). This analytical process has separation inefficiencies of its own, but has proven to be the most suitable for spiral performance quantification in the heavy mineral sands industry in the past. The float fraction is referred to as FLT.

3.7.4 Throughput

Spiral throughput refers to the mass of dry solids being fed to a unit process in a period of time, usually expressed in tons per hour (t/h). A spiral cannot process dry solids, and water act as the carrier medium at roughly 60 %-70 % by mass.

3.7.5 Solids Concentration

The solids concentration is expressed as the mass percentage of dry mass in total mass of water and solids, in other words, solids concentration or % solids is expressed on a wet basis.

3.7.6 Slimes Content

The slimes mass fraction is defined as the mass of material less than 45 µm, since that is the screen aperture size, which still allows for reasonable wet screening times. The typical D_{90} (90 % of mass passing this aperture size) of the slimes fraction is usually around 30 µm. Slimes content is therefore expressed as the mass percentage of material finer than 45 µm in the total solid mass.

3.7.7 Particle Class

This term is used to group particles with similar size and density attributes in this investigation. Each particle class will have its own size and density distribution. The mass of a class is determined by a size range and a density range. For example, all particles smaller than 150 µm and larger than 100 µm with density greater than 3.0 g/cm^3 and less than 4.0 g/cm^3 reports to this specific particle class. The class will be presented by the mass of particles that complies with the size and density criteria.

Part II

Literature Review

Chapter 4

Qemscan® as Material Characterisation Technique

This chapter focuses on material characterisation in heavy mineral sands and how Qemscan® is applied using its particle size and particle density quantification capabilities.

4.1 Introduction

In the processing of typical heavy mineral particles (between 50 µm and 500 µm in diameter) their physical attributes are used to separate valuable minerals from gangue. The main particle attributes that are exploited are size, density, magnetic susceptibility and electrical resistivity. The products from separation processes are typically analysed by means of chemical or mineralogical assaying to determine grade and recovery of a certain element or mineral to the product.

In the characterisation of typical heavy mineral particles the same particle attributes are used, but on a smaller scale with higher separation efficiencies. Examples are a sieve shaker at specific sieve apertures to characterise size separation, TBE sink-float to characterise gravity separation, electromagnetic lift magnet to characterise magnetic separation at increasing magnetic field intensities, and small high tension roll to characterise electrostatic separation at increasing electrical potentials. The general approach is to characterise a process through the measurement of the particle properties that are exploited during separation. For example, spiral products can be fractionated magnetically by means of a lift type electromagnet, but it is not ideal since there is no magnetic property being exploited during spiral separation. A better particle measurement would be one that measures or fractionates particles into different size-density classes.

This physical separation or fractionation of process products has the following two main advantages. The first is that the concentration of similar type particles will increase, making further analyses more effective. For example, if the concentration of a certain particle class is below 1 % and only a thousand particles are analysed, only 10 particles can possibly be analysed, which makes the description of that particle class less accurate. If the particle concentration could be upgraded to 10 % by some fractionation method it will increase the analysis accuracy significantly. The second benefit is that physical fractionation provides an indication of the particles' process separability, linking it to potential product qualities and recoveries, decreasing the processing risk. The result of the fractionation process is a physical particle population or mass that can be analysed or fractionated further by utilising a different particle attribute. For example, a typical run-of-mine sample can be screened on 1 mm and 0.045 mm, followed by sink-float. The sink fraction can be magnetically fractionated and the non-magnetic fraction can be separated on electrical conductivity to perform a high level simulation of a typical heavy

mineral separation process.

The physical fractionation of process products has the following two main disadvantages. The first is, there are limitations and separation inefficiencies in the fractionation method. For example, a standard TBE sink-float method will be suitable to separate quartz particles ($2.63\,g/cm^3$) from pure zircon particles ($4.63\,g/cm^3$) based on the large density difference between the particles. Separating quartz particles from lower density garnet particles ($3.40\,g/cm^3$) will cause separation inefficiencies or misplacement in the typical sink-float process - garnet particles will be trapped in the float fraction containing the quartz particles. Furthermore, the homogeneous mediums associated with higher density fractionation are either too toxic and/or too expensive for large numbers of analyses. The second disadvantage is that accurate physical fractionation requires skilled operators and specialised equipment with significant time and cost associated.

It is within these constraints that material characterisation by means of quantitative electron microscopy can make a significant contribution. Although quantitative electron microscopy does not separate the particles into physical fractions, the information gathered per particle is available to separate particles mathematically into different classes based on different particle attributes.

Since the spiral separates on particle size and particle density, these are the two main attributes that are discussed in further detail in the sections to follow. Particle shape is not considered in detail in this study based on the assumption discussed previously in Section 3.6.1.

4.2 Quantitative Electron Microscopy

In the field of quantitative electron microscopy there are various analysis systems such as Micro CT (Micro Computed Tomography), MLA (Mineral Liberation Analyser), Qemscan® (Quantitative Evaluation of Minerals by SCANning Electron Microscopy), CCSEM (Computer Controlled Scanning Electron Microscopy) and PTA (Particle Texture Analysis) to name a few. Each one of these analysis systems are owned by a different company with different detector numbers and detector types, with different proprietary software classes performing the automated data acquisition. Each system has its unique application with associated strength in one area and weakness in another area. (FEI 2014)

The analysis system that was utilised in this study, due to its availability in the specific research domain, was Qemscan®, referred to in the rest of the document as Qemscan®. The other analysis systems were not considered nor compared in this study due to availability, time and cost constraints. Qemscan® is a fully automated analysis system that produces mineralogical data from inorganic materials such as rocks and minerals. The data acquisition has been proven to be fast, statistically reliable and highly repeatable (FEI 2014). The specific Qemscan® system that was utilised had four light-element energy-dispersive X-ray spectra (EDX) detectors. These detectors capture the elemental composition at each of the measurement points on a predetermined grid size. The back-scattered electron (BSE) images provide information on textural properties such as particle size and particle shape. Figure 4.1 illustrates the process by which Qemscan® data is generated.

4.3 Particle Size and Density Quantification

The way mineral particles are presented to Qemscan® is to split a small number of particles, usually 2 to 5 g and mixing it with a resin. This mixture solidifies, setting the particles in a fixed matrix called a sample block, usually a round disc 30 mm in diameter and 10 to 15 mm thick. Figure 4.1 illustrates the sample block at the beginning of the process. The top layer

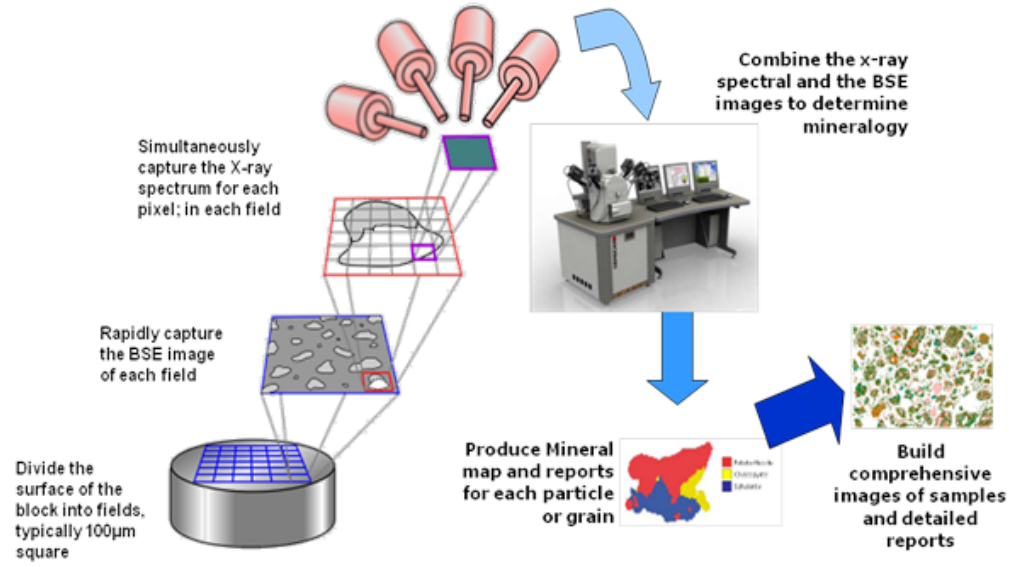

Figure 4.1: Process description of Qemscan® analysis. (Ayala 2009)

of the sample block, usually 50-70 µm in thickness, is removed and levelled through polishing (also termed polished block). This exposes the particles' internal composition.

Qemscan® integrated analysis system has the capability to characterise the individual particles exposed on the surface of a polished block. The combination of the EDX and BSE information reconstitutes the physical particle digitally, presenting a picture of the particles with each individual particle containing all the associated analytical information. These particles can be sorted digitally and classified according to different mineralogical or textural attributes (Ayala 2009). Figure 4.2 illustrates an example where the particles are digitally arranged in a 'washing line' after analysis, since they were not set in that orderly fashion in the preparation of the sample block. No classification was performed on the particles presented in Figure 4.2 and particles are presented in the sequence in which they were analysed.

4.4 Analysis Modes

Qemscan® can analyse a population of particles set in a resin mixture in different analysis modes with different data outputs depending on the information and detail required. It is important for the user to understand each analysis mode's application to leverage the analytical strength while being aware of the analytical weakness.

4.4.1 Bulk Modal Analysis (BMA)

This analysis performs several line scans across the polished block surface. The textural data is ignored and the BSE image is only utilised to direct the measurement point on the particle surface as the line of EDX analysis moves across the polished block. This analysis will give the highest quality of compositional information. It is fast since there is no image processing required and the operator can increase or decrease the number of line scans across the block. Figure 4.3 illustrates this analysis mode.

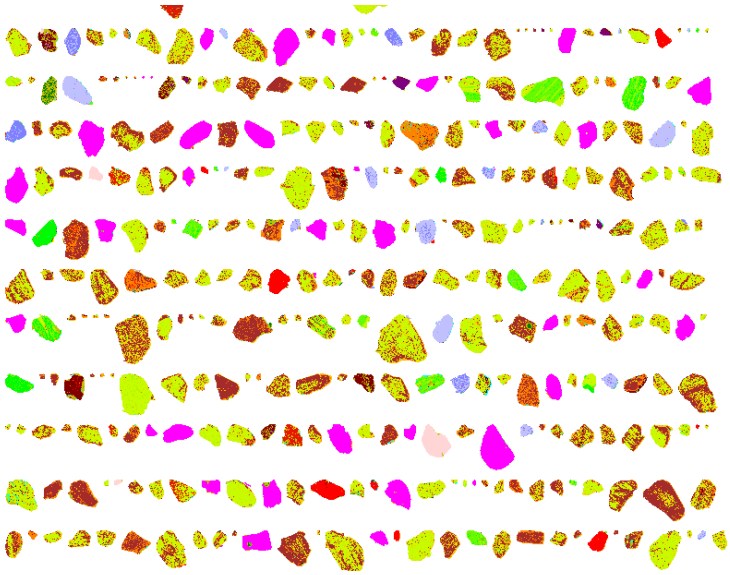

Figure 4.2: Particle map from Qemscan® particle mineral analysis. (Each colour represents a different mineral phase.)

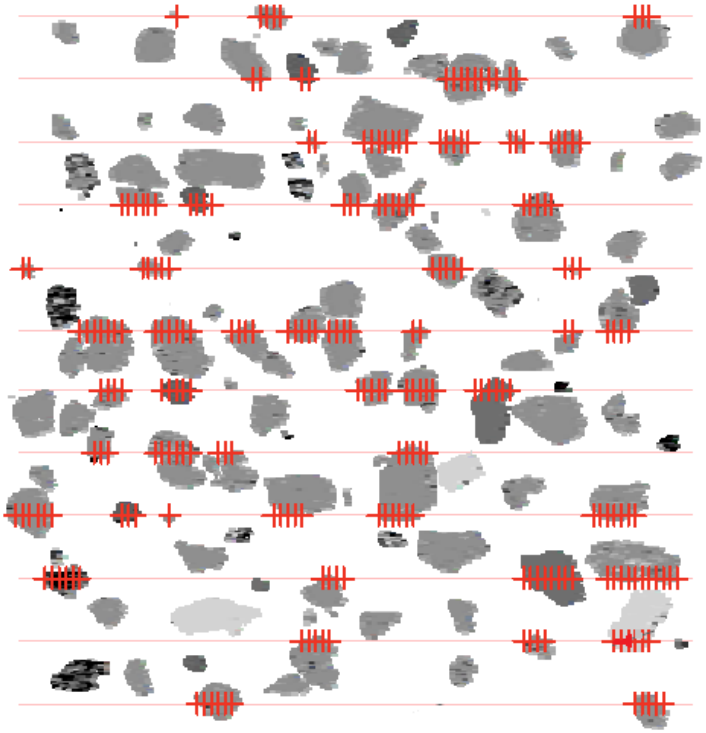

Figure 4.3: Demonstration of Qemscan® bulk mineral analysis (BMA) procedure. (Ayala 2009)

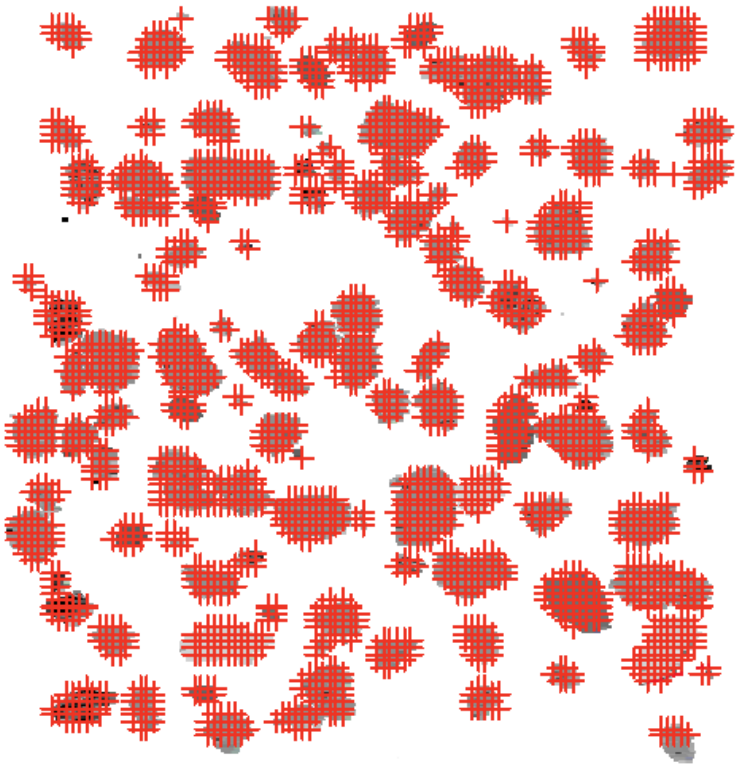

Figure 4.4: Demonstration of Qemscan® particle mineral analysis (PMA) procedure. (Ayala 2009)

4.4.2 Centroid Analysis

This analysis utilises the BSE image as the primary analysis image in which the different particles are considered as separate entities. The EDX measurement point is focused on the centre of each particle where it performs a single compositional analysis and assigns the analysed composition to the entire particle. This analysis is fast and provides high quality textural data (particle size and shape) since a large population can be analysed in a short period of time. If large numbers of multi-phase mineral particles are present this compositional variance will be ignored. Mineral association and liberation information is not available.

4.4.3 Particle Map Analysis (PMA)

This analysis uses the BSE image to identify the boundaries of each of the individual particles. A certain number of particles are selected based on a raster scan pattern. The particle is analysed through an EDX measurement point per pixel (can be set by user, usually 5 µm by 5 µm). Image analysis reconstructs the particle matching the compositional analysis per pixel within the particle. This analysis supplies the largest amount of information per particle, including mineral association, liberation and textural information (FEI 2014). It also takes the longest depending on the number of particles to be analysed. Figure 4.4 illustrates this analysis mode and Figure 4.2 presents a typical output.

4.5 Application and Validation

From 2003 Intellection Pty Ltd. developed, marketed and sold Qemscan® technology solutions. Qemscan® technology is now owned and marketed by FEI Company. From the start of

Qemscan® application in mineral processing industries various people could identify the benefit of using this technique in metallurgical studies, not just for accurate mineral quantification but also utilising the particle attributes to better understand separation performance. With the improvement in analytical methods there was also an improvement in the understanding of mineral resources and their process performance. The true profitability of a mineral resource can only be quantified if the economically valuable mineral and its variation are fully understood in the context of how it will behave in the separation process (Sutherland and Gottlieb 1997). The literature review in this investigation did not focus on the application of Qemscan® as mineral quantification tool in mineral processing, but rather on the application of the particle size and particle density quantification capability of Qemscan®.

4.5.1 Particle Size Analysis

A particle surface area from the sample block analysis is converted to a particle volume with effective particle diameter through stereological correction equations built into the proprietary software of the integrated Qemscan® analysis system. The general rule of thumb is that if a sufficient number of particles is analysed, a representative estimate of the actual particle size distribution of the material being evaluated will be obtained (Ayala 2009).

Since particle size is a normal output from Qemscan® analysis, several metallurgical studies have utilised this information to better understand the separation performance of different ores. Lotter (2003) utilised the particle size data output from Qemscan® to better understand flotation performance of nickel ore linked with the other mineral attribute outputs from Qemscan®, such as mineral liberation to the surface of the particle. Geo-metallurgical investigations by Philander and Rozendaal (2014) mentioned the importance of including particle size as part of an in-situ property for better quantifying process performance of mineral sands. Pascoe, Power, and Simpson (2007) utilised the particle size output from Qemscan® for improved understanding of the Mozley laboratory mineral separator in the separation of chromite ores.

In all of the studies, with the exception of the work from Pascoe, Power, and Simpson (2007), Qemscan® particle size output was utilised without a validation attempt on the accuracy of the particle size output. The underlining assumption was that Qemscan® size distribution did compare with the actual size distribution. Pascoe, Power, and Simpson (2007) performed a theoretical evaluation considering the probability of intersecting perfect spheres of different sizes during the preparation of the sample block. They also did a high level comparison between Qemscan® and the Malvern laser sizer using fine chromite ore that indicated agreement. The conclusion from the validation test-work from Pascoe, Power, and Simpson (2007) on this specific material is that Qemscan® can be used for size distribution if a sufficient number of grains are analysed. It was further noted that if the same method used to produce a separation model is used to analyse the independent sample, the separation model predictions should be valid.

4.5.2 Density Analysis

Particle density is used in the specie identification protocol (SIP-file) to convert particle volume to particle mass. The particle mass is important since it would influence recovery and grade of all the minerals under investigation. Accurate quantification of particle mass is also one of the major benefits of automated microscopy (Qemscan®) over grain counting (light microscopy).

Particle densities used in the Qemscan® SIP-file are predominantly sourced from literature sources on minerals and crystal structures. The chemical composition from the EDX analysis is converted to a mineral phase through the SIP-file. The SIP assigns a density to the mineral

phase at the specific analysis point. The particle density is a weighted sum of all the mineral phase densities analysed on the surface. No specific literature sources could be identified where the particle density output from Qemscan® was compared with actual density measurements on particle populations or individual particles.

4.6 Summary on literature review

The application of the mineral quantification capability of Qemscan® within the mineral processing industry is well established, to such an extent that automated mineralogy has become the standard for mineral quantification. The specific application of particle size and particle density outputs from Qemscan® in describing and understanding mineral processing performance was less common, but there were a number of references in the literature. The validation of the particle size and particle density output from Qemscan® was virtually non-existent in the literature. This investigation could contribute to literature through the validation attempts as well as the application to spiral separation performance data.

Chapter 5

Research Design

This chapter provides an overview of the research effort. Chapters 1 to 5 provide the background to the research and the remaining chapters are presented in the structure demonstrated in Figure 5.1. Figure 5.4 and Figure 5.5 illustrate the detail of the standard and enhanced material characterisation. The research approach involved evaluating the response of two materials on two spirals in a controlled test-work environment. The spiral products from test-work were characterised with standard and the newly developed enhanced methods to illustrate the benefit of more detailed characterisation approach. The test-work data were presented with the Holland-Batt equation which was improved through minor adjustments. The end result was a new, enhanced spiral performance analysis method, which can be compared with the enhanced approach. The following sections elaborate on the detail of the research approach.

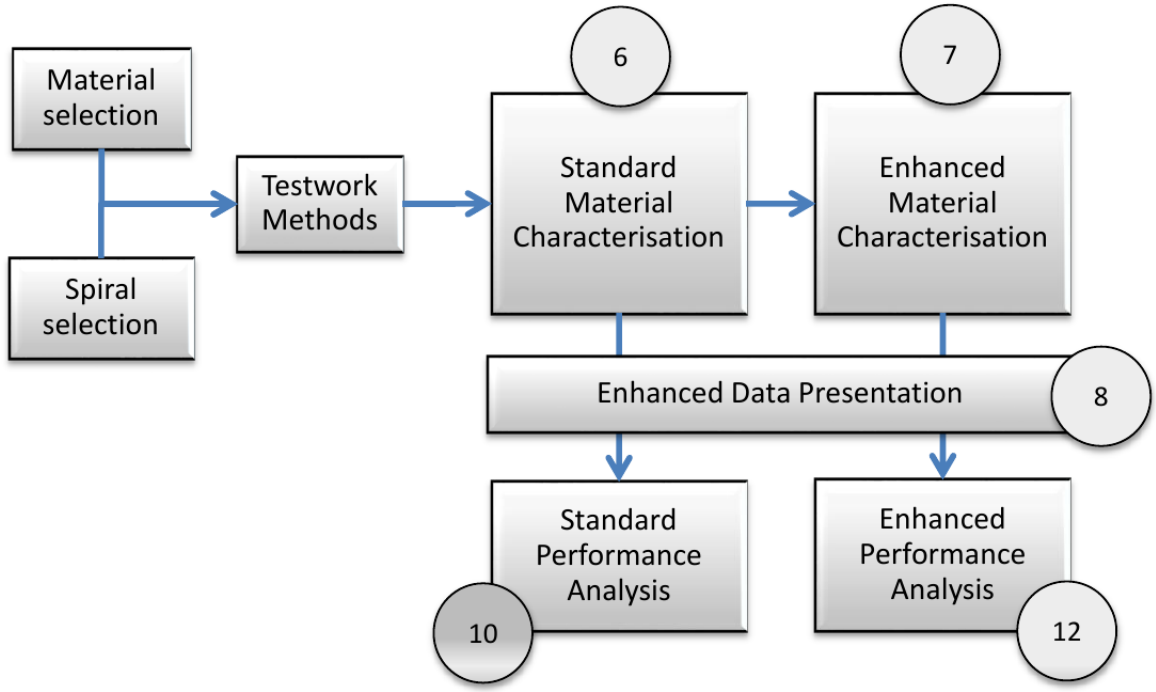

Figure 5.1: Research approach applied in the project. (Grey circles refer to the chapters in which it is discussed.)

5.1 Material Selection

Material 1 originated from the southwest coast of Madagascar. The deposit is approximately 15 km east of the coast line. This deposit was being evaluated as part of a feasibility study

during the material selection period. As part of the feasibility study a pilot plant was operated that was used to produce a bulk concentrate by means of spiral separation for further mineral processing in South Africa (Grobler 2007). During excavation of the feed material for the pilot plant a bulk sample of approximately 500 kg was taken by means of shovels and loaded into bulk bags that were transported back to South Africa for test-work. The sample contained roughly 2 % moisture. The following procedure was applied to the bulk sample as part of feed preparation prior to any test-work. The bulk sample, around 500 kg, was dried in large drying pans at temperatures below 150 °C to enable splitting and dry screening. The oversize material, greater than 1 mm, was removed by screening the total sample. This fraction was insignificant, consisting of mostly organic material. This sample is considered to be representative of the material from that specific block within the ore body since an entire block of undisturbed in-situ material was removed.

Material 2 originated from the west coast of South Africa. The deposit is approximately 5km east of the coast line. This deposit was being evaluated as part of process optimisation at an existing heavy mineral sands operation, the Namakwa Sands west primary concentration plant. Feed to the plant is prepared through a trommel screen (8 mm aperture), linear screen (1 mm aperture) and desliming cyclone to remove a portion of the slime. The feed is distributed to multiple spiral starts through a slurry distributor. One of the slurry starts was disconnected and used to fill several buckets totalling roughly 500 kg of dry mass. The sand and slime was left to settle where-after clean water was decanted. The wet sample, containing roughly 30 % moisture was transported to Pretoria where it was prepared in the same manner as Material 1. There was no oversize (+1 mm) material in the sample. This sample was considered to be representative of the material that was fed to the spiral plant on that specific day since the total feed stream to a spiral start was sampled for a period and no solids were discarded prior to transportation.

5.2 Spiral Selection

Two spirals from a single spiral manufacturer were selected for this investigation. Spiral A was a newer generation spiral with higher processing capacity, which implies more throughput capacity for a similar plant footprint. Spiral B was an older version and installed in many operational heavy mineral sands processing plants. Refer to Table 5.1 for a summary of the two spiral profiles utilised.

Table 5.1: Spiral profile information.

Spiral Ref	**Name**	**Description**	**Supplier**	**Design Feed Rate (dry t/h)**	**Design Solids Concentration**
A	HC1	High capacity	Mineral Technologies	5	35-40%
B	MG4	Medium grade	Mineral Technologies	2.2	30-35%

The design information was sourced from the supplier and is illustrated in Figure 5.2 and Figure 5.3. These two figures illustrate the optimal feed conditions for typical feed materials and are dependent on THM feed grade as well as the different types of mineral that are to be separated. A general rule is that throughput and solids concentration (pulp density) need to decrease when the material is more 'difficult' to separate.

The reason for the selection of Spiral A on Material 1 was a new plant design (feasibility study) with the smallest possible footprint for mobility considerations. The reason for the selection of Spiral A and Spiral B on Material 2 was based on a project that considered the possible replacement of the old worn out MG4 spirals with higher capacity HC1 spirals in an

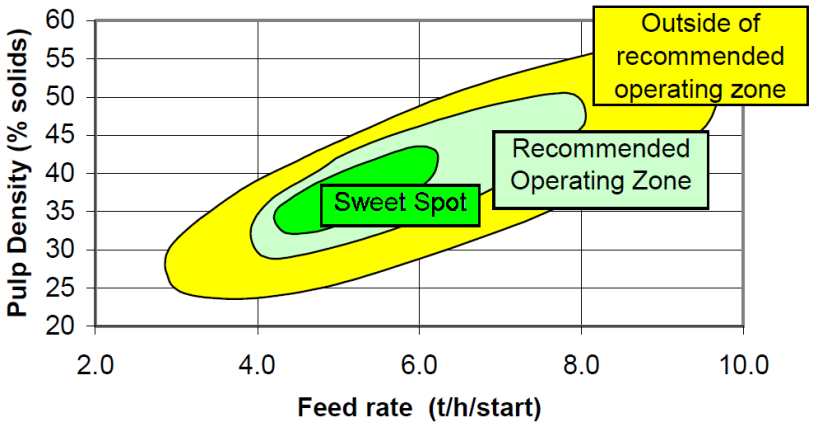

Figure 5.2: Recommended operating window as a function of pulp density and feed rate for spiral A. (Mineral Technologies 2014)

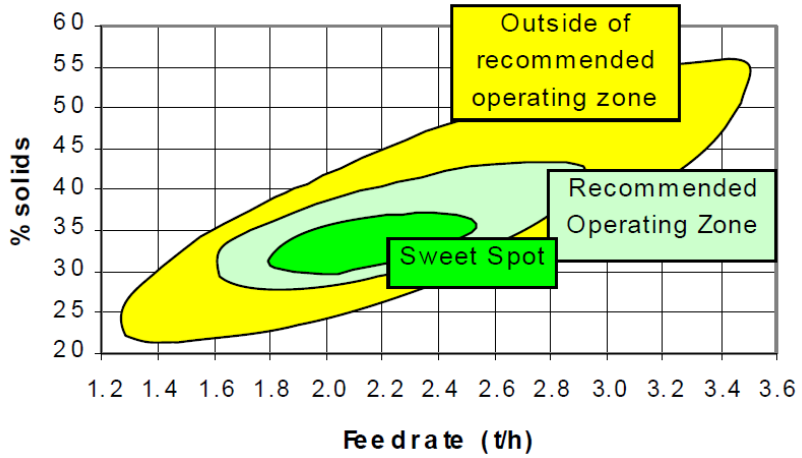

Figure 5.3: Recommended operating window as a function of pulp density and feed rate for spiral B. (Mineral Technologies 2014)

existing operation, which could assist with potential plant expansion later on. There are many more considerations when replacing low capacity spirals with high capacity spirals, but for the purpose of this investigation it was spiral separation performance.

5.3 Test-work Methods

Spiral test-work involved the evaluation of the two different spiral profiles (A and B) and the two materials (1 and 2), which produced three sets of test-work data (Material 1 on Spiral A, Material 2 on Spiral A and Material 2 on Spiral B). The test-work equipment was configured to control three operating parameters namely throughput, solids concentration and slimes content. The results of the individual tests were classified in terms performance (high, medium, low). The three selections (material and profile) and three performance brackets produced nine test-work groups as numbered 1 to 9 in Table 5.2. The equipment configuration and sampling techniques that were applied are discussed in the Section 6.1 and Section 6.2.

Table 5.2: Summary of test groupings and average operating parameters.

Group nr.	Performance	Feed material	Spiral profile	Nr. of tests	Ave. feed rate (t/h)	Average %solids	Average %slimes	Average %THM
1	High	1	A	3	4.40	39.5	2.6	14.0
2	Med	1	A	8	5.71	44.4	3.3	13.7
3	Low	1	A	3	6.93	50.6	3.7	13.8
4	High	2	A	5	5.60	36.4	4.1	11.7
5	Med	2	A	4	5.51	35.4	4.8	11.1
6	Low	2	A	2	5.35	34.1	7.1	10.9
7	High	2	B	3	1.87	36.7	4.5	12.3
8	Med	2	B	5	2.03	37.1	5.8	10.5
9	Low	2	B	6	2.17	35.4	6.5	10.9

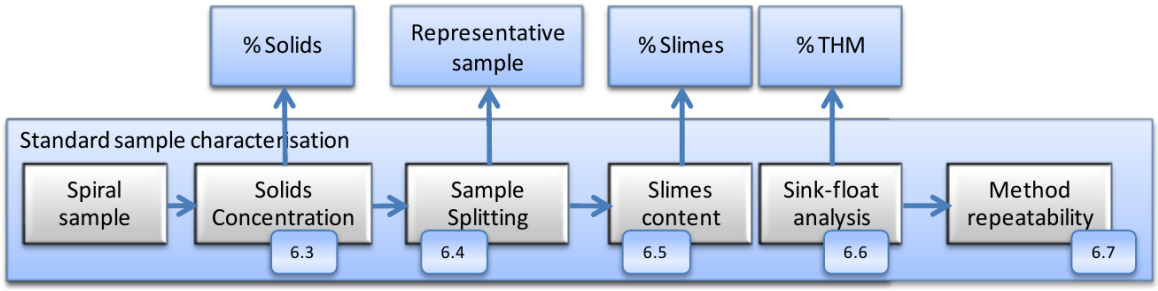

Figure 5.4: Description of standard sample characterisation. (Numbered block has reference to specific section in which it was discussed.)

5.4 Standard Material Characterisation Methods

The solids concentration (%Solids), slimes content (%Slimes) and total heavy mineral content (%THM) were determined using standard methods well known in industry. The characterisation process and the applied methods are presented schematically in Figure 5.4. Water was first separated from the sand-slime mixture to determine solids concentration. This was followed by separating the sand from the slimes to determine slimes content. Finally the high-density particles were separated from the low-density ones to determine the THM content. Representative solid material samples were split out during the process. Splitting procedures are critical in heavy minerals due to the large density differences that cause segregation and various sizes of rotary splitters were used in all cases. The reproducibility of the combination of these methods had to be demonstrated to provide confidence in the standard characterisation step. Details on the reproducibility and on the individual methods are provided in Chapter 6 in the sections indicated in Figure 5.4.

5.5 Enhanced Material Characterisation Methods

During enhanced characterisation rich data sets of material properties were created. Figure 5.5 shows the different methods involved in this step. These methods are introduced briefly here and discussed in detail in Chapter 7. The input to the enhanced material characterisation step is the sink and float mass fractions produced with the standard methods. These samples were split carefully to isolate small, representative particle populations for further characterisation. The particles were then set in resin and polished to produce polished blocks ready for Qemscan® analysis. The data set produced by the Qemscan® describes the size and density of the analysed population of particles. Details of the methods are presented in Chapter 7 in

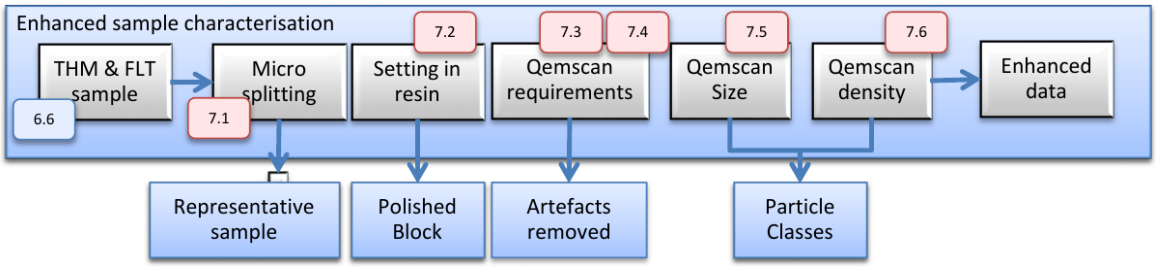

Figure 5.5: Description of enhanced material characterisation. (Numbered block has reference to specific section in which it was discussed.)

the sections indicated in Figure 5.5. Other important aspects, including how to ensure representative analyses and comparison of Qemscan® result with that of other characterisation techniques, are also addressed in Chapter 7. The requirements to ensure representative particle attribute outputs, over and above sample preparation, are to be adhered to so as to ensure minimum introduction of analysis artefacts. The confidence in the particle size output data from Qemscan® is demonstrated in the comparison with conventional screening. The confidence in the particle density output data from Qemscan® is demonstrated in the comparison with conventional density analysis. The combination of particle size and density output from Qemscan® allowed for setting up different particle classes as required by the user.

5.6 Enhanced Data Presentation

Once data sets had been prepared with the standard and enhanced characterisation methods, it was necessary to present the data in a manner that would clearly demonstrate the underlying nature and behaviour of the material on the different spirals. The Holland-Batt equation was selected to present the data. Some improvements were done to the equation as part of the investigation to increase the accuracy and speed of the fit to data sets. The enhanced equation showed a simple and accurate fit of the data that represented the relationship between cumulative recovery of different particle classes and cumulative yield to concentrate on the spiral profiles tested. The enhanced data presentation method was applied to both the data from the standard product characterisation as well as the data from the enhanced product characterisation, which are discussed in Chapters 10 and 12.

5.7 Standard Performance Analysis

The standard performance analysis utilised the data extracted from standard industry characterisation, which is the sink-float data. This data was plotted in relation with the four main separation attributes of yield, recovery, grade and separation efficiency. From these relationships spiral separation performance conclusions could be derived. This is discussed in more detail in Chapter 10.

5.8 Enhanced Performance Analysis

The enhanced performance analysis involved taking the rich data sets of material properties that was extracted from the sink and float fractions and plotting it in the same manner using the four main separation attributes of yield, recovery, grade and separation efficiency. The difference was that more performance data became available that described the spiral performance on a

level not done previously. The large step change in performance data is described in Chapter 11 with a comparison between the standard and enhanced performance analysis approaches.

Chapter 6

Standard Methods

Various references were made to standard methods in the previous chapter (research design). This chapter focuses on the detailed description of how each of these methods was executed.

6.1 Spiral Test-work

A closed-loop circulation configuration was used in which a sand and water mixture was pumped to a two-way distributor. The one line from the distributor was fed to the spiral while the second line was returned to the sump. The size of the orifice in the return line determined the flow rate to the spiral. The pump was fitted with a variable speed drive to provide an additional control parameter. The return line from the distributor was injected into the sump in a manner that provided sufficient agitation of the slurry at the pump's suction point. The pipe bends and distributor were carefully designed to limit solids segregation as far as possible. Refer to Figure 6.1 for a flow diagram of the physical apparatus.

Solids concentration was controlled by the systematic addition of sand to the sand-water mixture. Both throughput and solids concentration were measured by sampling the entire spiral trough for approximately 6 seconds. The total slurry mass was measured, the water decanted and returned to the sump. The moist sand was weighed with a moisture assumption to approximate the dry solids throughput prior to sampling to ensure that the throughput and solids concentration were within the target operating ranges. After calculation the sample used for feed rate approximation was returned to the sump and 5 minutes were allowed for pump stabilisation to reach a steady state condition. This was significantly longer than the sump's residence time of 1 minute. The actual throughput and solids concentration were determined by the material that was sampled for product characterisation. The approximated and actual measured values for throughput and solids concentration correlated well. The medium viscosity was increased by the addition of concentrated slimes (ultra-fines, smaller than 45 µm). Medium viscosity was decreased by the removal of slimes rich water and replacing it with equal volumes of clean water. "In process" slimes content was measured by means of medium density determination.

During the prolonged circulation of slurry in a closed-loop configuration two artificial effects might have been introduced. The first was a slurry temperature increase due to friction and the second was that the particles were scrubbed through the pump impeller action that could have increased the slimes content. Temperature was not specifically measured but the test was not allowed to run for longer than 30 minutes before samples were taken and fresh (cold) material and water was added again. Slimes content was measured prior to sampling to ensure that the target slimes content was correct.

During test-work the above mentioned spirals were easily interchanged in the same test-work configuration shown in Figure 6.1. With the interchangeable orifice in the slurry feed line and

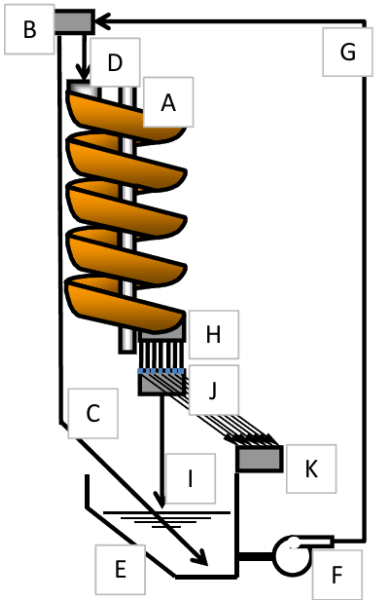

A	Spiral trough
B	Distribution box
C	Slurry return line
D	Slurry feed line
E	Slurry sump
F	Slurry pump
G	Pump delivery line
H	Mouth organ cutter
I	Normal flow line
J	Seven way sampler
K	Sample exit point

Figure 6.1: Spiral test-work apparatus.

the variable speed drive on the slurry pump higher and lower tonnages could be easily achieved to test the two spirals within the required operating window.

6.2 Spiral Product Sampling Method

Each spiral was fitted with a mouthorgan splitter to divide the spiral trough into seven cuts. The material continuously flowed through the seven stream sampler and returned to the sump. Refer to Figure 6.1 for detail on the flow through the sampler. During sampling all seven cuts were sampled simultaneously through a pneumatic cylinder pushing the diverter plates across, causing the material to divert into sample containers instead of returning to the sump. Care was taken not to exceed the residence time on the spiral during sampling because it would have compromised sample integrity. When a sample is removed out of the circulating loop the steady state condition is compromised and the feed composition to the spiral could change. Feed rates were calculated using the actual sample taking period.

Material residence time is calculated based on the number of turns, the trough diameter and the average slurry speed. The spiral under consideration has 7 turns with a 600 mm diameter and an average slurry speed of 1 m/s (determined by direct measurement of residence time of specific spiral profile). Refer to Equation 6.1.

$$t = \frac{\text{average distance}}{\text{average speed}} = \frac{7\,\text{turns} \times \pi \times 0.6\,\text{m}}{1\,\text{m/s}} = 13\,\text{s} \tag{6.1}$$

6.3 Solids Concentration Determination

To measure solids concentration the sample was first weighed in its wet, "as sampled", state to determine its "wet mass". It was allowed to settle out to allow for the decanting of clear water without any slimes loss. Siphoning was done on samples with low solids concentration. Addition of small amounts of flocculent assisted with speeding up the settling process. The flocculent did not influence the solids concentration or slimes content and the flocculated slimes material was not used for other test-work. The total solid mass in the wet sample was dried in a convection oven at 150 °C to remove all moisture. The sample was weighed in its dry state

to determine its "dry mass". The "dry mass" divided by the "wet mass" was termed solids concentration. No sample splitting was performed on the sample in its wet state and the total "as sampled" mass was handled in this manner.

6.4 Sample Splitting

The term sample splitting is used to describe the process in which a representative sub-sample is divided or cut from a larger sample. The equipment that was used for this process is called a rotary divider. Each size rotary divider has a maximum and minimum allowable feed sample size. The rotary divider also has a minimum number of revolutions (60) that it has to turn for the sub-sample to be representative. All the rotary dividers (Dickie and Stockler units) that were used in this investigation are fitted with turret orifice feeders as opposed to the normal vibrating chute feeders. Heavy minerals tend to segregate on a vibrating chute introducing possible bias during the splitting operation. The splitting procedure for heavy mineral samples is crucial since the density differences between particles are significant, which leads to segregation in any splitting device. This must be minimized through laboratory equipment selection. The feed samples used in the spiral test-work apparatus to supply the circulating loop were also split with a large rotary divider.

6.5 Slimes Content Determination

After drying, the material tended to lump together because of the slimes. The sample was therefore screened on a 1 mm screen to de-lump the material prior to splitting. A portion of the total "dry mass" was split through two rotary sample dividers to produce a 400 to 500 g sample that was wet screened on 45 µm aperture. The sample was manually scrubbed on the 45 µm screen until the water draining from the screen was clear. The plus 45 µm mass fraction was retained and the minus 45 µm mass fraction was discarded. The plus 45 µm mass fraction was dried and weighed to determine the "dry sand mass". The "minus 45 µm mass fraction" (calculated by difference) divided by the "dry mass" prior to screening was termed the slimes content.

6.6 Sink-float Analysis

The sand fraction from which all the slimes material was liberated and removed was processed by means of a sink-float funnel containing TBE. The detail of the sink-float test is discussed in Chapter 2, page 35. The dried sand fraction was fractionated into THM (total heavy minerals) and FLT (float) masses. The sink-float funnel had a feed mass limitation of 250 g. The sample was split in two and recombined after sink-float fractionation. Both fractions were cleaned from any organic liquid residue and dried. The dry "sink mass" divided by the dry sand mass fed to the sink-float funnel was termed the THM content. In the case where the THM content was below 1 %, more mass was split (700 - 800 g) for the sink-float fractionation. The sink fractions of three sink-float funnel separations were combined which produced sufficient material for further fractionations.

6.7 Evaluation of Method Consistency

6.7.1 Background

During measurement of spiral separation performance the influence of a combination of operating parameters had to be considered. These parameters had to be well controlled to ensure steady state separation conditions. Steady state conditions were required to make reasonable conclusions about spiral separation performance. To demonstrate that the test-work apparatus could deliver reproducible results many of the sampling sets were done in triplicate. These three tests were evaluated on four critical aspects, namely solid mass distribution, THM distribution, water distribution and slimes distribution across the spiral trough. All of them had to be the same within a reasonable degree of variation. At the same time the solids concentration, throughput, slimes content and THM content, back calculated from the products had to match the feed sample attributes closely.

6.7.2 Results

Table 6.1 summarises the feed conditions from the three tests that were repeated. Figures 6.2 to 6.5 present the variability in the four critical mass components of solids content, THM content, slimes content and water content. The raw data for these figures are presented in Appendix 2 to 6.

The weighted sum of the measurement differences is given in Table 6.2 and expressed by Equation 6.2. The purpose of this table is to quantify the variability between the tests with a single number. The distribution of the mass component (x_i) of each test across the seven spiral fractions is subtracted from the average ($\bar{x}$) of the three tests. The absolute differences are multiplied by the mass (x_i) it represents. For example, the dry mass distribution difference between Test 3 and the average (Test 1 to 3) for Cut 7 is 1.01 (29.26 - 28.25). This difference is multiplied by the 28 % of mass it represents of the total, contributing to more than half (0.29) of the total difference of 0.43 in Table 6.2.

$$\text{sum of weighted differences} = \sum_{i=1}^{7} \frac{|\bar{x} - x_i|}{100} x_i \tag{6.2}$$

Table 6.1: Operating parameters of repeatability tests.

Test	Feed Rate (t/h)	%Solids	%Slimes	%THM
1	4.34	38.76	2.42	14.23
2	4.50	39.70	2.63	14.19
3	4.37	39.94	2.77	13.55

Table 6.2: Weighted sum of measurement differences (test value versus average).

Mass Component Measurement	Test 1 vs. Ave	Test 2 vs. Ave	Test 3 vs. Ave
Dry mass	0.33	0.23	0.43
THM	0.23	0.21	0.19
Slimes	0.74	0.30	0.47
Water	0.57	0.57	0.04

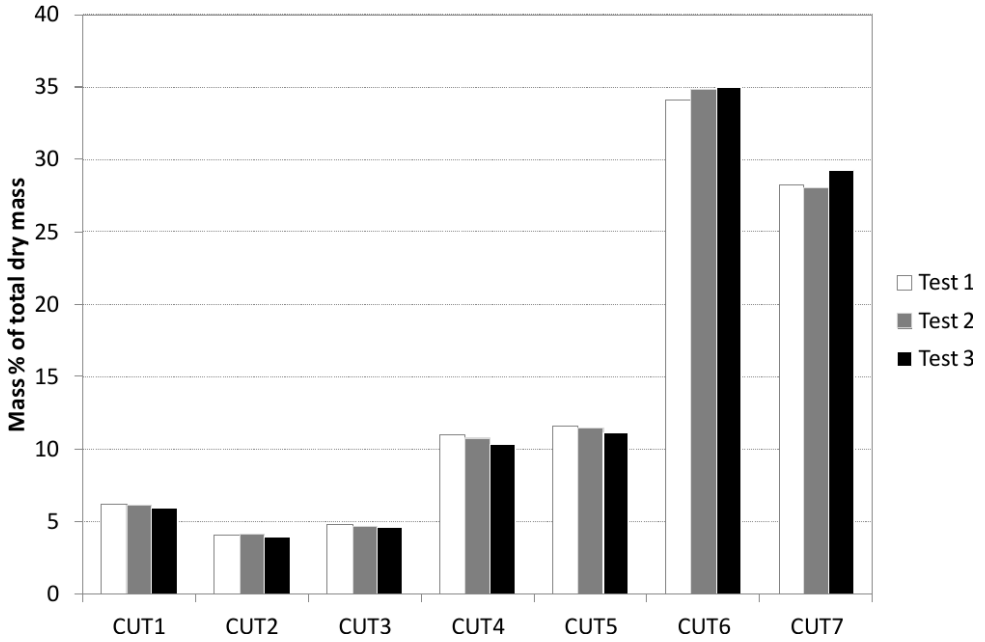

Figure 6.2: Solids content distribution across the spiral trough for repeated tests.

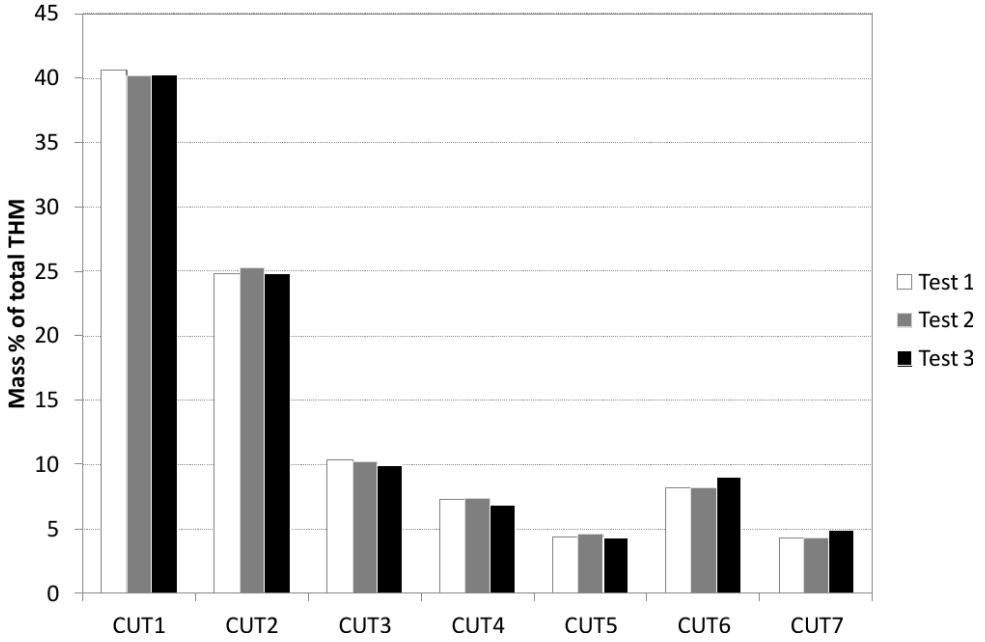

Figure 6.3: THM content distribution across the spiral trough for repeated tests.

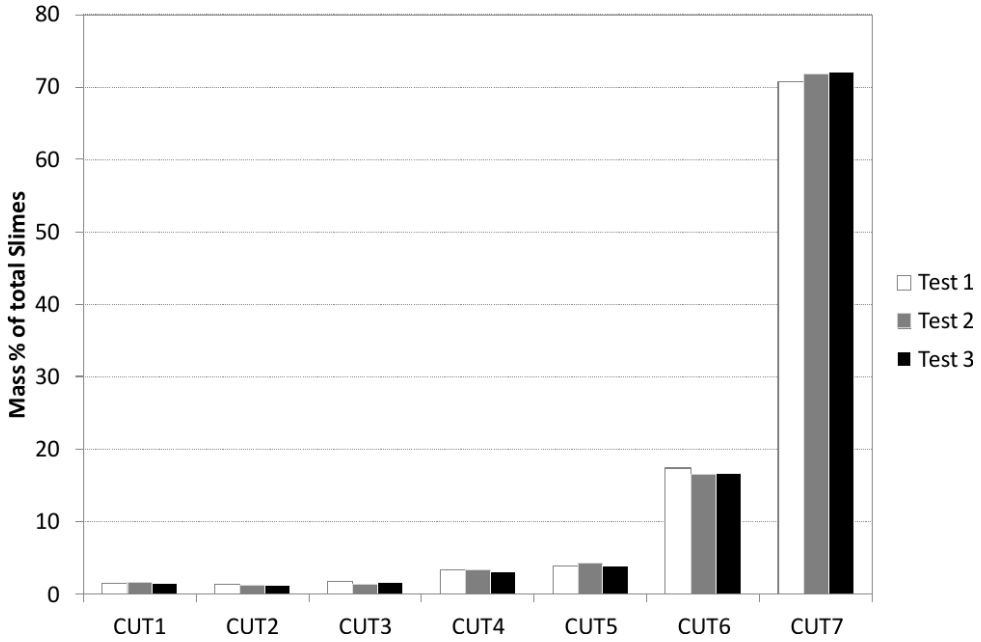

Figure 6.4: Slimes content distribution across the spiral trough for repeated tests.

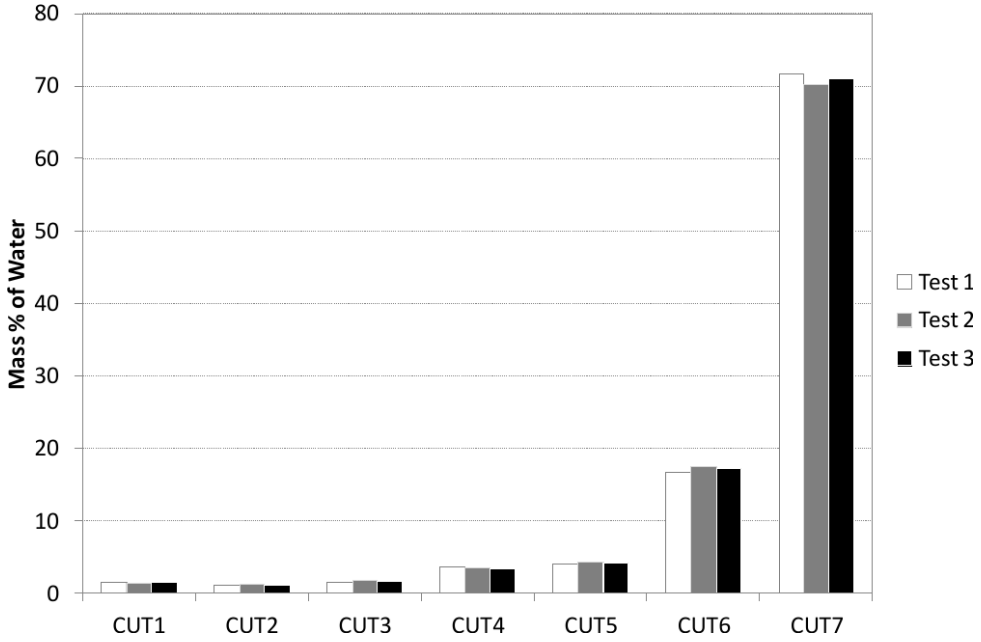

Figure 6.5: Water content distribution across spiral trough for repeated tests.

6.7.3 Discussion

The three repeat tests showed a high degree of consistency for all four mass attributes. Keep in mind that the consistency of these mass attributes not only reflects the test-work apparatus, but also the sample preparation and characterisation that was performed after samples were taken. These sample analyses included wet and dry weighing, sample drying, sample splitting, wet screening to determine slimes content and sink-float analysis. Table 6.2 provides the summary of the weighted measurement differences between the test value and average test value demonstrated in the four figures. From Table 6.2 it can be seen that THM showed the highest consistency and slimes the lowest consistency, but with an overall high level of consistency in the repeat tests.

During spiral separation the slimes distributed homogenously through the water to form part of the separating medium rather than the solids. The implication of this behaviour was that the water and the slimes had similar mass percentage distribution across the spiral trough. This can be clearly seen when comparing Figure 6.4 and Figure 6.5. The slimes content determination of samples containing small amounts of slimes and large volumes of water is notoriously difficult. Special attention was given to retain slimes within these samples and achieve consistent analysis results. Flocculation and removing water through siphoning was used. These consistent results gave the necessary confidence in the ability of the test-work apparatus and in the sample preparation methods to accurately measure spiral separation performance with limited artefacts.

Chapter 7

Enhanced Material Characterisation Methods

The 'enhanced methods' presented here did not replace the standard methods discussed in Chapter 6, but aimed to provide characterisation information in addition to the THM and FLT fractions produced by the standard methods. This relationship is illustrated in Figure 5.5. In this chapter the detail of the different methods and their validation results are presented and discussed.

7.1 Micro Splitting

The term 'micro splitting' is used to describe the process in which a representative sub-sample (1 to 2 g) is divided or cut from a sample weighing less than 10 g. The equipment that was used for this process is called a micro rotary riffler (or micro rotary divider). Figure 7.1 shows the unit that was utilised in this investigation. All the samples that were prepared for Qemscan® analysis were representatively divided by means of micro splitting. This is a standard splitting method for typical mineral analysis laboratories, but it is discussed under enhanced methods as the first critical step.

7.1.1 Consistency Evaluation

Since the micro splitting procedure played such a crucial role in this investigation it was necessary to confirm splitting consistency. This test was done by comparing the chemical composition

Figure 7.1: Rotary micro riffler. (Quantachrome 2014)

of the different sub-samples produced by a series of rotary dividers including the rotary micro riffler. As preparation for the chemical analysis with ICP-OES the sub-samples were crushed to fine powder, which limited the bias in the chemical analysis itself. Differences in the assays of the sub-samples were attributed to splitting accuracy.

7.1.2 Consistency Results

Table 7.1 presents the chemical assays of five different sub-samples that were produced through a series of rotary dividers. Note that not all the elements are indicated in the table. The assays show a high level of consistency with a low level of variability considering that there were over 30 different minerals present in the samples. Table 7.2 presents a similar comparison used in Table 6.2, calculated with Equation 6.2. The results from these tables provided the necessary confidence in the sample splitting method that was used as the basis of the other enhanced methods.

Table 7.1: Chemical assays of six sub-samples from rotary dividers. (C.V. = coefficient of variation)

	SiO_2 %	Al_2O_3 %	Fe_2O_3 %	TiO_2 %	CaO %	MgO %	ZrO_2 %	CeO_2 %	Th %	LOI %	Tot %
Split 1	4.59	2.67	40.6	42.2	0.1	0.58	4.29	0.76	2417	1.74	100.85
Split 2	4.86	2.7	41.38	42.56	0.09	0.59	4.07	0.78	2471	0.21	100.55
Split 3	4.69	2.8	40.46	41.11	0.1	0.58	4.4	0.8	2586	1.88	100.26
Split 4	4.71	2.8	39.89	42.31	0.1	0.58	3.8	0.8	2538	1.83	100.27
Split 5	4.67	2.81	40.37	41.24	0.09	0.57	4.37	0.83	2561	1.84	100.24
Split 6	4.73	2.9	40.06	41.31	0.08	0.57	4.48	0.82	2585	1.81	100.32
Avg.	4.71	2.78	40.46	41.79	0.09	0.58	4.24	0.80	2526	1.55	100.42
Std. Dev.	0.09	0.08	0.52	0.64	0.01	0.01	0.25	0.03	68	0.66	0.24
C.V.	0.019	0.03	0.013	0.015	0.087	0.013	0.06	0.032	0.027	0.425	0.002

Table 7.2: Weighted sum of measurement differences (split value versus average).

Mass Component Measurement	Split1 vs. Ave	Split2 vs. Ave	Split3 vs. Ave	Split4 vs. Ave	Split5 vs. Ave	Split6 vs. Ave
Splitting	0.25	0.75	0.31	0.49	0.29	0.39

7.2 Sample Block Preparation

Qemscan® analysis required that the particles be set in resin. A small representative sample of less than 2 g was mixed with a liquid resin having a viscosity similar to that of toothpaste. This resin had to be sufficiently viscous to limit particle segregation but liquid enough to allow air bubbles to comfortably escape from the mixture. The ratio of resin to particles was equally important to ensure a high density of particles within the resin. Carbon was mixed into the resin to limit contact between mineral particles. The resin mixture was placed in a small cylindrical mould and left to dry. This solidified resin-impregnated disc, also referred to as a sample block, had a typical diameter of 30 mm and was 15 mm thick. Once solidified completely, the top layer of the block was polished away to expose cross sections of the particles. The thickness of the layer that was to be removed had to match the thickness of half of the average sized particle (roughly 60 µm).

From the above description it can be seen that the block preparation method is sensitive to operator influence. An unskilled operator can introduce many sample analysis errors through

inconsistent preparation. The operator that was responsible for the block preparation in this investigation was highly skilled and had more than 15 years of experience. The operator skill had been proven with regards to reproducing mineralogical assays. The difference, however, with this investigation was that particle texture properties, namely particle size and particle shape, were now measured as well, which required an even higher standard of sample preparation consistency. Two critical questions had to be answered regarding sample block preparation. The first was to determine the influence of block preparation on Qemscan® analysis accuracy. The second was to determine the influence of the number of particles analysed on Qemscan® analysis accuracy. These two questions are answered in the next two sections.

7.2.1 Block Preparation Consistency

The micro splitting method produced three representative samples. Each sample was prepared with the same block preparation method described above. The material that was selected for this comparison was a total heavy mineral sample that contained the whole spectrum of different mineral particles. (THM from Cut 5 in Test 3 was selected. Refer to Appendix A.). Three particle property distributions were compared. The first was the particle density distribution, the second was the particle size distribution and the third was the particle shape distribution. Particle density was determined by Qemscan® particle composition analysis and is discussed in section 7.3.2. Particle size and shape was determined by Qemscan® software and are discussed in Section 7.3.1 and Section 7.3.3. The Qemscan® particle size distributions of the three blocks are presented in Figure 7.2a. These three distributions had a high degree of correlation. More variation was detected at the coarser size fractions.

Table 7.3: Weighted sum of measurement differences for different sample blocks.

Mass Component Measurement	Block1 vs. Ave	Block2 vs. Ave	Block3 vs. Ave
Size	0.34	0.45	0.42
Density	0.56	0.70	0.94
Shape	0.53	0.58	0.55

Qemscan® particle density distributions of the three blocks are presented in Figure 7.2b. These three distributions had a high degree of correlation. Some variation could be detected at the lower density fractions. The greatest variability was 5 % between Block 1 and 3 at a Qemscan® particle density between 3.3 and 3.4 g/cm^3

Qemscan® particle shape factor distributions of the three blocks are presented in Figure 7.2c. These three distributions had a high degree of correlation. Some variation could be detected at the higher shape factors. The greatest variability was 3.5 % between Block 2 and 3 at a Qemscan® particle shape factor of 19. Note that particle shape factor was not considered in the rest of the investigation and was only used as textural comparison other than particle size to validate preparation consistency.

The indicated variation gives the accuracy window in which these results should be interpreted. The greatest variation detected is 5 % on cumulative mass for the particle density distribution at a specific interval. Table 7.3 quantifies the variation and demonstrates that density distribution had the greatest variation. This variation is a combination of the sample preparation method as well as the block analysis, since the comparison was done on analysis results. Although this method is not new to mineralogical analysis techniques, its consistency had to be validated for textural properties (particle size and shape), since these properties are critical outputs of the enhanced characterisation method. The high level of compositional (density) and textural (size and shape) correlation in the three sample blocks gave confidence in the sample preparation method as part of enhanced characterisation.

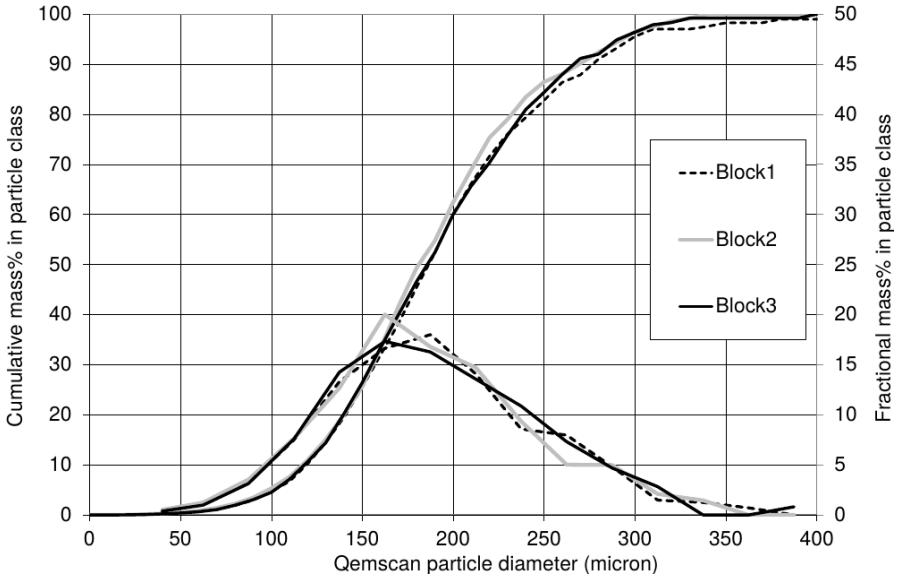

(a) Size distribution.

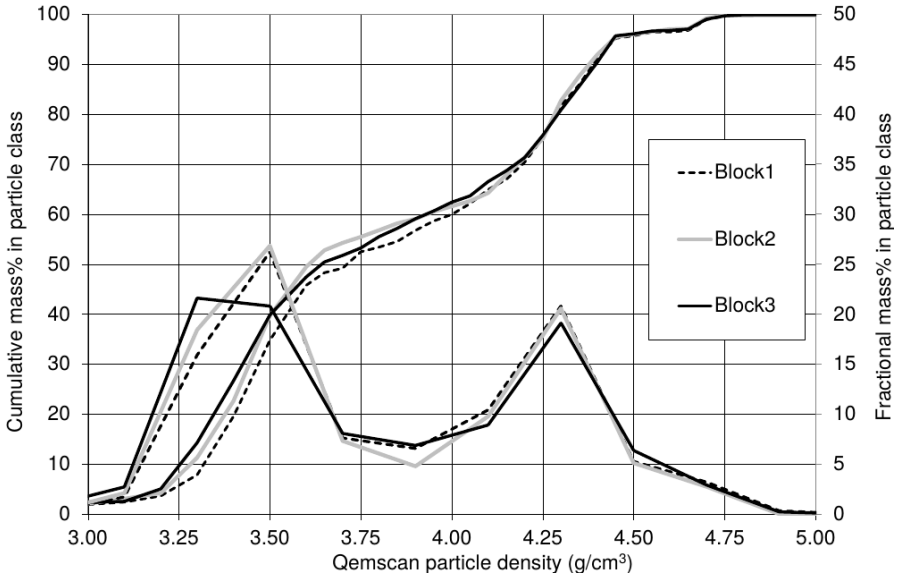

(b) Density distribution.

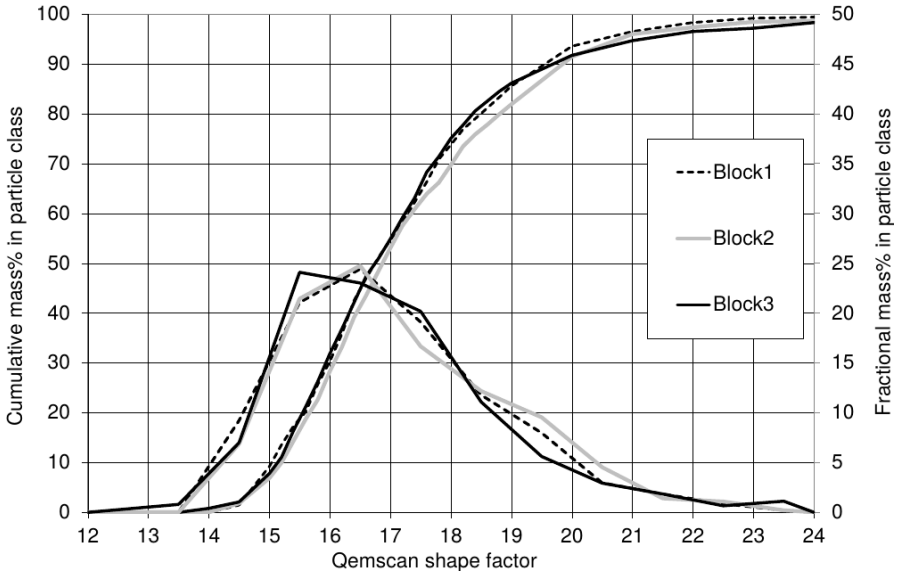

(c) Shape factor distribution.

Figure 7.2: Comparison of different sample blocks. (Sample = THM, test 3, cut 5, 3215 particles analysed)

7.2.2 Particle Population Size

A minimum number of particles is required to accurately represent larger particle populations. A single sample block was analysed at increasing numbers of particles, 1000, 2501, 4922 and 9849. These four analyses were compared to determine the minimum particle number to accurately measure the three mentioned particle property distributions (size, density, shape). The sample used for this evaluation was THM from Cut 1 in Test 3; refer to Appendix A for more specific sample attributes.

Figure 7.3a presents the cumulative size distributions of the four particle populations. All the lines correlated well with the exception of the 1000 particle line that showed a minor break away towards the coarser particle sizes. The same trend was observed in the block preparation data, which indicates a weakness in Qemscan® to analyse over a wide particle size range. If there are a significant number of particles above 300 µm, it should be considered to screen these particles out, prepare a separate block and analyse them separately.

Table 7.4: Weighted sum of measurement differences for different particle population sizes.

Mass Component Measurement	4922 **vs.** 9849	2501 **vs.** 9849	1000 **vs.** 9849
Size	0.13	0.42	0.46
Density	0.18	0.48	0.63
Shape	0.16	0.30	0.51

Figure 7.3b presents the cumulative density distributions of the four particle populations. All the lines show a high degree of correlation. Particle density is derived from particle composition, an internal particle property, and would be less sensitive to particle population size. Figure 7.3c presents the cumulative particle shape factor distributions of the four particle populations. All the lines show a high degree of correlation, although less than the density distribution and more than size distribution.

Table 7.4 summarises the weighted measurement differences per particle class with the largest population as reference. The values do not have physical meaning and are used for relative comparison. From this table it could be seen that all three particle property distributions are influenced with density slightly more affected. From Table 7.4, the decreasing number of particles that were analysed indicated that the most significant drop in consistency occurred between 4922 and 2501 particles. The ideal will be to analyse close to 5000 particles but definitely more than 2500 particles. The limitation on the amount of particles analysed is analysis time. A balance between short analysis times and consistent analysis results are therefore required. A standard of more than 2500 particles was chosen for this study with the typical number of analysed particles around 3800 to 4000. Although the variation in particle population size in Table 7.4 was less than for block preparation in Table 7.3, it still provided a guideline for the particle population size required not to introduce additional analytical bias. All these errors are cumulative in nature and where possible, it should be minimised. The variation in the block preparation procedure was double that of particle population variation for small populations when comparing values in Table 7.3 and Table 7.4. This illustrates the importance of accurate physical sample preparation procedures. Qemscan® program selections and data processing parameters, such as particle population size, grid size, and counts per second can all be easily modified and repeated to increase the quality of the data, but sample block quality is determined by its once-off preparation (splitting, mixing, setting and polishing).

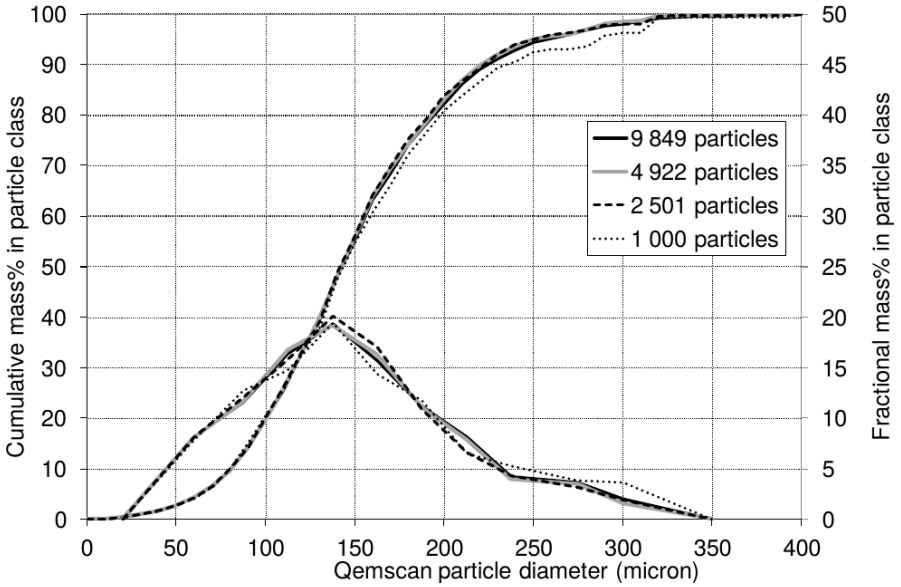

(a) Size distribution.

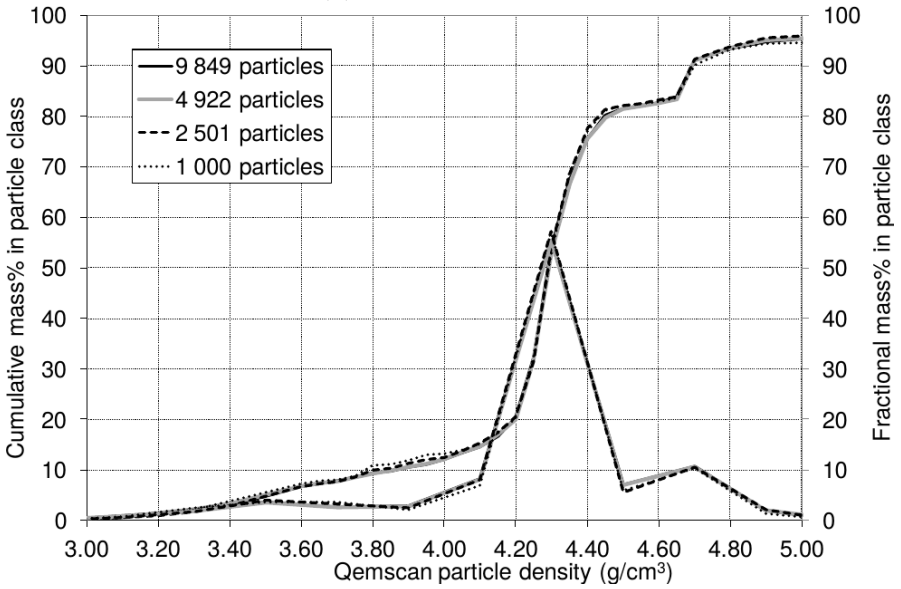

(b) Density distribution.

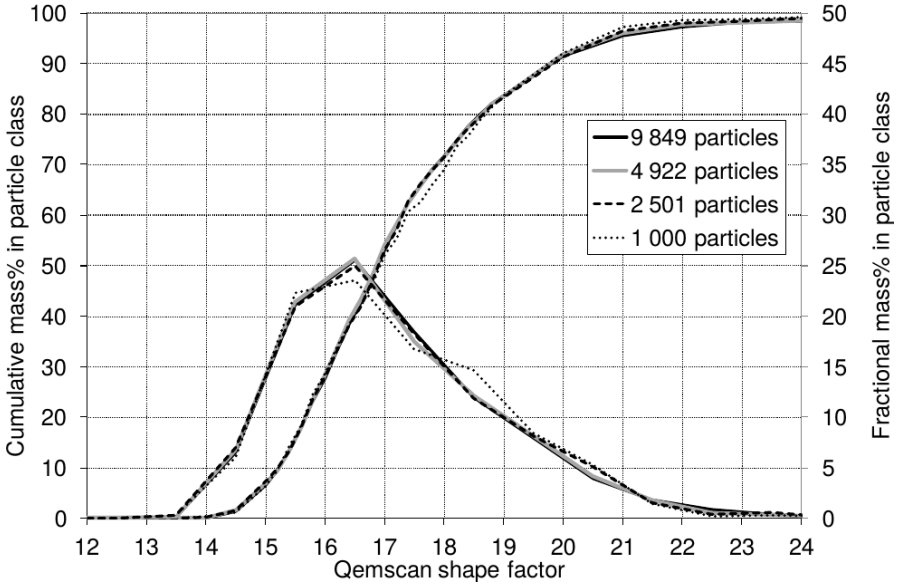

(c) Shape factor distribution.

Figure 7.3: Comparison of different particle population sizes.

7.3 Qemscan® Analysis

Qemscan® is an automated mineralogical analyser commonly used in the mineral processing industry to determine mineral composition. In this study Qemscan® was however utilised as a particle analyser, linking textural (size and shape) and compositional (mineral and density) data to individual particles. The sample block presented a two dimensional view (cross section) of the particles to Qemscan®. From this cross section Qemscan® produced a two-dimensional compositional image, see Figure 4.2, page 53, (from reflected light, backscattered electrons and energy dispersive x-ray) that is converted to a numerical list of three-dimensional particles that is used for calculations and interpretations. Qemscan® software does consider the stereological effect in the assignment of a diameter to the particle (Intellection 2009). There are numerous articles discussing the theory behind stereological corrections (**gay2004**; Gay and Keith 2001). It is, however, not the purpose of this investigation to validate Qemscan® two-dimensional to three-dimensional conversion, neither to demonstrate the statistical basis of the process. This investigation validated Qemscan® particle characterisation output with comparison to other methods and used this data to develop and validate an enhanced analysis method to better understand spiral separation performance. The next three sections briefly explain the method of quantifying particle properties such as size, density and shape. Particle shape was not applied in the interpretation of the spiral separation performance results but it was utilised in the validation of Qemscan® particle characterisation results. The apparatus used in this study is described in Table 7.5.

Table 7.5: Particulars of the Qemscan® apparatus used in this study.

Product	Qemscan® 4300 on Zeiss Evo 50 SEM platform.
Detector type	Bruker Xflash
X-ray data resolution	5 µm point spacing
Accelerating voltage	25 kV
Specimen current	5 nA

7.3.1 Particle Size

A combination of reflected light and backscattered electrons in the Qemscan® analysis chamber provides the particle outlines due to their contrast with the carbon-resin mixture in which it was set. These two dimensional images (surface area and surface shape) contain sufficient information to assign a particle diameter to each individual particle with the assistance of processing software within Qemscan®. The outcome from this process is a list of unique particles each with its assigned diameter. Stereological relationships contained within the software convert the area of the particle into particle volume. The mass of the particle is dependent on the density of the particle, which is discussed next.

7.3.2 Particle Density

Qemscan® measures particle density by dividing the intersected particle surface into a user-defined grid pattern (for this study a 5×5 µm grid was selected). The elemental composition of each grid block is determined by energy dispersive x-ray captured by Qemscan® detectors. The elemental composition is converted to mineralogical composition by a specie identification protocol (SIP) file. Each mineralogical composition will have its matching density in the software system. The final density of the particle is the weighted average of all the individual grid block analyses. Once the particle density is known the particle volume can be converted to particle mass. The outcome from this process is a list of unique particles, each with its assigned particle diameter, density and mass.

7.3.3 Particle Shape

During particle size determination the surface of the particle become available. The perimeter, longest axis and shortest axis of the particle surface are also available. From surface perimeter and surface area a basic particle shape factor, explained by Equation 2.7, page 36, is determined.

7.4 Qemscan® Analysis Requirements

Since the particle attributes of size and density from Qemscan® were used in the study and not just the total mineral composition, it required a detailed look at all the parameters that could possibly influence particle characterisation integrity. A list of requirements were developed that enables the user to minimize artefacts from Qemscan® application in this enhanced characterisation method.

7.4.1 Sample Block Preparation Consistency

As discussed in Section 7.2.1 the reproducibility of the particle characterisation output data from the same head sample is paramount. The block preparation method will also include the bias from the micro splitting method and might need to be evaluated separately. The evaluation method used in this study can be applied as a guideline to ensure that the total sample preparation bias is measured and minimized as far as possible.

7.4.2 Particle Population Size Selection

As discussed in Section 7.2.2 the selection of the number of particles to be analysed needs consideration. Smaller particle populations will allow for faster analysis times with insignificant compositional variances. However, when particle characterisation outputs from Qemscan® are pursued it will require the user to select a minimum of 2500 particles to be analysed to ensure consistency in Qemscan® output.

7.4.3 SIP-file Development

The SIP-file (specie identification protocol) is the term used in Qemscan® terminology to describe the relationship between mineral data and analysed elemental data. This relationship is used to convert the raw output from electron detectors to mineral output. It is therefore important that this relationship is correct to ensure the correct mineral data output and correct interpretation. The SIP-file is developed and validated with other analytical methods such as X-ray diffraction, X-ray fluorescence, induced coupled plasma (ICP) and iron titration. These analytical methods were previously performed to confirm the accuracy of the SIP-file that was used in this study, and this validation data does not form part of this study. Without a tried and proven SIP-file, the outputs from Qemscan® are subject to error. The accuracy of the SIP-file can be measured with a correlation analysis done on the back calculated chemistry from the mineralogy (after SIP conversion) and the chemical assay from XRF or ICP. If the correlation is poor it implies that the SIP-file is inadequate and unable to convert the EDX spectrum to the correct mineralogical composition. A SIP-file might be accurate for one type of mineralogy (location dependant) and inadequate for another. For this reason SIP-files are developed and refined for specific deposits. New deposits are usually analysed with generic SIP-files before the detail development can commence.

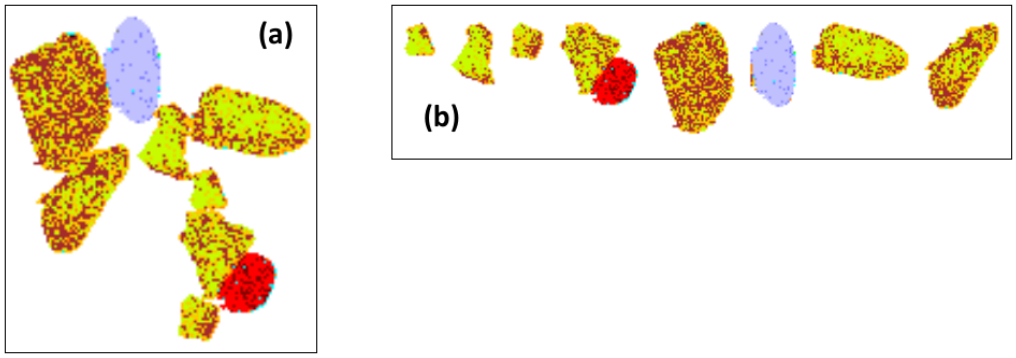

Figure 7.4: Visual presentation of particle de-clustering. (Particle cluster caused by setting particles in resin (a) and particles de-clustered after processing with Qemscan® touching particles pre-processor (b).)

7.4.4 De-clustering of Particles

The textural data from Qemscan® need to be 'corrected' to characterise particle size. The discrepancy occurs during the sample preparation process. During setting of thousands of particles in resin there are many instances of particles that are touching each other. Qemscan® would not recognize that these particles are not individual particles and see it as a single large particle with an abnormally large particle diameter and irregular shape with a weighted mineral density of all the particles present in the particle cluster, as shown in Figure 7.4.

To overcome this problem the particle information firstly had to be processed and saved in the particle manager (Qemscan® software) after ripping the clusters apart "digitally" as far as possible so that the analysis represents single particles. The de-clustering process can increase the number of analysed particles from 2000 up to 3500 particles, thus increasing the particle population significantly. Excessive de-clustering will alter the true size distribution and create small artefacts. These artificial particles can be filtered out. The particle shape trends of the population before and after the de-clustering process assist the operator in selecting the correct settings. There is also an option to identify touching particles that are suspect in the sense that they might not be reflecting the true nature of the sample but rather a preparation artefact. These particles could be selected and removed from the population. An example of this phenomenon can be seen in Figure 7.4 where the red and yellow particles are closely touching. The chances of these two particles being naturally cemented as indicated is highly improbable, and it could therefore also be excluded from the particle population during the de-clustering and correction process. After the correction process, that was de-clustering and raw particle-by-particle data export, the "picture" output is converted to a numerical output - a list of approximately 3500 particles, each particle with its unique mass, diameter, density and shape factor.

The number of touching particles can be reduced through the addition of carbon in the resin during the sample block preparation step, but this will also limit the number of particles that are exposed on the surface of the sample block.

7.4.5 Mineral Density Confirmation

Qemscan® software requires the user to specify the densities of the primary mineral phases as contained in the SIP-file. These densities are used to convert an analysed particle surface to particle mass. It was therefore important that the correct densities are used as supported by various sources in literature (Webmineral 2014; Mindat 2014) to ensure that the mass conversion was done correctly and that the particle density calculation was accurate.

7.4.6 Exclusion of Ultra-fine particles

During sample block polishing some particle fragments are physically ripped off from larger particles, but remains behind in the resin of the polished block and are also analysed. Since all the samples were wet screened at 45 µm and subjected to sink-float analysis with TBE it is highly unlikely that there would be particles smaller than 45 µm. This artefact increases the ultra-fine particle population. To overcome this problem, Qemscan® software allows the user to specify a particle size threshold below which particles will not be analysed and excluded from the particle population, or the particles can be removed afterwards. In this study all particles smaller than 45 µm were ignored and excluded from the particle population. The effect of this artificial fine particle population is demonstrated in the next section.

7.5 Qemscan® Particle Size Validation

7.5.1 Method Background

A Qemscan® size distribution was compared with one determined with the standard screening method to validate Qemscan® particle size measurement. Standard screening utilises 150 to 200 g of sample on a sieve shaker using standard Tyler series screens (200 mm diameter) and separates the sample into sized mass fractions. The laboratory sieve shaker unit, discussed in Section 2.5.1, was utilised to determine the particle size distribution. The screen measures the smallest particle dimension, where a slightly elongated particle would pass vertically through a square hole if sufficient time was given to reach that specific orientation.

7.5.2 Validation Results and Discussion

Figure 7.5 illustrates two particle size measurement methods, standard screening and Qemscan® analysis, performed on a THM sample from Material 1. Other heavy mineral sample types such as final products (ilmenite, zircon, rutile), quartz and different magnetic fractions were also evaluated in a similar manner. The particles were de-clustered as described in Section 7.4.4. A sufficient number of particles were analysed (2899 particles) to exceed the minimum number of particles (2500). Mineral densities within SIP-file were evaluated and confirmed on all the mineral species with a compositional percentage greater than 0.5 % in the different samples evaluated. The SIP-file was confirmed with a high degree of correlation between chemical assay and calculated assay from Qemscan® mineralogy. Sample block consistency was checked and confirmed as discussed in Section 7.2.1. Note that the fine particle population was not removed and its influence is demonstrated and discussed.

In Figure 7.5 the screen distribution shows the sharpest gradient. Qemscan® distribution and screen distribution intersected close to the D_{50} value. Qemscan® distribution indicated a larger fine particle population with 10 % minus 75 µm, while the screen showed no minus 75 µm particles. Qemscan® distribution also indicated a larger coarse particle population with 10 % plus 210 µm, while the screen showed only 3 % plus 210 µm particles. These trends were similar for the other samples evaluated.

Considering the fine particle population in Qemscan® distribution: setting spheres with equal diameters in resin and cutting them at various diameters, depending on the depth from the surface, it would produce a population of spheres with diameters smaller than the original spheres. The size distribution that was produced would be finer than the original population of equal sized spheres since in most cases the sphere would not be cut at its maximum possible diameter as indicated in Figure 7.6a. This effect is commonly referred to as the iceberg effect.

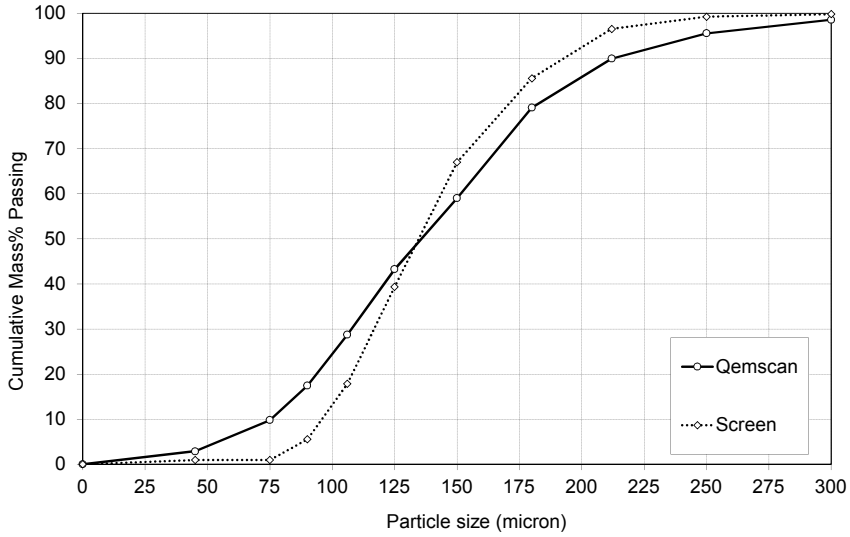

Figure 7.5: THM particle size distribution comparison between Qemscan® and screening. (Sample = Total heavy mineral, Qemscan® on 2899 particles)

The effect was more prominent in high-density resin mixtures, since the second layer of particles would just start to be intersected before the top layer of particles was intersected in the middle.

A second aspect to consider is that during sample block polishing some smaller particles are physically ripped off from large particles but remain behind in the resin of the polished block and are also analysed. Most of the samples analysed by Qemscan® indicated up to 4 % minus 45 µm, which was highly unlikely since the sample was de-slimed at 45 µm and fine particles would also remain behind in the heavy liquid medium that was used to do the sink-float analysis prior to sample block preparation. These particle fragments artificially increase the finer particle population, but had little effect in terms of shifting the PSD finer because the mass percentage contribution of these particles is small. The above mentioned two reasons caused Qemscan® D_{10} to be significantly smaller than screening D_{10}.

Screening, on the other hand, allows bigger dimension particles to go through the square wire mesh, especially with egg or elongated particle shapes, while that is not the case with Qemscan®. Qemscan® assigns a particle diameter based on equivalent spherical diameter. Figure 7.6b illustrates this difference in particle size due to particle shape. This caused a larger D_{90} value for Qemscan®. The larger D_{90} and smaller D_{10} value resulted in a less steep slope for Qemscan® distribution compared to screen distribution. The two lines are crossing somewhere between D_{40} to D_{60} in almost all the samples that were evaluated. The more rounded the particles are, the less the D_{90} will differ although there will always be smaller particles because of the sample preparation method.

In the case of quartz particles that are more irregular with sharper edges, Qemscan® can have a finer size distribution for coarser particle populations than screening. Figure 7.6c demonstrates the effect of particle shape on screen diameter and Qemscan® diameter. The more irregular and sharp the particles are the less the differences with larger particles. Figure 7.7 demonstrates how Qemscan® correlated better with coarse particle populations for sharp edged particles. The iceberg effect is still applicable causing Qemscan® to show an increased finer particle population. The iceberg effect will also be more prominent with sharp edged particles as opposed to rounded particles.

The effect of particle shape was further investigated by identifying a sample with little to no shape variation, which was a spherical ferrosilicon sample with narrow size distribution. Figure 7.8a demonstrates the particle size distribution of this spherical ferrosilicon sample as measured by Qemscan® and screening. The large difference in the fine particle population (15 % difference

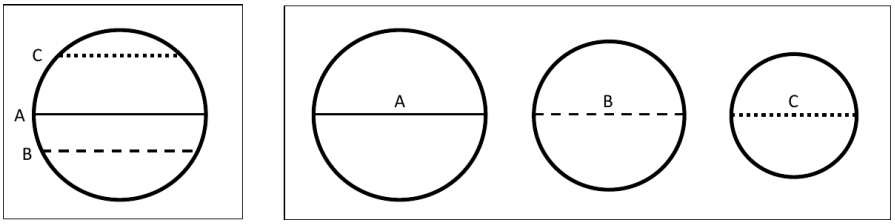

(a) Finer size distribution due to cutting spheres in resin.

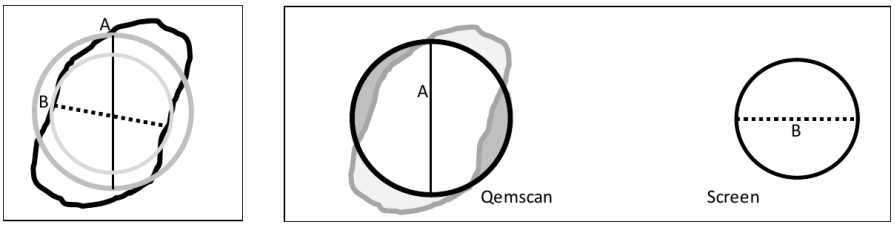

(b) Coarser size distribution due to particle shape.

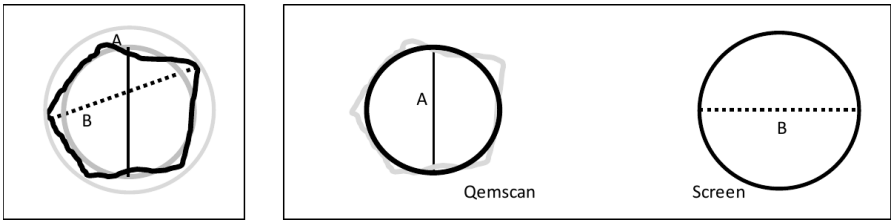

(c) Finer size distribution due to particle shape.

Figure 7.6: Qemscan® size distribution errors due to different factors.

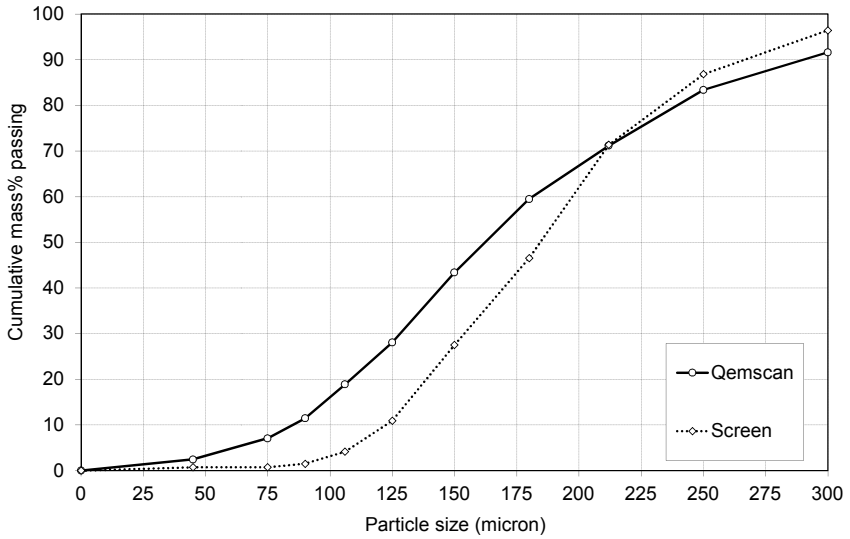

Figure 7.7: Quartz particle size distribution comparison between Qemscan® and screening. (Sample = Quartz, Qemscan® on 2870 particles)

in the minus 75 µm) and relatively small difference in the coarser particle population confirm the arguments in the previous paragraphs. The different intersection depths in the spheres produced finer particles that explained the finer population. Since the particles analysed were almost perfect spheres the screen did not 'allow' larger egg-shaped particles through (there was none) creating a similar coarse particle population to Qemscan®.

The bottom size of the ferrosilicon sample was known to be 75 µm. This correction was made to the Qemscan® distribution by removing the artificial fine particle population. Figure 7.8b illustrates the same distribution from Figure 7.8a, but without the particles smaller than 75 µm. This correction resulted in a close correlation between Qemscan® and screen size distribution, as shown by Figure 7.8c.

Since particle shape plays an important role in the explanation of particle size distribution differences between screening and Qemscan®, particle shape factor distribution was drawn up to illustrate the shape differences. Figure 7.9 demonstrates the differences in particle shape factor distribution of the different materials used to compare the sizing methods. Clear differences are visible.

The effect of particle shape on Qemscan® and screen size distribution was further investigated by considering a larger population of heavy mineral and quartz samples. The aim of this evaluation was to determine if there is a consistent particle shape relationship that would differentiate the heavy mineral particles (more rounded) and quartz particles (more sharp edged) from each other. Before the data was plotted the fine particle population (artificial small particles) was removed. Figure 7.10 demonstrates the results of this comparison and is plotted in similar manner as in Figure 7.8c.

Data points above the correlation line imply that Qemscan® size is larger than screening size. Points below the line indicate that Qemscan® size is smaller than screening size.

A clear distinction between the heavy mineral samples and quartz samples can be seen in Figure 7.10. This difference is primarily explained at the hand of particle shape differences as illustrated in Figure 7.9, where the quartz particles are shown to be less rounded than compared to heavy mineral particles.

For heavy mineral particles the screen analysis showed a finer particle size distribution compared to Qemscan®. This effect is easily explained by the fact that most heavy mineral particles were closer to 'egg shapes' as opposed to 'rounded balls'. This egg shape would be measured by the screen on its shortest diameter passing vertically through a square hole while Qemscan® would intersect the egg shaped particles at different angles that would present larger particles. Refer to Figure 7.6b.

For the quartz mineral particles the screen analysis showed a coarser particle size distribution compared to Qemscan®. This effect is easily explained by the fact that most quartz mineral particles were less rounded with sharp edges. These sharp edges would hinder the particle to go through square wire mesh. Qemscan® measured the intersected particle and the sharp edges will be less prominent in the calculation of the particle diameter. Refer to Figure 7.6c.

A close correlation between screening and Qemscan® size analysis could be achieved if the controlling parameters were well understood. The first influence of particle shape was addressed by using highly spherical ferrosilicon particles. The second influence of artificially fine particles was addressed by simply removing them from Qemscan® population since the sample was screened beforehand to remove any small particles. The conclusion from this size analysis method comparison and shape effect investigation is that Qemscan® size distribution did reflect a true particle property distribution and not just an analytical artefact. Qemscan® sensitivity for wide particle size ranges should be noted especially for particles larger than 300 µm. Qemscan® particle size distribution accuracy can be improved by screening into two size fractions and preparing a fine and coarse sample block for Qemscan® analysis.

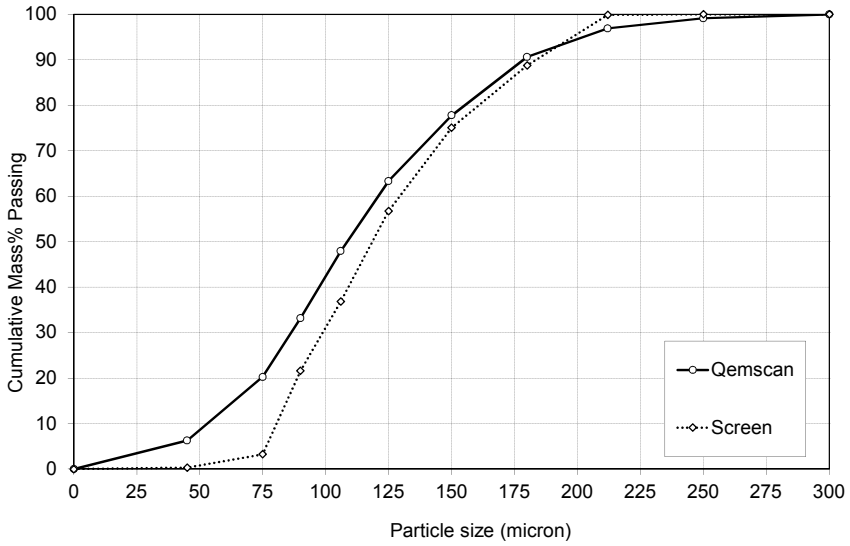

(a) Before correction.

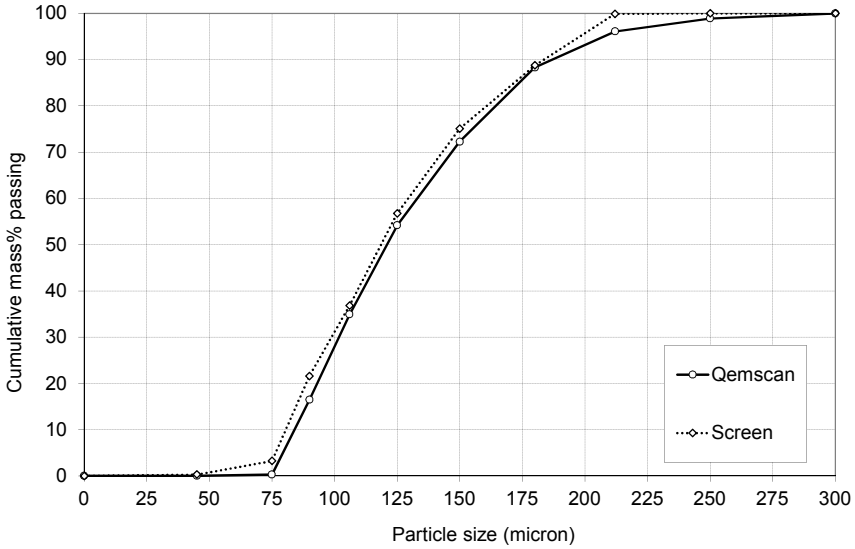

(b) After correction.

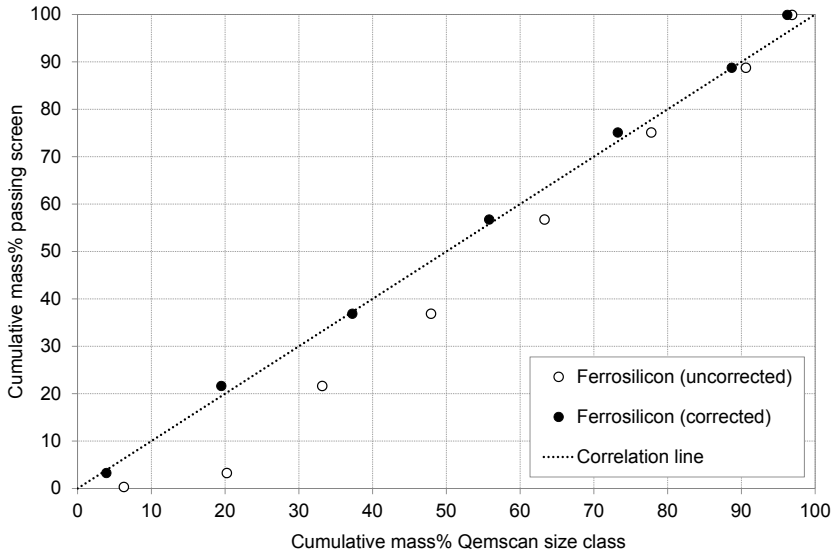

(c) Correlation between screening and Qemscan®.

Figure 7.8: Ferrosilicon particle size distribution comparison: Qemscan® vs screening. (Sample = Spherical ferrosilicon, Qemscan® on 2625 particles)

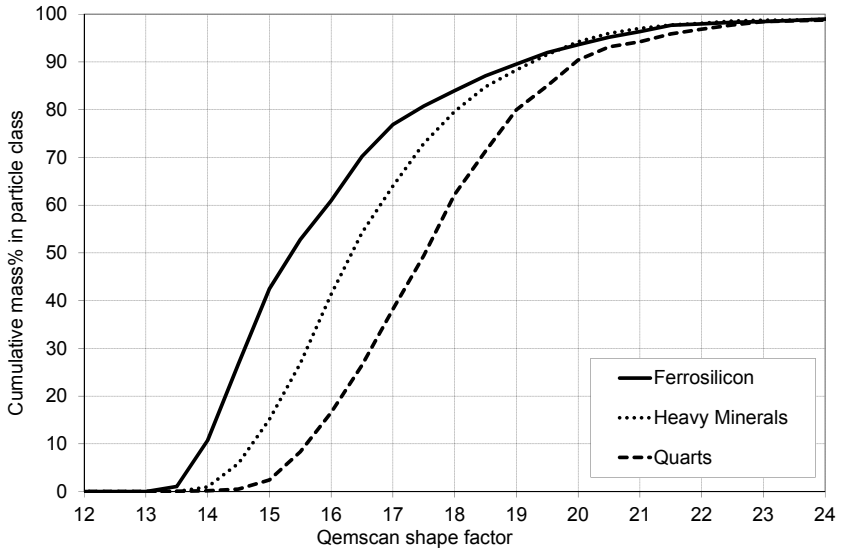

Figure 7.9: Shape distribution comparison of different materials. (spherical ferrosilicon, total heavy mineral and quartz)

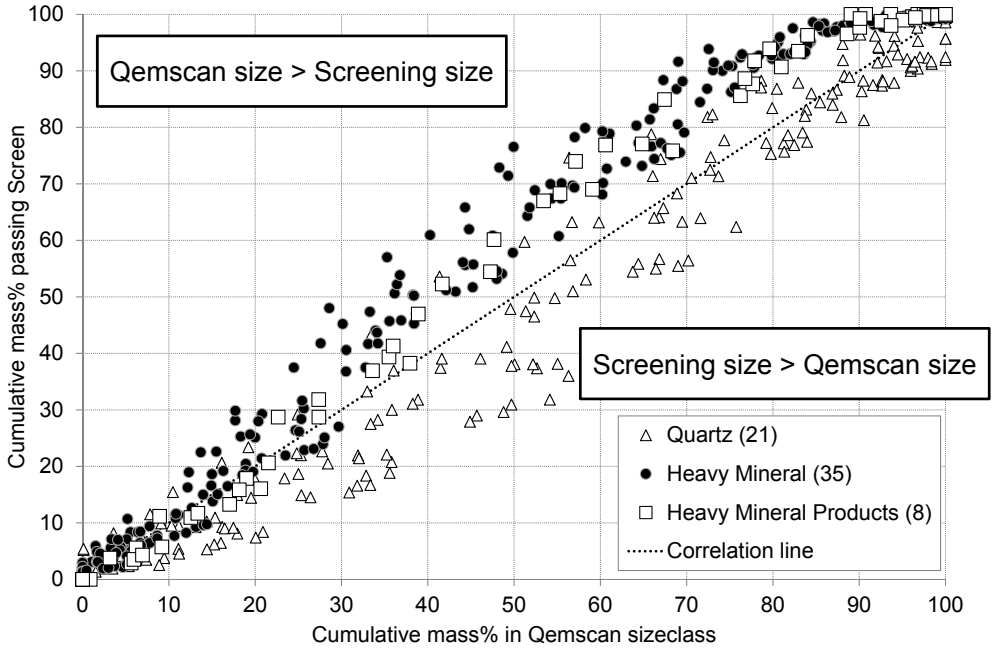

Figure 7.10: Comparison between Qemscan® and screening for multiple samples.(All samples were analysed with more than 2500 particles, 35 heavy mineral samples, 21 quartz samples, 8 heavy mineral product samples)

7.6 Qemscan® Density Validation

7.6.1 Method Background

The density of individual particles could not be measured during this investigation and only particle classes were measured. The density of a particle class was measured by means of alcohol displacement in a small volumetric flask. Particle classes with different densities were produced by final product samples, such as zircon, rutile, and ilmenite as well as various gravity fractions using shaking table. These samples were measured as a whole through alcohol displacement and compared with Qemscan® density that was derived from the weighted average of all the measured individual particles. The alcohol test for determining density is well known and showed a reasonable degree of repeatability. There was also a significant difference in the population size being measured between the two methods. Qemscan® density was determined by the analysis of 2500 to 3000 particles equating to 2 to 3 mg of sample, while the density measurement makes use of between 50 and 100 g. This is more than 3 orders of magnitude difference in mass.

Another method that was used to evaluate the consistency of Qemscan® density measurement was to fractionate a sample by means of a spiral to vary the mass split and density in each individual split. The density of each mass fraction was measured separately by means of alcohol displacement and Qemscan® . The weighted sum of all the density fractionated samples for a specific test had to correlate back to the head sample density for all the spiral tests since the same head sample was used in each case.

Particle porosity is an attribute that can cause discrepancy between alcohol displacement and Qemscan® density. Alcohol displacement is a wet method and displaces any air that is entrapped in the pores, cracks or crevices of the particles, while Qemscan® assumes a crystalline particle with the density of the analysed mineral. Qemscan® also analyses the inside of the particle and any surface porosity effects are ignored. The assumption was made in this investigation that particle porosity effects can be neglected based on the nature of the material that was used. The mineral sand sample was crystalline with limited to no porosity effects. If the Qemscan® density method is applied to a porous material, this effect needs to be well quantified beforehand.

7.6.2 Results and Discussion

Figure 7.11 demonstrates the correlation between Qemscan® density of particle classes as weighted averages of all analysed particle densities and the measured particle density by means of alcohol displacement

Table 7.6: Comparison between Qemscan® and wet density measurement. (Back calculated head feed density for various gravity fractionated samples. C.V. = coefficient of variation)

	Measured Density g/cm^3	**Qemscan® Density** g/cm^3
Test 1	4.13	4.23
Test 2	4.27	4.21
Test 3	4.34	4.20
Test 4	4.26	4.21
Test 5	4.29	4.21
Avg.	4.26	4.21
Std. Dev.	0.08	0.01
C.V.	0.018	0.0026

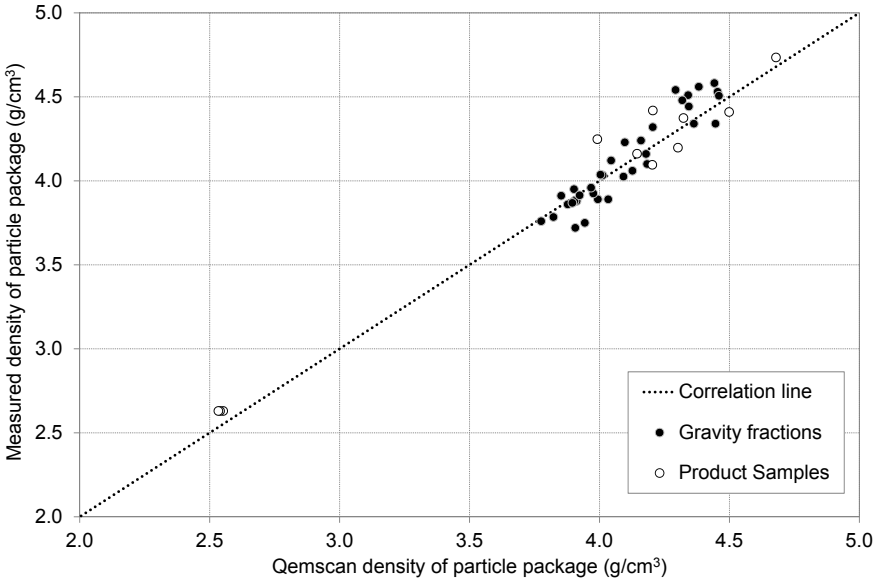

Figure 7.11: Comparison between Qemscan® and wet density measurement for various samples. (All Qemscan® samples were analysed with more than 2500 particles, 11 different product samples, 35 gravity fraction samples.)

The tests in Table 7.6 were gravity separation tests utilising the same head sample. The values in column 2 were measured with alcohol displacement measurement. The results in column 3 were back calculated from Qemscan® measurement. The numbers should be similar since the same head sample was used in each case.

Although the particle density could not be directly compared and validated, the comparison of measured particle classes density and Qemscan® weighted particle density did contribute to the investigation. Figure 7.11 indicates that the densities are comparable although it could be improved by carefully investigating the assigned mineral densities used in Qemscan® software. The consistency of Qemscan® density measurement was significantly better compared to the alcohol displacement density measurement as seen in Table 7.6.

The values from Qemscan® were comparable for the different head samples, while the other density measurement method showed a higher degree of variance. The density attribute is important since this number is used to convert the volume estimate to particle mass. If the densities were not comparable it would be advised to update Qemscan® software databases before any other analysis work continued. It could be concluded from this investigation that the density numbers from Qemscan® did correspond with actual measurements and could be applied in the characterisation of this specific material under investigation.

Chapter 8

Data Presentation Methods

The purpose of this chapter is to explain the data presentation method that was improved and applied in this study as well as the rationale behind it. The same separation attributes of yield, recovery, grade and separation efficiency were used in the same format as discussed in previous chapters.

8.1 Ideal Equation Fit

One of the standard methods to present data is using a straight line connecting test-work data points. Any test-work error will force the data trend into a specific direction, which is not desirable. The ideal when plotting test-work data is to have a mathematical equation that can be accurately and consistently fitted to test-work data points to describe the phenomenon that is being investigated. There are many equations that can be used to fit series of data points, but these may not be consistent over the different test-work conditions that were applied in the investigation. Its area of applicability may be very small and will require recalibration once the operating area has shifted. This is typically the nature of an empirical model. The ideal equation is one that describes the physical performance or separation behaviour of the process under investigation. This implies a model of a more fundamental nature. Such a relationship needs to be supported by large amounts of test-work data and/or fundamental analysis before it can be accepted as an equation suitable to fit test-work data.

8.2 Holland-Batt Spline Function

Holland-Batt (1990) proposed a combination of two simple equations to fit spiral recovery data in 1990. A simple power law equation and a linear equation were combined and it was referred to as a double-spline function (Equation 8.1). This function could be fitted effortlessly to all the yield-recovery data from this writer's test-work as well as spiral test-work data from other researchers. All of the test-work data from this investigation could also be fitted reasonably well using this function. The benefit of this relationship is that it provides structure to the data within which outliers can be easily identified, investigated and explained. It furthermore gives a continuous relationship over the entire yield range. Once a continuous expression was available for the yield-recovery relationship, the yield-grade and yield-efficiency relationships could also be calculated and plotted continuously over the entire yield range. Figure 8.1 provides an illustration of the Holland-Batt equation fitted on the yield-recovery data from one of the tests in this investigation.

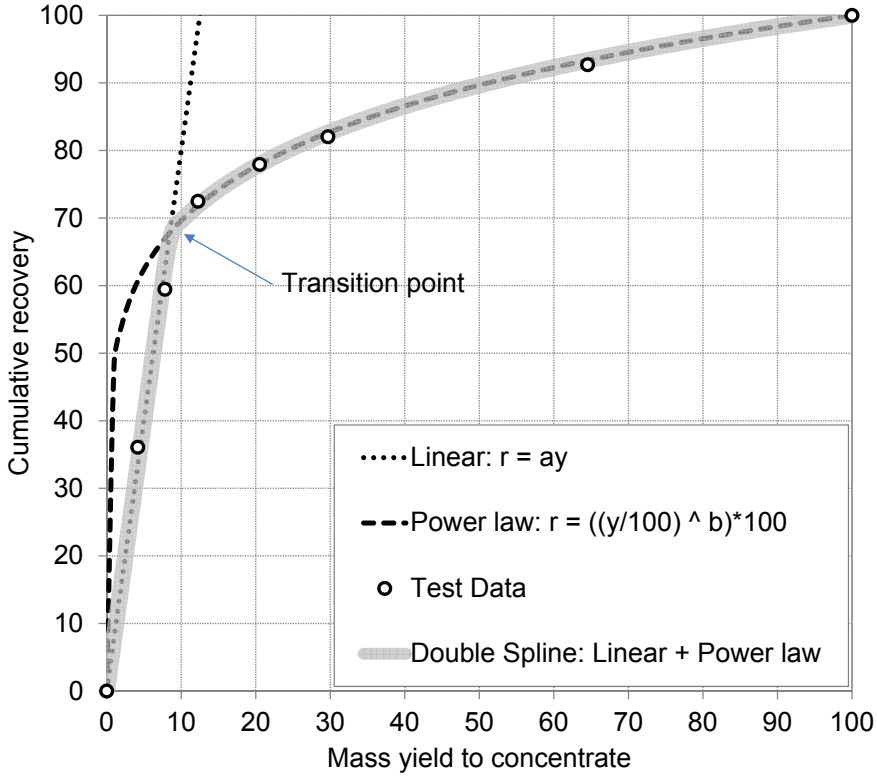

Figure 8.1: Double-spline Holland-Batt equation fitted to test-work data.

$$r = \min\left(ay, 100\left(\frac{y}{100}\right)^{b}\right) \qquad (8.1)$$

r cumulative recovery
y mass yield to concentrate
a gradient of straight line
b exponent of power law

8.3 Enhanced Holland-Batt

Although the Holland-Batt double-spline shows reasonable fits to test-work data, the fit can be improved. This is especially true at the transition point from the linear section to the power law section, as illustrated in Figure 8.1. Four improvements were made to the Holland-Batt equation to streamline the entire equation fitting process with regards to accuracy and calculation speed. These improvements are a polynomial fit for the transition zone, Excel Visual Basic programming for user friendly application of equation, automated fitting of parameters to test-work data using Excel Solver and plotting low-density lines. These improvements are discussed in the following sections.

8.3.1 Polynomial Fit for Transition Zone

The yield-recovery curve can be divided into three zones, namely the grade zone, the transition zone and the decay zone, as illustrated in Figure 8.2a. The grade zone is primarily defined by the number of high-density particles that are concentrated at the inner side of the spiral trough and is described by the straight line portion of the spline. An increase in the number of high-density particles would result in a decrease in the gradient of the straight line and a greater part of the spline would be presented by the straight line. The decay zone that is described by the power law is the result of higher density particles remaining in the bulk of low-density particles demonstrating a steady decrease in concentration. The decay zone is influenced by the

Table 8.1: Enhanced Holland-Batt triple-spline formulae and parameter limits for high-density material fractions.

Spline Segment	**Formula**	**Parameter Limits**
Linear	$r_{\text{lin}}(y) = ay$	$1 < a < 100$
Polynomial	$r_{\text{pol}}(y) = d_3y^3 + d_2y^2 + d_1y + d_0$	$0 < c < [a(100^{(b-1)})]^{\frac{1}{b-1}}$ for $0 < y < 50$
		$0 < c < 100 - [a(100^{(b-1)})]^{\frac{1}{b-1}}$ for $50 < y < 100$
Power Law	$r_{\text{pow}}(y) = 100(\frac{y}{100})^b$	$0.001 < b < 1$

sum of all the factors that could inhibit movement of high-density particles into the grade zone. Influencing factors may include increased throughput, increased solids concentration, increased viscosity (slimes content) and increased concentration of medium density particles. Since these two zones are completely different in nature and in the separation mechanism involved, there is naturally a transition zone between them. The gradient of the curve in the transition zone would be less than that of linear segment, but greater than the gradient of the power law. The suggested enhancement to the Holland-Batt equation is to fit a third order-polynomial function between the linear and power law functions.

The gradient of the polynomial function must match the gradient of the linear segment on the left side and match the gradient of the power law on the right side. This way there would always be a smooth transition between the two main separation zones. This enhancement results in a triple-spline that is made up by a linear segment, a polynomial segment and a power law segment. The width of the transition zone can be varied to improve the quality of fit.

The data points surrounding the transition point in Figure 8.2a are enlarged in Figure 8.2b to demonstrate the different equations used to determine the most suitable parameters to fit the triple spline to test-work data points. The coefficients of the third order-polynomial equation are solved using the relationships with the linear and power law segments. The result of all the calculations is summarised with Equation 8.2.

Considering Figure 8.2b, the triple spline for the high-density particles is a combination of the three curves. The three parameters that describe the triple spline for high-density fractions are a, b and c. The formulae for the three segments and the limits of the parameters are provided in Table 8.1.

Parameter 'a' describes the gradient of the linear segment that always starts from the origin $(0, 0)$. This part is primarily influenced by the grade of the particle class it represents. The higher the grade of the particle class the lower the gradient. This parameter is constrained at the y-axis and the gradient is rarely greater than 100 (based on experience) and cannot be less than 1. If the gradient is 1, no separation occurs with regards to the particle class it represents. If the gradient is less than one it is described by the low-density triple spline, with its origin at $(100, 100)$. This is discussed in Section 8.3.4.

Parameter 'b' is the coefficient of the power law. This part of the spline is primarily influenced by the decaying nature of high-density particles that are distributed among other particle classes towards the outer edge of the spiral. The higher the coefficient the more the dilution of the particle class into the bulk material and the lower the separation efficiency. This parameter is constrained at the recovery = 100 % line, which is close to 0.001, and at the zero separation line, which equates to a value of less than 1. This curve always ends in the $(100, 100)$ point where 100 % of the particle class is recovered in 100 % of the mass. From a recovery point of view this parameter has the strongest influence on the high-density spline.

Parameter 'c' is the half distance of the transition zone. The transition zone is the portion

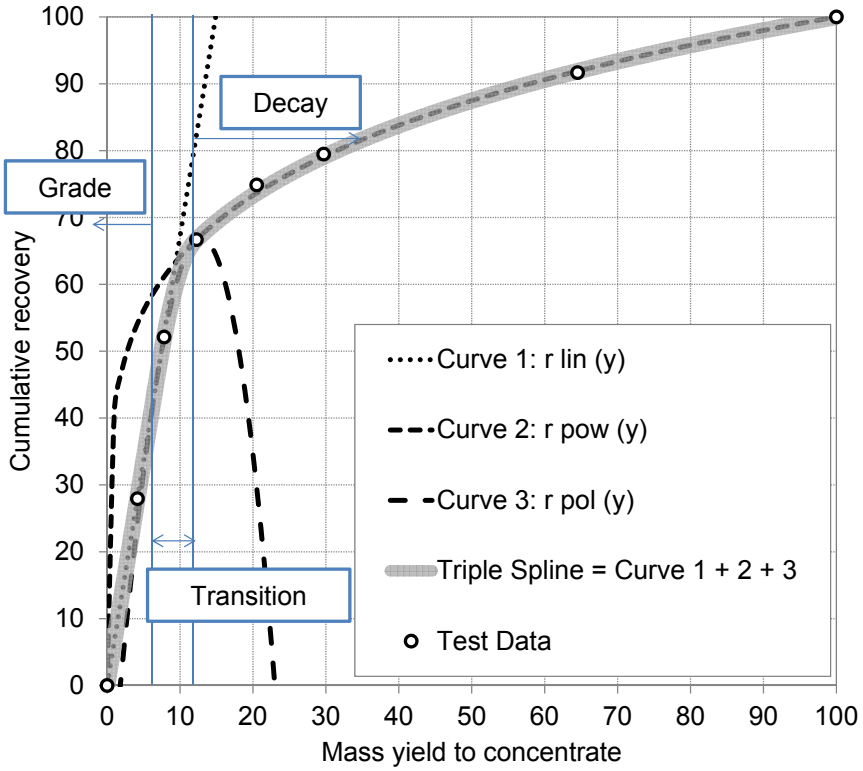

(a) Three zones covered by the triple spline.

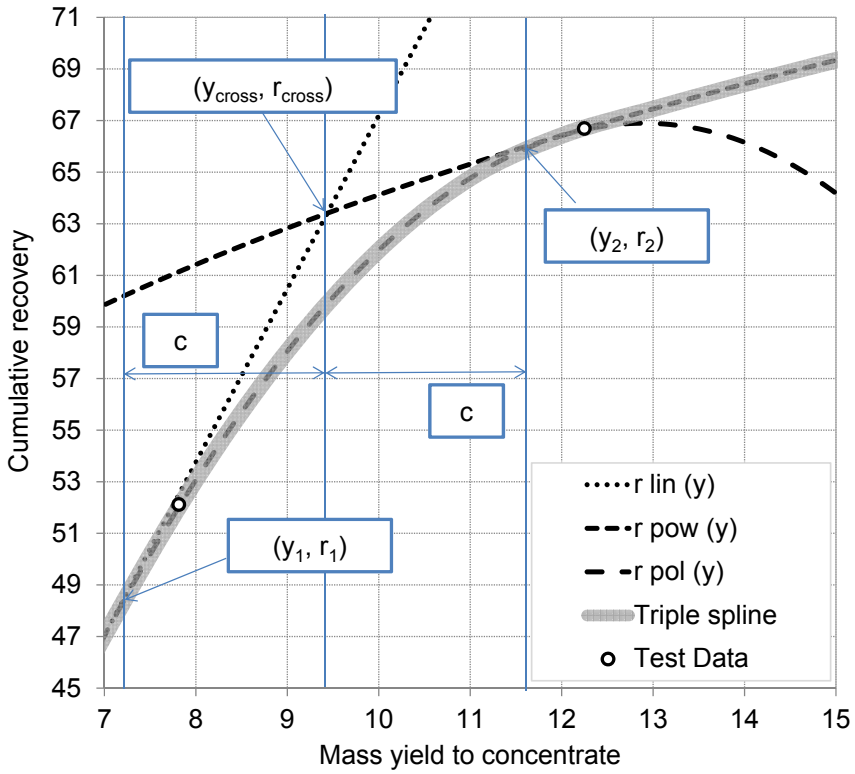

(b) Details of the transition zone.

Figure 8.2: Enhanced Holland-Batt triple spline for high-density material.

of the spline that is described by neither the linear segment nor the power law segment, but rather by the third-order polynomial. The purpose of the curve is to ensure a smooth transition between the linear and power law segments. The higher this parameter the larger portion of the spline is described by the polynomial segment. The parameter is constrained so that it cannot exceed the value of y_{cross} and cannot be zero or less than zero. If c is larger than y_{cross} the spline does not contain a linear segment and does not pass through the origin for y-values smaller than 50. For y values greater than 50, c may not exceed the value of $100 - y_{cross}$ since then the power law segment is absent and the spline function does not pass through the $(100, 100)$ point.

$$r_{\text{lin}}(y_{\text{cross}}) = r_{\text{pow}}(y_{\text{cross}})$$
$$y_{\text{cross}} = \left[a\left(100^{b-1}\right)\right]^{\frac{1}{b-1}}$$

The four unknown parameters d_0, d_1, d_2 and d_3 in $r_{\text{pol}}(y)$ can be solved for the conditions where $r_{\text{lin}}(y)$ and $r_{\text{pow}}(y)$ join $r_{\text{pol}}(y)$ exactly. With reference to Figure 8.2b, the first joining point (y_1, r_1) is where the values and gradients of $r_{\text{lin}}(y)$ and $r_{\text{pol}}(y)$ are equal:

$$\begin{aligned} \text{At point } (y_1, r_1): \quad & r_{\text{lin}}(y_1) = r_{\text{pol}}(y_1) \\ \text{and} \quad & \frac{dr_{\text{lin}}}{dy}(y_1) = \frac{dr_{\text{pol}}}{dy}(y_1) \qquad \left(\text{or } r'_{\text{lin}}(y_1) = r'_{\text{pol}}(y_1)\right) \end{aligned}$$

At the second joining point (y_2, r_2) the values and gradients of $r_{\text{pow}}(y)$ and $r_{\text{pol}}(y)$ are equal:

$$\begin{aligned} \text{At point } (y_2, r_2): \quad & r_{\text{pow}}(y_2) = r_{\text{pol}}(y_2) \\ \text{and} \quad & \frac{dr_{\text{pow}}}{dy}(y_2) = \frac{dr_{\text{pol}}}{dy}(y_2) \qquad \left(\text{or } r'_{\text{pow}}(y_2) = r'_{\text{pol}}(y_2)\right) \end{aligned}$$

These two conditions result in four unknowns (d_0, d_1, d_2 and d_3) and four equations as illustrated below:

$$r(y_1) = d_3 y_1^3 + d_2 y_1^2 + d_1 y_1 + d_0 = a y_1$$

$$r'(y_1) = 3d_3 y_1^2 + 2d_2 y_1 + d_1 = a$$

$$r(y_2) = d_3 y_2^3 + d_2 y_2^2 + d_1 y_2 + d_0 = 100\left(\frac{y_2}{100}\right)^b$$

$$r'(y_2) = 3d_3 y_2^2 + 2d_2 y_2 + d_1 = 100^{(1-b)} b y_2^{(b-1)}$$

This is a system of linear equations in d_i that can be solved by matrix algebra. The four equations expressed in matrix notation are presented below:

$$\begin{bmatrix} y_1^3 & y_1^2 & y_1 & 1 \\ 3y_1^2 & 2y_1 & 1 & 0 \\ y_2^3 & y_2^2 & y_2 & 1 \\ 3y_2^2 & 2y_2 & 1 & 0 \end{bmatrix} \begin{bmatrix} d_3 \\ d_2 \\ d_1 \\ d_0 \end{bmatrix} = \begin{bmatrix} a y_1 \\ a \\ 100\left(\frac{y_2}{100}\right)^b \\ 100^{(1-b)} b y_2^{(b-1)} \end{bmatrix}$$
$$\mathbf{Y}\mathbf{d} = \mathbf{r}$$

The system can be solved by using the matrix inverse as follows:

$$\mathbf{d} = \mathbf{Y}^{-1}\mathbf{r}$$

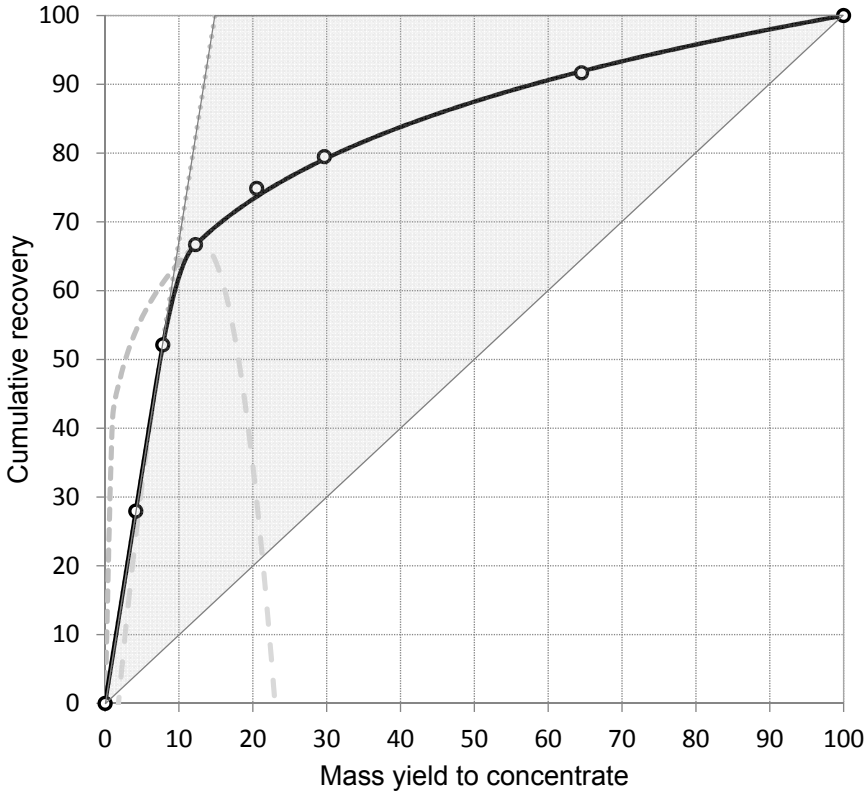

Figure 8.3: Permissible separation envelope for high-density line (indicated in grey).

Combining all the information, Equation 8.2 supplies the three curves for the high-density triple spline.

$$r(y) = \begin{cases} r_{\text{lin}}(y) = ay, & \text{if } 0 \leq y < (y_{\text{cross}} - c) \\ r_{\text{pol}}(y) = d_3y^3 + d_2y^2 + d_1y + d_0, & \text{if } (y_{\text{cross}} - c) \leq y < (y_{\text{cross}} + c) \\ r_{\text{pow}}(y) = 100\left(\frac{y}{100}\right)^b, & \text{if } (y_{\text{cross}} + c) \leq y < 100 \end{cases} \tag{8.2}$$

8.3.2 Excel Visual Basic Programming

The combination of the three spline sections and the simultaneous adjustment of the different parameters involve a large number of calculations in Microsoft Excel. All these calculations were programmed in a Visual Basic module in Excel. The result is a user-defined function that is selected and only three parameters are specified. The first parameter is the gradient of the straight line (parameter 'a'), the second is the exponent of the power law (parameter 'b') and the third is the half-width of the transition zone (parameter 'c'). All the calculations are done in the background, which makes it user friendly and keeps the data sheets dealing with large volumes of data neat and clear. The Visual Basic programming for the high-density line can be seen in Appendix C.1, page 159. The limiting conditions for the permissible envelope of separation were also considered and programmed to ensure a robust function over the entire range of possibilities. An error message guides the user if spline parameter values are specified that cause it to go outside the permissible separation envelope. The permissible envelope is limited on the right side by the zero separation line that intersects the origin and the (100,100) point. The envelope is further limited on the left side by the theoretical grade line (recovery $= \frac{100}{\text{grade}} \times$ yield) as well as the recovery = 100 horizontal line. Figure 8.3 shows this envelope.

Table 8.2: Enhanced Holland-Batt triple-spline formulae and parameter limits for low-density material fractions.

Spline Segment	**Formula**	**Parameter Limits**
Linear	$r^*_{\text{lin}}(y^*) = ay^*$	$1 < a < 100$
Polynomial	$r^*_{\text{pol}}(y^*) = d_3(y^*)^3 + d_2(y^*)^2 + d_1(y^*) + d_0$	$0 < c < [a(100^{(b-1)})]^{\frac{1}{b-1}}$ for $0 < y^* < 50$
		$0 < c < 100 - [a(100^{(b-1)})]^{\frac{1}{b-1}}$ for $50 < y^* < 100$
Power Law	$r^*_{\text{pow}}(y^*) = 100(\frac{y^*}{100})^b$	$0.001 < b < 1$

8.3.3 Automated Fitting with Excel Solver

Selecting the three spline parameters ('a', 'b' and 'c') for the three spline sections to yield the best fit to test-work data can take thousands of iterations and may be counter intuitive to the user. Different users can also have different parameter selection results on the same test-work data set. Therefore the Excel Solver facility was programmed in Excel Visual Basic to select the set of parameters that would produce the best fit to test-work data by minimizing the differences between the triple spline and the test-work data points. Equation 8.3 provides the function that should be minimised in the Excel Solver by changing parameter 'b' first followed by parameter 'a' and 'c' for the fitting of the high-density spline (7 data points available for fitting). For the low-density spline, parameter 'a' is changed first, followed by 'b' and 'c'. The parameter limits, demonstrated in Table 8.1 and Table 8.2, should be added to the constraint list of Excel Solver. This curve fitting process takes only a few seconds after initiating the Solver programme and many data fits could be done in a short period of time.

$$\text{sum of squared errors} = \sum_{i=1}^{7} (r_{\text{i (actual)}} - r_{\text{i (spline)}})^2 \tag{8.3}$$

8.3.4 Plotting Low-density Lines

In almost all relevant literature references (Henderson and MacHunter 2003; Richards and Palmer 1997; Holland-Batt 1995) only the high-density lines are plotted and the low-density lines (FLT) are omitted and as a result not fitted. The position and consistency of the low-density lines were crucial for this investigation since it represented the bulk of the mass on the spiral (80% plus) and a small movement in these lines would result in a significant influence on mass yield. The Holland-Batt equation was further enhanced to accommodate low-density lines. The power law had to be mirrored to the $(100, 100)$ point as the new origin for the power law to function correctly. The only two differences compared with the calculations of the high-density line is that (y) becomes (y^*) and (r) becomes (r^*). The two mirror equations are shown by Equation 8.4. The recovery mirror equation is applicable to all three sections (linear, power law, polynomial) of the low-density spline. The mirror equations are also applied to the boundary conditions. The result of this replacement can be seen in Table 8.2

$$\text{Mirror} \begin{cases} \text{Yield} & y^* = 100 - y, \\ \text{Recovery} & r^* = 100 - r \end{cases} \tag{8.4}$$

As expected the low-density fit is dominated by the grade zone, with the grade zone of the low-density particles located on the outside of the spiral. Figure 8.4a demonstrates the different spline sections for a low-density line and Figure 8.4b supplies the detail of the different lines

in the transition zone. The permissible separation envelope for the low-density line is also significantly smaller, see Figure 8.5, since it represents the bulk of the mass on the spiral.

The parameter descriptions for the low-density spline in comparison with the high-density spline parameters are as follows: Parameter '*a*' still describes the gradient of the linear part of the spline, but starts from the (100, 100) point. This part is primarily influenced by the grade of the low-density particle class it represents. This parameter is constrained at the yield = 100 line and the gradient is rarely greater than 100 and cannot be less than 1. From a recovery point of view this parameter has the strongest influence on the low-density spline.

Parameter '*b*' still describes the power law coefficient. This parameter is constrained at the recovery = 0 line, which is close to '*b*' value of 0.001 and at the zero separation line, which equates to a '*b*'-value of just less 1. This curve always ends in the (0,0) point where 0 % of the particle class is recovered in 0 % of the mass.

Parameter '*c*' still describes the half distance of the transition zone, same as for the high-density spline. The parameter is constrained that it cannot exceed the value of y_{cross} and cannot be zero or less than zero. The same boundary conditions apply as with the high-density spline.

The result of all the calculations is summarised with Equation 8.5. The Visual Basic programming for a low-density line can be seen in Appendix C.2, page 161.

$$r(y) = \begin{cases} r^*_{\text{lin}}(y^*) = ay^*, & \text{if } 0 \leq y^* < (y_{\text{cross}} - c) \\ r^*_{\text{pol}}(y^*) = d_3(y^*)^3 + d_2(y^*)^2 + d_1(y^*) + d_0, & \text{if } (y_{\text{cross}} - c) \leq y^* < (y_{\text{cross}} + c) \\ r^*_{\text{pow}}(y^*) = 100\left(\frac{y^*}{100}\right)^b, & \text{if } (y_{\text{cross}} + c) \leq y^* < 100 \end{cases} \quad (8.5)$$

8.4 Summary

The following list is a summary of the main points from this chapter.

- This data presentation method (curve fitting) is robust and is supported by large amounts of curve fits on test-work data from many other researches as well as the test-work data from this investigation.
- The mathematical equations used are simple with only three parameters (a, b, and c). These triple spline parameters can also be correlated well to spiral separation behavior (grade, decay and transition).
- The enhancements made to the Holland-Batt equation in this study have considerable benefits when dealing with large amounts of data, and they also improved the accuracy and calculation speed of the fitting process. This enhanced method is applied in the presentation of the test-work data in the chapters to follow.

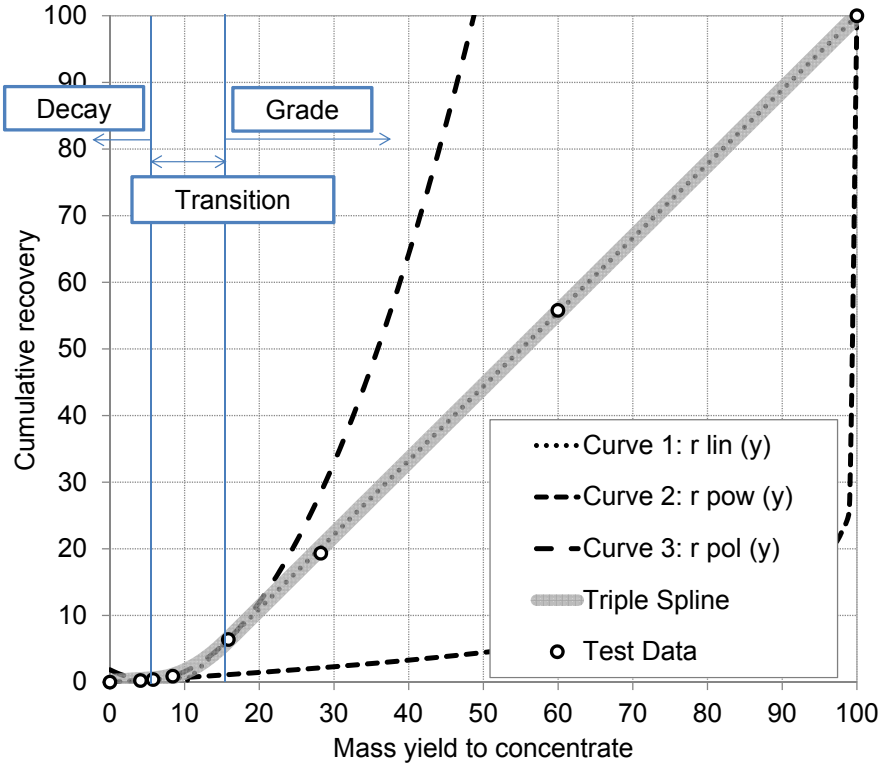

(a) Three zones covered by the triple spline.

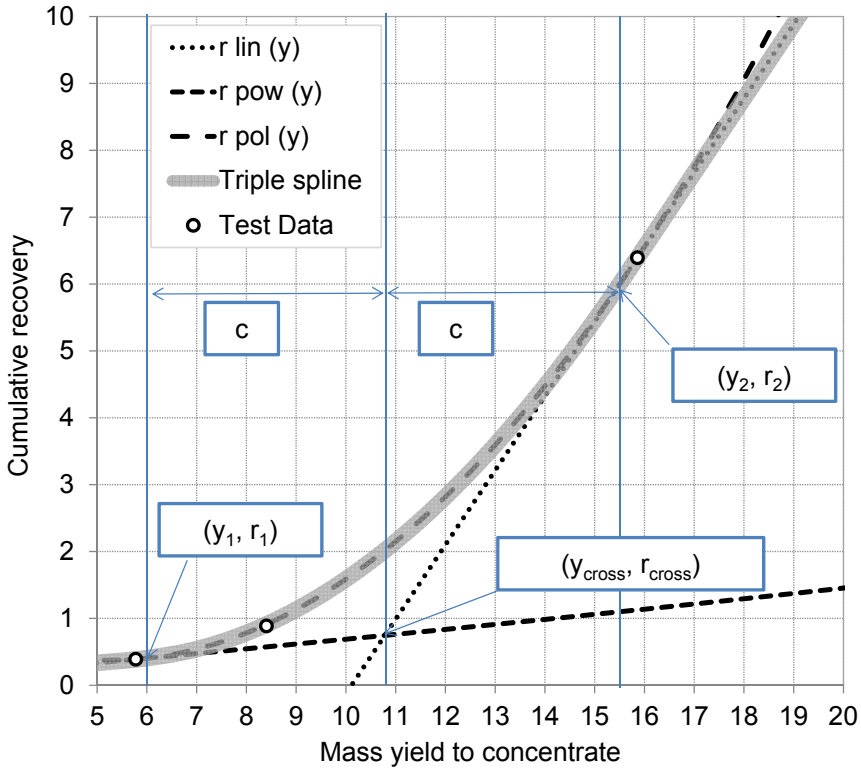

(b) Details of the transition zone.

Figure 8.4: Enhanced Holland-Batt triple spline for low-density material.

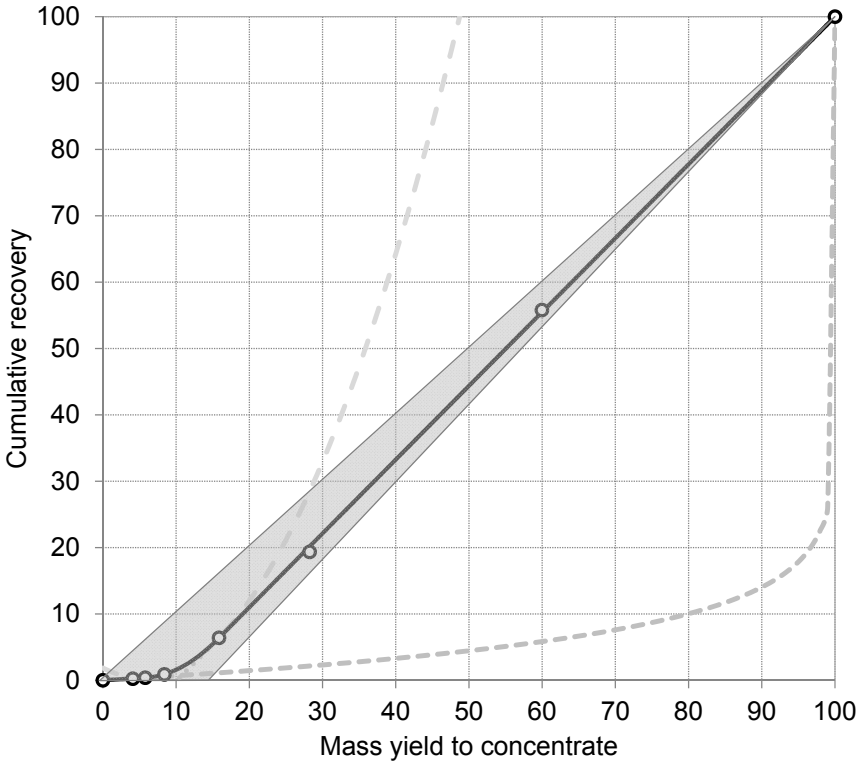

Figure 8.5: Permissible separation envelope for low-density line (indicated in grey).

Part III

Results and Discussion

Chapter 9

Feed Material Characterisation

Feed material characterisation aims to improve understanding of the material to be processed, in this case by the spiral. If the different feed materials are well characterised, it will be beneficial in understanding and explaining separation behaviour differences that are observed. This chapter aims to illustrate the information that is typically made available after standard feed characterisation techniques were applied (first part) and then to compare that with the information that is made available after enhanced feed characterisation techniques were applied (second part)The significant character difference between the two feed materials used in this investigation is demonstrated in this chapter.

9.1 Standard Feed Characterisation

Usually a sink-float analysis is performed on the feed material followed by a chemical analysis of the sink (THM) fraction. The elements from the chemical analysis are usually assigned to specific minerals based on historical data from the specific deposit. For example 5 % of the titanium is assigned to rutile while the rest is assigned to ilmenite. All the zirconium is assigned to zircon. A more thorough standard feed characterisation will consider a mineralogical analysis on the sink fraction followed by a particle size distribution on the sink and float fractions. Table 9.1 presents the data from standard characterisation methods applied to material 1 and 2.

Table 9.1: Standard characterisation of the two feed materials.

		Material 1	**Material 2**
Particle size:			
D_{50} of the sink fraction	µm	140	120
D_{50} of the float fraction	µm	200	220
Mineralogical composition:			
Slimes content	mass%	3.5	6.1
Total heavy mineral content	mass%	13.9	12.6

9.1.1 Particle Density (sink-float)

The sink-float analysis of the two materials gave similar THM values. The method discussed in Section 2.5.1, page 34, was used. Material 1 has 13.9 % heavy minerals and Material 2 has 12.6 %. There are however significant differences between the minerals present and their respective densities. Table 9.2 illustrates the density differences between the two materials. The mass weighted density indicates significant overall density differences between the two materials. From this analysis a significant separation behaviour difference is expected since

the density difference between the THM and FLT (quartz) gives an indication of the level of interference in the transition zone of the spiral trough. The greater the density difference the less the interference. Therefore it is expected that Material 1 will separate more efficiently than Material 2.

Table 9.2: Density differences between materials 1 and 2 based on mineralogical composition.

Material 1 THM	**Mass %**	**Density**	**Material 2 THM**	**Mass %**	**Density**
Zircon	4.0	4.63	Zircon	6.3	4.63
Rutile	2.2	4.15	Rutile	5.7	4.15
Leucoxene	6.7	3.85	Leucoxene	1.3	3.85
Ilmenite	47.8	4.37	Ilmenite	20.1	4.37
Altered ilmenite	17.4	4.30	Ti-Hematite	3.3	4.60
Goethite	14.6	3.60	Garnet	17.8	3.95
Iron oxides	4.6	4.60	Clinopyroxene	34.4	3.25
Monazite	1.6	4.80	Others	11.2	3.55
Others	1.2	3.55			
Weighted density		4.22	Weighted density		3.82
Total THM content	13.9		Total THM content	12.6	

9.1.2 Particle Size

Standard screen analyses were conducted on the sink (THM) and float (FLT) fractions. The method as discussed in Section 2.5.1 on page 35 was applied. Figure 9.1 and Figure 9.2 illustrate the particle size distribution of Material 1 and Material 2. The D_{50} difference between the THM and FLT fractions for Material 1 is around 60 µm. For Material 2 this difference is more pronounced at 100 µm. It is expected that a smaller size difference between the low-density and high-density material would improve separation between the two fractions on the spiral trough, since the influence of particle size will be less pronounced while particle density will be more pronounced.

The fraction of particles larger than 300 µm also differs significantly for the two material types. Material 1 contains almost no +250 µm in the THM fraction and contains around 10 % +300 µm for the FLT fraction. Material 2 contains around 12 % +250 µm in the THM fraction and contains around 22 % +300 µm for the FLT fraction. It is expected that the increased coarse fraction (+300 µm) would hinder effective separation since the coarse particles tend to be circulated back to the concentrate band by secondary fluid flow.

9.2 Enhanced Feed Characterisation

9.2.1 Material 1 and Material 2

To visually illustrate the benefit of characterising feed material by means of Qemscan® particle size and density classes, Material 1 and Material 2 were divided into a 9×9 set of size-density particle classes. This is illustrated in Figure 9.3 and Figure 9.4.

9.2.2 Materials Differences

The following major feed materials differences could be identified comparing Figure 9.3 and Figure 9.4:

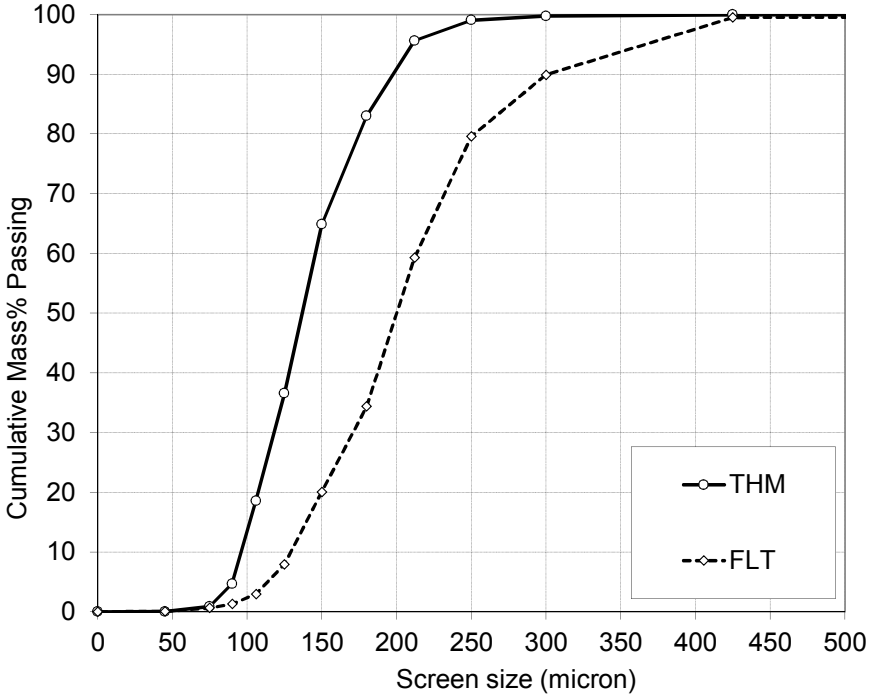

Figure 9.1: Particle size distributions of Material 1 THM and FLT fractions.

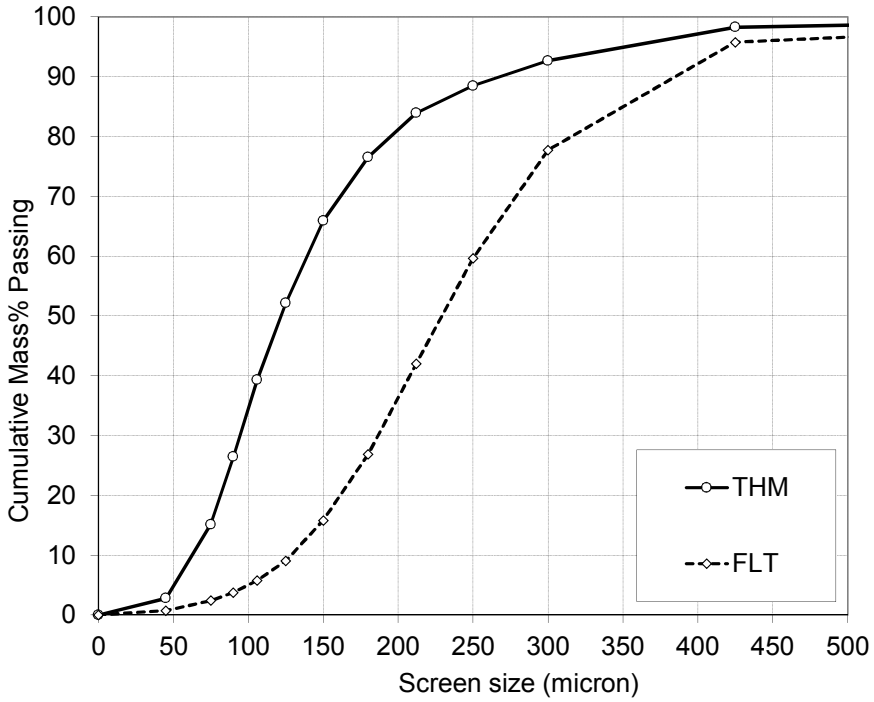

Figure 9.2: Particle size distributions of Material 2 THM and FLT fractions.

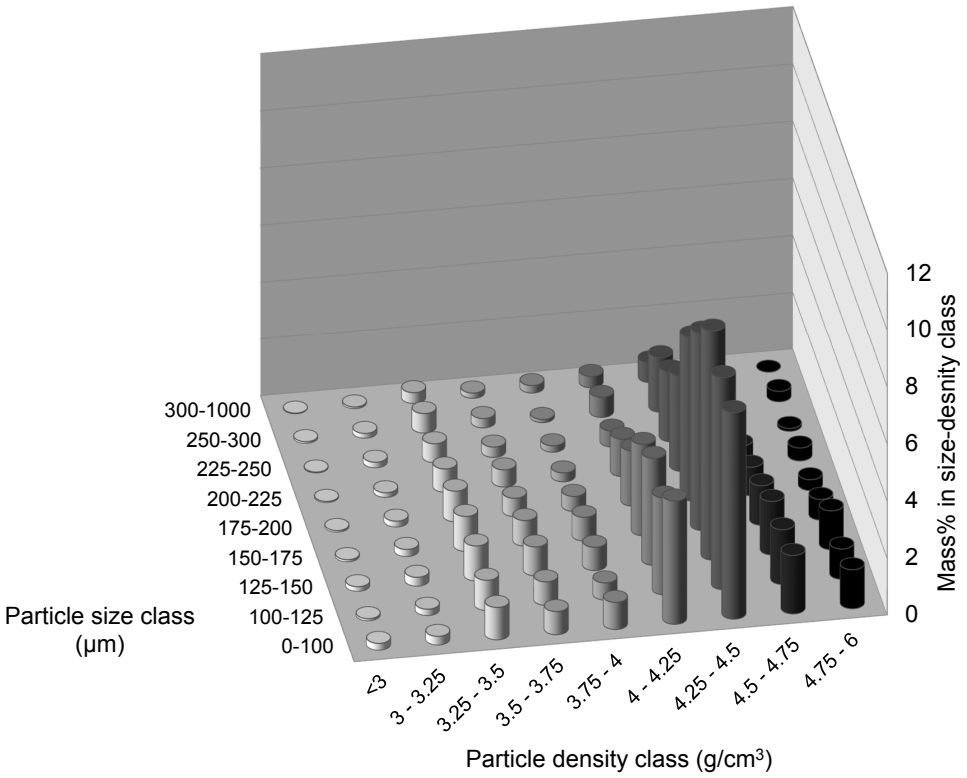

Figure 9.3: Qemscan® size-density data for Material 1 THM.

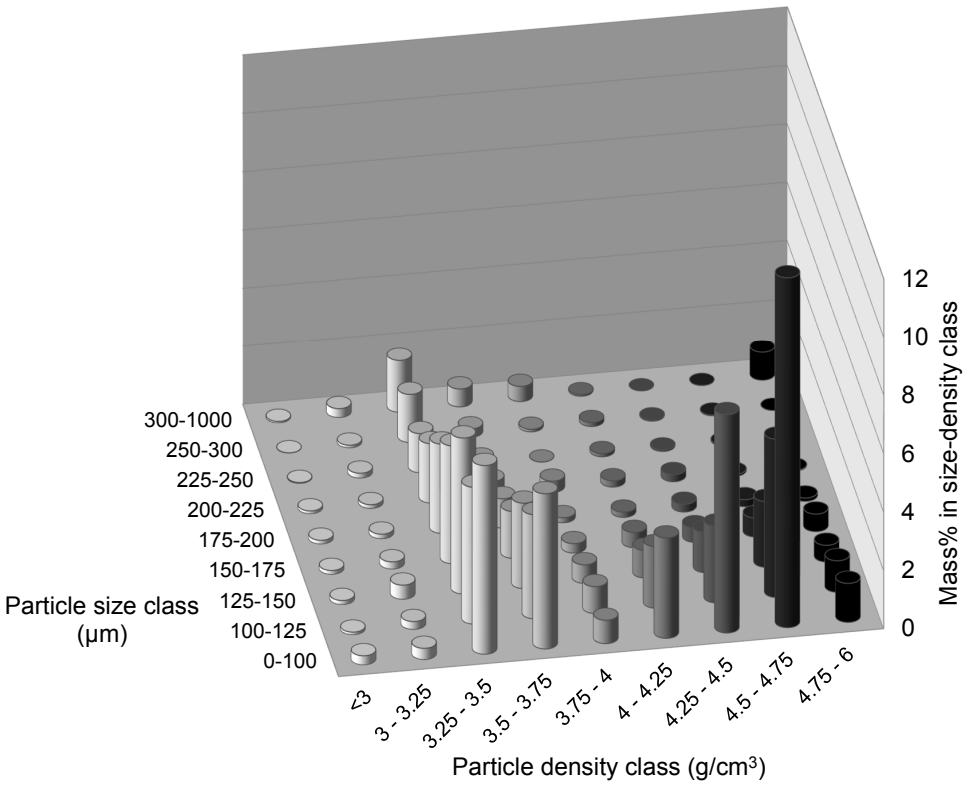

Figure 9.4: Qemscan® size-density data for Material 2 THM.

1. Material 2 contains a significant mass percentage of lower density (3.25-3.75) particles while Material 1 contains only a small percentage of material in that class.

2. The high-density particles in Material 2 is mostly concentrated in the 0-100 µm class, while the high-density particles form Material 1 is distributed to the larger particle size classes.

3. Material 2 contains little mass in the larger particle size classes while Material 1 contains more material in the larger particle classes.

4. The presence of mass in the 300-1000 µm class could be seen for Material 2 and significantly less mass for Material 1. This correlated with the particle size distributions in Figure 9.1 and Figure 9.2.

From this simple and quick analysis the feed material difference could be clearly demonstrated before any separation test-work was conducted. This information is valuable in explaining separation behaviour differences in the two chapters to follow.

9.3 Summary

The following summarises the feed material characterisation chapter:

- A more detailed feed characterisation, in addition to the standard feed characterisation, using mineralogical analysis of the THM fraction and screening of both the THM and FLT fractions will aid significantly in understanding the material differences.

- A single Qemscan® analysis conducted on the THM and FLT fractions clearly demonstrated the feed material differences in terms of particle size and particle density.

Chapter 10

Standard Analysis of Spiral Separation Performance

This chapter presents the results and discussion of standard product characterisation required for spiral separation performance analysis for the three test-work data sets (Table 5.2, page 60) produced in this investigation. It considers only two density classes (THM and FLT) that resulted from the standard sink-float analysis. The enhanced Holland-Batt triple spline, as discussed in Chapter 8, was fitted to the test-work data. For each test-work data set a summary table depicting the operating conditions is shown, followed by six figures that illustrate the three separation attributes for the THM and FLT fractions separately. A discussion follows after each data set. The chapter closes with a summary of the most important observations and conclusions.

10.1 Influence of Operating Parameters

10.1.1 Spiral A, Material 1

Table 10.1 demonstrates the operating conditions during sampling for all the tests conducted on Spiral A with Material 1. The fourteen tests were divided into three performance groups. Group 1 (3 tests - black lines in figures to follow) was higher performance, Group 2 (8 tests - grey lines in figures to follow) medium performance and Group 3 (3 tests - dotted lines in figures to follow) lower performance based on the separation attributes of yield, recovery, grade and efficiency that are illustrated in Figure 10.1. These performance groups are relative to each other and have no other test-work references. The THM and FLT density classes that resulted from the standard sink-float analyses are plotted separately. The background to these specific plotted relationships is discussed in Section 2.4.1 on separation attributes, page 22.

Figure 10.1a illustrates the high degree of repeatability in the three different groups. The tests in each performance group had similar operating conditions. The curves that were fitted through the test-work data points are based on the enhanced Holland-Batt triple spline described in Chapter 8. The model fit showed a high degree of fitting accuracy.

In Figure 10.1a, Group 1 had a 5 % higher THM recovery when compared to Group 2. The reason for this was lower throughput (4.4 versus 5.7 t/h), lower percentage solids (39.5 % versus 44.4 %) and lower percentage slimes (2.6 % versus 3.3 %). Group 3 had almost a 5 % lower THM recovery when compared to Group 2. The reason for this was higher throughput (6.9 versus 5.7 t/h), higher percentage solids (50.6 % versus 44.4 %) and higher percentage slimes (3.7 % versus 3.3 %). It was difficult to estimate which of the three operating conditions between throughput, percentage solids and percentage slimes played the most significant role in the increased and decreased recovery to concentrate for similar mass to concentrate. More test

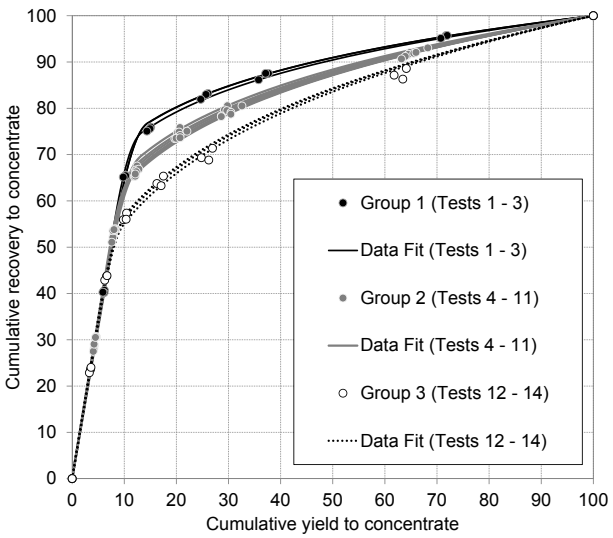

(a) THM cumulative recovery.

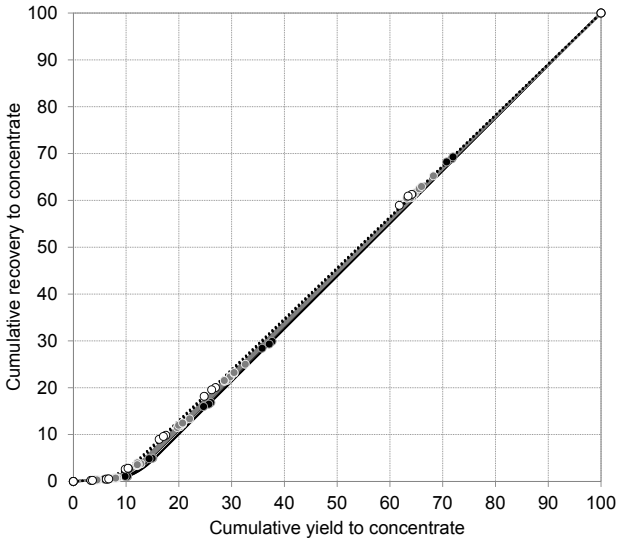

(b) FLT cumulative recovery.

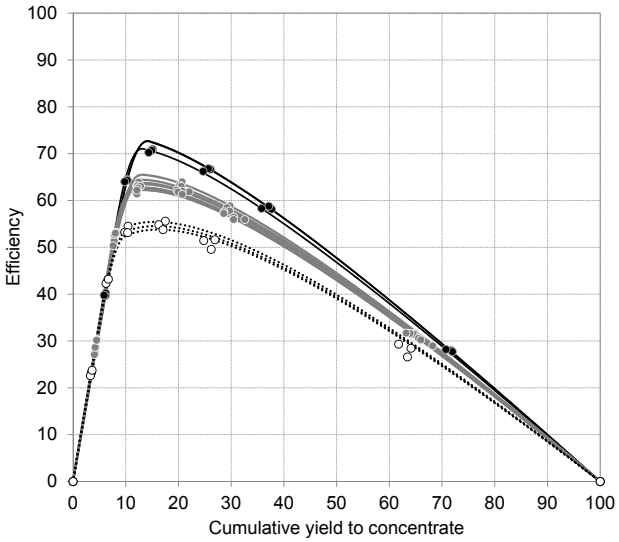

(c) THM separation efficiency.

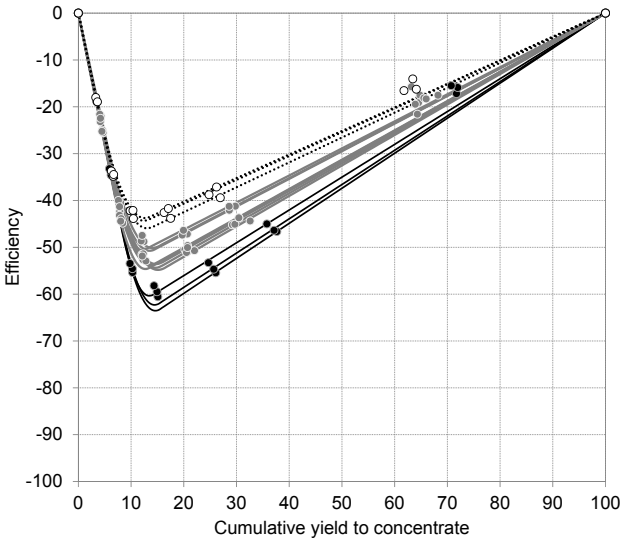

(d) FLT separation efficiency.

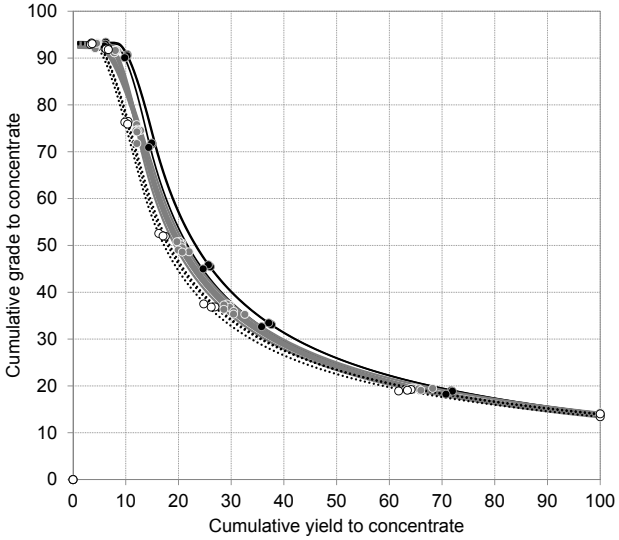

(e) THM cumulative grade.

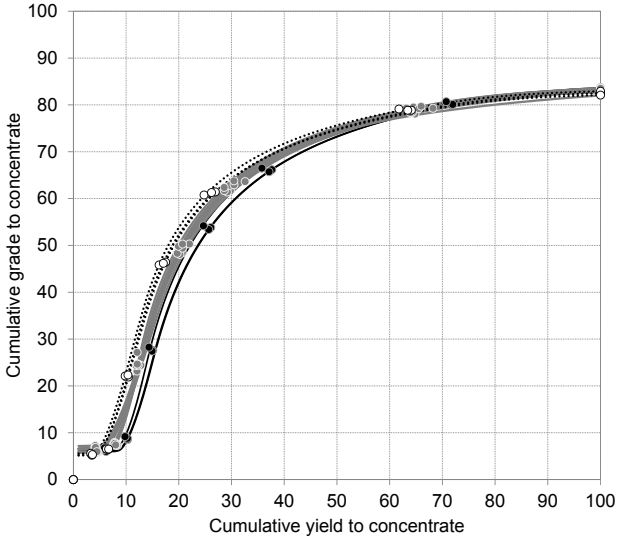

(f) FLT cumulative grade.

Figure 10.1: Spiral performance for different tests for Spiral A, Material 1.

Table 10.1: Operating conditions for Spiral A, Material 1 tests.

Performance Group	Test Nr	Feed Rate (t/h)	%Solids	%Slimes	%THM
1 - HIGH	1	4.34	38.76	2.42	14.23
	2	4.50	39.70	2.63	14.19
	3	4.37	39.94	2.77	13.55
	Avg.	4.40	39.47	2.61	13.99
2 - MEDIUM	4	5.52	43.01	4.21	13.77
	5	5.87	43.79	3.14	13.76
	6	5.88	43.64	2.64	13.74
	7	5.39	46.15	2.81	14.28
	8	5.92	44.52	3.67	13.63
	9	5.52	45.87	3.08	13.83
	10	5.93	43.65	3.85	13.30
	11	5.67	44.23	2.80	13.67
	Avg.	5.71	44.36	3.28	13.75
3 - LOW	12	6.79	49.56	3.56	13.91
	13	7.13	51.77	3.67	13.41
	14	6.89	50.33	3.87	14.03
	Avg.	6.93	50.55	3.70	13.78

work will be required on single parameter changes to determine the separate contribution of a specific operating parameter. The feed grades (THM) of the different spiral tests were similar.

In Figure 10.1b the lines seem to be on top of each other and the difference seems insignificant. The enhanced Holland-Batt equation fitted the test-work data points quite accurately. The FLT fraction represented on average 86 % of the mass and a slight movement in this line implied a significant grade difference in the concentrate. The higher efficiency tests in Group 1 were to the right while the lower efficiency tests in Group 3 were to the left. This implied that more of the quartz in the Group 3 FLT reported earlier in the heavy mineral concentrate compared to the Group 1 FLT which is detrimental to concentrate grade. Figure 10.1e and Figure 10.1f confirm the lower THM grade and higher FLT grade in the poorer performing Group 3 tests, and the higher THM grade and lower FLT grade in the better performing Group 1 tests.

Figure 10.1c and Figure 10.1d indicate the separation efficiency that is a combination of recovery, grade and yield to concentrate. The highest efficiency is around the 14 % mass yield to concentrate, which is similar to the THM grade in the feed.

The overall recovery of Spiral A with Material 1 was not satisfactory considering that this was a rougher spiral duty and the recovery under the best test conditions (Group 1) was poor. Only 80 % of the THM could be recovered with a 20 % mass yield to concentrate.

10.1.2 Spiral A, Material 2

Table 10.2 demonstrates the operating conditions during sampling for all the tests conducted on Spiral A with Material 2. The eleven tests were divided into three performance groupings. Group 4 (5 tests - black lines) was higher performance, Group 5 (4 tests - grey lines) medium performance and Group 6 (2 tests - dotted lines) lower performance based on the separation attributes of yield, recovery, grade and efficiency that are illustrated in Figure 10.2. These performance groupings are relative to each other and have no other test-work references. The THM and FLT density classes that resulted from the standard sink-float analysis were plotted separately. Table 10.2 also illustrates that for this data set there were no repeat tests done at

similar operating conditions but rather that a spectrum of operating parameters was evaluated. The background to these specific plotted relationships is discussed in Section 2.4.1, page 22.

Table 10.2: Operating conditions for Spiral A, Material 2 tests.

Performance Group	Test Nr	Feed Rate (t/h)	%Solids	%Slimes	%THM
4 - HIGH	15	4.86	35.74	4.37	10.39
	16	5.33	33.81	3.35	14.86
	17	5.74	36.50	3.71	11.33
	18	6.47	38.94	4.18	10.80
	19	5.58	37.12	4.65	11.26
	Avg.	5.60	36.42	4.05	11.73
5 - MEDIUM	20	5.25	33.38	2.85	11.52
	21	5.66	37.23	5.13	11.11
	22	5.71	35.54	5.68	10.94
	23	5.42	35.55	5.37	10.85
	Avg.	5.51	35.42	4.76	11.11
6 - LOW	24	5.17	33.26	6.63	9.83
	25	5.52	34.93	7.63	11.90
	Avg.	5.35	34.09	7.13	10.86

In Figure 10.2 it is clear that variability in operating conditions produced a range of spiral separation performances. Figure 10.2a shows a gradual change in THM recovery with the exception of test 25 (the last test), which shows significantly poorer performance. This can be directly related to the higher slimes content (7.6 %). The operating differences between tests 15 to 25 were not significant in terms of feed rate and solids concentration changes. The gradual increase of slimes content was considered to be the main parameter negatively influencing spiral separation performance.

The fit of the enhanced Holland-Batt equation was acceptable for the first few data points, but was unsatisfactory for the data points to the right of the Figure 10.2 graphs. The reason for this poor fit was the density distribution within the THM material itself. The THM is a single particle class containing particles with densities ranging from 3.0 to 5.0 g/cm^3. There is a natural density distribution across the spiral trough with the high-density particles (within THM) on the inside of the spiral and the lower density particles (within THM) on the outside of the spiral. When plotting the THM yield-recovery relationship the average particle density reaction will be fitted using the enhanced Holland-Batt triple spline. This relationship will be different for lower density particles and therefore not falling on the same line, but rather below the line as illustrated for the data points to the right in Figure 10.2a. If there are significant amounts of low-density particles within the THM fraction, these particles will be on a different yield-recovery line than the high-density particles. This is a further motivation for a more detailed density fractionation when evaluating spiral separation performance.

The other significant difference that Test 16 showed in comparison with the other tests was a different grade performance in Figure 10.2e and Figure 10.2f. This was expected since the THM feed grade in the sample was higher compared to the other tests (14.8 % versus 11 %). In this test the THM grade was artificially increased by the addition of material with higher THM content.

The overall recovery of Spiral A with Material 2 was not satisfactory considering that this is a rougher spiral duty and the recovery under the best test conditions (Group 4) was poorer than the poorest performing group (Group 3) with Material 1. Only 50 % of the THM could be recovered with a mass yield to concentrate of 20 %. This gave the indication that material

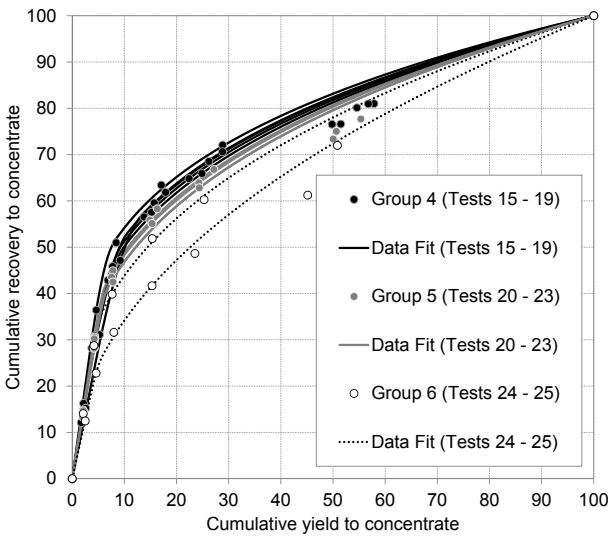

(a) THM cumulative recovery.

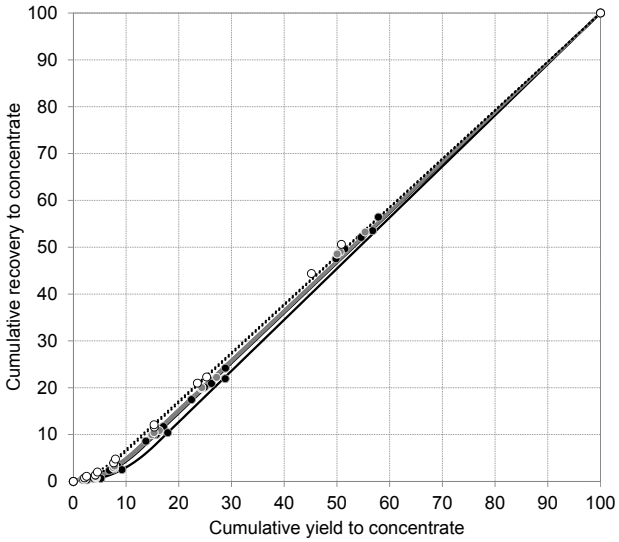

(b) FLT cumulative recovery.

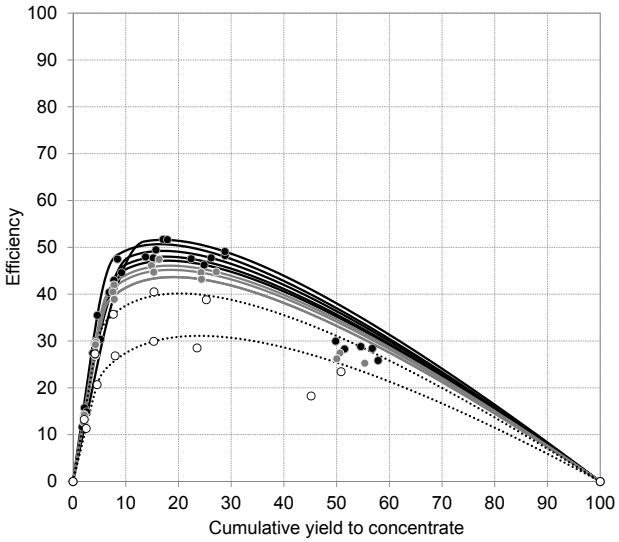

(c) THM separation efficiency.

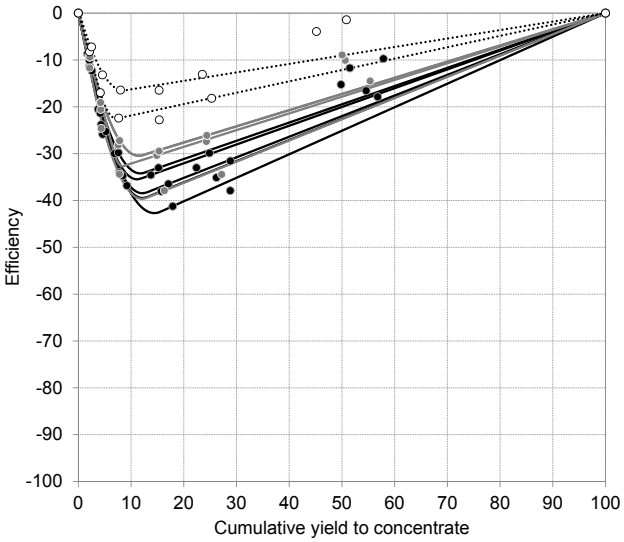

(d) FLT separation efficiency.

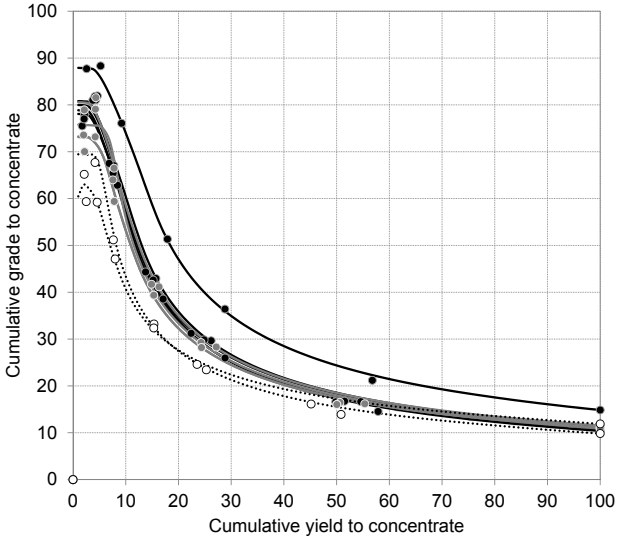

(e) THM cumulative grade.

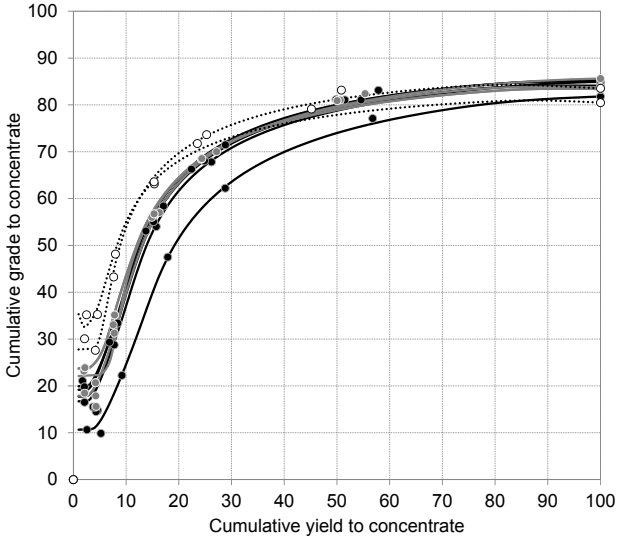

(f) FLT cumulative grade.

Figure 10.2: Spiral performance for different tests for Spiral A, Material 2.

type played a significant role in spiral separation performance since the operating conditions were not significantly different between Material 1 tests and Material 2 tests.

10.1.3 Spiral B, Material 2

Table 10.3 demonstrates the operating conditions during sampling for all the tests conducted on Spiral B with Material 2. The fourteen tests were divided into three performance groupings. Group 7 (3 tests - black lines) was higher performance, Group 8 (5 tests - grey lines) medium performance and Group 9 (6 tests) lower performance based on the separation attributes of yield, recovery, grade and efficiency, which are illustrated in Figure 10.3. These performance groupings are relative to each other and have no other test-work references. The THM and FLT density classes that resulted from the standard sink-float analysis are plotted separately. Table 18 also illustrates that for this data set there were no repeat tests done at similar operating conditions, but rather that a spectrum of operating parameters was evaluated. The background to these specific plotted relationships is discussed in Section 2.4.1, page 22

Table 10.3: Operating conditions for Spiral B, Material 2 tests.

Performance Group	Test Nr	Feed Rate (t/h)	%Solids	%Slimes	%THM
7 - HIGH	26	2.07	38.44	4.22	11.30
	27	1.38	36.10	5.00	11.27
	28	2.15	35.64	4.26	14.39
	Avg.	1.87	36.73	4.49	12.32
8 - MEDIUM	29	1.97	34.57	5.38	9.60
	30	1.99	41.55	4.71	11.65
	31	2.02	32.49	6.90	7.61
	32	2.33	37.54	5.60	11.85
	33	1.86	39.54	6.26	11.87
	Avg.	2.03	37.14	5.77	10.51
9 - LOW	34	1.83	34.74	7.05	12.10
	35	2.15	36.27	6.12	11.82
	36	2.20	34.37	5.64	5.99
	37	2.34	35.03	6.57	11.40
	38	2.29	37.51	6.51	12.00
	39	2.20	34.19	7.07	12.04
	Avg.	2.17	35.35	6.49	10.89

In Figure 10.3a it is clear that the variability in the operating conditions produced a range of spiral separation performances for Spiral B. The variability with regards to feed rate and solids concentration could be seen in all three the test groups. Slimes content was again identified as the parameter with the strongest influence on spiral separation performance for this material and spiral profile. It was observed that higher feed rates and higher pulp densities can be tolerated if the slimes content was low. Once the slimes content was more than 5 %, increased feed rate and percentage solids negatively impacted on spiral separation performance. The other side was also true, where higher slimes content could be tolerated if the feed rate and percentage solids were below design feed conditions.

THM feed grade did not influence spiral separation efficiency, but the difference in feed grade can be clearly seen in Figure 10.3e and Figure 10.3f, as well as the gradients of the initial part of the graph in Figure 10.3a and Figure 10.3b.

The overall recovery of Spiral B with Material 2 was better compared to Spiral A with Material 2. The THM recovery was still low and only 80 % of the THM could be recovered

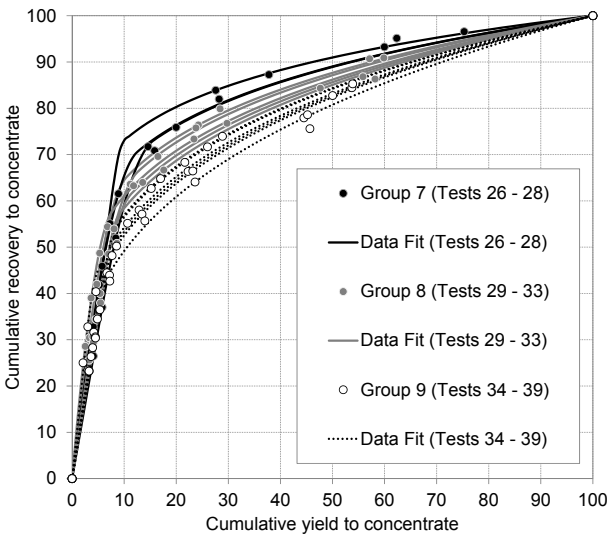

(a) THM cumulative recovery.

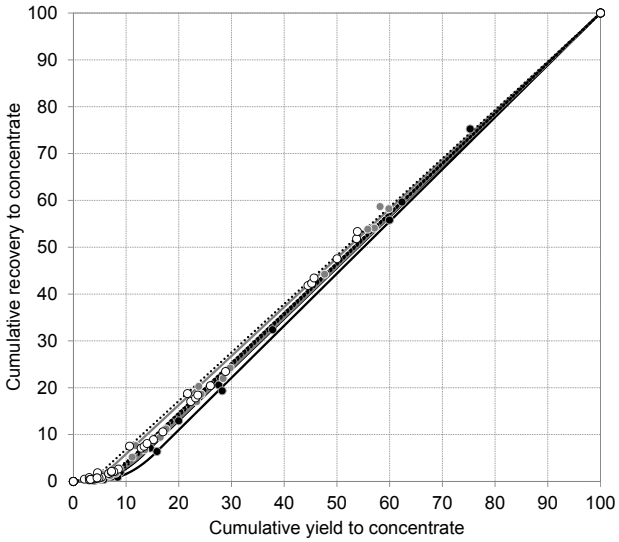

(b) FLT cumulative recovery.

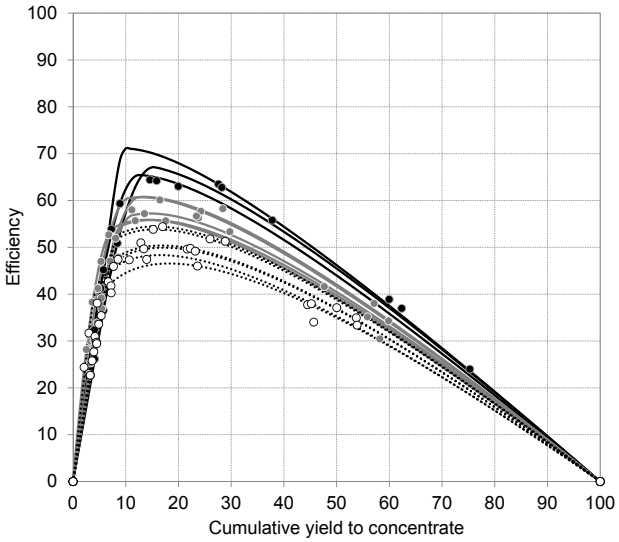

(c) THM separation efficiency.

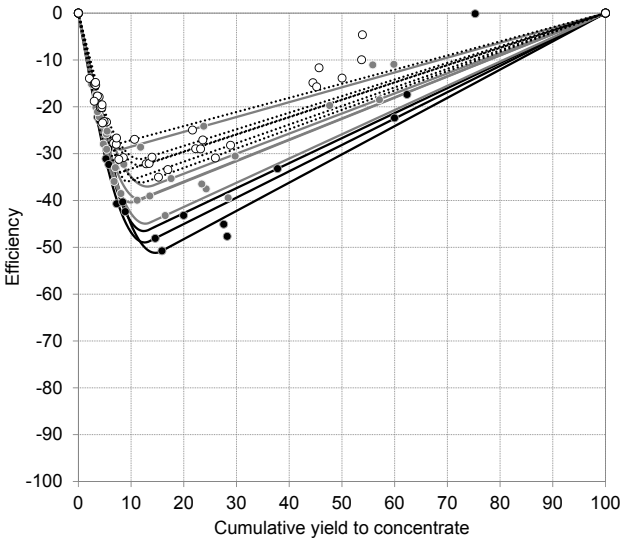

(d) FLT separation efficiency.

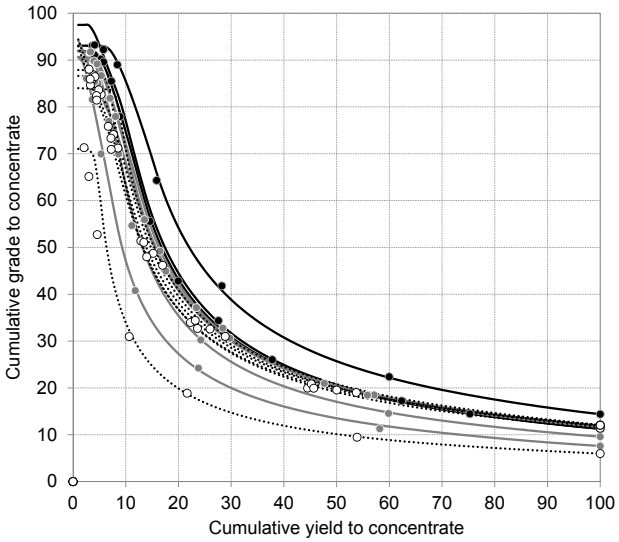

(e) THM cumulative grade.

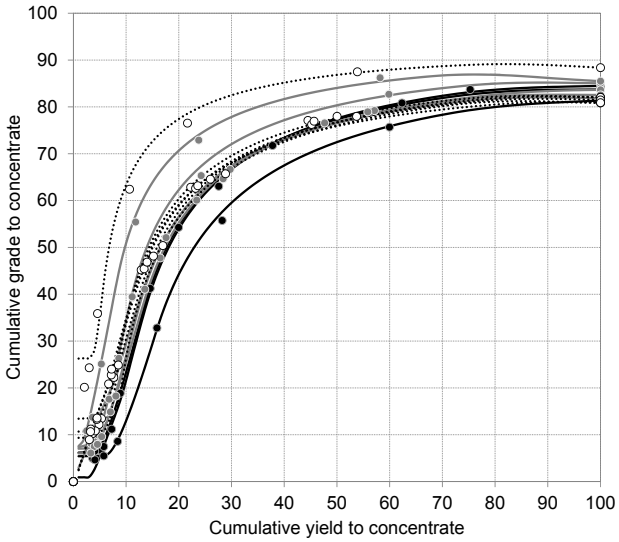

(f) FLT cumulative grade.

Figure 10.3: Spiral performance for different tests for Spiral B, Material 2.

with a mass yield to concentrate of 20 %. This gives an indication that the spiral trough played a significant role in separation performance, since the operating conditions were not significantly different between Spiral A and B other than that the design throughput tonnages differed.

10.2 Summary

The following is a summary of the main points from this chapter.

- The two feed materials and two spiral profiles differed vastly from each other and could be clearly seen in the spiral separation performance depicted by the figures in this chapter.
- From an operating parameter point of view, slimes content was identified as a strong influence especially once it exceeded some critical value.
- THM grade variances (within the tested ranges) seemed to have limited to no influence on performance.
- Material 1 and 2 performed vastly different on the same Spiral A, which illustrates the importance of understanding the influence of material type on a spiral trough.
- Spiral A and B performed vastly different with the same material (Type 2), which illustrates the importance of matching a specific spiral profile to a specific feed material.
- The enhanced Holland-Batt equation provided consistency in the test-work data with reasonably good fits across all the test-work points although the fitting of the data points associated with the outside of the spiral showed some concern.
- The poor fits to the right of the figures are explained as a result of plotting a particle population with wide density distribution as a single line instead of multiple lines.
- In all the tests none of the results gave satisfactory THM recoveries for the materials tested.

Chapter 11

Enhanced Product Characterisation

Chapter 10 illustrated and discussed the results of standard product characterisation, where the spiral trough was divided in 7 products and characterised by means of sink-float analysis. This information was presented using the three combinations of the 4 separation attributes yield, grade, efficiency and recovery. This chapter illustrates the benefit of enhanced product characterisation over standard product characterisation by comparison. The sink and float fractions are further characterised using Qemscan®, which is the reason for the term enhanced characterisation. The chapter starts with a motivation for enhanced characterisation. The spiral separation performance results based on enhanced characterisation are discussed in Chapter 12.

11.1 Motivation

Particle size and particle density variation across the spiral trough are presented in Figure 11.1, Figure 11.2 and Figure 11.3. Figure 11.1 and Figure 11.2 illustrate the data obtained from screening the different mouth-organ samples taken across the spiral trough. The THM and FLT particle size distribution data is presented separately since the size distribution differed significantly. Only a single spiral test (Test1) is presented since the data from the other spiral tests showed similar trends. Refer to Appendix D.1 for more data.

The particle density distribution data in Figure 11.3 was obtained from Qemscan®. In this case the sample was not physically separated into different density fractions, but it was calculated from the minerals as identified on the particle cross sections from the polished block as discussed in Section 4.5.2, page 55. Refer to Appendix D.2 for the data.

It can be seen from Figure 11.1, Figure 11.2 and Figure 11.3 that there is a significant variation of both particle size and particle density across the spiral trough during separation. The D_{50} value in the THM particle class differed with more than 40 µm between the inner and outer sections of the spiral trough. The D_{50} value in the FLT particle class differed with more than 80 µm between the inner and outer sections of the spiral trough. The ρ_{50} value in THM particle class differed with more than 0.7 g/cm^3 between the inner and outer sections of the spiral trough. This implied that the THM particle class and FLT particle class had a significant variability in terms of particle size and particle density. If the THM particle class was to be combined, as with standard characterisation, this variation would not be visible and only the 'averaged' spiral separation performance would be measured. The combination of the different size and density particle classes could hide certain operating inefficiencies or advantages of spiral separation performance for a specific material composition on a specific spiral trough. This particle size variation for a certain particle density class was also identified by (**bazin2014**), providing additional supporting evidence to the importance of quantifying particle size and density simultaneously.

The basis of the enhanced characterisation was to separate the FLT and THM into different

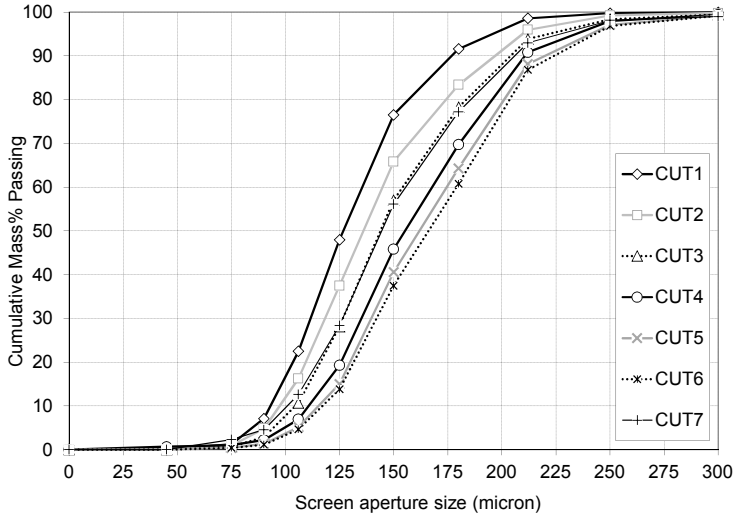

Figure 11.1: THM particle size distribution variation across spiral trough. (Cut 1 to Cut 7 represent the different samples from the mouth-organ sampler, Material 1, Spiral A)

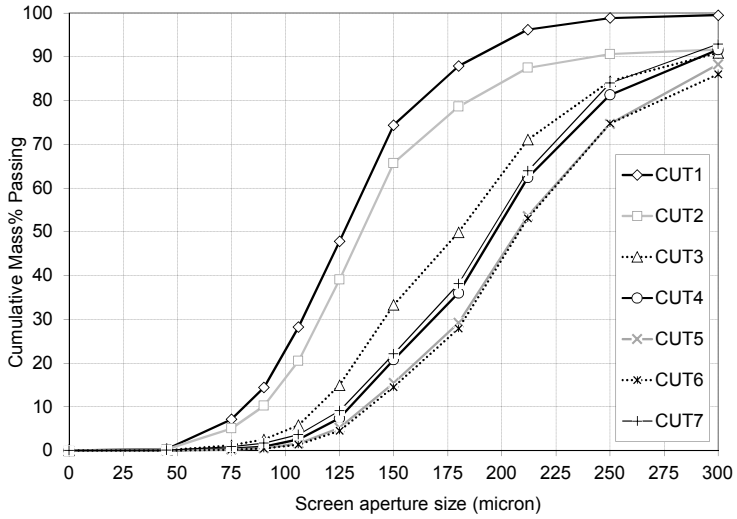

Figure 11.2: FLT particle size distribution variation across spiral trough.

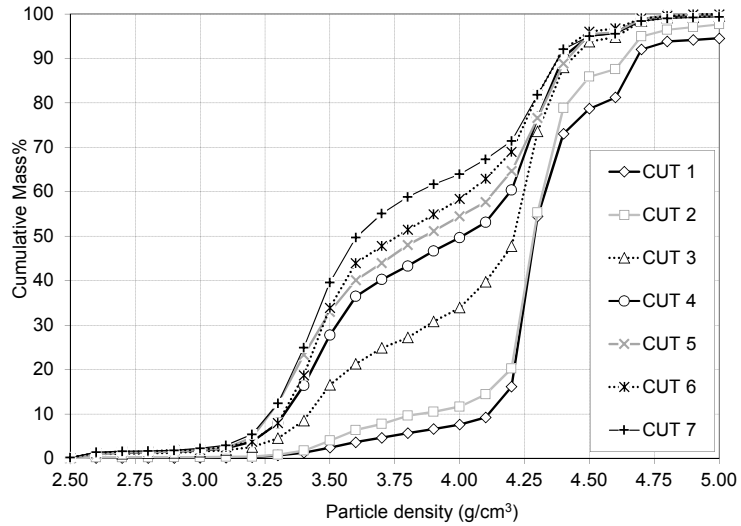

Figure 11.3: THM particle density distribution variation across spiral trough. (Cut 1 to Cut 7 represent the different samples from the mouth-organ sampler, Material 1, Spiral A)

Table 11.1: Naming convention for standard characterisation.

		Density Range (g/cm^3)	
		0.0 - 3.0 (Lo)	3.0 - 6.0 (Hi)
Size Range	0 - 1000	FLT	THM

Table 11.2: Material 1 average sand composition (mass%) based on standard characterisation.

		Density Range (g/cm^3)	
		0.0 - 3.0 (Lo)	3.0 - 6.0 (Hi)
Size Range (µm)	0 - 1000	86.2	13.8

size and density classes by means of a simple analytical method to measure this particle size and particle density variation across the trough during spiral separation. This information would enable the evaluator to select the most suitable spiral trough for application on a specific feed material.

The standard method is neither able to supply the particle size and density information required to make informed decisions on matching a spiral with specific feed material, nor to explain the reasons for poor or good spiral separation performance. Enhanced product characterisation using Qemscan® provides a simple and cost effective solution to this information gap.

11.2 Standard vs Enhanced

After illustrating the significant size and density variations within the THM and FLT fractions for the different spiral products, the next section compares the data output from the standard and enhanced methods to demonstrate the additional valuable information from the enhanced method.

11.2.1 Material 1 Products

The standard method had two density classes and one size class which resulted in two mass classes as seen in Table 11.1. These two classes were termed THM and FLT based on a sink-float fractionation as applied and discussed in previous chapters. Material 1 contained an average of 86.2 % mass in the FLT class and 13.8 % in the THM class shown in Table 11.2. Only the sand fraction was considered in this evaluation since the slimes formed part of the separation medium and not the particles.

Figure 11.4 demonstrates the mass distribution from Table 11.2 in a cylinder graph. These cylinders were broken down into seven mass fractions by means of spiral separation. This fractionation produced Figure 11.5, which illustrates the mass and density variation across the spiral trough in Cut 1 to Cut 7. Figure 11.4 plots the data of spiral performance using the standard characterisation method applied. The three dimensional plot allows for particle class on the x-axis, spiral trough position on the y-axis and mass percentage on the z-axis. The dark coloured cylinders represent the higher density classes and the light coloured cylinders represent the lower density classes.

The enhanced method divides the material into nine size-density classes instead of the normal two (THM and FLT). The material below density of 3.0 g/cm^3, mainly FLT, was divided into three size classes. The material above density of 3.0 g/cm^3, mainly THM, was divided into six size-density classes. Each one of the particle classes are assigned a specific name, which is used in the results in the rest of the chapter. In Table 11.3 the size and density ranges of each of the nine particle classes are illustrated as well as the assigned labels of each class are

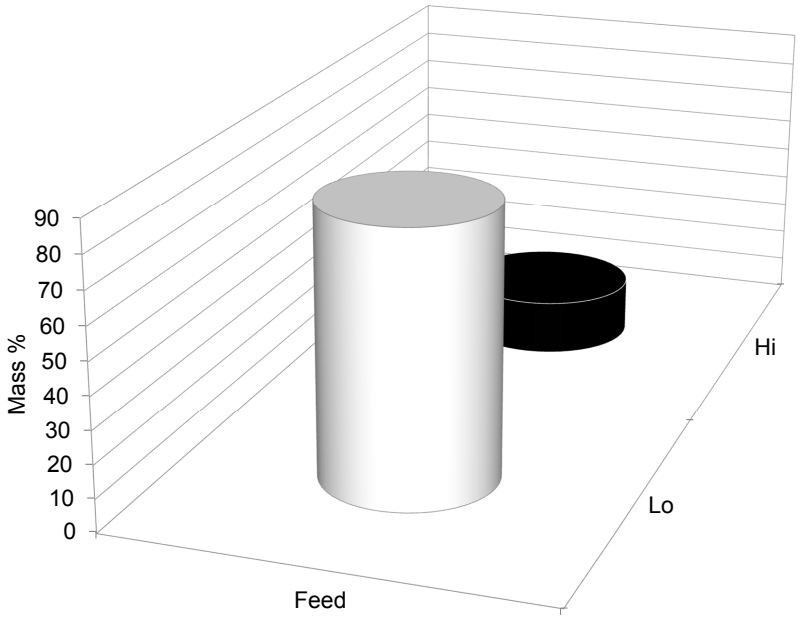

Figure 11.4: Material 1 particle density distribution using standard characterisation. (Lo = float fraction, Hi = sink fraction)

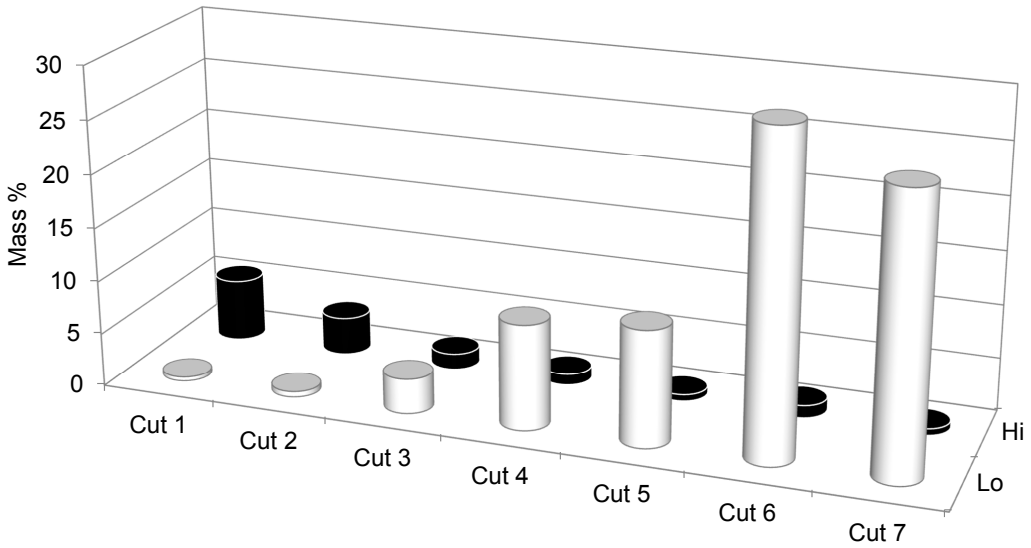

Figure 11.5: Material 1 particle density distribution across spiral trough using standard characterisation. (Cuts 1 to 7 represent the different mouth-organ sampler cuts, Lo: $<3\,\mathrm{g/cm^{-3}}$, Md = 3-4 $\mathrm{g/cm^3}$, Hi: $>4\,\mathrm{g/cm^3}$)

indicated. The first part of the name refers to the size of the class (Fine, Med, Crs), the second part of the name refers to the density of the class (Lo, Md, Hi). Table 11.4 illustrates the mass percentage distribution of the feed material into the different particle classes. The sum of the mass percentages in the "Lo" density class should correspond to the FLT mass and the sum of the mass percentages in the "Md" and "Hi" classes should correspond to the THM mass. These numbers would not be exactly the same, since the sink-float fractionation was not an exact separation and there were still some high-density particles trapped in the floats. Since Qemscan® analysed the particles in the FLT fraction, the correction could be made causing some mass percentage increase in the back calculated THM value. This mass increase would be more in the lower density ranges between 3.0 and 3.5 g/cm^3 since these medium density particles were more easily entrapped in the FLT fraction during sink-float fractionation. Compare Table 11.2 with back calculated values in Table 11.4.

The feed material was characterised on a 9×9 particle class, refer to Figure 9.3 on page 101, while the product was characterised on a 3×3 particle class. It should be noted that since the enhanced characterisation does not involve any physical fractionation, the number of size and density classes can be selected and the material divided accordingly. This investigation selected a 3×3 particle class based on the following reasons:

1. To demonstrate the enhanced characterisation technique the number of particle classes were minimised for simplicity.

2. Valuable heavy minerals are typically above a density of 4.0 gcm^3 and non-valuable heavy minerals between 3.0 and 4.0 g/cm^3, therefore the 3 density classes (Lo, Md, Hi) were a good balance between simplicity and additional information worth.

3. The majority of the heavy mineral particles are below 200 µm, which motivates this particle size boundary.

4. Heavy mineral particles below 100 µm have generally lower recoveries, although there are usually significant amounts present. It made sense to track this population as well.

5. Particle classes with little to no mass make the fitting of the test-work data from spiral separation inaccurate and troublesome.

Other mineral sands deposits or commodities will have different particle size and density class boundaries. These should be considered when defining the particle classes. The selection of a square matrix is helpful when plotting data, but it is not a requirement. If there is a specific size density class of significant mass that needs to be tracked separately, it can be done with minimal effort. It should also be noted that the particle class that is selected will have its own size and density distribution, and the average size and density of the material in a specific class might differ significantly from the midpoint of the particle class. For example, the 'MedHi' class in Table 11.4 contains 7 % mass in a density range between 4.0 and 6.0 g/cm^3. The actual average density of the class will be close to 4.5 g/cm^3 instead of the midpoint density, 5.0 g/cm^3, of the particle class. It was for this reason that bar charts were used in presenting the data instead of continuous surface graphs.

The mass percentage distribution of the nine particle classes in the feed from Table 11.4 is plotted to produce Figure 11.6. Similar to Figure 11.5, the mass percentages can be further divided as it was fractionated with the spiral. Figure 11.7a presents all the mass percentages across the spiral trough for the nine different size-density classes. Figure 11.7b presents the same data, but without the three low-density particle classes to increase the resolution in the medium- and high-density particle classes.

Table 11.3: Naming convention for enhanced characterisation. (Med = medium size, Crs = coarse size, Lo = low density, Md = medium density, Hi = high density)

		Density Range (g/cm^3)		
		0.0 - 3.0	3.0 - 4.0	4.0 - 6.0
Size Range (µm)	0 - 100	FineLo	FineMd	FineHi
	100 -200	MedLo	MedMd	MedHi
	200 -1000	CrsLo	CrsMd	CrsHi

Table 11.4: Material 1 average sand composition (mass%) based on enhanced characterisation.

		Density Range (g/cm^3)		
		0.0 - 3.0	3.0 - 4.0	4.0 - 6.0
Size Range (µm)	0 - 100	13.3	0.8	2.5
	100 -200	42.8	2.0	7.5
	200 -1000	28.8	0.8	1.9
Sum	0 -1000	85.0	15.0	

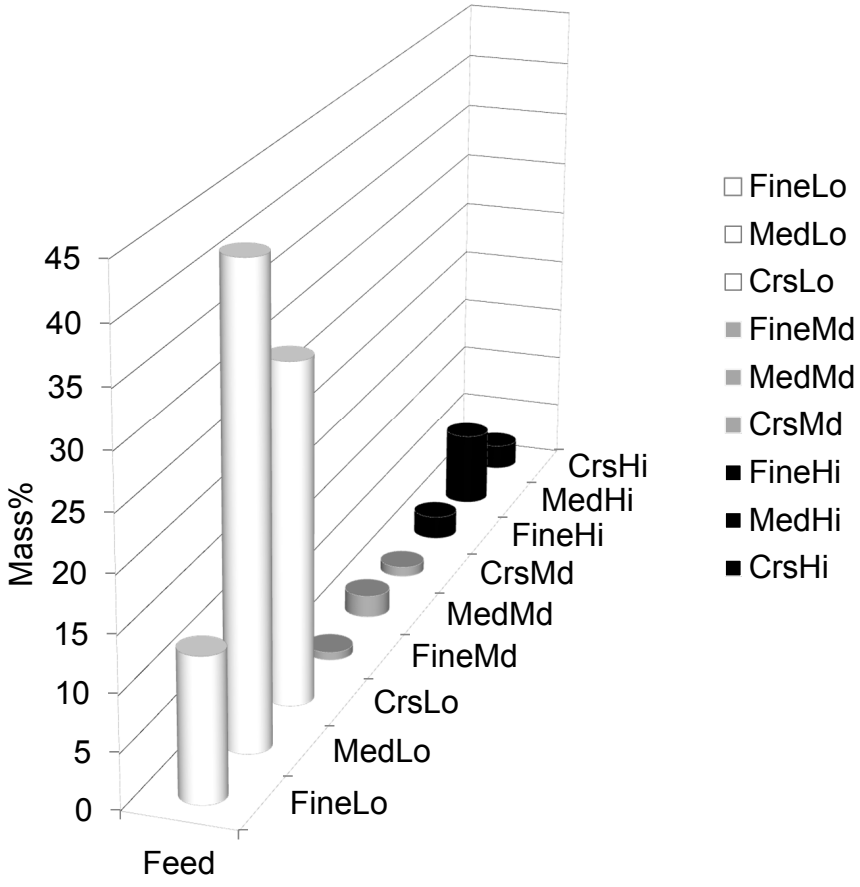

Figure 11.6: Material 1 particle density distribution using enhanced characterisation. (Lo: <3 g/cm^{-3}, Md = 3-4 g/cm^3, Hi: >4 g/cm^3)

Table 11.5: Legend for the result presentation.

Particle Class	Lo	Md	Hi
Fine Size	**X**	**X**	**X**
Medium Size	**X**	**X**	**X**
Coarse Size	**X**	**X**	**X**

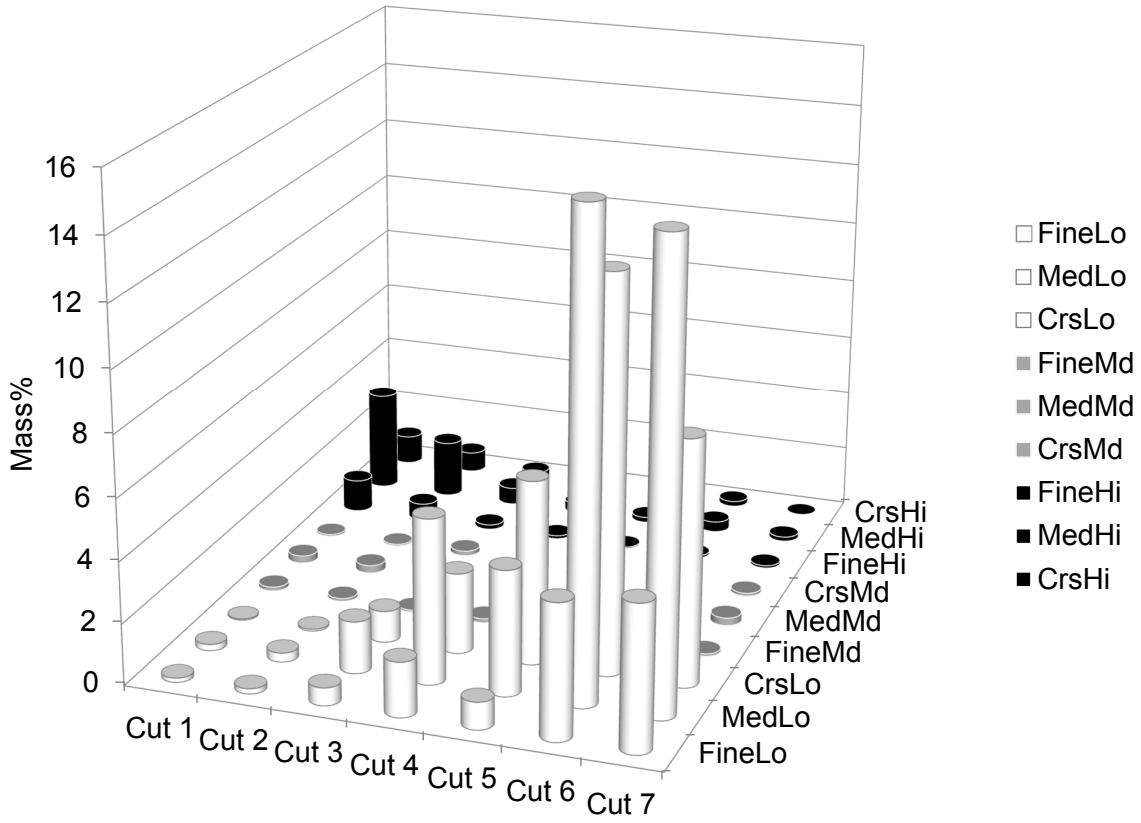

(a) All classes.

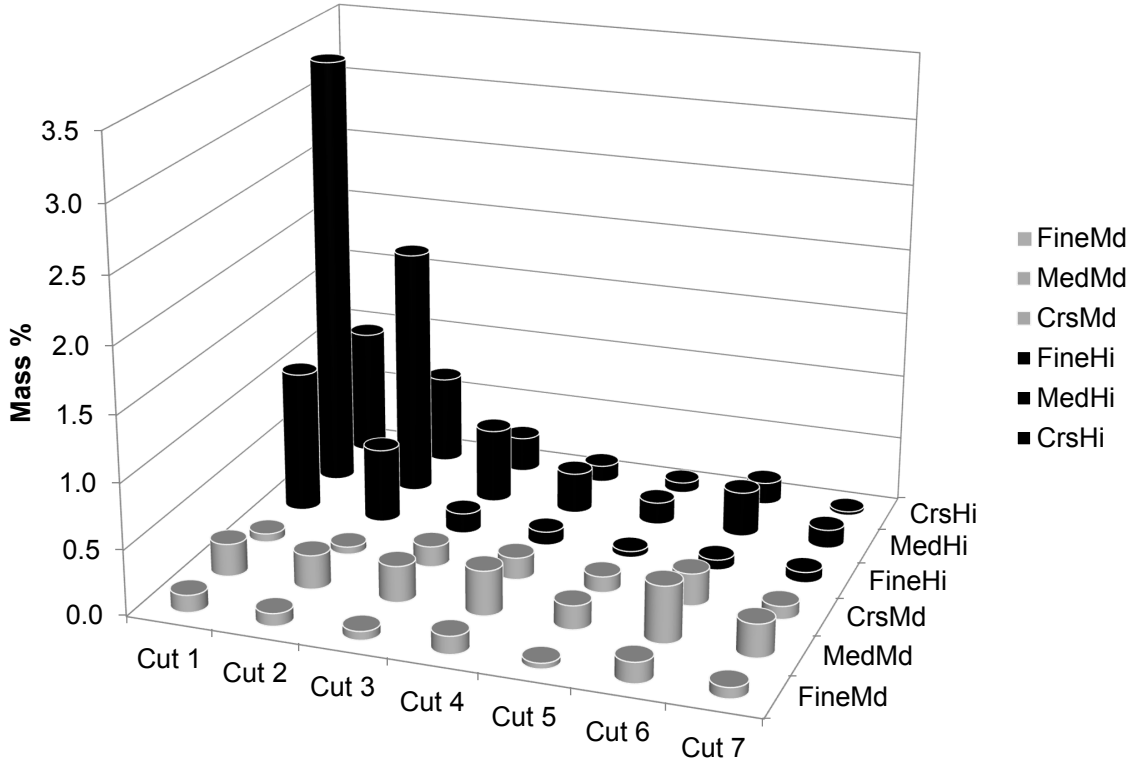

(b) High-density classes only.

Figure 11.7: Material 1 particle size-density distribution across spiral trough using enhanced material characterisation. (Cuts 1 to 7 represent the different mouth-organ sampler cuts. Refer to Table 11.4 for a density and size definition of particle class labels.)

Table 11.6: Material 2 average sand composition (mass%) based on standard characterisation.

		Density Range (g/cm^3)	
		0.0 - 3.0 (Lo)	3.0 - 6.0 (Hi)
Size Range (µm)	0 - 1000	88.8	11.2

Table 11.7: Material 2 average sand composition (mass%) based on enhanced characterisation.

		Density Range (g/cm^3)		
		0.0 - 3.0	3.0 - 4.0	4.0 - 6.0
Size Range (µm)	0 - 100	3.1	2.0	2.1
	100 -200	22.1	5.7	2.8
	200 -1000	58.0	3.7	0.5
Sum	0 -1000	83.2	16.8	

For the purpose of presenting the results in the next sections of this chapter, the legend in Table 11.5 is used to indicate which one of the nine particle classes is presented in a specific figure. This legend corresponds with Table 11.3 and Table 11.4. If three crosses are indicated in the legend it implies that it represents the combination of the three particle classes. The same would apply for six crosses. If only one cross is indicated, only that specific particle class is presented in the graph.

11.2.2 Material 2 Products

For Material 2 the same tables were populated as for Material 1. The same size-density classes were also utilised for ease of comparison. The back-calculated mass percentage of the "Md" and "Hi" particle classes combined were higher than the THM value. Material 2 contained predominantly medium density particles in the THM which were more easily entrapped in the float fraction during the sink-float fractionation. Therefore the Qemscan® correction of the value was higher compared to Material 1.

The data in Table 11.6 is presented in graphical form in Figure 11.8. An example of how the spiral fractionated these two density classes across the spiral trough is shown in Figure 11.9. Table 11.7 is represented in graphical form in Figure 11.10. The spiral fractionated the particle class masses from Figure 11.10 into the masses presented in Figure 11.11.

In Chapter 12 the standard and enhanced characterisation are compared with one another for different operating conditions. The cylinder graphs presented earlier would make the comparison of different spiral tests too complicated. Therefore, the cumulative yield versus cumulative particle class recovery was used to demonstrate the differences between the standard and enhanced product characterisation methods. A single spiral test (Test 28) is presented in Figure 11.12 to illustrate the structure for the next chapter. Figure 11.12a illustrates the single THM particle class from sink-float analysis, while Figure 11.12b illustrates the six particle classes that make up the THM.

The standard characterisation method (sink-float) application on Material 1 and Material 2 indicates that Material 1 had a slightly higher THM content (13.8 %) compared to Material 2 (11.2 %). Material 2 had poorer separation performance on Spiral A compared to Material 1. A possible conclusion from the standard result could be that Spiral A's separation performance was sensitive to THM grade.

The enhanced characterisation method (Qemscan® classification) applied to Material 1 and Material 2 indicated a significant difference in the intermediate density fraction (between 3.0 and 4.0 g/cm^3) and medium particle size class in the FLT fraction (between 100 µm and 200 µm). The Material 1 THM fraction had less than 25 % medium density particles, while the Material 2 THM fraction contained more than 67 % of medium density particles. The Material 1 FLT

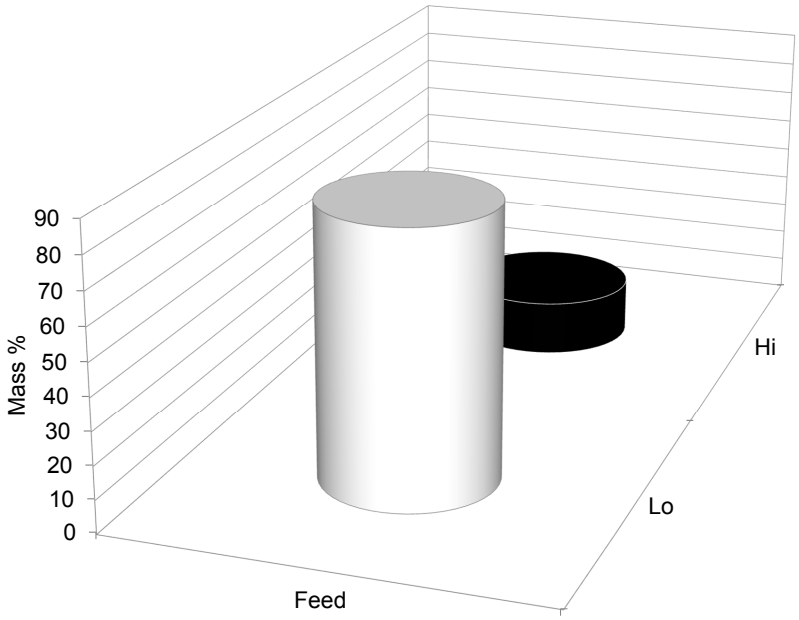

Figure 11.8: Material 2 particle density distribution using standard characterisation. (Sink-float analysis data corrected after Qemscan® analysis - back calculated.)

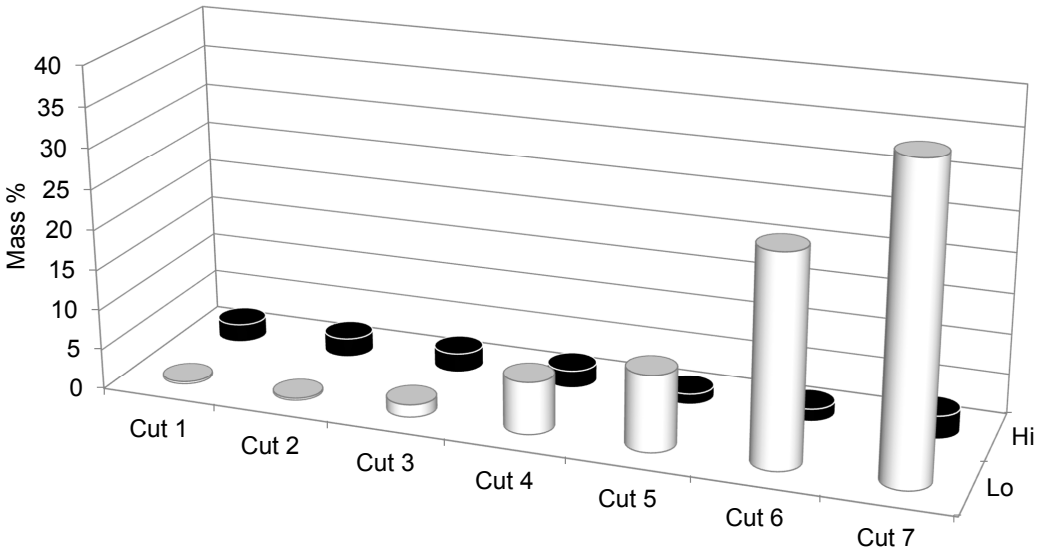

Figure 11.9: Material 2 particle density distribution across spiral trough using standard characterisation. (Cuts 1 to 7 represent the different mouth-organ sampler cuts, Lo: $<3\,g/cm^{-3}$, Md = 3-4 g/cm^3, Hi: $>4\,g/cm^3$)

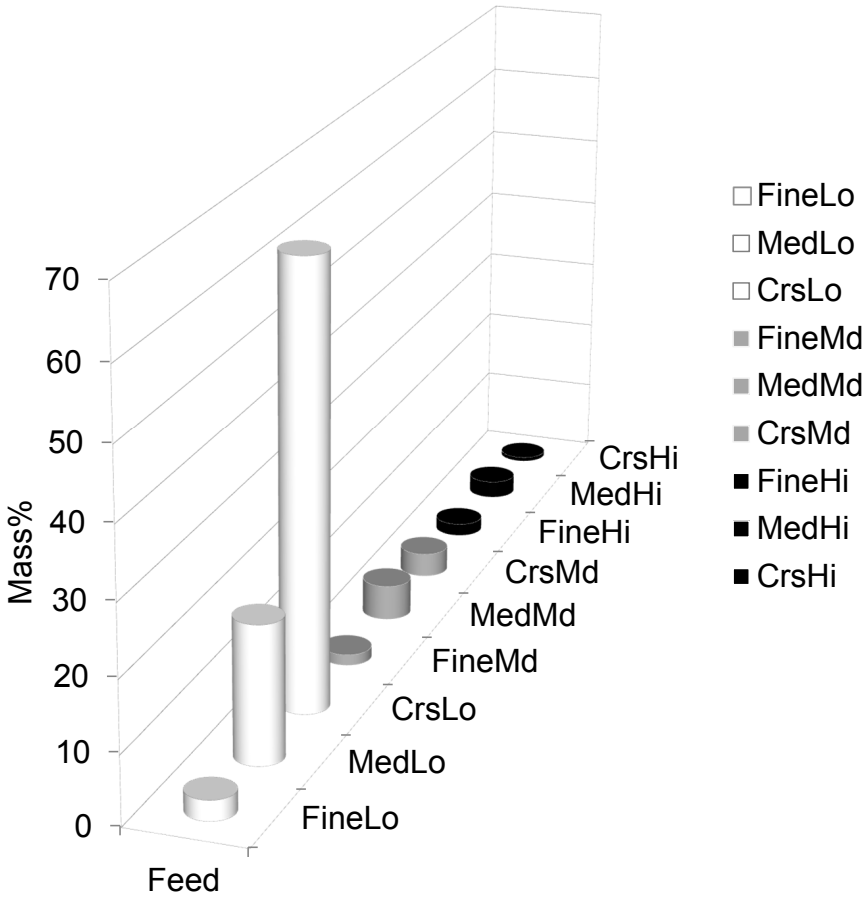

Figure 11.10: Material 2 particle density distribution using enhanced characterisation. (Lo: $<3\,g/cm^{-3}$, Md = 3-4 g/cm^3, Hi: $>4\,g/cm^3$)

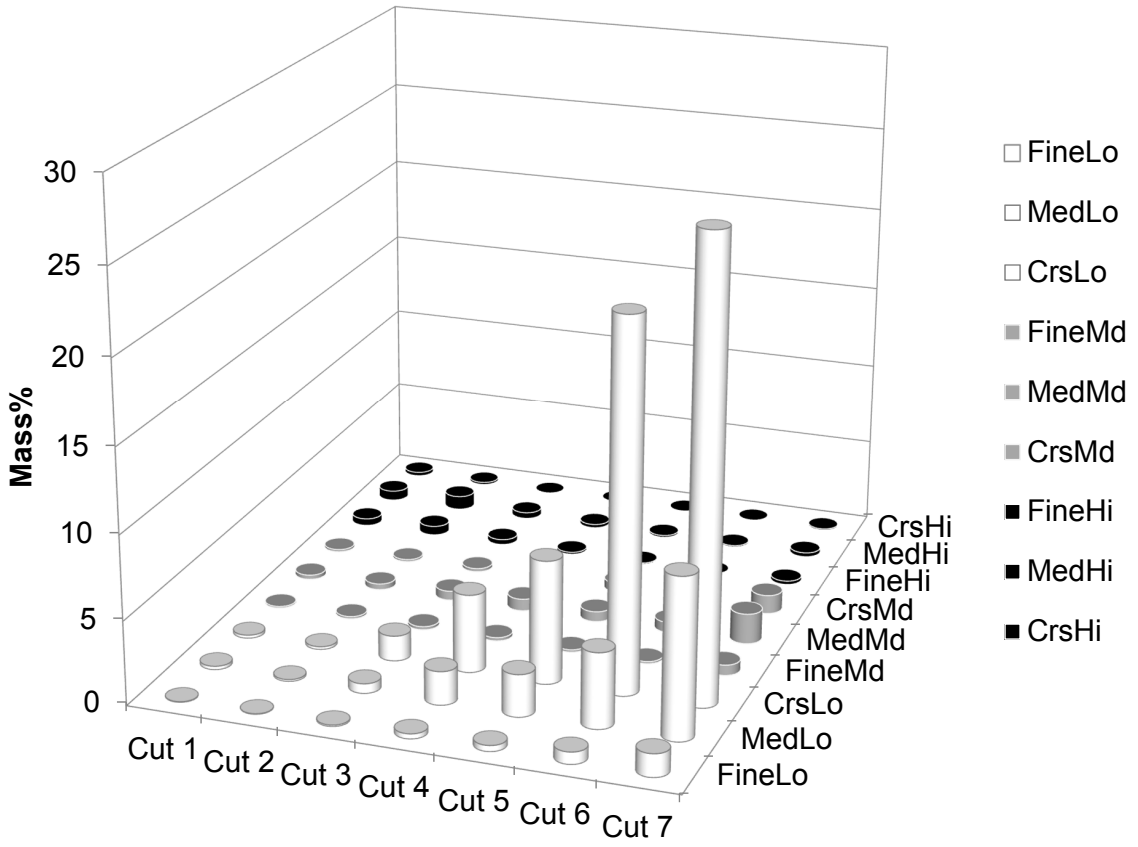

(a) All classes.

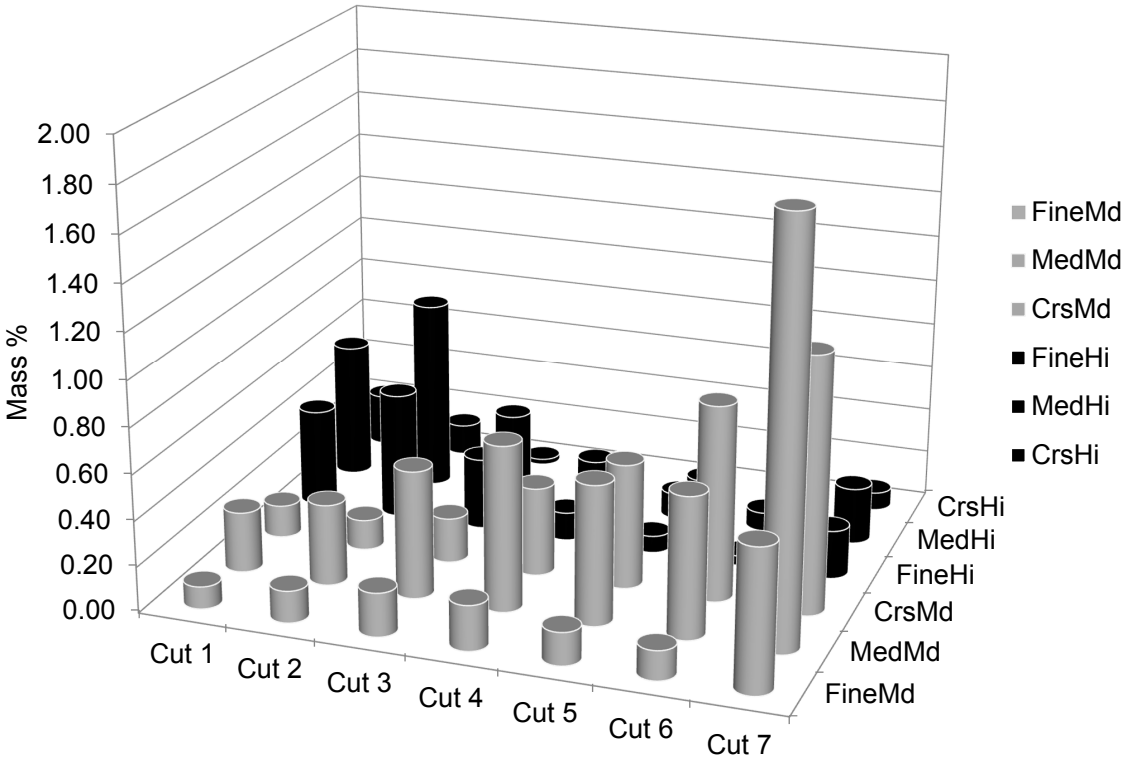

(b) High-density classes only.

Figure 11.11: Material 2 particle size-density distribution across spiral trough using enhanced material characterisation. (Cuts 1 to 7 represent the different mouth-organ sampler cuts. Refer to Table 11.7 for a density and size definition of particle class labels.)

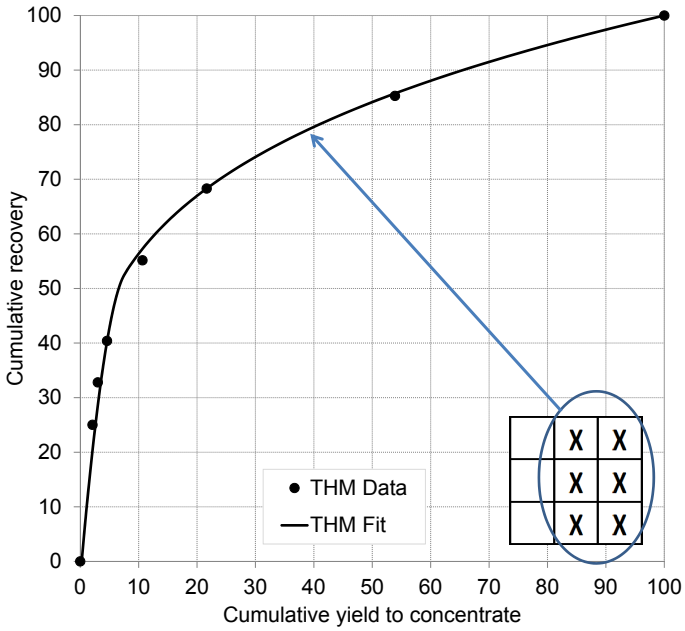

(a) Standard characterisation.

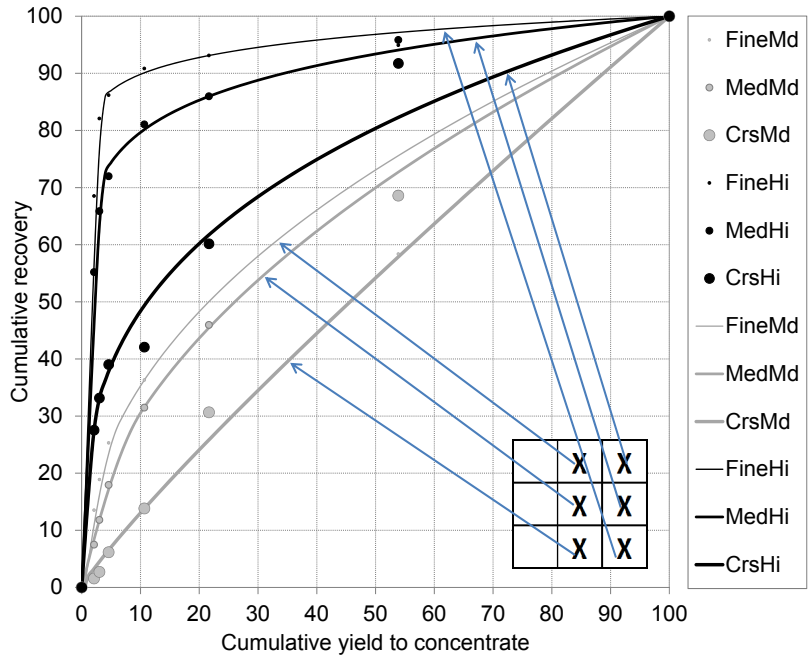

(b) Enhanced characterisation.

Figure 11.12: Comparison of THM recovery visualisation between standard and enhanced characterisation.

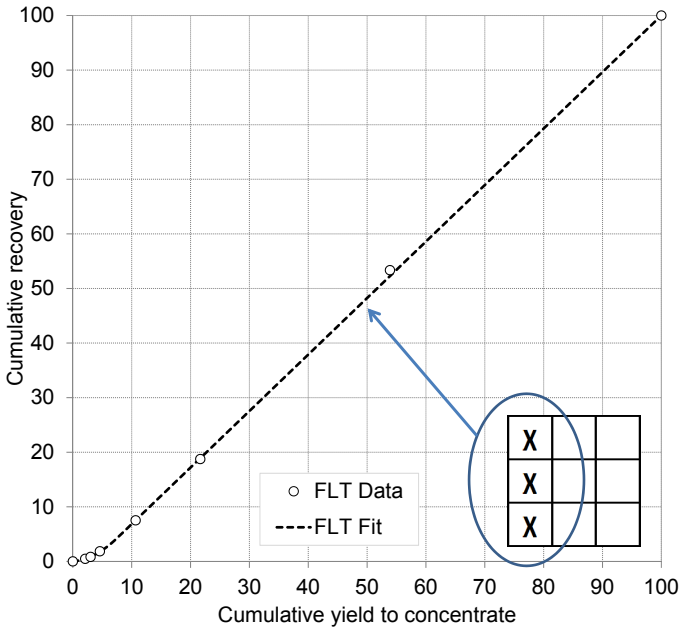

(a) Standard characterisation.

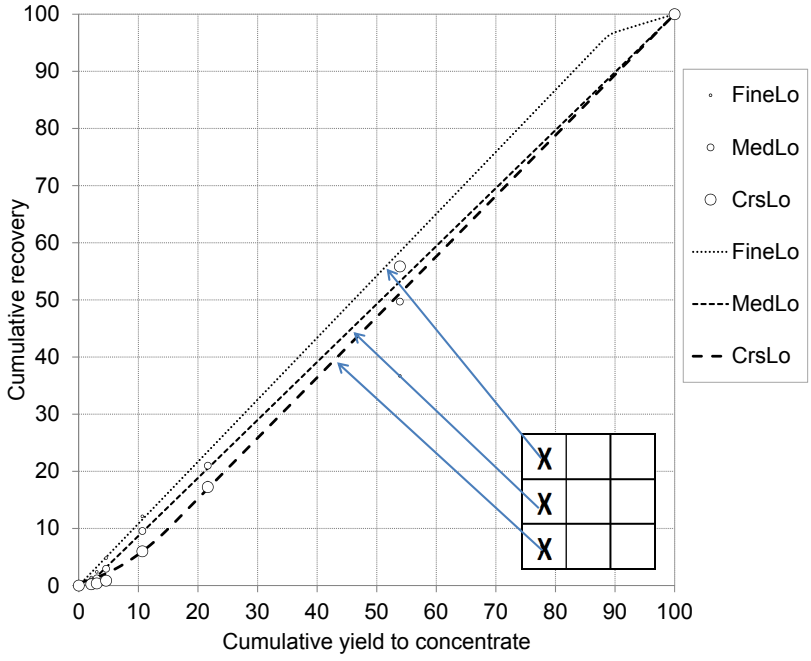

(b) Enhanced characterisation.

Figure 11.13: Comparison of FLT recovery visualisation between standard and enhanced characterisation.

fraction had more than 40 % medium-sized particles and around30 % coarse-sized particles. The Material 2 FLT fraction had less than 20 % medium-sized particles and more than 60 % coarse-sized particles.

These two material differences would have a significant impact on the spiral separation performance. If these critical particle size and density parameters were not measured and understood in the light of the particle size and density fractionation that occurred on the spiral, it would result in the wrong conclusions. The enhanced characterisation data is plotted as cylinder graphs in Figure 11.6 and Figure 11.10. These figures illustrate how the nine size-density classes varied across the spiral trough for the two material types. This same information is plotted on cumulative recovery graphs. Figure 11.12 illustrates the wide variation in cumulative recovery for the six different size-density particle classes when compared to the single THM line. Figure 11.13 illustrates the wide variation in cumulative recovery for the three different size particle classes when compared to the single FLT line.

11.3 Summary

The following is a summary of the main points from this chapter.

- The importance of enhanced product characterisation was demonstrated by the wide separation spectrum of the nine different particle classes contained within the THM and FLT particle classes obtained from only standard characterisation.
- Materials 1 and 2 that were expected to separate similarly based on the standard analysis, separated very differently. This observation corresponded well with the expectations from the enhanced feed material characterisation in Chapter 9.
- The selection of the boundaries and the number of particle classes were dependant on the material and would need to be considered carefully when another material is evaluated.
- The enhanced product characterisation method is critical to ensure that the correct conclusions are made with regards to spiral separation performance for specific material. The greater the size and density range of the material under investigation, the greater the need for enhanced product characterisation. In other words, if there are only two minerals present with narrow particle size ranges, enhanced product characterisation will produce similar conclusions to the standard product characterisation.
- The particle class yield-recovery relationship was selected to illustrate the advantages of the enhanced product characterisation in Chapter 12, when the different operating conditions are compared with each other.

Chapter 12

Enhanced Analysis of Spiral Separation Performance

This chapter is divided in three sections. Each section illustrates and discusses the spiral separation performance for a spiral profile-material combination using enhanced product characterisation data. The focus is on the influence of operating conditions and relating those to the spiral separation performance. This chapter has a similar structure to Chapter 10, which discussed the influence of operating parameters but used the data from standard product characterisation. For ease of comparison, the operating parameters and summary of the standard product characterisation are repeated from Chapter 10. The line formatting remains the same from Chapter 10. The size and density definition of the particle classes are the same as discussed in Chapter 11.

12.1 Influence of Operating Parameters

12.1.1 Spiral A, Material 1

Figure 12.1 illustrates the FLT cumulative recovery for all the operating conditions evaluated on Spiral A, Material 1 using standard product characterisation. All the data from standard product characterisation are indicated with a grey background on the figures. Figure 12.2 illustrates the three different particle classes that make up the FLT fraction, as extracted from enhanced product characterisation. Table 12.1 presents the summarised operating conditions for this section.

Table 12.1: Summarised operating conditions for Spiral A, Material 1 tests.

Performance Group	Test Nr	Feed Rate (t/h)	%Solids	%Slimes	%THM
1 - HIGH	1-3	4.40	39.47	2.61	13.99
2 - MEDIUM	4-11	5.71	44.36	3.28	13.75
3 - LOW	12-14	6.93	50.55	3.70	13.78

The three particle classes for the FLT fraction do not show significant variation across the spiral trough. The fine class (less than 100 µm) in Figure 12.2 shows a slightly poorer separation, with its line being closer to the zero separation line compared to the two coarser classes. The slight variation with operating condition changes is consistent with the variation picked up from the standard characterisation. The coarse particle class demonstrates the best separation efficiency being the furthest from the zero separation line. Figure 12.3 illustrates the THM cumulative recovery for all the operating conditions evaluated on Spiral A and Material 1 using standard product characterisation. In Figure 12.4, the six graphs illustrate the six different

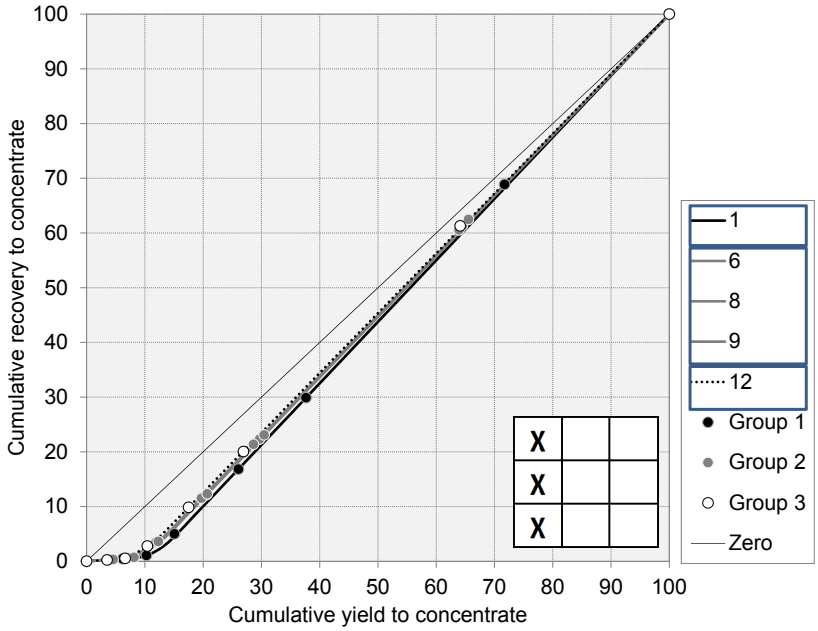

Figure 12.1: Spiral A, Material 1 low-density particle class recoveries. (Standard characterisation for different operating conditions. 85.0 % of mass)

particle classes separately that made up the THM fraction as extracted from enhanced product characterisation. Operating conditions are indicated in Table 12.1.

The standard product characterisation of the THM fraction divided the data into three groups of low, medium and high performance as illustrated in Figure 12.3. This same grouping was applied to the enhanced product characterisation to compare and determine if the performance classification was still similar. The enhanced product characterisation on Spiral A, Material 1 shows a similar performance ranking when compared to the standard product characterisation, illustrated in Figure 12.4. The best performing tests, Group 1 in Figure 12.3, show a THM recovery around 80 % at 20 % mass yield to concentrate for the standard product characterisation. The fine-high-density (FineHi) and medium-high-density (MedHi) particle classes show a THM recovery just below 90 % in the enhanced product characterisation, as indicated by Group 1 in Figure 12.4b and Figure 12.4d. A 90 % recovery might be acceptable in a certain process application, but not an 80 % recovery. This illustrates that the enhanced product characterisation demonstrates the true recovery of the valuable particle (high density, suitable size range) portion within the THM, as opposed to the standard product characterisation that demonstrate only an average recovery on the total THM fraction.

The fit of the enhanced Holland-Batt equation on the test-work data points shows a high level of consistency. In the two cases where the masses of the particle classes were low, below 1 % for FineMd and CrsMd in Figure 12.4, the fit was less consistent with some of the actual test-work data points not lying on the enhanced Holland-Batt lines. If the particle class contained only a small mass, represented by only a few particles during analysis, the potential for error was greater.

12.1.2 Spiral A, Material 2

Figure 12.5 illustrates the cumulative FLT recovery for all the operating conditions evaluated on Spiral A, Material 2 using standard product characterisation. Figure 12.6 (a), (b) and (c) illustrate the three different particle classes separately that made up the FLT fraction extracted from enhanced product characterisation. The operating conditions from Chapter 10

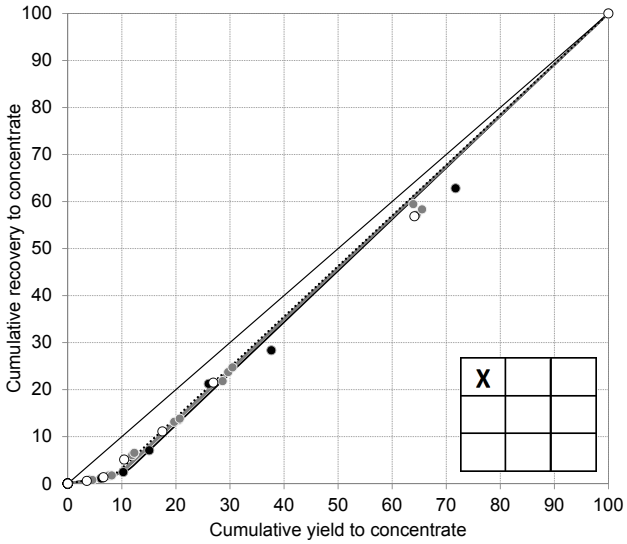

(a) Fine particles. Average content 13.3 %.

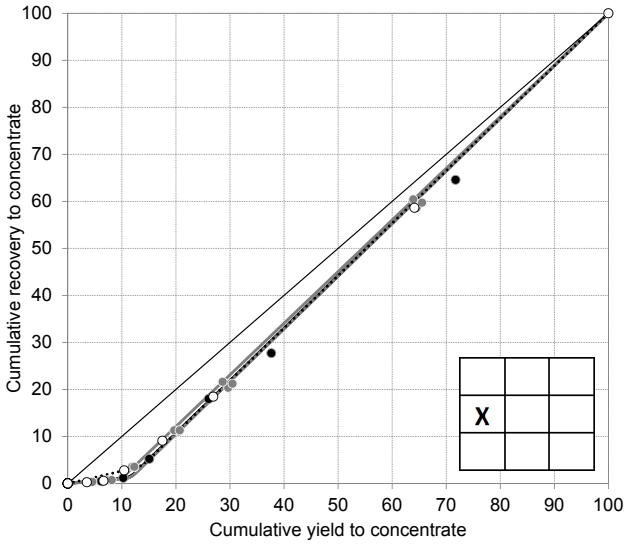

(b) Medium-sized particles. Average content 42.8 %.

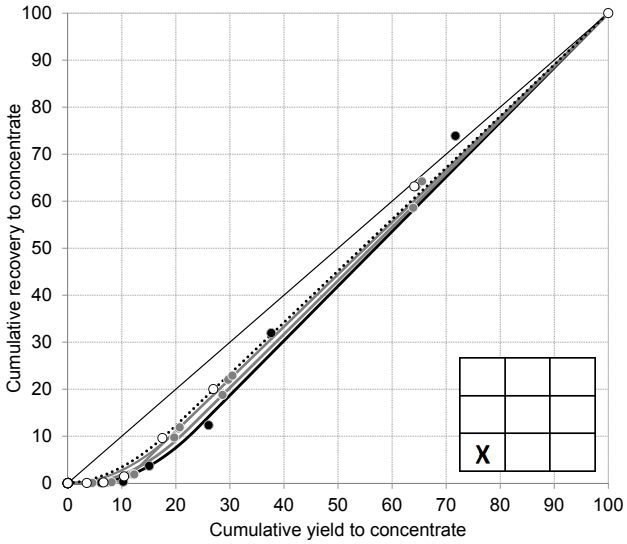

(c) Coarse particles. Average content 28.8 %.

Figure 12.2: Comparison of Spiral A, Material 1 low-density particle class recoveries. (Legend from Figure 12.1 applies)

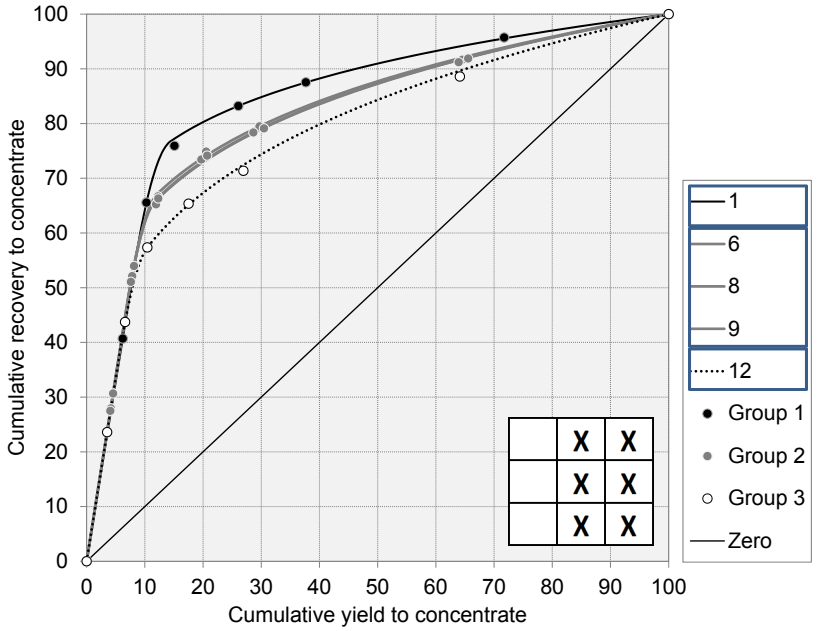

Figure 12.3: Spiral A, Material 1 high and medium density particle class recovery combined. (Standard characterisation for different operating conditions.)

are repeated in Table 12.2.

Table 12.2: Operating conditions for Spiral A, Material 2 tests.

Performance Group	Test Nr	Feed Rate (t/h)	%Solids	%Slimes	%THM
4 - HIGH	15	4.86	35.74	4.37	10.39
	16	5.33	33.81	3.35	14.86
	17	5.74	36.50	3.71	11.33
	18	6.47	38.94	4.18	10.80
	19	5.58	37.12	4.65	11.26
	Avg.	5.60	36.42	4.05	11.73
5 - MEDIUM	20	5.25	33.38	2.85	11.52
	21	5.66	37.23	5.13	11.11
	22	5.71	35.54	5.68	10.94
	23	5.42	35.55	5.37	10.85
	Avg.	5.51	35.42	4.76	11.11
6 - LOW	24	5.17	33.26	6.63	9.83
	25	5.52	34.93	7.63	11.90
	Avg.	5.35	34.09	7.13	10.86

The three particle classes for the FLT fraction show more variation across the spiral trough compared to Spiral A, Material 1. The fine class (less than 100 µm) shows the greatest variation in Figure 12.6, but has the lowest mass fraction (3.1 %) of the three classes. Figure 12.8 illustrates the THM cumulative recovery for all the operating conditions evaluated on Spiral A, Material 2 using standard product characterisation. In Figure 12.8, the six graphs illustrate the six different particle classes separately that made up the THM fraction extracted from enhanced product characterisation.

A trend was identified with the inconsistent fitting to the test-work data points towards the outside of the spiral trough for the THM lines in Figure 12.7, and the different particle classes lines in Figure 12.8. In almost all of the cases the test-work data points are lower than what

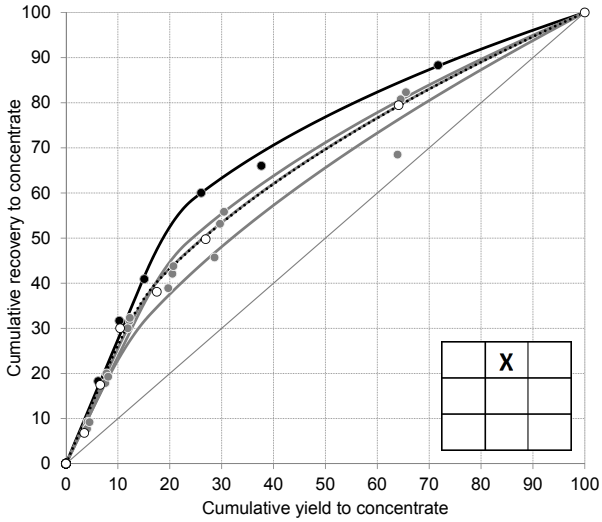

(a) Fine medium-density particles.
Average content 0.8 %.

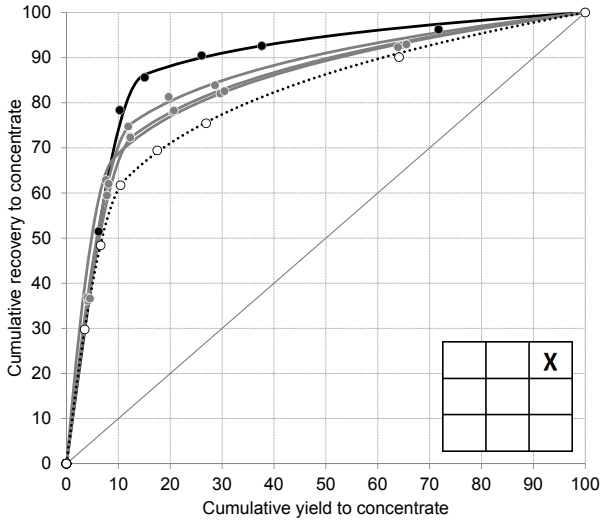

(b) Fine high-density particles.
Average content 2.5 %.

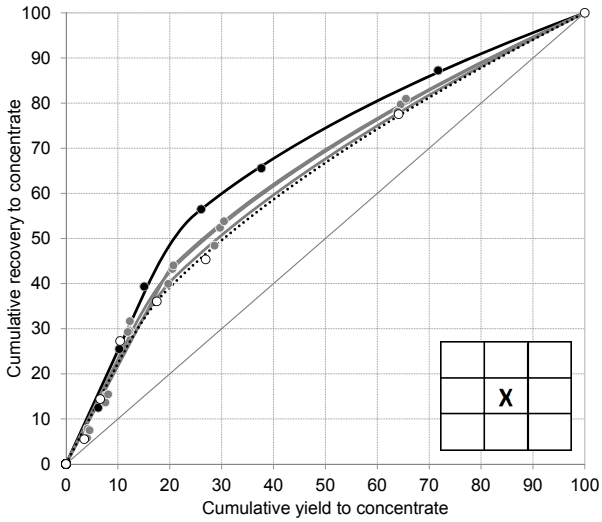

(c) Medium-sized medium-density particles.
Average content 2.0 %.

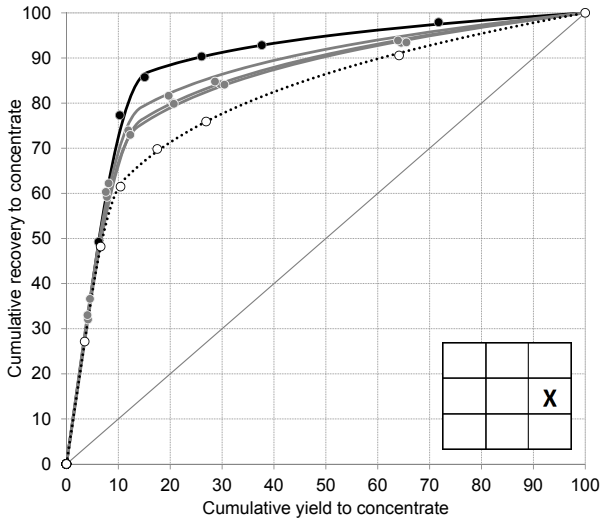

(d) Medium-sized high-density particles.
Average content 7.0 %.

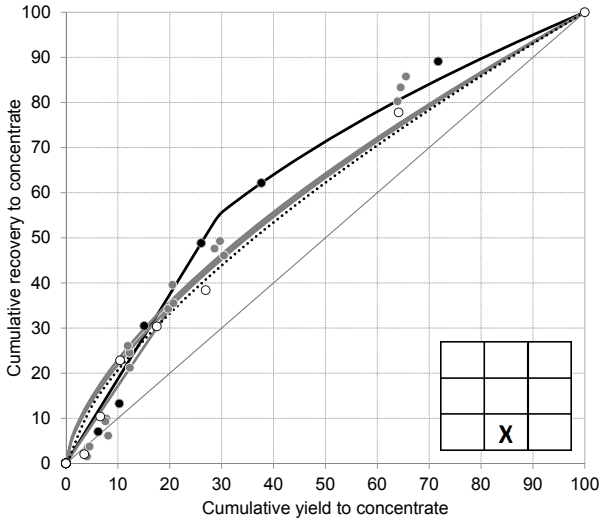

(e) Coarse medium-density particles.
Average content 0.8 %.

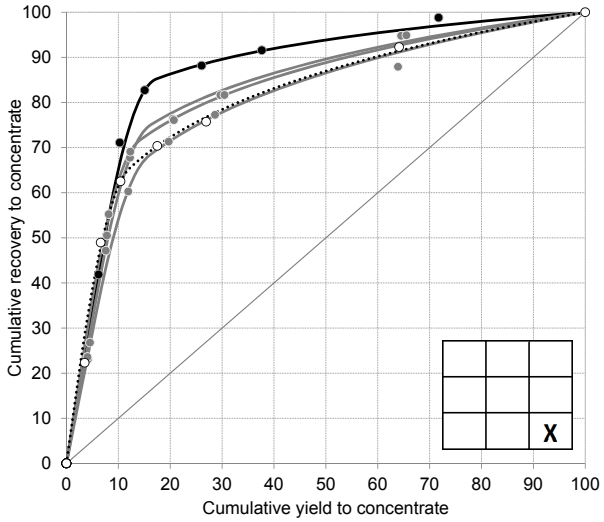

(f) Coarse high-density particles.
Average content 1.9 %.

Figure 12.4: Comparison of Spiral A, Material 1 med- and high-density particle class recoveries. (Legend of Figure 12.3 applies)

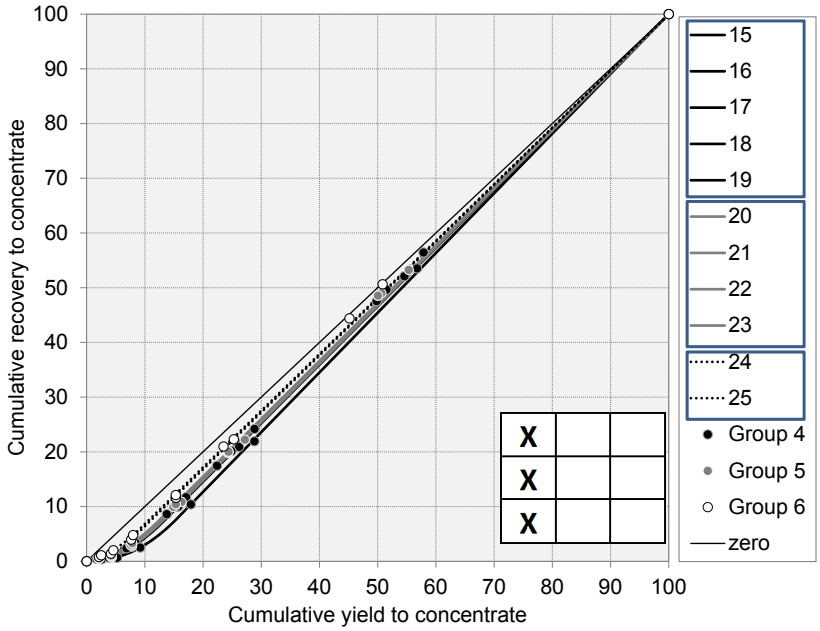

Figure 12.5: Spiral A, Material 2 low-density particle class recoveries. (Standard characterisation for different operating conditions. 85.0 % of mass)

the enhanced Holland-Batt line indicated it to be. This inconsistency could be explained on the basis of density differentiation in the particle class itself. For example, the MedMd particle class had density range boundaries of greater than 3.0 g/cm^3 and less than 4.0 g/cm^3. Even with this enhanced classification this is still a wide density range and further density differentiation could easily occur within this particle class.

Table 12.3 demonstrates the density variation within the MedMd particle class as an example. A difference of close to 0.2 g/cm^3 between the inner part of the trough (cut 1) and outer part of the trough (cut 7) could be identified. The coarser particle classes indicated a density difference of more than 0.3 g/cm^3 between the inner and outer regions of the spiral trough. This explained why the test-work data points to the right of the curve was on a 'lower density Holland-Batt line' compared to the test-work data points to the left of the curve in Figure 12.7 and Figure 12.8. The fit of the Holland-Batt equation would be most accurate if there were limited to no density differentiation in a specific particle class across the spiral trough. A possible solution to this problem is to divide the particle population into more density classes, but the risk is that the mass in the particle class will become too small, which will create data inconsistencies.

Table 12.3: Density variation within a single particle class (MedMd).

Trough Position	Cut 1	Cut 2	Cut 3	Cut 4	Cut 5	Cut 6	Cut 7
Density in g/cm3	3.65	3.57	3.58	3.53	3.47	3.48	3.46

The operating conditions that were evaluated in Group 4, 5 and 6, Figure 12.5 to Figure 12.8, produced a wider range of spiral separation performance when enhanced product characterisation was applied. Recovery differences of more than 30 % for a specific particle class were identified as opposed to only 18 % of difference between the THM lines for the same operating conditions for standard product characterisation. When comparing the six particle classes with the one THM particle class, the recovery range at 10 % mass yield to concentrate ranged between 10 and 90 %, in Figure 12.8, while the THM ranged only between 35 and 55 % recovery, in Figure 12.7 (standard). The enhanced product characterisation produced higher resolution

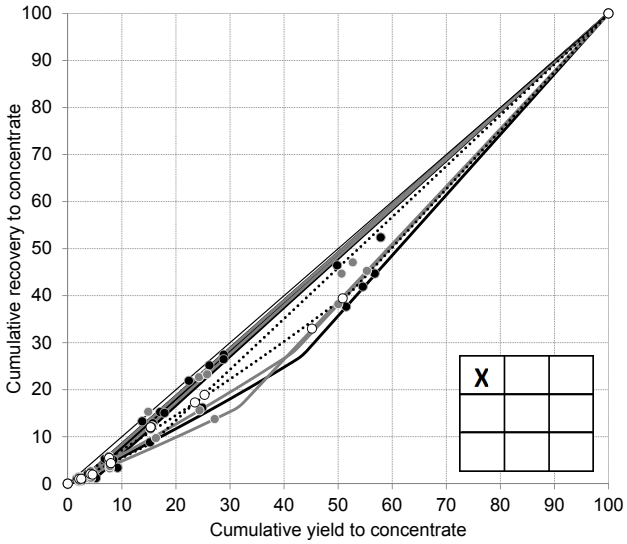

(a) Fine particles. Average content 3.1 %.

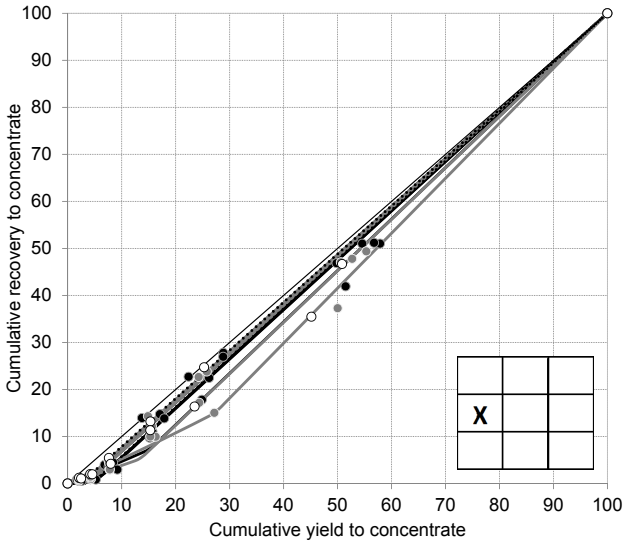

(b) Medium-sized particles. Average content 22.1 %.

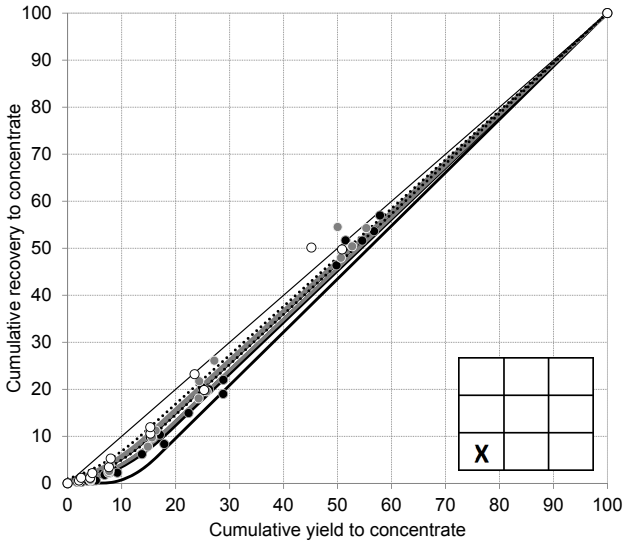

(c) Coarse particles. Average content 58.0 %.

Figure 12.6: Comparison of Spiral A, Material 2 low-density particle class recoveries. (Legend of Figure 12.5 applies)

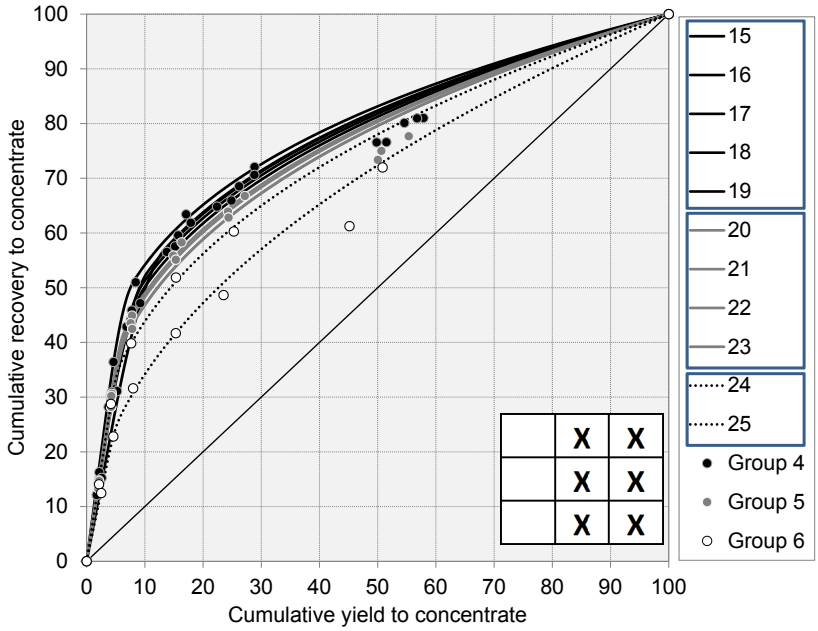

Figure 12.7: Spiral A, Material 2 high and medium density particle class recovery combined. (Standard characterisation for different operating conditions. 16.8 % of mass)

data to identify performance weaknesses and strengths for specific spiral troughs separating specific feed materials.

12.1.3 Spiral B, Material 2

Figure 12.9 illustrates the FLT fraction cumulative recovery for all the operating conditions evaluated on Spiral B, Material 2 using standard product characterisation. Figure 12.10 (a), (b) and (c) illustrate the three different particle classes that made up the FLT fraction separately, extracted from enhanced product characterisation. The operating conditions from Chapter 10 are repeated in Table 12.4.

Comparing the low-density particle classes in Figure 12.10 with the combined FLT class shows that for a certain higher performing test, the fine low-density fraction behaved more like the medium density particle class being on the left hand side of the zero separation line, as opposed to the normal position on the right hand side of the line. This might indicate a weakness in this spiral trough (Spiral B) to separate fine quartz from high-density particles under certain operating conditions. More data will be required to confirm this weakness since it was only seen with one specific test.

Figure 12.11 illustrates the THM cumulative recovery for all the operating conditions evaluated on Spiral B, Material 2 using standard product characterisation. In Figure 12.12, the six graphs illustrate the six different particle classes separately that made up the THM fraction extracted from enhanced characterisation.

The performance ranking developed on the THM class data from the standard characterisation was fairly consistent with that of the enhanced characterisation, but with the following differences to be considered. One of the tests, with lower grade of high-density particles, performed better, Figure 12.12b, indicating the same principal of competing medium density particles allowing only a certain separation volume for the high-density particle class. If the concentration of the medium density classes was lower, there would be more space for efficient separation of the high-density classes.

The particle class CrsHi, in Figure 12.12f, shows a significant difference with the THM

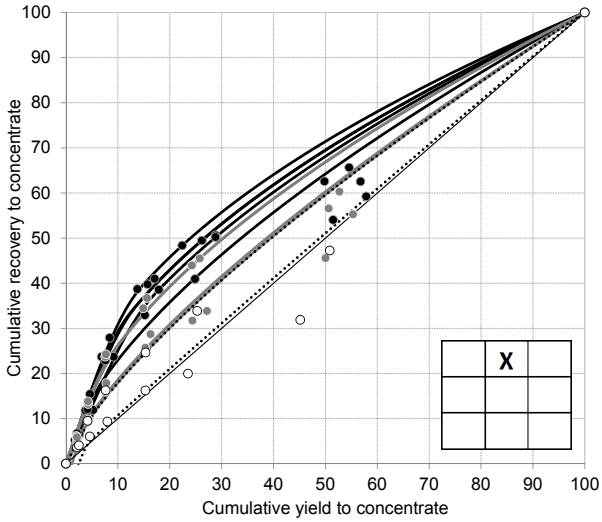

(a) Fine medium-density particles.
Average content 2.0 %.

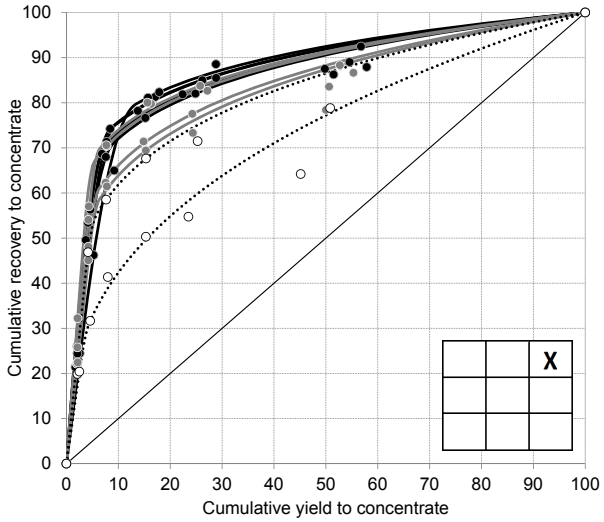

(b) Fine high-density particles.
Average content 2.1 %.

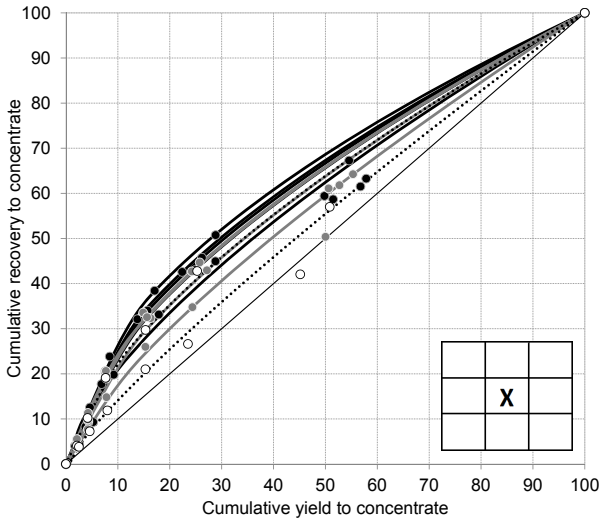

(c) Medium-sized medium-density particles.
Average content 5.7 %.

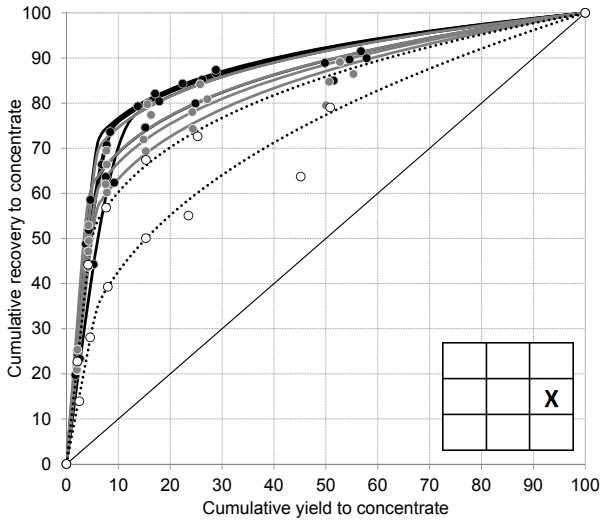

(d) Medium-sized high-density particles.
Average content 2.8 %.

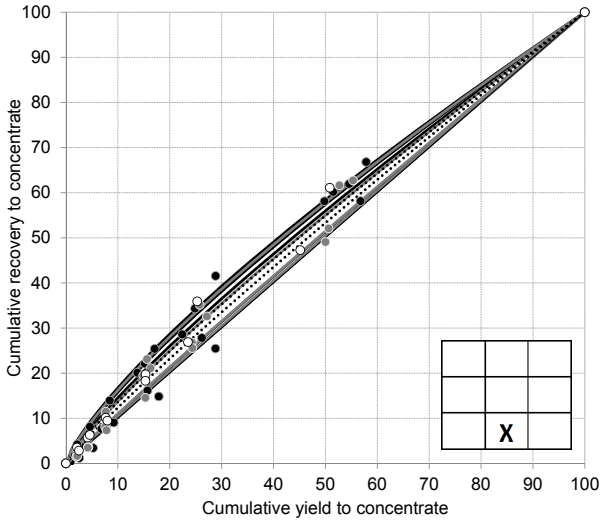

(e) Coarse medium-density particles.
Average content 3.7 %.

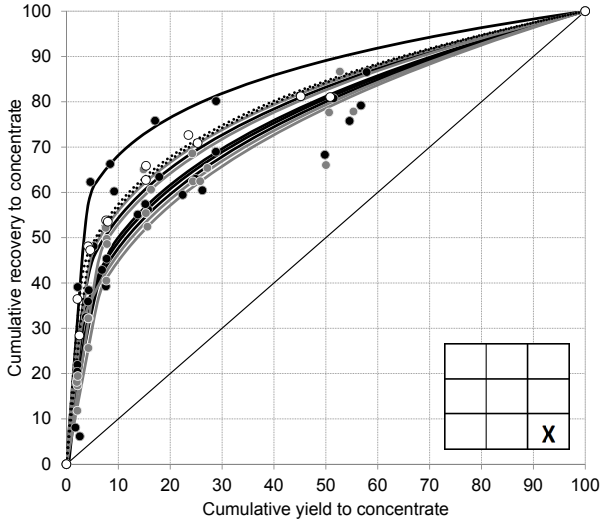

(f) Coarse high-density particles.
Average content 0.5 %.

Figure 12.8: Comparison of Spiral A, Material 2 med- and high-density particle class recoveries. (Legend of Figure 12.7 applies)

Table 12.4: Operating conditions for Spiral B, Material 2 tests.

Performance Group	Test Nr	Feed Rate (t/h)	%Solids	%Slimes	%THM
7 - HIGH	26	2.07	38.44	4.22	11.30
	27	1.38	36.10	5.00	11.27
	28	2.15	35.64	4.26	14.39
	Avg.	1.87	36.73	4.49	12.32
8 - MEDIUM	29	1.97	34.57	5.38	9.60
	30	1.99	41.55	4.71	11.65
	31	2.02	32.49	6.90	7.61
	32	2.33	37.54	5.60	11.85
	33	1.86	39.54	6.26	11.87
	Avg.	2.03	37.14	5.77	10.51
9 - LOW	34	1.83	34.74	7.05	12.10
	35	2.15	36.27	6.12	11.82
	36	2.20	34.37	5.64	5.99
	37	2.34	35.03	6.57	11.40
	38	2.29	37.51	6.51	12.00
	39	2.20	34.19	7.07	12.04
	Avg.	2.17	35.35	6.49	10.89

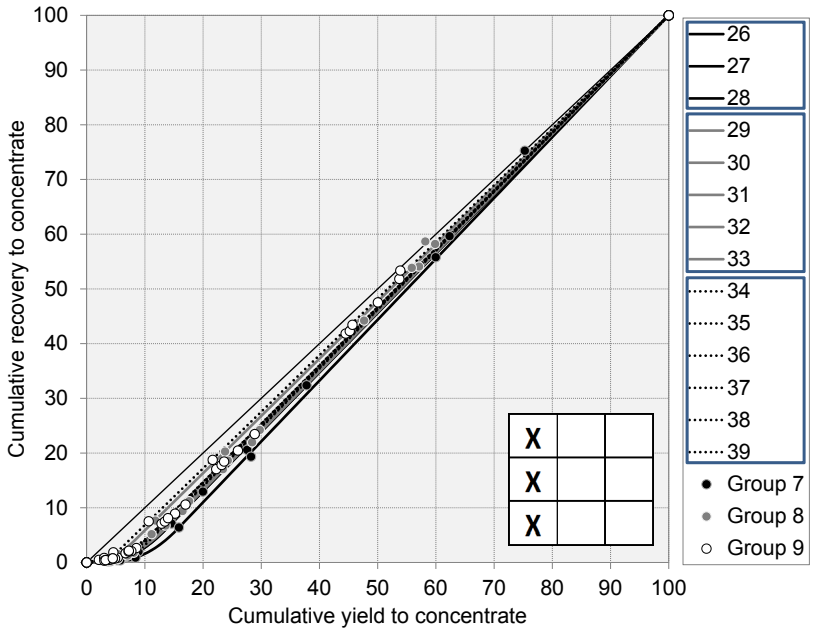

Figure 12.9: Spiral B, Material 2 low-density particle class recoveries. (Standard characterisation for different operating conditions. 83.6 % of mass)

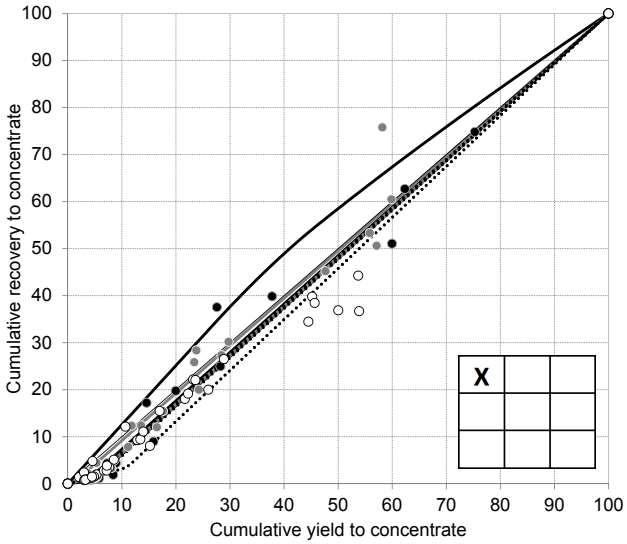

(a) Fine particles. Average content 3.4 %.

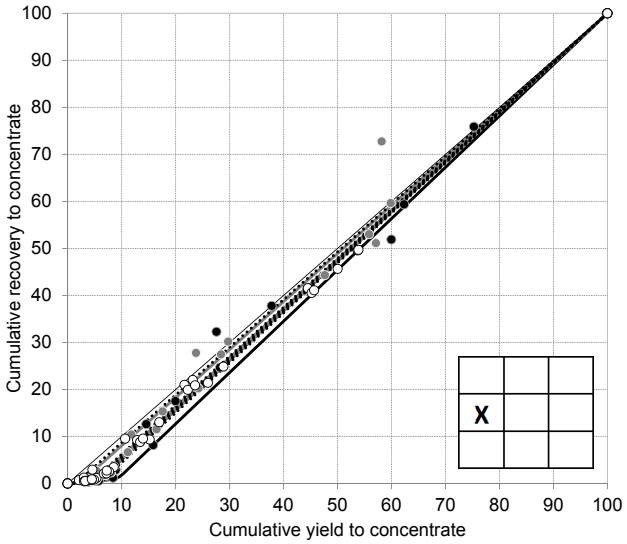

(b) Medium-sized particles. Average content 24.2 %.

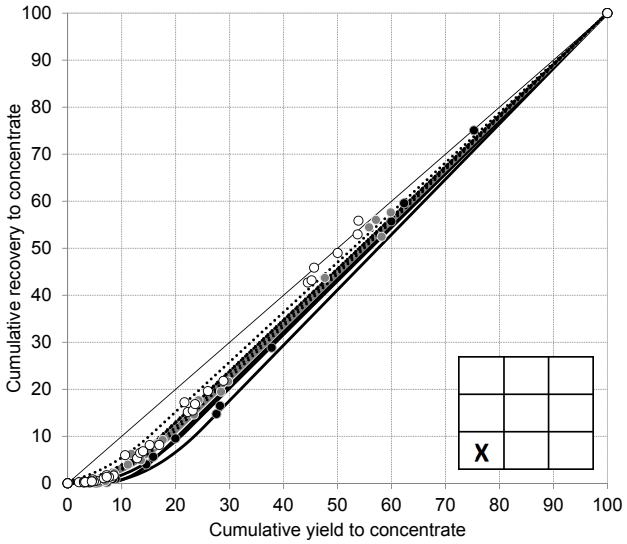

(c) Coarse particles. Average content 56.0 %.

Figure 12.10: Comparison of Spiral B, Material 2 low-density particle class recoveries. (Legend from Figure 12.9 applies)

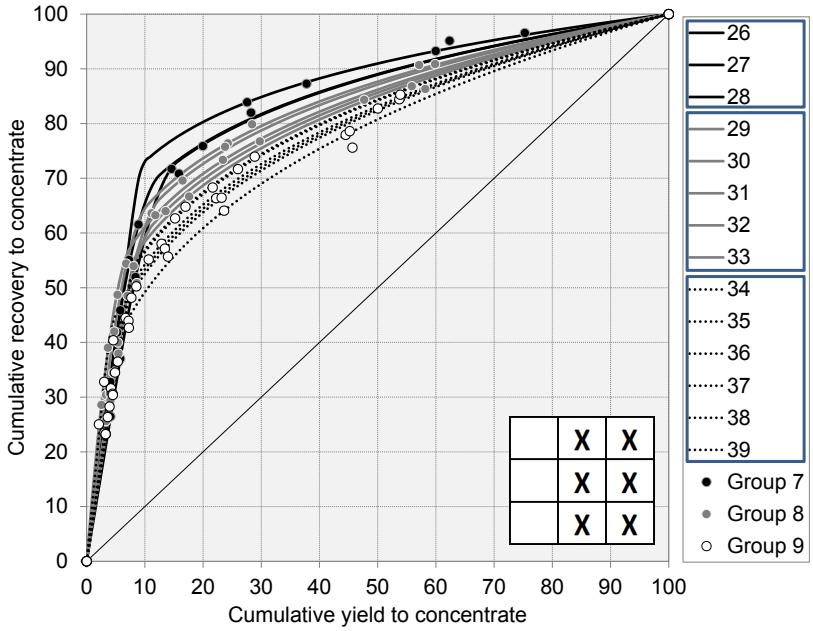

Figure 12.11: Spiral B, Material 2 high and medium density particle class recovery combined. (Standard characterisation for different operating conditions. 16.4 % of mass)

class performance ranking. At the same time the test-work data points do not show a high consistency fit with the enhanced Holland-Batt lines, which might indicate analysis or sampling inaccuracies considering that the average mass of the class was below 0.5 % mass.

Spiral B showed an overall better performance on Material 2 as compared to Spiral A. There were several tests that showed more than 90 % recovery at 10 % mass yield in the two critical particle classes (FineHi and MedHi) for Spiral B as seen in Figure 12.12d. The medium density particle classes showed more differentiation across the operating condition spectrum for Spiral B compared to Spiral A, also indicating better overall separation.

This data set indicates that the higher resolution data from the enhanced characterisation enable a better comparison with the different spiral troughs on the same feed material. The concentration of the different particle classes had a more significant effect on spiral separation performance when the enhanced product characterisation data were compared with the standard product characterisation data. The standard characterisation data did not have sufficient resolution to accurately determine the effect of particle class concentration, since the performance was averaged.

12.2 Summary

The following is a summary of the main points from this chapter.

- The enhanced product characterisation demonstrates a different performance ranking for the different operating conditions compared to the performance ranking based on standard product characterisation. This further supports the case for enhanced product characterisation to ensure the correct decisions are made with regards to spiral selection and trouble shooting.

- The six particle classes (medium- and high-density) gave significantly more information on spiral separation performance than the single THM class. The well-sized, high-density particle class (MedHi) recovery is a better indicator of true spiral performance compared

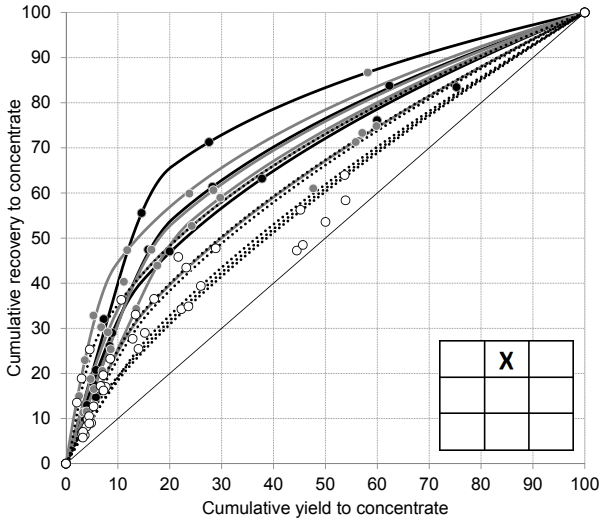

(a) Fine medium-density particles.
Average content 2.1 %.

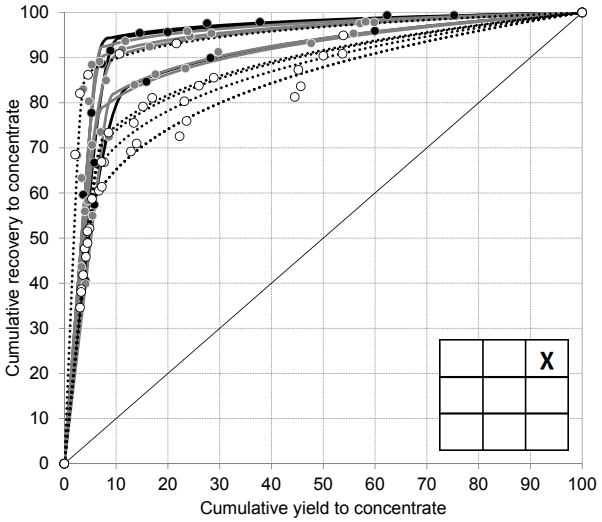

(b) Fine high-density particles.
Average content 2.4 %.

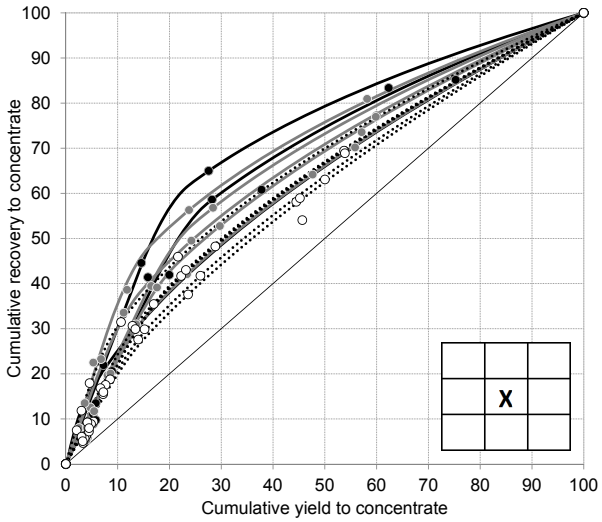

(c) Medium-sized medium-density particles.
Average content 5.7 %.

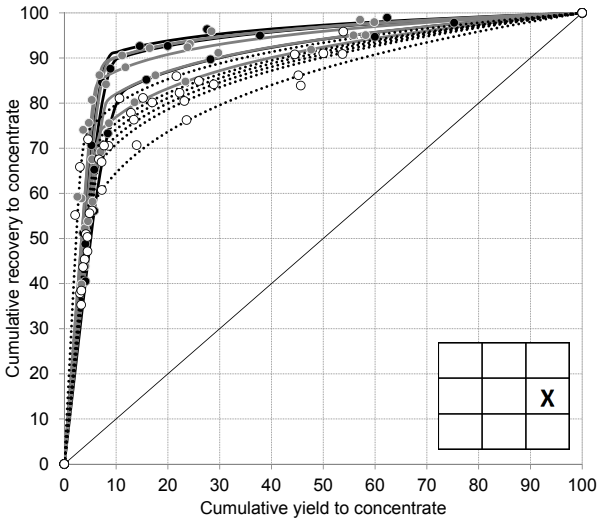

(d) Medium-sized high-density particles.
Average content 2.4 %.

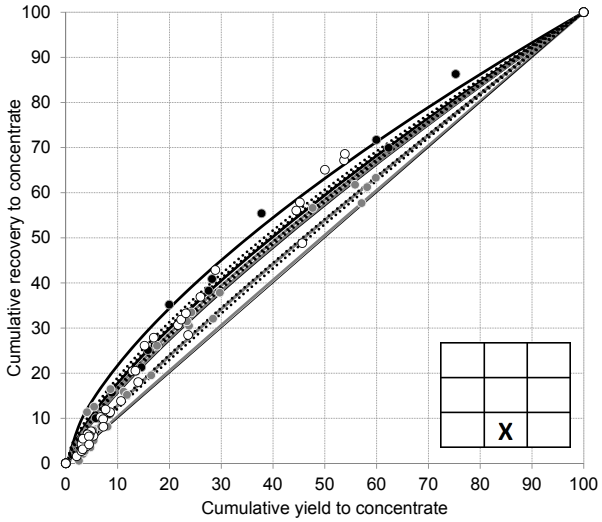

(e) Coarse medium-density particles.
Average content 3.4 %.

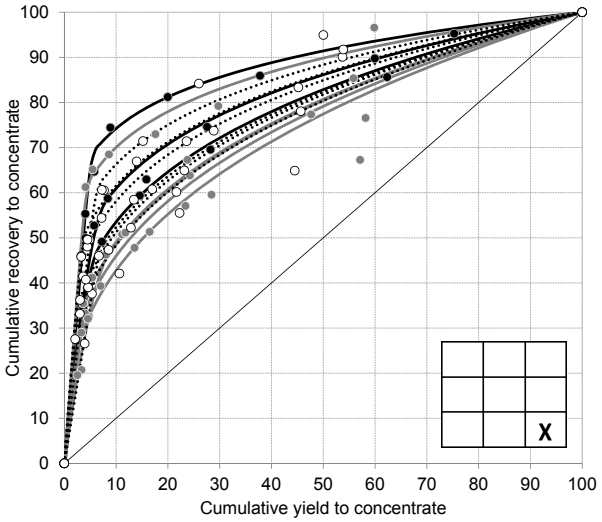

(f) Coarse high-density particles.
Average content 0.5 %.

Figure 12.12: Comparison of Spiral B, Material 2 med- and high-density particle class recoveries.(Legend from Figure 12.11 applies)

to THM recovery since the THM can contain large amounts of medium density particles that cannot be effectively separated by the spiral.

- Even with the narrow density particle classes there was still a density range that made the fit of the Holland-Batt equation less accurate. The narrower the density range within a particle class, the more accurate the fit will be.
- The enhanced product characterisation indicates that particle class concentration has a more pronounced effect on spiral separation performance compared to the conclusions from the standard product characterisation.

Part IV

Closure

Chapter 13

Closure

13.1 Summary

Enhanced feed material characterisation is required to identify material differences that will impact spiral separation performance, since standard feed material characterisation is insufficient.

Standard spiral separation performance analysis indicates slimes content to be the most significant influence from the operating parameters and ranges evaluated, with grade changes having limited to no influence.

Enhanced spiral separation performance analysis illustrated the differences over the standard spiral separation performance analysis, especially with wider particle density ranges present in THM. Particle class concentration (grade) has a more pronounced effect, which would otherwise not have been identified through standard analysis.

The enhanced characterisation and analysis techniques applied on both the feed and products of the spiral do not only supply a wealth of additional information, but is also critical to make the right decisions with regards to spiral profile suitability to specific feed materials.

13.2 Conclusions

13.2.1 Test-work Apparatus

The test-work apparatus that was utilised in this investigation to sample the spiral under different operating conditions demonstrated a high degree of repeatability with regards to total mass, THM and water distribution across the trough. This was a necessary starting point to ensure the quality of the data going forward into the different detailed analyses. The mouth-organ sampler that was used in this study to divide the spiral trough into seven cuts was crucial to achieve good mass data presentation across the total mass yield range. The standard sample preparation methods that were applied showed a high degree of repeatability and consistency with back calculation checks. Therefore, the test-work apparatus and standard methods applied introduced limited to no measurable bias into the test-work data, providing a solid base to make conclusions.

13.2.2 Standard Characterisation - Spirals and Materials

An increase in throughput and percentage solids caused a decrease in the separation efficiency in a consistent incremental nature, which is in agreement with literature. Slimes content was identified as a stronger influence. Once it has gone over some critical percentage, it influenced

separation efficiency significantly. THM grade variances seemed to have limited to no influence on performance.

Material type 1 and 2 performed vastly different on the same Spiral A, which illustrated the importance of understanding the influence of a specific material on a spiral trough. Spiral A and B performed vastly different with the same material (Type 2), which illustrated the importance of matching a specific spiral trough to a specific feed material. In all the tests none of the results gave satisfactory THM recoveries for the materials tested (all tests were below 90 % THM recovery with concentrate grade below 40 %).

The standard characterisation results successfully supplied the 'base case' with which the enhanced characterisation methods could be compared to illustrate the purpose and benefit of this investigation.

13.2.3 Curve Fitting Consistency

The fitting of the enhanced Holland-Batt triple spline to the test-work data of all the characterisation work showed a high degree of consistency. This greatly benefited the quality of data presentation for this investigation. The enhancements that were made to the original Holland-Batt equation improved the quality of fit to the data but also significantly improved the ease and consistency of the fitting process through the Excel Visual Basic programmed function. This technique, which was refined in this investigation, is a valuable contribution to the industry since it can be applied easily on any spiral recovery-yield data.

13.2.4 Material Characterisation Method Development

The application of the mineral quantification capability of Qemscan® within the mineral processing industry is well established, to such an extent that automated mineralogy had become the standard in mineral quantification. The specific application of particle size and particle density outputs from Qemscan® in describing and understanding mineral processing performance was less common, but a number of references were found in literature. The validation of particle size and particle density output from Qemscan® was virtually non-existent in literature. This investigation contributed to literature through the validation work, as well as the application to spiral separation performance data.

Qemscan® sample preparation methods (sample block preparation) that were applied showed some variation in the repeatability test-work results. Any analytical method will show some degree of variation and the accuracy of the application of the data should be in line with the measurement accuracy. The fractional particle size, shape and density comparisons were the most stringent comparison method with regards to the evaluation of the size and density output from Qemscan®. The different sample preparation steps that were evaluated still gave a reasonable repeatability consistency. This work also demonstrated the importance of understanding the constraints and risks when preparing samples for Qemscan® analysis, specifically for size and density outputs.

The analytical requirements with regards to the correction of the raw data are crucial if Qemscan® results are to be successfully applied to quantify particle size and particle density distributions. The most important requirements include the minimum number of particles to be analysed, the removal of artificial ultra-fine particles (below 45 µm) and de-clustering of touching particles.

The particle size distribution from Qemscan®, after the analytical requirements were met, shows a high degree of comparison with conventional screening. The influence of particle shape is well quantified in the size analysis method comparisons. The particle density validation is limited due to the lack of an accurate high-density fractionation alternative (fine particles above

3.0 g/cm^3. This shortcoming also confirmed the importance of ensuring that particle density data applied within Qemscan® are correct.

Validation test-work results indicates that the particle size and particle density output from Qemscan® can be utilised for material characterisation in the density separation environment, provided that the constraints and conditions are fully understood and applied correctly. The most important constraint is the material type. Irregular shaped particles, highly porous particles or a wide range of particle sizes (30 to 1000 µm) would require separate validation test-work.

Qemscan® quantification of particle size and particle density offers an accurate, time- and cost-effective alternative to physical fractionation. There is no separation inefficiency to consider since all the particles are analysed. The benefit of instantly calculating different particle classes from the same analyses data source cannot be overstated.

13.2.5 Enhanced Material Characterisation

The enhanced characterisation method demonstrates clear benefits when compared to the standard characterisation methods. The most important benefits include: (1) A clear characterisation of the different feed materials upfront allows for better understanding of the separation performance that was observed. (2) The influence of particle class concentration (grade) is overlooked during the standard characterisation, which would lead to incorrect conclusions. (3) The weakness of Spiral B to reject fine quartz would be overlooked if only standard characterisation is considered. (4) The recovery of the valuable particle classes (correct size and density) from the enhanced method differs significantly from the THM recovery of the standard method since all the performances are averaged in the standard method.

The enhanced spiral separation performance analysis demonstrates significant value in the ability to identify the most suitable spiral to match a specific feed material within the expected operating ranges, therefore significantly reducing installation risk and improving long term business profitability with clear indications of sustainable recovery improvement. The enhanced characterisation method also delivers process data that can be utilised to identify strengths and weaknesses in spiral trough designs, that can greatly assist in future spiral design work.

13.3 Recommendations

13.3.1 Modelling

The high degree of test-work data fitting accuracy that the triple spline demonstrates, opens various opportunities for detailed spiral separation performance modelling using this simple equation. The equation fitting method can be coupled with an enhanced characterisation method that can describe particle classes (size-density) that will be influenced most in the separation zone.

The development of a spiral model that can predict the separation performance of a specific spiral trough based on a specific feed material characteristic and a selection of a combination of operating conditions, is a natural consequence of this work. Particle classes can have a characteristic performance on a spiral profile that can be measured once through test-work and modelled for the remainder of the other operating conditions. This tool can potentially save a significant amount of costly test-work.

The model parameters can be determined through testing of an artificial sample with specific size and density attributes as feed material to a specific spiral trough to analyse the spiral separation performance under specific operating conditions. This sample can be selected in such a way that density fractionation can be done magnetically to simplify the sample analysis process. Large volumes of operating data can be gathered in a time and cost effective manner.

If the colours of the different density mineral particles are carefully chosen, the movement on the spiral trough can be measured by means of a stationary camera. Viscosity can be adjusted with some modifier to keep the separation medium clear. The measurement of medium viscosity rather than percentage slimes should be considered in future spiral work.

13.3.2 Enhanced Characterisation Continued

The confirmation of mineral density within the Qemscan® database coupled with the validation of the particle density output from Qemscan® should be investigated. Methods to measure the actual density of small numbers of similar particles and comparing it with Qemscan® particle population density should be evaluated. High speed cameras and sensitive scales are constantly improving, decreasing the size of particles that can be measured. Currently 1 mm particles are being evaluated and finer particles are also considered.

Size and magnetic fractionation followed by Qemscan® centroid analysis can potentially remove the requirement to perform sink-float analysis prior to enhanced characterisation. For a specific mineral sand sample screening can be done on 300 µm to remove the majority of the quartz. The minus 300 µm material can be fractionated magnetically into three fractions. These four samples can be prepared into polished blocks and analysed by Qemscan® centroid to provide a full size and density picture at high resolution. The four centroid analyses will take similar Qemscan® processing time compared to a single particle mineral analysis.

Particle shape and particle size should be combined into a single parameter called particle spiral drag. Elongated particles can be added as a particle class to determine the influence that particle shape has on spiral separation performance.

Bibliography

Allen, J. (1982). *Sedimentary Structures: Their Character and Physical Basis*. Elsevier.

Ayala, J. (2009). "The Qemscan solution - Applications". In: URL: http://www.minsoc.ru/FilesBase/QemScan0803.pdf.

British Geological Society (2014). *Heavy media separation and analysis*. URL: http://www.bgs.ac.uk/scienceFacilities/laboratories/mpb/media.html.

Cooke, G. (2011). "Adjustable spiral concentrator". Pat. US20110186487 (United States of America).

FEI (2014). *Metallurgical Testing and Flow Sheet Design. Quantitative mineralogy solutions for metallurgical testing*. URL: http://www.fei.com/natural-resources/metallurgical-testing/.

Fritsh (2014). *Vibratory Sieve Shaker ANALYSETTE 3 PRO*. URL: http://www.fritsch-milling.com/products/sieving/vibratory-sieve-shakers/analysette-3-pro/description..

Gay, S. and J. Keith (2001). "Stereological correction of the surface area of particle". In: Brisbane.

— (2014). "Geometric probability based stereological corrections. Applied Mathematics". In: *Journal of the Australian Mathematical Society*. B 45, pp. 618–631.

Grobler, J. (2007). "Wet heavy mineral pilot plant design, assembly, commissioning and operation for a remote location". In: *The Southern African Institute of Mining and Metallurgy*.

Grobler, J. and J. Bosman (2009). "Gravity separator performance evaluation using Qemscan particle mineral analysis". In: *Journal of the South African Institute of Mining and Metallurgy*.

— (2010). "Spiral concentrator modelling using Qemscan®". In: *Journal of the South African Institute of Mining and Metallurgy*.

— (2011). "Gravity separator performance evaluation using Qemscan® particle mineral analysis". In: *Journal of the South African Institute of Mining and Metallurgy* 111, pp. 401–408.

Henderson, D. and D. MacHunter (2003). "A review of spiral technology for fine gravity beneficiation". In: *MD Mineral Technologies*.

Holland-Batt, D. (1990). "Interpretation of spiral and sluice tests". In: *Transactions Institution of Mining and Metallurgy* 99, pp. 11–20.

— (1995). "Some design considerations for spiral separators". In: *Mineral Technologies*, pp. 1–16.

Iluka (2013). *Mineral Sands Industry. Fact Book*. Iluka. URL: http://www.zircon-association.org/Websites/zircon/images/The_Mineral_Sands_Industry_Factbook.pdf (visited on 04/01/2015).

Intellection (2009). URL: http://www.intellection.com.au-iQ-0710-04GrainSizeExternal.doc.

Kapur, P.C. and T.P. Meloy (1998). "Spirals Observer". In: *International Journal of Mineral Processing* 53, pp. 15–28.

Kapur, P.C. and T.P. Meloy (1999). "Industrial modeling of spiral for optimal configuration and design: spiral geometry, fluid flow and forces on particles." In: *Powder Technology* 102, pp. 244–252.

Lotter, N. (2003). "Sampling and flotation testing of Sudbury Basin drill core for process mineralogy modelling". In: *Minerals Engineering* 16, pp. 857–864.

Mindat (2014). URL: `http://www.mindat.org` (visited on 2014).

Mine Engineer (2014). *Spiral Concentrators*. URL: `http://mine-engineer.com/mining/minproc/spiral.htm` (visited on 2014).

Mineral Technologies (2014). *Gravity Separation Technology*. URL: `http://www.mineraltechnologies.com/gravity-separation-technology` (visited on 2014).

Multotec (2014a). *Coal Spiral Concentrators*. URL: `http://www.multotec.com.au/coal-spiral-concentrators.html` (visited on 09/01/2014).

— (2014b). *Heavy Mineral Spiral Concentrators*. URL: `http://www.multotec.com.au/heavy-mineral-spiral-concentrators.html`.

Pascoe, R., M. Power, and B. Simpson (2007). "Qemscan analysis as a tool for improved understanding of gravity separator performance". In: *Minerals Engineering* 20, pp. 487–495.

Philander, C. and A. Rozendaal (2014). "A process mineralogy approach to geometallurgical model refinement for the Namakwa Sands heavy minerals operations, west coast of South Africa". In: *Minerals Engineering* 65, pp. 9–16.

Quantachrome (2014). *Rotary Micro Riffler. Rotary Sample Splitter*. URL: `http://www.quantachrome.co.uk/en/Rotary_Sample_Splitters-Rotary_Riffler.asp` (visited on 2014).

Richards, R. and M. Palmer (1997). "High capacity gravity separators - a review of current status". In: *Minerals Engineering* 10, pp. 973–982.

Richards, R. et al. (2000). "Gravity separation of ultrafine (-0.1mm) minerals using spiral separators". In: *Minerals Engineering* 13, pp. 65–77.

Sutherland, D. and P. Gottlieb (1997). "Application of automated quantitative mineralogy in mineral processing". In: *Minerals Engineering* 4, pp. 753–762.

Thompson, J. V. (1969). *History of the Humphreys Spiral Concentrator*. The MINES Magazine.

Webmineral (2014). URL: `http://webmineral.com`.

Wright, D., R. Richards, and M. Cross (1986). "The development of mineral sands separation technology - solving today's problems, anticipating tomorrow's". In: *AusIMM*.

Wright, D. C. (1982). "Spiral separator". Pat. EP0077049NWA1 (Europe).

Glossary

ρ_{50} The medium density at which 50 % of the mass of a material will sink.

concentrate The product mass stream containing valuable minerals.

cut A mass fraction on a spiral trough (cut 1 on inside, cut 7 on outside).

D_{50} The aperture size at which 50 % of the mass will pass through a screen.

efficiency The ability to achieve a high recovery and high grade.

FLT Dry mass percentage of sand particles that floated on heavy liquid (density less than 2.98 g/cm^3) in all sand particles greater than 45 µm.

grade Concentration of particular component (usually THM) in product.

Holland-Batt Spline function (surname of researcher of spiral separation performance).

ICP-OES A chemical analysis method employing inductively coupled plasma and optical emission spectrometry.

KZN Kwa-Zulu Natal, a province of the Republic of South Africa.

Material 1 Material originated from Madagascar.

Material 2 Material originated from Namakwa Sands.

middling The mass stream between the concentrate and tailing.

mouth organ Sampling device to fractionate the spiral trough outlet stream.

particle class Group of particles with similar attributes (density and size).

particle shape factor Factor used to quantify particle shape based on the relationship between perimeter and cross-sectional area).

performance Behaviour of the spiral under different operating conditions.

PMA Particle mineral analysis (Qemscan® analysis mode).

Qemscan® Quantitative Evaluation of Minerals by SCANning electron microscopy.

recovery Mass % of a particular component (usually THM) that ends up in product.

SIP Specie identification protocol (used in Qemscan® software).

slimes content Dry mass percentage of particles finer than 45 µm in all solid particles..

solids percentage Mass percentage of dry solids in mass of liquid (water) and dry solids combined.

Spiral A High capacity spiral.

Spiral B Normal capacity spiral.

spline function Combination of two or more equations (functions).

start Single spiral trough feed point.

tailings The mass stream containing non-valuable minerals.

THM Dry mass percentage of total heavy minerals (density greater than 2.98 g/cm^3) in all sand particles greater than 45 µm..

throughput Dry solids flow rate (usually expressed in ton / hour).

trough Surface of the spiral on which the separation occurs.

viscosity Thickness of liquid in which separation occurs.

yield Mass% of dry material to product or concentrate.

Part V

Appendices

Appendix A

Spiral Test Data

This appendix presents the test configurations and some of the raw data collected during the spiral tests.

Table A.1: Spiral test operating parameters.

Test Identification				Operating Parameters			
Profile	**Material**	**Group**	**Test**	**Feed Rate** t/ h	**Solids Content** %	**Slimes Content** %	**THM Content** %
A	1	1	1	4.34	38.76	2.42	14.23
A	1	1	2	4.50	39.70	2.63	14.19
A	1	1	3	4.37	39.94	2.77	13.55
A	1	2	4	5.52	43.01	4.21	13.77
A	1	2	5	5.87	43.79	3.14	13.76
A	1	2	6	5.88	43.64	2.64	13.74
A	1	2	7	5.39	46.15	2.81	14.28
A	1	2	8	5.92	44.52	3.67	13.63
A	1	2	9	5.52	45.87	3.08	13.83
A	1	2	10	5.93	43.65	3.85	13.30
A	1	2	11	5.67	44.23	2.80	13.67
A	1	3	12	6.79	49.56	3.56	13.91
A	1	3	13	7.13	51.77	3.67	13.41
A	1	3	14	6.89	50.33	3.87	14.03
A	2	4	15	4.86	35.74	4.37	10.39
A	2	4	16	5.33	33.81	3.35	14.86
A	2	4	17	5.74	36.50	3.71	11.33
A	2	4	18	6.47	38.94	4.18	10.80
A	2	4	19	5.58	37.12	4.65	11.26
A	2	5	20	5.25	33.38	2.85	11.52
A	2	5	21	5.66	37.23	5.13	11.11
A	2	5	22	5.71	35.54	5.68	10.94
A	2	5	23	5.42	35.55	5.37	10.85
A	2	6	24	5.17	33.26	6.63	9.83
A	2	6	25	5.52	34.93	7.63	11.90
B	2	7	26	2.07	38.44	4.22	11.30
B	2	7	27	1.38	36.10	5.00	11.27
B	2	7	28	2.15	35.64	4.26	14.39
B	2	8	29	1.97	34.57	5.38	9.60
B	2	8	30	1.99	41.55	4.71	11.65
B	2	8	31	2.02	32.49	6.90	7.61
B	2	8	32	2.33	37.54	5.60	11.85
B	2	8	33	1.86	39.54	6.26	11.87
B	2	9	34	1.83	34.74	7.05	12.10
B	2	9	35	2.15	36.27	6.12	11.82
B	2	9	36	2.20	34.37	5.64	5.99
B	2	9	37	2.34	35.03	6.57	11.40
B	2	9	38	2.29	37.51	6.51	12.00
B	2	9	39	2.20	34.19	7.07	12.04

Table A.2: Spiral test solids distribution results.

Test Identification				Product Solid Mass Per Cut							
Profile	**Material**	**Group**	**Test**	**1**	**2**	**3**	**4**	**5**	**6**	**7**	**Tot.**
				%	%	%	%	%	%	%	%
A	1	1	1	6.20	4.08	4.80	10.98	11.60	34.07	28.27	100.00
A	1	1	2	6.13	4.13	4.67	10.75	11.44	34.84	28.04	100.00
A	1	1	3	5.90	3.90	4.55	10.33	11.09	34.98	29.26	100.00
A	1	2	4	4.30	3.72	4.42	8.24	9.11	35.02	35.19	100.00
A	1	2	5	4.20	3.66	4.21	8.15	9.00	35.09	35.69	100.00
A	1	2	6	4.16	3.65	4.43	8.27	9.17	34.83	35.48	100.00
A	1	2	7	4.69	3.72	4.40	9.22	10.56	35.64	31.77	100.00
A	1	2	8	4.07	3.54	4.32	7.79	8.94	35.28	36.08	100.00
A	1	2	9	4.55	3.59	4.18	8.40	9.76	35.07	34.46	100.00
A	1	2	10	4.20	3.62	4.29	7.84	8.66	34.57	36.82	100.00
A	1	2	11	4.48	3.55	4.09	8.59	9.74	35.53	34.02	100.00
A	1	3	12	3.52	3.08	3.83	7.07	9.42	37.19	35.88	100.00
A	1	3	13	3.30	2.95	3.58	6.44	8.52	36.98	38.23	100.00
A	1	3	14	3.62	3.08	3.66	6.71	9.15	37.23	36.56	100.00
A	2	4	15	2.17	2.45	3.81	8.66	11.76	29.03	42.13	100.00
A	2	4	16	2.58	2.65	3.98	8.69	10.92	27.95	43.23	100.00
A	2	4	17	2.13	2.19	3.43	7.98	10.48	28.38	45.42	100.00
A	2	4	18	1.73	2.03	3.10	6.91	8.64	27.42	50.17	100.00
A	2	4	19	2.10	2.07	3.44	7.61	9.67	26.63	48.50	100.00
A	2	5	20	2.14	2.18	3.46	8.53	10.86	28.16	44.66	100.00
A	2	5	21	2.01	2.24	3.31	7.33	9.39	26.36	49.37	100.00
A	2	5	22	2.19	2.03	3.60	7.49	9.06	25.66	49.97	100.00
A	2	5	23	2.12	2.12	3.46	7.93	10.16	26.93	47.28	100.00
A	2	6	24	2.12	2.05	3.48	7.69	9.94	25.56	49.15	100.00
A	2	6	25	2.50	2.08	3.40	7.33	8.21	21.64	54.84	100.00
B	2	7	26	3.66	1.58	2.04	7.30	13.00	34.77	37.66	100.00
B	2	7	27	4.06	1.71	3.13	11.07	17.81	37.49	24.72	100.00
B	2	7	28	4.09	1.69	2.63	7.46	12.37	31.73	40.03	100.00
B	2	8	29	3.33	1.41	2.05	4.38	13.08	35.61	40.14	100.00
B	2	8	30	3.98	1.39	2.69	8.42	11.94	28.70	42.88	100.00
B	2	8	31	2.53	1.11	1.66	6.51	11.98	34.40	41.82	100.00
B	2	8	32	3.31	1.26	2.45	6.54	9.85	24.26	52.34	100.00
B	2	8	33	4.09	1.37	3.17	8.98	12.14	26.11	44.15	100.00
B	2	9	34	3.94	1.40	3.20	8.45	11.89	24.85	46.28	100.00
B	2	9	35	3.63	1.24	2.81	7.52	10.80	24.03	49.97	100.00
B	2	9	36	2.10	.91	1.57	6.08	10.99	32.23	46.11	100.00
B	2	9	37	3.04	1.13	2.52	6.18	9.39	22.24	55.50	100.00
B	2	9	38	3.30	1.16	2.73	6.24	9.75	22.02	54.80	100.00
B	2	9	39	3.26	1.24	2.75	6.72	9.64	22.06	54.33	100.00

Table A.3: Spiral test THM content results.

Test Identification				Product THM Content Per Cut							
Profile	**Material**	**Group**	**Test**	**1**	**2**	**3**	**4**	**5**	**6**	**7**	**Tot.**
				%	%	%	%	%	%	%	%
A	1	1	1	93.40	86.74	30.75	9.44	5.30	3.42	2.15	14.23
A	1	1	2	92.97	86.80	30.86	9.75	5.66	3.33	2.15	14.19
A	1	1	3	92.57	86.30	29.62	9.00	5.17	3.47	2.26	13.55
A	1	2	4	92.36	90.00	44.65	13.89	7.12	4.53	3.10	13.77
A	1	2	5	92.35	90.61	46.33	14.03	7.43	4.62	3.31	13.76
A	1	2	6	92.34	90.91	45.17	13.59	6.93	4.81	3.23	13.74
A	1	2	7	93.20	89.75	41.83	12.69	7.40	5.02	3.12	14.28
A	1	2	8	92.13	90.81	44.70	14.36	7.53	4.96	3.32	13.63
A	1	2	9	93.23	89.82	40.86	12.89	7.07	5.03	3.26	13.83
A	1	2	10	92.01	90.07	36.54	13.90	7.18	4.79	3.37	13.30
A	1	2	11	93.14	89.68	40.12	12.44	7.15	5.14	3.18	13.67
A	1	3	12	93.23	90.78	49.56	15.72	8.86	6.45	4.42	13.91
A	1	3	13	92.90	90.84	49.02	16.27	8.78	6.46	4.51	13.41
A	1	3	14	93.07	90.33	46.76	15.16	8.49	6.59	5.26	14.03
A	2	4	15	77.99	85.40	39.71	14.91	7.65	3.20	4.68	10.39
A	2	4	16	87.72	88.93	59.98	25.11	11.93	5.50	6.55	14.86
A	2	4	17	78.93	83.15	49.34	19.52	9.69	4.63	4.96	11.33
A	2	4	18	75.51	85.68	51.15	21.35	10.34	4.62	5.04	10.80
A	2	4	19	77.01	86.66	45.60	19.79	9.75	4.51	5.43	11.26
A	2	5	20	78.92	84.10	47.66	18.08	8.99	4.46	5.76	11.52
A	2	5	21	73.57	84.05	44.66	18.70	9.55	4.68	5.62	11.11
A	2	5	22	70.01	76.57	43.29	18.47	9.30	4.50	5.83	10.94
A	2	5	23	75.36	80.91	42.47	17.46	9.37	4.27	5.47	10.85
A	2	6	24	65.18	70.30	31.36	15.36	8.33	4.50	5.60	9.83
A	2	6	25	59.36	59.04	30.80	16.34	10.09	6.93	8.41	11.90
B	2	7	26	93.04	83.55	73.46	25.75	10.58	3.65	1.46	11.30
B	2	7	27	91.08	86.02	56.45	14.60	7.21	2.79	1.57	11.27
B	2	7	28	93.22	89.87	81.87	36.45	12.96	5.11	2.43	14.39
B	2	8	29	87.53	79.04	58.20	20.16	9.38	3.90	2.18	9.60
B	2	8	30	89.79	77.80	60.48	21.66	10.04	4.39	2.53	11.65
B	2	8	31	86.08	71.37	44.44	17.01	7.95	2.34	2.49	7.61
B	2	8	32	91.74	82.46	68.21	28.03	11.28	5.37	3.55	11.85
B	2	8	33	85.39	73.94	48.26	20.91	9.87	4.58	3.54	11.87
B	2	9	34	86.81	70.95	52.07	20.88	9.31	5.11	4.07	12.10
B	2	9	35	85.88	77.16	57.54	22.80	9.85	5.45	4.08	11.82
B	2	9	36	71.30	50.97	28.93	14.54	7.16	3.15	1.91	5.99
B	2	9	37	88.04	82.22	58.25	24.97	10.11	5.94	4.53	11.40
B	2	9	38	84.67	76.02	58.47	25.41	11.46	6.63	4.69	12.00
B	2	9	39	85.93	69.68	53.74	23.28	10.51	6.29	5.41	12.04

Table A.4: Spiral test FLT content results.

Test Identification				Product FLT Content Per Cut							
Profile	**Material**	**Group**	**Test**	**1**	**2**	**3**	**4**	**5**	**6**	**7**	**Tot.**
				%	%	%	%	%	%	%	%
A	1	1	1	6.00	12.47	68.37	89.82	93.89	95.34	91.79	83.35
A	1	1	2	6.37	12.46	68.40	89.45	93.35	95.42	91.11	83.18
A	1	1	3	6.76	12.84	69.41	90.18	93.88	95.20	90.91	83.68
A	1	2	4	6.64	8.84	54.37	84.92	91.63	92.01	89.36	82.03
A	1	2	5	6.67	8.42	52.51	84.88	91.35	92.56	91.59	83.10
A	1	2	6	7.27	8.65	54.29	86.18	92.63	93.81	91.00	83.61
A	1	2	7	5.83	9.24	56.96	86.28	91.42	93.59	90.73	82.92
A	1	2	8	6.78	8.27	54.08	85.02	91.19	91.88	90.42	82.71
A	1	2	9	5.95	9.03	57.84	86.02	91.63	93.34	90.48	83.09
A	1	2	10	6.87	8.73	62.55	84.80	91.26	93.34	88.92	82.85
A	1	2	11	5.97	9.20	58.51	86.42	92.51	93.36	90.94	83.53
A	1	3	12	5.20	7.82	48.60	82.62	89.27	91.51	89.05	82.52
A	1	3	13	5.63	7.57	49.39	82.03	89.25	91.43	89.04	82.92
A	1	3	14	5.33	7.94	51.27	83.00	89.47	91.21	87.75	82.10
A	2	4	15	18.53	11.42	56.03	82.71	90.49	94.70	88.15	85.24
A	2	4	16	10.65	9.11	38.53	74.26	86.35	92.47	87.95	81.80
A	2	4	17	16.52	12.58	46.70	78.56	88.54	93.31	89.62	84.95
A	2	4	18	21.11	10.74	46.11	76.61	87.32	93.27	88.90	85.03
A	2	4	19	19.79	11.02	51.39	78.40	88.45	93.22	87.33	84.10
A	2	5	20	18.46	12.82	50.82	80.53	89.56	94.34	89.62	85.62
A	2	5	21	23.16	13.12	52.53	79.66	88.07	92.70	86.54	83.76
A	2	5	22	23.90	17.22	52.08	79.26	88.48	92.66	85.86	83.38
A	2	5	23	21.49	16.12	55.03	81.00	88.90	93.53	85.52	83.78
A	2	6	24	30.07	25.06	62.04	82.88	89.88	92.57	83.93	83.54
A	2	6	25	35.19	35.32	65.51	80.40	86.99	87.11	81.61	80.48
B	2	7	26	4.96	10.68	22.76	71.22	87.50	94.93	90.53	84.48
B	2	7	27	6.52	9.74	39.87	82.74	91.35	95.75	83.79	83.72
B	2	7	28	4.64	7.57	15.39	60.08	85.14	93.43	89.83	81.35
B	2	8	29	8.17	14.15	35.34	73.37	87.38	94.53	88.49	85.03
B	2	8	30	7.50	15.63	35.58	75.99	87.98	93.62	89.54	83.64
B	2	8	31	10.83	20.36	50.03	80.11	90.12	95.42	84.48	85.49
B	2	8	32	6.10	12.81	27.84	69.21	86.28	92.50	87.98	82.55
B	2	8	33	11.28	19.79	48.57	76.86	87.74	92.94	85.59	81.87
B	2	9	34	10.64	21.41	43.99	76.16	87.62	92.22	84.17	80.84
B	2	9	35	10.23	17.92	39.65	74.63	87.66	92.51	86.15	82.07
B	2	9	36	20.14	33.88	58.09	82.43	90.23	94.86	89.40	88.37
B	2	9	37	8.95	15.85	37.49	71.48	87.06	91.37	85.97	82.03
B	2	9	38	11.22	19.05	38.25	71.60	86.28	90.57	85.81	81.48
B	2	9	39	10.66	21.20	41.05	71.48	86.80	91.68	84.21	80.89

Table A.5: Spiral test slimes content results.

Test Identification				Product Slimes Content Per Cut							
Profile	**Material**	**Group**	**Test**	**1**	**2**	**3**	**4**	**5**	**6**	**7**	**Tot.**
				%	%	%	%	%	%	%	%
A	1	1	1	0.60	0.79	0.88	0.74	0.81	1.24	6.06	2.42
A	1	1	2	0.66	0.74	0.74	0.80	0.99	1.24	6.74	2.63
A	1	1	3	0.67	0.85	0.98	0.82	0.96	1.32	6.84	2.77
A	1	2	4	1.01	1.16	0.98	1.19	1.25	3.46	7.54	4.21
A	1	2	5	0.98	0.97	1.16	1.09	1.23	2.83	5.11	3.14
A	1	2	6	0.38	0.44	0.54	0.23	0.45	1.38	5.77	2.64
A	1	2	7	0.97	1.02	1.21	1.03	1.18	1.39	6.15	2.81
A	1	2	8	1.10	0.91	1.21	0.62	1.28	3.16	6.27	3.67
A	1	2	9	0.82	1.15	1.30	1.09	1.30	1.64	6.27	3.08
A	1	2	10	1.12	1.21	0.91	1.30	1.55	1.87	7.71	3.85
A	1	2	11	0.89	1.12	1.37	1.14	0.34	1.51	5.88	2.80
A	1	3	12	1.58	1.40	1.83	1.66	1.86	2.04	6.53	3.56
A	1	3	13	1.47	1.59	1.60	1.70	1.96	2.11	6.45	3.67
A	1	3	14	1.60	1.73	1.97	1.84	2.04	2.20	6.99	3.87
A	2	4	15	3.48	3.18	4.26	2.37	1.86	2.10	7.17	4.37
A	2	4	16	1.64	1.97	1.49	0.63	1.72	2.04	5.50	3.35
A	2	4	17	4.55	4.27	3.96	1.92	1.77	2.06	5.42	3.71
A	2	4	18	3.38	3.57	2.74	2.04	2.35	2.11	6.06	4.18
A	2	4	19	3.20	2.32	3.01	1.81	1.81	2.27	7.24	4.65
A	2	5	20	2.62	3.08	1.52	1.39	1.45	1.19	4.62	2.85
A	2	5	21	3.26	2.83	2.81	1.64	2.39	2.62	7.84	5.13
A	2	5	22	6.09	6.22	4.63	2.28	2.22	2.85	8.31	5.68
A	2	5	23	3.15	2.97	2.49	1.53	1.73	2.19	9.02	5.37
A	2	6	24	4.74	4.64	6.60	1.76	1.79	2.93	10.46	6.63
A	2	6	25	5.46	5.64	3.69	3.26	2.92	5.96	9.99	7.63
B	2	7	26	2.00	5.76	3.78	3.03	1.92	1.42	8.01	4.22
B	2	7	27	2.40	4.24	3.68	2.66	1.44	1.46	14.64	5.00
B	2	7	28	2.14	2.56	2.74	3.47	1.90	1.45	7.74	4.26
B	2	8	29	4.29	6.81	6.46	6.47	3.24	1.56	9.33	5.38
B	2	8	30	2.72	6.57	3.94	2.35	1.98	1.99	7.94	4.71
B	2	8	31	3.09	8.27	5.52	2.87	1.93	2.24	13.03	6.90
B	2	8	32	2.16	4.73	3.96	2.76	2.44	2.14	8.48	5.60
B	2	8	33	3.33	6.26	3.17	2.23	2.38	2.48	10.87	6.26
B	2	9	34	2.55	7.63	3.94	2.96	3.07	2.67	11.76	7.05
B	2	9	35	3.89	4.92	2.81	2.57	2.50	2.04	9.77	6.12
B	2	9	36	8.56	15.15	12.98	3.03	2.61	1.99	8.69	5.64
B	2	9	37	3.01	1.93	4.26	3.55	2.82	2.69	9.49	6.57
B	2	9	38	4.11	4.93	3.28	2.99	2.26	2.80	9.50	6.51
B	2	9	39	3.41	9.12	5.20	5.24	2.69	2.03	10.38	7.07

Table A.6: Spiral test solids concentration results.

Test Identification				Product Solids Concentration Per Cut							
Profile	**Material**	**Group**	**Test**	**1**	**2**	**3**	**4**	**5**	**6**	**7**	**TOTAL**
				%	%	%	%	%	%	%	%
A	1	1	1	6.00	12.47	68.37	89.82	93.89	95.34	91.79	83.35
A	1	1	2	6.37	12.46	68.40	89.45	93.35	95.42	91.11	83.18
A	1	1	3	6.76	12.84	69.41	90.18	93.88	95.20	90.91	83.68
A	1	2	4	6.64	8.84	54.37	84.92	91.63	92.01	89.36	82.03
A	1	2	5	6.67	8.42	52.51	84.88	91.35	92.56	91.59	83.10
A	1	2	6	7.27	8.65	54.29	86.18	92.63	93.81	91.00	83.61
A	1	2	7	5.83	9.24	56.96	86.28	91.42	93.59	90.73	82.92
A	1	2	8	6.78	8.27	54.08	85.02	91.19	91.88	90.42	82.71
A	1	2	9	5.95	9.03	57.84	86.02	91.63	93.34	90.48	83.09
A	1	2	10	6.87	8.73	62.55	84.80	91.26	93.34	88.92	82.85
A	1	2	11	5.97	9.20	58.51	86.42	92.51	93.36	90.94	83.53
A	1	3	12	5.20	7.82	48.60	82.62	89.27	91.51	89.05	82.52
A	1	3	13	5.63	7.57	49.39	82.03	89.25	91.43	89.04	82.92
A	1	3	14	5.33	7.94	51.27	83.00	89.47	91.21	87.75	82.10
A	2	4	15	18.53	11.42	56.03	82.71	90.49	94.70	88.15	85.24
A	2	4	16	10.65	9.11	38.53	74.26	86.35	92.47	87.95	81.80
A	2	4	17	16.52	12.58	46.70	78.56	88.54	93.31	89.62	84.95
A	2	4	18	21.11	10.74	46.11	76.61	87.32	93.27	88.90	85.03
A	2	4	19	19.79	11.02	51.39	78.40	88.45	93.22	87.33	84.10
A	2	5	20	18.46	12.82	50.82	80.53	89.56	94.34	89.62	85.62
A	2	5	21	23.16	13.12	52.53	79.66	88.07	92.70	86.54	83.76
A	2	5	22	23.90	17.22	52.08	79.26	88.48	92.66	85.86	83.38
A	2	5	23	21.49	16.12	55.03	81.00	88.90	93.53	85.52	83.78
A	2	6	24	30.07	25.06	62.04	82.88	89.88	92.57	83.93	83.54
A	2	6	25	35.19	35.32	65.51	80.40	86.99	87.11	81.61	80.48
B	2	7	26	4.96	10.68	22.76	71.22	87.50	94.93	90.53	84.48
B	2	7	27	6.52	9.74	39.87	82.74	91.35	95.75	83.79	83.72
B	2	7	28	4.64	7.57	15.39	60.08	85.14	93.43	89.83	81.35
B	2	8	29	8.17	14.15	35.34	73.37	87.38	94.53	88.49	85.03
B	2	8	30	7.50	15.63	35.58	75.99	87.98	93.62	89.54	83.64
B	2	8	31	10.83	20.36	50.03	80.11	90.12	95.42	84.48	85.49
B	2	8	32	6.10	12.81	27.84	69.21	86.28	92.50	87.98	82.55
B	2	8	33	11.28	19.79	48.57	76.86	87.74	92.94	85.59	81.87
B	2	9	34	10.64	21.41	43.99	76.16	87.62	92.22	84.17	80.84
B	2	9	35	10.23	17.92	39.65	74.63	87.66	92.51	86.15	82.07
B	2	9	36	20.14	33.88	58.09	82.43	90.23	94.86	89.40	88.37
B	2	9	37	8.95	15.85	37.49	71.48	87.06	91.37	85.97	82.03
B	2	9	38	11.22	19.05	38.25	71.60	86.28	90.57	85.81	81.48
B	2	9	39	10.66	21.20	41.05	71.48	86.80	91.68	84.21	80.89

Appendix B

Method Validation Data

This appendix presents data used to validate some of the experimental methods used. This includes the influence of block preparation on Qemscan® property measurement results, as well as the influence of Qemscan® particle population size.

Table B.1: Data indicating the influence of block preparation on property measurement results. Three blocks were analysed, and all properties were measured by Qemscan®.

Particle Size				**Particle Density**				**Particle Shape Factor**			
	1	2	3		1	2	3		1	2	3
µm	%	%	%	kg/ m^3	%	%	%		%	%	%
0	0.00	0.00	0.00	2.00	0.00	0.00	0.00	0.0	0.00	0.00	0.00
10	0.00	0.00	0.00	2.50	0.06	0.46	0.00	2.0	0.00	0.00	0.00
20	0.03	0.04	0.03	2.60	1.27	1.19	0.96	4.0	0.00	0.00	0.00
30	0.06	0.09	0.06	2.70	0.29	0.18	0.30	6.0	0.00	0.00	0.00
40	0.11	0.16	0.11	2.80	0.01	0.03	0.19	8.0	0.00	0.00	0.00
50	0.19	0.22	0.19	2.90	0.24	0.18	0.14	10.0	0.00	0.00	0.00
60	0.27	0.32	0.26	3.00	0.03	0.05	0.73	10.5	0.00	0.00	0.00
70	0.45	0.54	0.41	3.10	0.50	0.97	0.22	11.0	0.00	0.00	0.00
80	0.76	0.85	0.87	3.20	1.22	1.12	2.49	11.5	0.00	0.00	0.00
90	1.09	1.23	1.11	3.30	4.23	7.08	9.22	12.0	0.00	0.00	0.00
100	1.72	1.83	1.46	3.40	11.68	11.34	12.37	12.5	0.00	0.00	0.00
110	2.02	2.31	2.60	3.50	15.21	17.04	13.21	13.0	0.00	0.00	0.00
120	3.50	3.35	3.51	3.60	11.00	9.80	7.59	13.5	0.00	0.00	0.00
130	4.31	4.13	3.80	3.65	2.52	3.34	2.98	14.0	0.00	0.00	0.80
140	4.97	4.93	5.79	3.70	0.91	1.46	1.32	14.5	1.46	1.80	1.28
150	5.98	5.59	6.15	3.75	3.27	1.20	1.48	15.0	7.75	5.06	5.70
160	6.38	7.60	6.93	3.80	0.91	1.31	2.29	15.2	4.31	3.07	3.26
170	6.41	8.48	6.70	3.85	1.14	1.39	1.66	15.4	3.79	4.42	5.38
180	7.27	7.72	6.65	3.90	2.22	0.89	1.89	15.6	2.85	4.34	4.77
190	6.80	5.34	5.79	3.95	1.90	1.46	1.57	15.8	5.49	3.92	5.05
200	7.76	7.65	7.52	4.00	1.31	1.05	1.74	16.0	4.63	5.70	5.62
210	6.08	6.55	5.74	4.05	2.14	1.07	1.28	16.2	5.55	4.86	4.96
220	5.43	6.37	4.60	4.10	2.84	1.62	2.87	16.4	6.70	5.97	5.29
230	4.46	3.66	5.54	4.15	2.02	3.65	2.16	16.6	4.44	4.39	5.31
240	3.29	4.46	5.14	4.20	3.42	3.44	2.60	16.8	4.11	4.79	3.45
250	3.41	3.02	3.39	4.25	4.95	3.73	4.46	17.0	3.62	4.75	4.01
260	3.61	1.61	3.58	4.30	6.42	7.61	5.10	17.2	3.48	4.51	4.27
270	1.51	2.09	3.20	4.35	4.13	4.91	4.73	17.4	4.06	3.26	3.94
280	3.14	2.20	0.87	4.40	5.30	4.31	4.82	17.6	4.10	3.08	5.20
290	2.20	2.07	2.84	4.45	4.00	3.51	5.27	17.8	4.53	2.26	3.10
300	2.32	2.04	1.50	4.50	0.50	0.57	0.42	18.0	2.93	3.56	3.67
310	1.48	1.05	1.52	4.55	0.75	0.56	0.53	18.2	3.09	3.72	2.64
320	0.00	1.05	0.43	4.60	0.01	0.47	0.13	18.4	2.12	2.40	2.84
330	0.00	0.56	0.88	4.65	0.33	0.04	0.29	18.6	2.13	1.94	1.95
340	0.55	0.89	0.00	4.70	2.15	2.13	1.96	18.8	2.19	2.11	1.96
350	0.70	0.00	0.00	4.80	0.72	0.56	0.68	19.0	2.26	1.99	1.67
360	0.00	0.00	0.00	4.90	0.32	0.01	0.21	20.0	7.97	9.53	5.61
370	0.00	0.00	0.00	5.00	0.00	0.00	0.01	21.0	2.95	4.53	2.93
380	0.71	0.00	0.00	5.10	0.00	0.00	0.00	22.0	1.83	1.40	1.84
390	0.00	0.00	0.00	5.20	0.00	0.00	0.00	23.0	0.87	1.08	0.66
400	0.00	0.00	0.81	5.40	0.00	0.00	0.00	24.0	0.21	0.20	1.12
500	1.04	0.00	0.00	5.60	0.00	0.00	0.00	26.0	0.10	0.75	1.09
600	0.00	0.00	0.00	5.80	0.00	0.14	0.00	28.0	0.12	0.45	0.13
700	0.00	0.00	0.00	6.00	0.06	0.11	0.12	30.0	0.05	0.06	0.09
800	0.00	0.00	0.00	6.20	0.00	0.00	0.00	40.0	0.30	0.09	0.38
900	0.00	0.00	0.00	6.40	0.00	0.00	0.00	50.0	0.03	0.00	0.00
1000	0.00	0.00	0.00	6.60	0.00	0.00	0.00	100.0	0.00	0.00	0.01

Table B.2: Data indicating the influence of particle population size on property measurement results. Four population sizes were analysed, and all properties were measured by Qemscan®.

Particle Size					**Particle Density**					**Particle Shape Factor**				
Range	9849	4922	2501	1000	Range	9849	4922	2501	1000	Range	9849	4922	2501	1000
µm	%	%	%	%	kg/ m^3	%	%	%	%		%	%	%	%
0	0.00	0.00	0.00	0.00	2.00	0.00	0.00	0.00	0.00	0.0	0.00	0.00	0.00	0.00
10	0.02	0.02	0.02	0.02	2.50	0.03	0.03	0.05	0.13	2.0	0.00	0.00	0.00	0.00
20	0.34	0.35	0.36	0.38	2.60	0.31	0.38	0.22	0.37	4.0	0.00	0.00	0.00	0.00
30	0.56	0.57	0.57	0.58	2.70	0.01	0.01	0.00	0.00	6.0	0.00	0.00	0.00	0.00
40	0.72	0.72	0.73	0.58	2.80	0.04	0.07	0.05	0.00	8.0	0.00	0.00	0.00	0.00
50	1.06	1.08	1.07	1.29	2.90	0.02	0.02	0.03	0.04	10.0	0.00	0.00	0.00	0.00
60	1.59	1.54	1.38	1.22	3.00	0.01	0.00	0.01	0.01	10.5	0.00	0.00	0.00	0.00
70	2.24	2.29	2.28	2.23	3.10	0.15	0.19	0.10	0.20	11.0	0.00	0.00	0.00	0.00
80	3.22	3.15	3.60	3.59	3.20	0.70	0.69	0.52	0.46	11.5	0.00	0.00	0.00	0.00
90	4.37	4.47	4.23	5.29	3.30	0.77	0.85	0.70	0.92	12.0	0.00	0.00	0.00	0.00
100	5.55	5.57	5.88	5.34	3.40	1.05	1.16	1.10	1.63	12.5	0.00	0.00	0.00	0.00
110	6.01	6.19	6.19	5.13	3.50	1.74	1.59	2.02	1.76	13.0	0.00	0.00	0.00	0.00
120	6.99	6.97	6.61	6.95	3.60	1.87	1.82	1.96	1.78	13.5	0.00	0.00	0.00	0.00
130	6.85	6.76	6.23	5.20	3.65	0.66	0.60	0.44	0.49	14.0	0.06	0.12	0.25	0.31
140	8.40	8.50	9.43	9.53	3.70	0.44	0.37	0.38	0.26	14.5	1.18	1.43	1.23	0.87
150	7.45	7.57	7.47	7.38	3.75	0.82	0.63	0.92	0.67	15.0	5.28	5.36	5.76	5.13
160	7.85	8.23	8.14	6.07	3.80	0.70	0.95	1.42	2.25	15.2	2.76	2.64	2.50	3.01
170	5.25	5.39	5.70	5.40	3.85	0.46	0.53	0.47	0.09	15.4	4.26	3.83	3.69	5.01
180	5.67	5.04	5.46	6.07	3.90	0.66	0.72	0.93	0.86	15.6	4.39	4.72	4.52	3.98
190	4.24	4.15	3.91	4.31	3.95	0.68	0.65	0.74	0.99	15.8	5.22	5.50	5.49	6.12
200	3.79	4.59	4.69	4.25	4.00	0.96	0.82	0.41	0.23	16.0	4.54	4.71	4.73	4.21
210	3.98	3.74	2.82	3.03	4.05	1.39	1.36	1.37	0.84	16.2	5.50	5.48	4.88	5.29
220	2.96	3.01	2.50	2.78	4.10	1.09	1.12	1.43	1.03	16.4	5.33	5.35	5.27	4.51
230	1.97	2.20	2.79	2.84	4.15	2.09	2.30	2.10	2.48	16.6	4.10	3.94	3.50	3.58
240	1.72	1.58	1.93	1.06	4.20	3.61	3.17	3.15	2.56	16.8	5.38	5.18	5.25	4.30
250	1.62	1.34	0.91	2.03	4.25	12.14	11.49	11.06	12.40	17.0	5.24	5.77	6.10	5.89
260	0.84	0.66	1.03	0.48	4.30	21.48	21.60	22.16	20.15	17.2	4.85	3.98	3.94	3.21
270	0.77	0.45	0.35	0.00	4.35	13.51	13.54	14.90	16.22	17.4	4.40	4.59	5.76	5.26
280	0.78	0.84	0.53	0.66	4.40	8.32	8.91	9.10	8.25	17.6	3.66	3.08	3.37	1.90
290	0.85	1.12	0.99	2.02	4.45	4.46	4.27	3.56	4.15	17.8	3.07	3.06	2.76	3.50
300	0.38	0.37	0.27	0.68	4.50	1.44	1.57	0.78	0.88	18.0	2.50	2.77	2.45	2.91
310	0.52	0.30	0.00	0.00	4.55	0.64	0.61	0.51	0.35	18.2	2.91	2.93	3.18	4.48
320	0.70	0.88	1.55	3.07	4.60	0.52	0.57	0.69	0.46	18.4	2.95	2.95	2.56	2.25
330	0.16	0.09	0.17	0.00	4.65	1.09	0.80	0.57	0.81	18.6	2.20	2.23	2.08	2.88
340	0.09	0.19	0.00	0.00	4.70	7.24	7.66	7.48	6.45	18.8	2.31	2.36	2.45	2.84
350	0.00	0.00	0.00	0.00	4.80	2.29	2.56	2.50	3.04	19.0	1.58	1.61	1.59	2.16
360	0.00	0.00	0.00	0.00	4.90	1.48	1.41	1.68	1.17	20.0	7.95	8.17	8.09	8.46
370	0.23	0.00	0.00	0.00	5.00	0.46	0.45	0.45	0.17	21.0	3.95	4.19	5.10	5.21
380	0.00	0.00	0.00	0.00	5.10	0.20	0.00	0.01	0.01	22.0	1.77	1.74	1.53	1.44
390	0.00	0.00	0.00	0.00	5.20	0.00	0.00	0.00	0.00	23.0	0.84	0.52	0.33	0.17
400	0.16	0.11	0.21	0.54	5.40	0.16	0.01	0.01	0.00	24.0	0.36	0.36	0.54	0.27
500	0.11	0.00	0.00	0.00	5.60	0.05	0.11	0.00	0.00	26.0	0.18	0.25	0.21	0.41
600	0.00	0.00	0.00	0.00	5.80	0.36	0.67	0.69	1.55	28.0	0.06	0.06	0.04	0.02
700	0.00	0.00	0.00	0.00	6.00	3.92	3.76	3.35	3.86	30.0	0.04	0.06	0.12	0.01
800	0.00	0.00	0.00	0.00	6.20	0.00	0.00	0.00	0.00	40.0	1.21	1.04	0.73	0.42
900	0.00	0.00	0.00	0.00	6.40	0.00	0.00	0.00	0.00	50.0	0.00	0.00	0.00	0.00
1000	0.00	0.00	0.00	0.00	6.60	0.00	0.00	0.00	0.00	100.0	0.00	0.00	0.00	0.00

Appendix C

Enhanced Holland-Batt Visual Basic Program

C.1 High Density Lines

```
Public Function Spline_HighDensity(a As Double, b As Double, c As Double, y As Double)

'The combination of three curves describes the cumulative recovery of certain
' mass class as a function of mass yield to concentrate.
'a is the gradient of the straight line, defined by rlin
'b is the power law, defined by rpow
'c is the distance at cross point of rlin and rpow
'y is the cumulative mass yield to concentrate
'r is the the cumulative recovery of certain mass class
'rpol is defined by the polynomial function that connects rlin and rpow
'cross point is defined by rlin and rpow intersection

Dim rlin As Double, rpow As Double
rlin = a * y
rpow = 100 * ((y / 100) ^ b)

Dim y_cross As Double
y_cross = (a * (100 ^ (b - 1))) ^ (1 / (b - 1))

Dim y1 As Double, y2 As Double, r1 As Double, r2 As Double
Dim r1_ As Double, r2_ As Double
y1 = y_cross - c
y2 = y_cross + c
r1 = a * y1
r2 = 100 * ((y2 / 100) ^ b)
r1_ = a
r2_ = ((100 * (((y_cross + c + 1) / 100) ^ b) - (100 * (((y_cross + c) / 100) ^ b)))) _
      / ((y_cross + c + 1) - (y_cross + c))

Dim Z As Variant
ReDim Z(4, 4) As Double
Z(1, 1) = (1)
Z(1, 2) = (y1)
Z(1, 3) = (y1 ^ 2)
Z(1, 4) = (y1 ^ 3)
Z(2, 1) = (1)
Z(2, 2) = (y2)
Z(2, 3) = (y2 ^ 2)
Z(2, 4) = (y2 ^ 3)
```

```
Z(3, 1) = (0)
Z(3, 2) = (1)
Z(3, 3) = (2 * y1)
Z(3, 4) = (3 * y1 ^ 2)
Z(4, 1) = (0)
Z(4, 2) = (1)
Z(4, 3) = (2 * y2)
Z(4, 4) = (3 * y2 ^ 2)

Dim R As Variant
ReDim R(4, 1) As Double
R(1, 1) = (r1)
R(2, 1) = (r2)
R(3, 1) = (r1_)
R(4, 1) = (r2_)

Dim Zinverse As Variant
Zinverse = WorksheetFunction.MInverse(Z)

Dim Coeff As Variant
Coeff = WorksheetFunction.MMult(Zinverse, R)

Dim d0 As Double, d1 As Double, d2 As Double, d3 As Double
d0 = Coeff(1, 1)
d1 = Coeff(2, 1)
d2 = Coeff(3, 1)
d3 = Coeff(4, 1)

Dim rpol As Double
rpol = d0 + d1 * y + d2 * y ^ 2 + d3 * y ^ 3

If y <= y1 And y >= 0 Then
    Spline_HighDensity = rlin
Else If y <= y2 And y > y1 Then
    Spline_HighDensity = rpol
Else If y > y2 And y <= 100 Then
    Spline_HighDensity = rpow
Else
    Spline_HighDensity = "unknown"
End If

End Function
```

C.2 Low Density Lines

```
Public Function Spline_LowDensity(a As Double, b As Double, c As Double, y As Double)

Dim y_
y_ = 100 - y

Dim r as Double
r = Spline_HighDensity(a,b,c,y_)

Dim r_ as Double
r_ = 100 - r

Spline_LowDensity = r_

End Function
```

Appendix D

Particle Population Variability Data

This appendix presents particle size and density distribution data for selected spiral tests.

D.1 Particle Size

Table D.1: Spiral test 1 particle size distribution results.

	Heavy Mineral Cuts							Light Mineral Cuts						
Size	**1**	**2**	**3**	**4**	**5**	**6**	**7**	**1**	**2**	**3**	**4**	**5**	**6**	**7**
µm	%	%	%	%	%	%	%	%	%	%	%	%	%	%
0	0.0	0.0	0.0	0.0	0.0	0.0	0.0	0.0	0.0	0.0	0.0	0.0	0.0	0.0
45	0.0	0.0	0.0	0.7	0.0	0.0	0.0	0.3	0.3	0.1	0.0	0.0	0.0	0.1
75	1.2	0.9	0.7	1.0	0.4	0.4	2.3	7.1	5.0	1.2	0.4	0.2	0.2	0.9
90	7.1	4.9	2.9	2.2	1.3	1.2	4.6	14.4	10.2	2.5	0.9	0.5	0.4	1.7
106	22.5	16.3	10.7	6.9	5.2	4.7	12.6	28.2	20.5	5.8	2.5	1.6	1.4	3.6
125	48.0	37.5	28.1	19.3	15.0	13.8	28.4	47.8	39.1	14.9	7.4	5.2	4.5	9.1
150	76.5	65.8	57.0	45.8	40.6	37.5	56.1	74.4	65.7	33.3	20.8	15.4	14.5	22.1
180	91.6	83.4	78.3	69.7	64.3	60.7	77.2	87.9	78.6	49.9	36.0	29.2	27.9	38.1
212	98.6	96.0	93.8	90.8	88.1	86.8	93.0	96.2	87.5	71.0	62.4	53.6	53.1	63.9
250	99.8	99.2	98.4	98.0	97.1	96.8	98.1	98.9	90.6	84.4	81.3	74.6	74.7	84.0
300	99.9	99.8	99.4	99.4	99.2	99.2	99.0	99.5	91.7	90.9	91.6	88.2	86.0	92.9
425	100.0	99.9	99.9	100.0	99.9	99.9	99.8	99.8	92.4	95.7	99.4	99.3	99.6	99.9
550	100.0	100.0	100.0	100.0	100.0	100.0	100.0	100.0	100.0	100.0	100.0	100.0	100.0	100.0

Table D.2: Spiral test 4 particle size distribution results.

	Heavy Mineral Cuts							Light Mineral Cuts						
Size	**1**	**2**	**3**	**4**	**5**	**6**	**7**	**1**	**2**	**3**	**4**	**5**	**6**	**7**
µm	%	%	%	%	%	%	%	%	%	%	%	%	%	%
0	0.0	0.0	0.0	0.0	0.0	0.0	0.0	0.0	0.0	0.0	0.0	0.0	0.0	0.0
45	0.1	0.0	0.0	0.0	0.0	0.0	-0.1	0.9	0.4	0.1	0.0	0.0	0.0	0.1
75	1.6	1.0	0.6	0.3	0.2	0.2	0.3	11.1	7.9	1.6	0.6	0.4	0.3	0.9
90	8.5	4.9	3.1	1.9	1.4	1.3	2.2	19.6	15.1	3.4	1.2	0.8	0.6	1.6
106	25.6	29.8	11.6	7.7	6.4	6.0	9.3	32.6	27.2	7.4	3.2	2.3	1.7	3.5
125	52.2	41.8	31.6	22.9	19.0	18.4	23.9	51.0	45.9	18.0	9.5	6.3	5.4	9.1
150	79.3	70.1	62.0	51.7	47.0	45.7	54.1	74.7	68.5	38.5	22.7	18.0	16.2	21.6
180	92.7	87.0	81.4	74.4	70.1	69.3	75.5	86.8	79.5	55.7	38.8	31.7	29.1	37.0
212	98.8	97.1	95.0	93.0	91.1	90.9	93.0	94.7	86.3	74.7	64.1	56.0	54.0	62.8
250	99.8	99.5	98.8	98.5	97.8	97.9	98.4	97.7	89.0	85.8	81.5	77.3	76.1	82.6
300	100.0	99.8	99.6	99.6	99.5	99.5	99.4	99.1	90.2	91.1	90.5	88.1	88.7	91.3
425	100.0	100.0	99.9	100.0	100.0	99.9	99.9	99.5	91.1	95.8	99.3	99.4	99.6	99.8
550	100.0	100.0	100.0	100.0	100.0	100.0	100.0	100.0	100.0	100.0	100.0	100.0	100.0	100.0

Table D.3: Spiral test 6 particle size distribution results.

	Heavy Mineral Cuts							Light Mineral Cuts						
Size	**1**	**2**	**3**	**4**	**5**	**6**	**7**	**1**	**2**	**3**	**4**	**5**	**6**	**7**
µm	%	%	%	%	%	%	%	%	%	%	%	%	%	%
0	0.0	0.0	0.0	0.0	0.0	0.0	0.0	0.0	0.0	0.0	0.0	0.0	0.0	0.0
45	0.0	0.0	0.0	0.0	0.0	-0.1	0.0	1.0	0.7	0.1	0.0	0.0	0.0	0.1
75	1.4	1.1	0.5	0.3	0.3	0.3	1.4	10.8	9.9	1.8	0.6	0.4	0.2	0.8
90	8.3	5.9	2.9	1.5	1.3	1.2	4.0	22.0	17.7	3.8	1.5	0.8	0.6	1.7
106	25.3	19.0	11.1	7.1	5.6	5.3	11.4	37.4	30.0	8.4	3.7	2.3	1.9	3.8
125	50.6	41.8	29.3	20.4	16.6	16.5	26.4	56.5	47.5	18.8	9.5	6.5	5.4	9.3
150	79.0	71.4	60.9	50.3	44.0	43.7	55.6	77.7	68.3	37.4	22.3	16.6	14.9	21.9
180	92.1	86.8	80.3	72.7	67.4	67.4	76.6	89.1	79.1	55.5	39.1	30.9	29.0	38.1
212	98.7	97.0	95.0	92.3	90.0	90.1	93.7	96.2	86.4	75.3	63.2	55.8	54.4	63.3
250	99.8	99.4	98.8	98.2	97.7	97.7	98.9	98.7	90.0	86.6	81.8	77.2	76.9	83.1
300	99.9	99.8	99.7	99.4	99.4	99.5	99.8	99.3	91.4	91.7	91.9	88.3	88.4	92.1
425	100.0	99.9	99.9	99.9	99.9	100.0	100.0	99.4	92.4	95.3	99.2	99.1	99.3	99.7
550	100.0	100.0	100.0	100.0	100.0	100.0	100.0	100.0	100.0	100.0	100.0	100.0	100.0	100.0

Table D.4: Spiral test 8 particle size distribution results.

	Heavy Mineral Cuts							Light Mineral Cuts						
Size	**1**	**2**	**3**	**4**	**5**	**6**	**7**	**1**	**2**	**3**	**4**	**5**	**6**	**7**
µm	%	%	%	%	%	%	%	%	%	%	%	%	%	%
0	0.0	0.0	0.0	0.0	0.0	0.0	0.0	0.0	0.0	0.0	0.0	0.0	0.0	0.0
45	0.0	0.0	0.0	0.0	0.0	0.0	0.0	0.6	0.8	0.0	0.0	0.0	0.0	0.1
75	1.3	1.0	0.6	0.5	0.1	0.3	0.6	9.7	9.5	1.6	0.5	0.3	0.2	0.8
90	8.3	5.3	3.1	2.0	1.7	1.4	3.1	18.6	17.9	3.5	1.3	0.7	0.6	1.6
106	25.1	19.2	11.4	7.7	5.8	6.4	10.8	31.8	31.1	8.1	3.4	2.1	1.9	3.8
125	50.2	41.7	30.2	21.9	18.6	18.0	26.1	51.0	49.8	18.3	9.2	6.2	5.3	9.0
150	78.9	68.9	60.8	50.9	47.4	45.3	55.7	72.5	71.4	38.1	22.7	16.7	15.4	21.4
180	92.4	86.3	80.5	73.2	69.9	68.1	77.2	86.0	81.8	56.7	41.1	31.8	29.6	37.8
212	98.8	97.0	95.2	92.1	91.5	90.5	94.2	94.4	87.9	75.7	64.1	56.4	55.0	64.0
250	99.8	99.5	99.2	97.7	98.2	98.0	98.9	97.6	90.4	87.4	82.0	77.4	77.2	83.4
300	100.0	99.9	99.7	98.8	99.5	99.6	99.9	98.6	91.2	92.3	91.5	88.1	88.9	94.0
425	100.0	100.0	99.9	99.2	100.0	100.0	100.1	99.4	91.9	95.7	99.3	99.3	99.6	99.8
550	100.0	100.0	100.0	100.0	100.0	100.0	100.0	100.0	100.0	100.0	100.0	100.0	100.0	100.0

Table D.5: Spiral test 12 particle size distribution results.

	Heavy Mineral Cuts							Light Mineral Cuts						
Size	**1**	**2**	**3**	**4**	**5**	**6**	**7**	**1**	**2**	**3**	**4**	**5**	**6**	**7**
µm	%	%	%	%	%	%	%	%	%	%	%	%	%	%
0	0.0	0.0	0.0	0.0	0.0	0.0	0.0	0.0	0.0	0.0	0.0	0.0	0.0	0.0
45	0.1	0.1	0.1	0.0	0.0	0.0	0.0	0.8	0.9	0.1	0.0	0.0	0.0	0.1
75	1.8	1.4	0.9	0.5	0.4	0.2	0.6	12.5	11.1	1.8	0.7	0.4	0.4	0.8
90	9.4	7.0	4.1	2.3	2.0	1.6	2.7	21.2	19.4	4.0	1.6	0.9	0.8	1.6
106	28.0	22.6	15.0	9.6	8.2	7.3	9.7	34.8	31.9	8.6	3.9	2.4	2.0	3.4
125	53.8	45.2	36.8	27.0	23.1	21.4	25.1	52.9	49.0	19.0	10.4	7.0	6.2	8.7
150	79.9	72.9	65.8	57.8	53.2	51.2	54.5	75.2	69.4	37.6	23.9	18.9	17.2	20.8
180	92.9	88.4	84.4	79.1	75.1	73.9	76.2	86.6	79.0	55.1	41.3	34.5	31.3	36.8
212	98.8	97.5	96.2	94.7	93.3	92.7	93.4	94.6	85.3	75.2	64.6	58.1	56.5	61.2
250	99.8	99.9	99.2	98.9	98.6	98.4	98.5	98.0	88.1	85.9	81.6	77.8	77.7	81.4
300	100.0	100.0	99.8	99.7	99.7	99.7	99.7	99.1	89.2	91.1	90.2	88.2	88.0	91.2
425	100.0	100.0	100.0	100.0	100.0	100.0	100.0	99.7	90.1	95.7	99.2	99.4	99.6	99.7
550	100.0	100.0	100.0	100.0	100.0	100.0	100.0	100.0	100.0	100.0	100.0	100.0	100.0	100.0

D.2 Particle Density

Table D.6: Spiral test 1 heavy mineral particle density distribution results.

Density kg/m^3	**Cut1** %	**Cut2** %	**Cut3** %	**Cut4** %	**Cut5** %	**Cut6** %	**Cut7** %
0.00	0.00	0.00	0.00	0.00	0.00	0.00	0.00
2.00	0.00	0.00	0.00	0.00	0.00	0.00	0.00
2.10	0.00	0.00	0.00	0.00	0.00	0.00	0.00
2.20	0.00	0.00	0.00	0.00	0.00	0.00	0.00
2.30	0.00	0.00	0.00	0.00	0.00	0.00	0.00
2.40	0.00	0.00	0.00	0.00	0.00	0.00	0.00
2.50	0.01	0.01	0.18	0.11	0.10	0.10	0.14
2.60	0.07	0.19	0.95	1.08	0.88	1.24	1.39
2.70	0.08	0.21	1.03	1.25	1.32	1.52	1.56
2.80	0.09	0.23	1.12	1.40	1.40	1.56	1.64
2.90	0.10	0.24	1.22	1.50	1.54	1.86	1.76
3.00	0.11	0.25	1.49	1.75	1.85	1.95	2.23
3.10	0.13	0.31	1.86	2.22	2.32	2.55	2.88
3.20	0.25	0.36	2.54	3.73	4.69	3.76	5.39
3.30	0.65	0.80	4.52	7.91	12.41	7.95	12.39
3.40	1.26	1.74	8.48	16.42	23.26	18.69	24.90
3.50	2.37	3.97	16.52	27.73	32.96	33.87	39.53
3.60	3.63	6.36	21.25	36.44	40.08	43.93	49.71
3.70	4.62	7.74	24.84	40.24	43.94	47.76	55.08
3.80	5.65	9.59	27.19	43.26	48.04	51.45	58.80
3.90	6.60	10.47	30.79	46.66	51.18	54.90	61.68
4.00	7.57	11.63	33.93	49.68	54.46	58.36	63.92
4.10	9.20	14.38	39.71	53.12	57.71	62.87	67.26
4.20	16.11	20.18	47.70	60.36	64.64	68.96	71.39
4.30	54.42	55.30	73.57	76.68	76.63	81.83	81.82
4.40	73.01	78.82	87.98	90.42	88.89	91.98	92.06
4.50	78.70	85.87	93.78	95.09	95.44	96.04	95.01
4.60	81.21	87.58	94.78	95.79	95.80	96.73	95.53
4.70	92.00	94.95	98.42	98.91	98.87	99.00	98.39
4.80	93.80	96.46	99.15	99.51	99.82	99.55	98.97
4.90	94.14	97.05	99.31	99.73	99.87	99.90	99.18
5.00	94.52	97.67	99.50	99.77	99.93	99.90	99.30
5.10	94.53	97.67	99.50	99.77	99.93	99.90	99.30
5.20	94.53	97.67	99.50	99.77	99.93	99.90	99.30
5.30	94.53	97.67	99.50	99.77	99.93	99.90	99.30
5.40	94.63	97.67	99.50	99.77	99.93	99.90	99.30
5.50	94.63	97.67	99.50	99.77	99.93	99.90	99.30
5.60	94.66	97.69	99.50	99.77	99.93	99.90	99.30
5.70	94.66	97.70	99.50	99.77	99.93	99.90	99.31
5.80	94.72	97.70	99.50	99.77	99.93	99.90	99.31
5.90	94.87	97.81	99.51	99.77	99.94	99.90	99.37
6.00	100.00	100.00	100.00	100.00	100.00	100.00	100.00
6.10	100.00	100.00	100.00	100.00	100.00	100.00	100.00
6.20	100.00	100.00	100.00	100.00	100.00	100.00	100.00
6.30	100.00	100.00	100.00	100.00	100.00	100.00	100.00
6.40	100.00	100.00	100.00	100.00	100.00	100.00	100.00
6.50	100.00	100.00	100.00	100.00	100.00	100.00	100.00

Appendix E

Mass Distribution for 3×3 Particle Classes

This appendix presents the distribution of mass between the different size-density classes for each of the tests, per spiral cut.

Table E.1: Mass distribution between low-density classes by test and by cut.

	1. Fine-particle Low-density Cuts								2. Medium-particle Low-density Cuts								3. Course-particle Low-density Cuts							
Test	**1**	**2**	**3**	**4**	**5**	**6**	**7**	**Tot.**	**1**	**2**	**3**	**4**	**5**	**6**	**7**	**Tot.**	**1**	**2**	**3**	**4**	**5**	**6**	**7**	**Tot.**
1	0.14	0.17	0.60	1.82	0.91	4.43	4.78	**12.85**	0.20	0.30	1.70	5.35	4.08	15.47	14.87	**41.96**	0.04	0.06	1.03	2.63	5.96	12.75	7.94	**30.40**
6	0.11	0.12	0.63	0.96	1.38	4.50	5.77	**13.47**	0.14	0.15	1.19	3.24	3.99	16.38	17.72	**42.81**	0.02	0.04	0.47	2.80	2.96	11.74	10.54	**28.57**
8	0.11	0.12	0.59	0.96	1.17	5.11	5.50	**13.57**	0.15	0.16	1.25	3.39	4.52	17.00	17.34	**43.81**	0.02	0.02	0.47	2.20	2.52	11.11	11.55	**27.90**
9	0.10	0.13	0.64	0.98	1.47	4.52	5.60	**13.45**	0.14	0.17	1.21	3.31	4.24	16.45	17.20	**42.71**	0.02	0.04	0.48	2.86	3.15	11.81	10.23	**28.58**
12	0.08	0.10	0.50	0.80	1.39	4.73	5.76	**13.36**	0.11	0.13	0.95	2.70	4.01	17.19	17.70	**42.79**	0.01	0.03	0.37	2.33	2.98	12.34	10.54	**28.60**
15	0.03	0.03	0.08	0.30	0.36	0.73	1.40	**2.93**	0.20	0.10	0.57	2.01	2.55	4.54	9.58	**19.56**	0.18	0.16	1.50	4.65	7.33	21.99	27.05	**62.86**
16	0.02	0.01	0.06	0.34	0.33	0.53	1.61	**2.91**	0.11	0.06	0.43	2.21	2.67	4.93	9.93	**20.34**	0.16	0.18	0.94	3.46	6.06	19.69	26.39	**56.89**
17	0.03	0.04	0.09	0.21	0.35	0.47	1.64	**2.83**	0.15	0.11	0.60	1.67	2.66	6.60	11.34	**23.14**	0.22	0.16	0.93	4.25	6.02	18.36	28.09	**58.03**
18	0.03	0.03	0.08	0.21	0.23	0.65	1.41	**2.64**	0.16	0.10	0.51	1.94	1.71	4.70	10.33	**19.45**	0.20	0.12	0.79	2.76	5.47	19.62	33.50	**62.45**
19	0.02	0.02	0.09	0.16	0.24	0.71	2.07	**3.31**	0.12	0.08	0.58	1.37	1.79	5.33	12.84	**22.11**	0.32	0.13	1.05	4.30	6.25	18.35	28.44	**58.83**
20	0.02	0.02	0.08	0.24	0.15	1.18	2.05	**3.74**	0.15	0.08	0.49	1.73	1.25	8.47	12.50	**24.68**	0.25	0.19	1.07	4.62	8.12	15.42	24.99	**54.67**
21	0.04	0.03	0.08	0.23	0.18	0.54	1.36	**2.46**	0.18	0.13	0.61	1.77	1.56	4.59	9.96	**18.81**	0.25	0.14	1.00	3.49	6.42	18.75	32.61	**62.67**
22	0.03	0.03	0.07	0.26	0.14	0.76	2.09	**3.38**	0.20	0.12	0.43	1.78	1.83	5.11	15.94	**25.41**	0.35	0.27	1.40	3.68	5.64	17.13	23.76	**52.24**
23	0.03	0.02	0.08	0.19	0.30	0.64	1.43	**2.71**	0.19	0.11	0.61	1.59	2.41	4.96	10.79	**20.67**	0.25	0.21	1.12	4.40	6.00	18.90	30.39	**61.27**
24	0.03	0.03	0.11	0.21	0.22	0.66	1.94	**3.20**	0.27	0.17	0.75	1.69	2.51	4.78	11.61	**21.78**	0.35	0.35	1.34	4.26	5.53	17.85	30.00	**59.69**
25	0.04	0.04	0.10	0.31	0.21	0.63	2.70	**4.03**	0.29	0.24	0.60	1.92	1.36	5.15	17.41	**26.98**	0.56	0.48	1.48	3.20	5.40	12.90	23.87	**47.88**
26	0.03	0.03	0.07	0.37	0.59	0.73	1.08	**2.88**	0.07	0.05	0.23	2.31	4.15	5.72	8.58	**21.11**	0.03	0.01	0.09	2.31	6.51	27.16	24.51	**60.62**
27	0.03	0.02	0.11	0.56	0.73	1.27	0.91	**3.62**	0.11	0.05	0.57	3.73	5.16	9.71	6.15	**25.48**	0.07	0.04	0.42	4.70	10.58	25.33	13.67	**54.81**
28	0.02	0.01	0.02	0.22	0.50	0.82	1.54	**3.14**	0.09	0.03	0.14	1.47	3.50	5.78	10.21	**21.21**	0.12	0.11	0.30	2.67	6.13	22.19	25.06	**56.57**
29	0.04	0.03	0.06	0.18	0.48	1.58	1.54	**3.90**	0.12	0.07	0.28	1.17	3.33	9.68	9.91	**24.55**	0.07	0.06	0.31	1.84	7.85	22.94	24.34	**57.41**
30	0.03	0.02	0.06	0.26	0.46	0.70	1.48	**3.00**	0.11	0.07	0.31	1.94	3.38	5.01	10.35	**21.17**	0.14	0.11	0.52	4.17	6.65	21.77	26.18	**59.54**
31	0.04	0.03	0.07	0.25	0.51	1.51	0.77	**3.19**	0.13	0.09	0.37	1.65	3.76	9.73	5.90	**21.65**	0.07	0.08	0.35	3.48	6.79	22.51	30.19	**63.47**
32	0.03	0.01	0.06	0.26	0.40	0.57	1.62	**2.95**	0.09	0.05	0.31	1.79	3.00	6.04	14.18	**25.47**	0.03	0.04	0.18	2.35	5.15	15.40	29.84	**52.99**
33	0.03	0.02	0.10	0.31	0.44	0.69	1.40	**2.99**	0.14	0.08	0.51	2.41	3.04	4.68	9.62	**20.48**	0.26	0.15	0.89	4.23	7.44	19.66	27.30	**59.92**
34	0.05	0.02	0.12	0.39	0.41	0.66	2.08	**3.74**	0.20	0.12	0.63	2.63	3.25	6.78	13.86	**27.48**	0.14	0.12	0.58	3.31	6.93	15.84	23.93	**50.85**
35	0.04	0.02	0.08	0.18	0.46	0.65	2.44	**3.86**	0.15	0.07	0.46	1.87	3.30	6.64	14.89	**27.39**	0.12	0.08	0.47	3.42	5.76	14.76	25.63	**50.25**
36	0.05	0.03	0.08	0.25	0.20	0.64	2.16	**3.42**	0.19	0.15	0.45	1.77	3.07	7.70	13.50	**26.83**	0.13	0.09	0.28	2.98	6.54	22.42	25.65	**58.08**
37	0.03	0.02	0.06	0.26	0.39	0.61	2.59	**3.95**	0.12	0.07	0.37	1.88	2.81	5.69	15.39	**26.32**	0.07	0.04	0.44	2.21	5.12	14.32	29.80	**52.01**
38	0.03	0.01	0.05	0.22	0.42	0.59	2.00	**3.32**	0.13	0.04	0.31	1.49	2.95	4.13	13.28	**22.34**	0.16	0.15	0.68	2.71	5.17	15.88	32.58	**57.33**
39	0.03	0.02	0.09	0.26	0.40	0.59	2.23	**3.63**	0.14	0.10	0.50	1.83	3.03	5.41	15.78	**26.78**	0.13	0.07	0.49	2.76	5.08	14.72	27.46	**50.72**

Table E.2: Mass distribution between medium-density classes by test and by cut.

	1. Fine-particle Medium-density Cuts								2. Medium-particle Medium-density Cuts								3. Course-particle Medium-density Cuts							
Test	**1**	**2**	**3**	**4**	**5**	**6**	**7**	**Tot.**	**1**	**2**	**3**	**4**	**5**	**6**	**7**	**Tot.**	**1**	**2**	**3**	**4**	**5**	**6**	**7**	**Tot.**
1	0.13	0.10	0.07	0.14	0.04	0.16	0.08	**0.72**	0.25	0.26	0.28	0.34	0.18	0.43	0.25	**1.99**	0.06	0.06	0.16	0.17	0.12	0.24	0.10	**0.91**
6	0.07	0.08	0.09	0.08	0.09	0.22	0.15	**0.78**	0.15	0.15	0.28	0.27	0.18	0.54	0.40	**1.97**	0.03	0.05	0.12	0.13	0.08	0.28	0.14	**0.84**
8	0.07	0.09	0.11	0.08	0.06	0.20	0.28	**0.88**	0.12	0.16	0.31	0.21	0.17	0.59	0.44	**2.00**	0.01	0.06	0.13	0.06	0.10	0.25	0.15	**0.75**
9	0.08	0.09	0.12	0.10	0.11	0.24	0.16	**0.90**	0.16	0.17	0.35	0.27	0.21	0.59	0.41	**2.16**	0.03	0.02	0.12	0.11	0.08	0.32	0.11	**0.80**
12	0.06	0.10	0.11	0.07	0.10	0.27	0.18	**0.89**	0.11	0.18	0.26	0.18	0.19	0.65	0.46	**2.03**	0.01	0.06	0.09	0.05	0.06	0.29	0.16	**0.73**
15	0.10	0.14	0.19	0.20	0.15	0.13	0.63	**1.53**	0.26	0.35	0.56	0.72	0.61	0.62	1.82	**4.94**	0.14	0.13	0.20	0.39	0.55	0.85	1.12	**3.37**
16	0.13	0.11	0.24	0.30	0.24	0.25	0.75	**2.01**	0.25	0.29	0.61	0.78	0.69	0.97	2.24	**5.83**	0.04	0.08	0.21	0.21	0.39	1.20	1.54	**3.69**
17	0.11	0.11	0.17	0.25	0.15	0.26	0.55	**1.59**	0.21	0.30	0.58	0.79	0.65	1.19	1.81	**5.53**	0.09	0.04	0.16	0.27	0.41	1.19	1.33	**3.48**
18	0.09	0.12	0.21	0.27	0.17	0.25	0.67	**1.79**	0.21	0.22	0.50	0.75	0.55	0.88	2.12	**5.23**	0.07	0.07	0.13	0.45	0.31	1.06	1.51	**3.60**
19	0.09	0.13	0.19	0.18	0.14	0.24	0.82	**1.79**	0.24	0.31	0.58	0.67	0.56	0.86	2.27	**5.49**	0.08	0.08	0.18	0.37	0.39	0.83	1.28	**3.22**
20	0.10	0.10	0.16	0.21	0.10	0.42	0.88	**1.98**	0.26	0.30	0.56	0.80	0.63	1.26	2.12	**5.92**	0.06	0.08	0.27	0.38	0.42	1.11	1.38	**3.69**
21	0.11	0.12	0.18	0.18	0.16	0.22	0.74	**1.71**	0.23	0.28	0.53	0.68	0.47	0.95	2.00	**5.15**	0.05	0.08	0.17	0.43	0.27	0.94	1.79	**3.73**
22	0.11	0.16	0.20	0.29	0.18	0.41	1.62	**2.98**	0.26	0.27	0.49	0.77	0.61	1.07	3.42	**6.88**	0.06	0.07	0.15	0.28	0.43	0.91	1.98	**3.88**
23	0.10	0.14	0.18	0.22	0.15	0.26	0.70	**1.76**	0.29	0.31	0.50	0.63	0.65	0.91	2.03	**5.32**	0.12	0.09	0.21	0.43	0.44	0.97	1.41	**3.66**
24	0.06	0.10	0.12	0.15	0.16	0.24	0.93	**1.76**	0.21	0.32	0.46	0.55	0.68	0.74	2.24	**5.21**	0.13	0.08	0.17	0.37	0.62	0.97	1.49	**3.84**
25	0.13	0.06	0.10	0.22	0.12	0.38	2.15	**3.16**	0.28	0.25	0.34	0.66	0.41	1.12	4.22	**7.29**	0.12	0.15	0.14	0.39	0.38	0.90	2.33	**4.42**
26	0.17	0.13	0.24	0.40	0.27	0.21	0.28	**1.70**	0.34	0.24	0.56	1.17	1.06	0.95	0.86	**5.18**	0.10	0.07	0.15	0.36	0.54	1.00	0.95	**3.15**
27	0.24	0.15	0.15	0.34	0.30	0.38	0.31	**1.88**	0.41	0.28	0.37	1.10	0.97	1.25	0.76	**5.15**	0.21	0.10	0.18	0.61	0.63	0.97	0.43	**3.13**
28	0.22	0.13	0.27	0.51	0.33	0.35	0.57	**2.39**	0.34	0.24	0.60	1.29	1.03	1.11	1.36	**5.96**	0.22	0.02	0.12	0.46	0.51	1.01	0.92	**3.26**
29	0.19	0.12	0.19	0.17	0.20	0.37	0.42	**1.65**	0.35	0.32	0.57	0.55	0.85	1.47	1.23	**5.35**	0.06	0.04	0.14	0.24	0.53	0.91	1.12	**3.04**
30	0.23	0.10	0.25	0.36	0.26	0.25	0.53	**1.97**	0.28	0.18	0.57	1.03	0.91	0.88	1.38	**5.22**	0.14	0.03	0.11	0.39	0.43	0.88	1.45	**3.42**
31	0.25	0.13	0.17	0.24	0.21	0.45	0.22	**1.67**	0.34	0.24	0.39	0.69	0.76	1.06	0.82	**4.30**	0.02	0.07	0.14	0.24	0.46	0.93	1.18	**3.04**
32	0.15	0.08	0.21	0.29	0.19	0.38	0.83	**2.13**	0.34	0.18	0.56	0.95	0.73	1.45	2.36	**6.58**	0.18	0.04	0.18	0.37	0.43	0.96	1.66	**3.84**
33	0.16	0.09	0.24	0.36	0.29	0.24	0.56	**1.94**	0.43	0.20	0.45	1.02	0.73	0.93	1.60	**5.36**	0.41	0.04	0.14	0.35	0.43	0.87	1.39	**3.63**
34	0.19	0.10	0.25	0.31	0.26	0.38	0.84	**2.32**	0.39	0.19	0.57	1.02	0.78	1.30	1.87	**6.14**	0.12	0.08	0.17	0.55	0.49	0.80	1.08	**3.30**
35	0.15	0.06	0.19	0.28	0.24	0.33	1.08	**2.32**	0.39	0.22	0.59	0.84	0.81	1.46	2.53	**6.85**	0.14	0.10	0.17	0.49	0.37	0.97	1.20	**3.45**
36	0.25	0.10	0.12	0.21	0.18	0.24	0.78	**1.87**	0.36	0.21	0.29	0.65	0.69	1.09	1.48	**4.77**	0.05	0.04	0.12	0.27	0.58	1.32	1.09	**3.47**
37	0.17	0.08	0.18	0.26	0.16	0.32	1.30	**2.47**	0.37	0.20	0.47	0.85	0.68	1.01	2.58	**6.17**	0.15	0.07	0.13	0.35	0.39	0.82	1.50	**3.41**
38	0.16	0.08	0.21	0.31	0.24	0.30	1.02	**2.33**	0.27	0.15	0.48	0.83	0.76	0.92	2.37	**5.76**	0.17	0.02	0.12	0.34	0.40	0.77	1.32	**3.13**
39	0.13	0.07	0.17	0.22	0.22	0.32	1.20	**2.33**	0.33	0.19	0.53	0.77	0.66	1.09	3.04	**6.61**	0.12	0.04	0.15	0.38	0.40	0.78	1.96	**3.83**

Table E.3: Mass distribution between high-density classes by test and by cut.

	1. Fine-particle High-density Cuts								2. Medium-particle High-density Cuts								3. Course-particle High-density Cuts							
Test	**1**	**2**	**3**	**4**	**5**	**6**	**7**	**Tot.**	**1**	**2**	**3**	**4**	**5**	**6**	**7**	**Tot.**	**1**	**2**	**3**	**4**	**5**	**6**	**7**	**Tot.**
1	1.09	0.57	0.15	0.10	0.05	0.08	0.08	**2.11**	3.33	1.90	0.57	0.31	0.17	0.34	0.14	**6.75**	0.97	0.68	0.27	0.13	0.08	0.17	0.03	**2.31**
6	0.87	0.56	0.31	0.13	0.10	0.26	0.18	**2.41**	2.33	1.98	1.01	0.51	0.30	0.67	0.48	**7.27**	0.44	0.52	0.33	0.16	0.10	0.25	0.10	**1.89**
8	0.90	0.63	0.29	0.16	0.06	0.21	0.19	**2.44**	2.28	1.88	0.94	0.53	0.22	0.63	0.42	**6.90**	0.42	0.42	0.23	0.19	0.10	0.19	0.21	**1.76**
9	0.97	0.68	0.27	0.16	0.11	0.28	0.19	**2.66**	2.61	1.83	0.77	0.49	0.30	0.67	0.47	**7.13**	0.43	0.46	0.22	0.11	0.09	0.21	0.08	**1.62**
12	0.81	0.51	0.36	0.21	0.16	0.40	0.27	**2.72**	1.90	1.47	0.93	0.58	0.43	1.02	0.66	**6.99**	0.42	0.50	0.26	0.15	0.10	0.31	0.15	**1.89**
15	0.43	0.56	0.31	0.12	0.07	0.04	0.21	**1.75**	0.60	0.84	0.37	0.21	0.11	0.08	0.25	**2.46**	0.23	0.13	0.02	0.06	0.03	0.04	0.08	**0.58**
16	0.78	0.69	0.60	0.55	0.20	0.13	0.24	**3.18**	1.05	0.94	0.81	0.81	0.31	0.19	0.38	**4.48**	0.04	0.28	0.08	0.02	0.04	0.07	0.14	**0.67**
17	0.51	0.62	0.36	0.20	0.08	0.08	0.23	**2.10**	0.66	0.70	0.49	0.24	0.13	0.12	0.27	**2.61**	0.15	0.12	0.05	0.08	0.03	0.11	0.17	**0.70**
18	0.55	0.72	0.49	0.24	0.09	0.14	0.32	**2.56**	0.40	0.58	0.35	0.26	0.10	0.09	0.22	**2.01**	0.02	0.07	0.03	0.03	0.01	0.02	0.09	**0.28**
19	0.53	0.56	0.30	0.18	0.11	0.09	0.28	**2.05**	0.61	0.68	0.45	0.30	0.15	0.14	0.41	**2.73**	0.10	0.07	0.02	0.09	0.03	0.08	0.09	**0.47**
20	0.59	0.45	0.24	0.17	0.05	0.07	0.24	**1.82**	0.65	0.90	0.53	0.35	0.11	0.18	0.43	**3.14**	0.06	0.05	0.06	0.04	0.02	0.05	0.08	**0.37**
21	0.47	0.55	0.30	0.19	0.13	0.13	0.35	**2.11**	0.58	0.73	0.42	0.28	0.17	0.19	0.43	**2.79**	0.10	0.17	0.02	0.07	0.02	0.05	0.13	**0.58**
22	0.57	0.57	0.41	0.20	0.10	0.13	0.55	**2.53**	0.50	0.47	0.37	0.20	0.11	0.12	0.45	**2.22**	0.09	0.06	0.08	0.03	0.03	0.02	0.17	**0.49**
23	0.50	0.55	0.32	0.18	0.07	0.09	0.23	**1.93**	0.58	0.63	0.38	0.24	0.10	0.11	0.25	**2.30**	0.05	0.05	0.06	0.05	0.04	0.09	0.05	**0.38**
24	0.27	0.37	0.16	0.13	0.05	0.10	0.29	**1.38**	0.60	0.57	0.33	0.28	0.14	0.17	0.55	**2.65**	0.18	0.06	0.03	0.06	0.02	0.05	0.09	**0.49**
25	0.39	0.22	0.19	0.17	0.09	0.18	0.69	**1.92**	0.52	0.53	0.42	0.40	0.19	0.32	1.35	**3.72**	0.17	0.11	0.04	0.06	0.06	0.05	0.11	**0.61**
26	1.32	0.40	0.24	0.15	0.05	0.04	0.01	**2.21**	1.42	0.54	0.39	0.22	0.10	0.07	0.03	**2.77**	0.13	0.03	0.03	0.04	0.06	0.04	0.06	**0.39**
27	1.27	0.54	0.68	0.11	0.06	0.04	0.02	**2.72**	1.18	0.40	0.54	0.12	0.06	0.07	0.05	**2.41**	0.45	0.08	0.08	0.05	0.04	0.08	0.04	**0.81**
28	1.55	0.65	0.61	0.43	0.20	0.23	0.16	**3.83**	1.27	0.49	0.54	0.37	0.14	0.16	0.17	**3.14**	0.25	0.01	0.03	0.02	0.03	0.10	0.05	**0.50**
29	1.06	0.28	0.15	0.04	0.05	0.05	0.04	**1.68**	1.27	0.36	0.23	0.09	0.06	0.10	0.04	**2.15**	0.05	0.03	0.04	0.01	0.03	0.09	0.01	**0.26**
30	1.57	0.41	0.40	0.21	0.08	0.06	0.07	**2.81**	1.22	0.36	0.39	0.19	0.09	0.06	0.04	**2.33**	0.18	0.04	0.03	0.03	0.04	0.04	0.17	**0.53**
31	0.93	0.20	0.07	0.07	0.03	0.03	0.03	**1.36**	0.64	0.16	0.07	0.08	0.05	0.03	0.05	**1.08**	0.05	0.04	0.01	0.03	0.04	0.02	0.06	**0.25**
32	0.98	0.33	0.34	0.24	0.08	0.13	0.15	**2.26**	1.31	0.46	0.50	0.36	0.15	0.23	0.27	**3.28**	0.15	0.02	0.04	0.04	0.05	0.10	0.12	**0.51**
33	0.99	0.37	0.43	0.34	0.12	0.10	0.11	**2.48**	0.97	0.31	0.38	0.23	0.11	0.09	0.11	**2.20**	0.61	0.04	0.03	0.04	0.06	0.06	0.14	**0.99**
34	1.49	0.34	0.46	0.24	0.14	0.17	0.28	**3.12**	1.19	0.28	0.38	0.25	0.11	0.18	0.24	**2.62**	0.11	0.05	0.04	0.06	0.06	0.07	0.04	**0.43**
35	0.94	0.23	0.33	0.28	0.10	0.15	0.22	**2.25**	1.39	0.38	0.48	0.34	0.12	0.20	0.29	**3.19**	0.18	0.04	0.05	0.05	0.06	0.05	0.02	**0.44**
36	0.53	0.10	0.03	0.04	0.02	0.01	0.04	**0.77**	0.33	0.06	0.04	0.06	0.03	0.06	0.03	**0.61**	0.05	0.01	0.01	0.01	0.03	0.06	0.02	**0.18**
37	0.82	0.27	0.35	0.21	0.08	0.21	0.44	**2.36**	1.04	0.36	0.46	0.28	0.12	0.23	0.25	**2.76**	0.20	0.02	0.03	0.03	0.02	0.05	0.19	**0.55**
38	1.14	0.38	0.45	0.26	0.14	0.21	0.37	**2.95**	0.94	0.29	0.41	0.23	0.10	0.14	0.34	**2.44**	0.18	0.01	0.03	0.02	0.03	0.07	0.07	**0.40**
39	0.89	0.25	0.29	0.22	0.12	0.18	0.38	**2.33**	1.12	0.38	0.43	0.32	0.18	0.24	0.51	**3.17**	0.28	0.02	0.07	0.04	0.03	0.04	0.13	**0.61**

DECLARATION ON PLAGIARISM
UNIVERSITY OF PRETORIA
Faculty of Engineering, the Built Environment and Information Technology
Department of Materials Science and Metallurgical Engineering

The University places great emphasis upon integrity and ethical conduct in the preparation of all written work submitted for academic evaluation. While academic staff teach you about systems of referring and how to avoid plagiarism, you too have a responsibility in this regard. If you are at any stage uncertain as to what is required, you should speak to your lecturer before any written work is submitted.

You are guilty of plagiarism if you copy something from a book, article or website without acknowledging the source and pass it off as your own. In effect you are stealing something that belongs to someone else. This is not only the case when you copy work word-by-word (verbatim), but also when you submit someone else's work in a slightly altered form (paraphrase) or use a line of argument without acknowledging it. You are not allowed to use another student's past written work. You are also not allowed to let anybody copy your work with the intention of passing it off as his/her work.

Students who commit plagiarism will lose all credits obtained in the plagiarised work. The matter may also be referred to the Disciplinary Committee (Students) for a ruling. Plagiarism is regarded as a serious contravention of the University's rules and can lead to expulsion from the University.

The declaration which follows must be appended to all written work submitted within the department. No written work will be accepted unless the declaration has been completed and attached.

I (full names) _____

Student number _____

Topic of work _____

Declaration
1. I understand what plagiarism is and am aware of the University's policy in this regard.
2. I declare that this report is my own original work. Where other people's work has been used (from a printed source, internet or any other source), this has been properly acknowledged and referenced in accordance with departmental requirements.
3. I have not used another student's past written work to hand in as my own.
4. I have not allowed, and will not allow, anyone to copy my work with the intention of passing it off as his or her own work.

Signature _____